



Compound Specific Isotope Analysis (^{13}C , ^{37}Cl , ^2H) to trace induced attenuation of chlorinated organic contaminants in groundwater

Carme Audí Miró

ADVERTIMENT. La consulta d'aquesta tesi queda condicionada a l'acceptació de les següents condicions d'ús: La difusió d'aquesta tesi per mitjà del servei TDX (www.tdx.cat) i a través del Dipòsit Digital de la UB (diposit.ub.edu) ha estat autoritzada pels titulars dels drets de propietat intel·lectual únicament per a usos privats emmarcats en activitats d'investigació i docència. No s'autoritza la seva reproducció amb finalitats de lucre ni la seva difusió i posada a disposició des d'un lloc aliè al servei TDX ni al Dipòsit Digital de la UB. No s'autoritza la presentació del seu contingut en una finestra o marc aliè a TDX o al Dipòsit Digital de la UB (framing). Aquesta reserva de drets afecta tant al resum de presentació de la tesi com als seus continguts. En la utilització o cita de parts de la tesi és obligat indicar el nom de la persona autora.

ADVERTENCIA. La consulta de esta tesis queda condicionada a la aceptación de las siguientes condiciones de uso: La difusión de esta tesis por medio del servicio TDR (www.tdx.cat) y a través del Repositorio Digital de la UB (diposit.ub.edu) ha sido autorizada por los titulares de los derechos de propiedad intelectual únicamente para usos privados enmarcados en actividades de investigación y docencia. No se autoriza su reproducción con finalidades de lucro ni su difusión y puesta a disposición desde un sitio ajeno al servicio TDR o al Repositorio Digital de la UB. No se autoriza la presentación de su contenido en una ventana o marco ajeno a TDR o al Repositorio Digital de la UB (framing). Esta reserva de derechos afecta tanto al resumen de presentación de la tesis como a sus contenidos. En la utilización o cita de partes de la tesis es obligado indicar el nombre de la persona autora.

WARNING. On having consulted this thesis you're accepting the following use conditions: Spreading this thesis by the TDX (www.tdx.cat) service and by the UB Digital Repository (diposit.ub.edu) has been authorized by the titular of the intellectual property rights only for private uses placed in investigation and teaching activities. Reproduction with lucrative aims is not authorized nor its spreading and availability from a site foreign to the TDX service or to the UB Digital Repository. Introducing its content in a window or frame foreign to the TDX service or to the UB Digital Repository is not authorized (framing). Those rights affect to the presentation summary of the thesis as well as to its contents. In the using or citation of parts of the thesis it's obliged to indicate the name of the author.

UNIVERSITAT DE BARCELONA

Departament de Cristal·lografia, Mineralogia i Dipòsits Minerals

Facultat de Geologia

COMPOUND SPECIFIC ISOTOPE ANALYSIS (^{13}C , ^{37}Cl , ^2H) TO TRACE INDUCED ATTENUATION OF CHLORINATED ORGANIC CONTAMINANTS IN GROUNDWATER

Tesi doctoral presentada per:

Carme Audí Miró

Per a aspirar a l'obtenció del títol de doctora per la Universitat de Barcelona
amb Menció Internacional.

Tesi realitzada dintre del Programa de Doctorat de Ciències de la Terra, sota la
co-direcció de la Dra. Neus Otero i el Dr. Albert Soler, i tutoritzada pel Dr. Albert
Soler

Dra. Neus Otero

Dpt. Cristal·lografia, Mineralogia
i Dipòsits Minerals
Universitat de Barcelona

Dr. Albert Soler

Dpt. Cristal·lografia, Mineralogia
i Dipòsits Minerals
Universitat de Barcelona

Barcelona, Març, 2014



Table of contents.

Acknowledgement	IX
Abstract	XIII
Chapter 1. General Introduction	1
1.1. Chlorinated compounds and their environmental impact	1
1.2. Remediation techniques	4
1.3. Permeable reactive barriers	6
1.3.1. ZVI-PRB treatment	7
1.3.1.1. Longevity of the ZVI-PRBs	9
1.3.1.2. Microbial activity in the ZVI-PRB	10
1.4. Chlorinated compounds degradation pathways	11
1.4.1. Biotic degradation pathways	12
1.4.2. Abiotic zero valent iron degradation pathways	13
1.5. Hydrolysis as a proposed chloroform remediation technique	15
1.6. Compound Specific Isotope Analyses (CSIA)	18
1.7. Study sites	26
1.7.1. ZVI-PRB study site	26
1.7.2. CF alkaline hydrolysis study site	27
1.8. Objectives	28
1.9. Publications derived from this thesis	30
Chapter 2. Results	33
2.1 Assessment of ZVI-PRB induced chlorinated ethenes degradation	33
2.1.1 Laboratory ZVI batch experiments	33
2.1.2 Laboratory microcosm experiments	35
2.1.3 ZVI-PRB field-scale application assessment	36

2.2. Assessment of the chloroform alkaline hydrolysis induced by concrete-based construction wastes	40
2.2.1. Laboratory experiments of induced CF alkaline hydrolysis	40
2.2.2 Field-scale experiments with concrete-based recycled construction wastes	41
Chapter 3. Discussion	45
3.1 Assessment of ZVI-PRB induced chlorinated ethenes degradation	45
3.1.1 Laboratory ZVI batch experiments	45
3.1.2 ZVI-PRB field-scale application assessment	50
3.2. Assessment of the chloroform alkaline hydrolysis induced by concrete-based construction wastes	54
3.2.1 Laboratory experiments	54
3.2.2 Field-scale experiments	55
Chapter 4. Conclusions	59
Bibliography	65
Annex	
Annex A: Cl and C isotope analysis to assess the effectiveness of chlorinated ethene degradation by zero-valent iron: Evidence from dual element and product isotope values.	1
Annex B: C, Cl and H compound-specific isotope analysis to assess natural versus Fe (0) barrier-induced degradation of chlorinated ethenes at a contaminated site.	13
Annex C: The use of alkaline hydrolysis as a novel strategy for chloroform remediation: feasibility of using construction wastes and evaluation of carbon isotopic fractionation.	47

List of figures

Figure 1.1. Frequency at which CF, PCE, TCE, <i>cis</i> -DCE and VC were found in one or more percent of 3500 water samples from the 100 different aquifer studies carried out by the USGS in concentration higher than 0.2 µg/L	3
Figure 1.2. Continuous permeable reactive barrier, the most commonly used configuration.	6
Figure 1.3. Sequential anaerobic reductive dechlorination of PCE to ethene.	13
Figure. 1.4. Hypothesized reaction pathways for the chlorinated ethenes and other intermediates during reduction by Fe ⁰ .	14
Figure 1.5. Instrumentation for carbon isotope analysis (GC-C-IRMS) by compound specific isotope analysis.	18
Figure 1.6. GC-CF-IRMS equipment for chlorine isotopes analysis; and GC-R-IRMS for hydrogen isotopes analyses.	20
Figure 1.7. Evolution of the isotopic composition of an original PCE molecule and its daughter products along their transformation reactions.	21
Figure 1.8. Evolution of the isotopic composition of an TCE over the degradation products in abiotic degradation reactions.	24
Figure 2.1. Carbon isotope values of residual TCE and <i>cis</i> -DCE fraction in a double logarithmic plot over the respective concentrations.	35
Figure 2.2. Isotope data of: δ ¹³ C and δ ³⁷ Cl of PCE; δ ¹³ C of TCE; and δ ¹³ C, δ ³⁷ Cl and δ ² H of <i>cis</i> -DCE.	37
Figure 2.3. Changes in δ ¹³ C over time of PCE and <i>cis</i> -DCE in wells OMW5 and BR1-11, and MW17 and BR1-9.5, respectively.	38
Figure 2.4A-B. δ ¹³ C of PCE in BR1, BR3 and BR4 in depth from Jun-12 and Mar-13 campaigns	39
Figure 2.5. Changes in concentration and δ ¹³ C of CF over time in the alkaline hydrolysis laboratory experiments: unfiltered concrete experiments, filtered concrete experiments, filtered cement experiments, buffer experiments and control experiments.	40
Figure 2.6. Variation over time of CF concentration and carbon isotope ratios (δ ¹³ C-CF) in the tank trench and pit trench during the studied period.	43
Figure 2.7. Estimation of the extent of chloroform degradation by alkaline hydrolysis induced by construction wastes in the tank trench and the pit trench using Equation 1.13.	43

Figure 3.1. Changes in concentration of TCE, from Dual Element TCE experiments, and its byproducts over time.	46
Figure 3.2. Changes in chlorine isotope values of TCE, as substrate, and <i>cis</i> -DCE, as product, during TCE combined Dual Element experiments	47
Figure 3.3. Dual isotope plot $\delta^{13}\text{C}$ versus $\delta^{37}\text{Cl}$ obtained from TCE and <i>cis</i> -DCE Dual Element combined experiments.	48
Figure 3.4. Isotope values of TCE and its by-products, with a 10‰ isotope difference between hydrogenolysis <i>cis</i> -DCE byproduct and β -dichloroelimination ethene and ethane by-products.	49
Figure 3.5. $\delta^{13}\text{C}$ versus $\delta^{37}\text{Cl}$ from Oct-12 campaign samples.	51
Figure 3.6. $\delta^{13}\text{C}$ versus $\delta^2\text{H}$ of <i>cis</i> -DCE in Oct-12 campaign all over the site showing a positive correlation between $\delta^2\text{H}$ and $\delta^{13}\text{C}$ shifts.	54

List of tables

Table 1.1. VOCs found in about 1 percent or more of aquifer samples, at an assessment level of 0.2 µg/L	2
Table 1.2. Compounds degradable by ZVI	8
Table 1.3. Processes that can degrade chloroethenes and chloromethanes	12
Table 1.4. Selected elements and relative abundance and mass differences of the international standards	18

ACKNOWLEDGMENTS/AGRAÏMENTS

En primer lloc, vull agrair als meus directors de tesi, al Dr. Albert Soler i a la Dra. Neus Otero, haver-me donat l'oportunitat de fer la tesi al grup MAIMA, confiant en mi des del primer moment. Sobretot, per haver-me ensenyat tantes coses durant aquests quatre anys que m'han permès desenvolupar-me científicament, per haver-me donat suport durant tota la tesi i, sobretot en l'últim tram, pels vostres consells, positivisme i recolzament. Us agraeixo també haver estat sempre propers i haver compartit junts tantes experiències divertides, sempre recordaré el tast del menjar del sopar de gala del congrés AIG-9, incloent l'elecció de les estovalles! Gràcies per tot, de tot cor.

Vull agrair molt especialment al Dr. Jordi Palau, qui em va introduir al grup i va fer que això fos possible. Recordo la nostra primera conversa d'isòtops al bar de la facultat, un món nou davant meu; els primers experiments amb ferro zero valent; la primera visita a l'emplaçament de Granollers; l'informe del màster. Van ser molt bons moments a nivell científic i personal. Gràcies per tota la ciència que em vas aportar mentre eres a Barcelona i en les posteriors trobades, per a mi ha estat molt valuosa.

Very special thanks to Dr. Martin Elsner, from the Helmholtz Zentrum of Munich. Thanks for trusting me and allowing me to work in your great group; I learned a lot during my stay in the Environmental Isotope Chemistry group. It was really an honor to receive your knowledge and share a project with you, a great scientist and a great person. Thanks for all your efforts during the revision of the two papers, I enjoyed very much these periods of the thesis. Also thanks to Dr. Stefan Cretnik, I spent a great time working together; I will always remember very good moments in the lab, in the canteen, in the barbecue at the roof... Thanks to all the nice people I met in the Institute of Groundwater Ecology.

Gràcies al Dr. Massimo Marchesi. Amb tu vam començar els primers experiments d'hidròlisi alcalina amb formigó, vaig fer les primeres planificacions experimentals, vaig posar-me en contacte amb els equips per primer cop... Gràcies per tots els teus bons consells. Però sobretot, et vull agrair l'acollida que tu i la Chiara em vau fer quan vaig ser a Toronto. Rebre'm a l'aeroport, el primer cap de setmana junts de barbacoa i les posteriors acollides a casa vostra quan ho requeria van ser claus per sentir-me no tant lluny de casa meva.

Thanks to Dr. Orfan Shouakar-Stash for showing me the hydrogen isotope technique and analyzing our field samples. Thanks to you, Orfan, and to Mirna Stas for being so kind and welcoming me so nicely when I was in Waterloo. Thanks to Mirna for the guided tour in Waterloo, it was a great time.

Thanks to Dr. Barbara Sherwood-Lollar for giving me the opportunity to work in the Stable Isotope Laboratory group. Thanks to all the staff there, that made the stay very pleasant, and most importantly to Dr. Georges Lacrampe-Coulome with whom it was a pleasure to work, not only for his great knowledge but also for the kindness he always gave me. Merci beaucoup, força gràcies.

Gràcies a l'Agència Catalana de l'Aigua que en tot moment s'ha interessat pels resultats d'aquest treball i que ha col·laborat com a ens promotor i observador aportant tant la informació disponible com idees. En particular a l'Emilio Orejudo; i molt especialment al Roberto Espinola, qui ha participat activament en aquest projecte sobretot durant la realització del seu Projecte de Final de Màster d'Enginyeria Ambiental.

Gràcies a l'Agència de Residus de Catalunya pel seu suport i informació aportada, concretament al Josep Anton Domènech i al Joan Bartoll.

Gràcies al Clapé Group per proporcionar-nos el ferro zero valent, instal·lar els pous multinivell i permetre'ns estudiar l'eficiència de la barrera permeable reactiva de ferro zero valent. Gràcies també a l'empresa Entorn, per facilitar-nos les tasques. I a l'Albert Ventayol i els sondistes que van instal·lar els pous multinivell, que van ajudar-nos amb el sistema de tubets multinivell i amb qui vam passar una setmana molt agradable al camp.

Gràcies a Geomar, especialment al Joan Martínez i a la Júlia Soler per haver instal·lat un nou punt de mostreig que ha estat clau per resoldre un dels objectius de la tesi.

Moltes gràcies als Centres Científics i Tecnològics (CCiT) de la Universitat de Barcelona, concretament a les Dres. Pilar Teixidor i Rosa Maria Marimón per haver dedicat temps a resoldre dubtes i problemes analítics que han anat sorgint durant la tesi. Especialment amb la Pilar hem passat molt bons moments, moments en que hem parlat de ciència i moments en que hem compartit anècdotes personals que han fet més agradable la feina. També vull agrair la col·laboració de la Pili i la Lourdes que sempre han estat allà per donar-me un cop de mà, a la vegada que també m'han fet passar moments molt divertits.

Moltes gràcies al personal de la Facultat de Geologia en general i a tots els membres del Departament de Cristal·lografia, Mineralogia i Dipòsits Minerals, amb qui durant tot aquest temps hem compartit dinars de Nadal, celebracions de tesis doctorals, converses de passadís, que sempre fan el dia a dia més agradable.

Gràcies a la resta de companys del grup de Mineralogia Aplicada i Medi Ambient (MAIMA). A l'Alba i la Diana, les últimes incorporacions pre-doc del grup, gràcies per ajudar-me en les campanyes de camp, m'ha encantat viure l'últim any de tesi amb vosaltres i començar aquesta amistat. Al Roger, al Raul i la Georgina, amb qui vivim i compartim els nervis de les últimes setmanes de tesi. A la Mercè per ser sempre un suport molt gran al laboratori, i per la seva ajuda al camp també, gràcies per tot. A la Paula per la seva calidesa com a persona, i per escoltar-me sempre. A l'Albert Folch, pel seu suport hidrogeològic, sempre disposat a ajudar. Tot i que no sigui MAIMA, com si ho fos, gràcies també a la Marta per aportar-me alegria i preocupar-se sempre per mi. A l'Àngels Canals, sempre riallera i amb ganes d'ajudar-te, gràcies. A la Manuela i la Cristina, últimes incorporacions post-doc del grup, per sempre estar allà amb el seu somriure i compartir agradables moments a l'hora de dinar. Cristina gràcies per la teva ajuda científica també, a l'hora d'escriure els articles. Vull fer especial menció a la Clara, amb qui he treballat molt directament tot aquest temps i ha suposat un gran pilar tant en la recerca com a nivell personal, gràcies per tot el que m'has aportat Clara i pels consells que sempre m'has donat. Finalment, a la meva companya de despatx i amiga, la Mònica. Gran científica i persona. De tu he après moltes coses, m'encanta quan em transmits la teva ciència i fas que resulti tot més fàcil, gràcies per escoltar-me i pels teus bons consells com a científica i com a amiga.

Vull agrair a totes les persones que han passat pel grup en les seves estades o projectes finals de carrera. Especialment als que han participat activament en les tasques d'aquesta tesi. A la Geneviève Bordeleau, l'Arnau Follia, el Dani Sancho, el Pol Pla. I sobretot, a l'Adriana Rossi, amb qui vaig començar una bonica amistat, gràcies pel teu carinyo i afecte.

Fora de l'ambient laboral vull agrair a la Reyes, la meva amiga mallorquina, la seva amistat i el seu suport durant aquest període, el qual hem viscut gairebé en paral·lel. Gràcies pels moments tan genials que hem viscut quan ens hem trobat, i per escoltar-me i entendre sempre encara que fos en la distància. A la Chari, la meva antiga companya de pis i amiga. Gràcies pel seu suport, al seu costat he viscut gairebé tots els moments de la tesi, fent el dia a dia més càlid i divertit. Gràcies a les meves amigues Judit, Txell i Raquel, per les quedades que hem anat fent durant aquest temps i que m'han fet gaudir encara més d'aquesta etapa. A la Tània, per l'última etapa de la tesi, que ens l'hem passat corrent, literalment parlant. Gràcies per la força que sempre em transmits.

A la meua amiga Núria. Quantes trucades de telèfon aquests anys, sempre preguntant-me per la tesi, els articles, i fent-me sentir que el que faig val molt la pena. Gràcies pel teu recolzament, i per tot. I a la meua amiga Blanca, pel seu suport en aquest temps, per emocionar-se amb les meves estades, i fer-me gaudir encara més d'aquesta experiència.

Thanks to Yoon-ji and Hana, my sweet friends in Canada. Toronto would not have been the same without you.

Gràcies també a la Tere, la Sara, el Jeremy i la Carme, amics que vaig fer al Departament de Fisiologia de la Facultat de Farmàcia. Al vostre costat vaig iniciar-me en la recerca, i la vaig disfrutar!

Un agraïment molt especial a la Laura Colom, artista del quadre de la portada. Moltíssimes gràcies per aquest regal tan especial Laura, per haver-te inspirat amb la meua tesi. Gràcies també per acompanyar-me en aquest final de tesi i sempre donar-me ànims.

Moltes gràcies a tota la família de Tortosa, en especial a la Iaia, que sempre es preocupa per mi i em dona suport per a que les coses em surtin bé, als "tios", als padrins, cosins i cosines, a la tia Tere i família, a tots. I a la família italiana, gràcies als 4. Gràcies a tots per recolzar-me durant la tesi, per estar pendents de mi durant tot aquest temps i durant les meves estades. Gràcies també a la nombrosa família menorquina, les escapades a Menorca han fet que aquest període fos encara millor.

Finalment, les persones més importants de tot plegat. Els meus pares, la Cinta i el Quim. Aquesta tesi ha estat possible gràcies a l'esforç previ dels meus pares, Josep i Maite. És el resultat de la formació que m'han donat i de la motivació i empenya que sempre m'han transmès. Gràcies per confiar en mi, per interessar-vos pel que faig, i per fins i tot voler entendre els isòtops i la barrera del camp, en definitiva, gràcies per estar sempre al meu costat i per estimar-me tant. Gràcies a la meua germaneta Cinta, amb qui he conviscut gairebé durant tota la tesi; hem passat innumbrables moments juntes durant aquests anys, moments molt feliços i que mai oblidaré, gràcies per cuidar-me i preocupar-te sempre per la meua felicitat; i gràcies a tu i al Vicent per fer-me sentir com a casa quan m'heu acollit a Barcelona durant la part final de la tesi. Per últim, gràcies al Quim, la persona que ha viscut de més a prop tota la tesi, m'ha escoltat en tot moment i ha sentit les mateixes alegries, preocupacions i emocions que jo durant aquest procés. Gràcies per ser-hi sempre.

Aquesta tesi s'ha realitzat amb el suport de la beca de Formació de Personal Investigador (FPI) del Ministeri d'Economia i Competitivitat del Govern d'Espanya. També s'ha beneficiat del finançament dels projectes CICYT CGL2008-06373-C03-01/03-BTE i CICYT CGL2011-29975-C04-01 del Ministeri d'Economia i Competitivitat del govern espanyol, l'ajut de suport al Grup Consolidat de recerca de Mineralogia Aplicada i Medi Ambient 2009SGR-00103 del Departament d'Universitats, Recerca i Societat de la Informació de la Generalitat de Catalunya, la "Marie Curie Career Integration Grant" del projecte IMOTEC-BOX (PCIG9-GA-2011-293808) dintre del 7è Programa Marc de la Unió Europea. També ha estat finançada pel Clapé Group a través de la Fundació Bosch i Gimpera de la Universitat de Barcelona amb el contracte n° 306611.

ABSTRACT

Chloroform (CF), tetrachloroethene (PCE) and trichloroethene (TCE) are dense chloro-aliphatic hydrocarbons (CAH) extensively used as industrial solvents. These compounds have been largely released to the environment due to poor waste management. In the aquifer, because they are denser than water, they migrate downwards through the saturated zone until they reach a confining layer, forming pools, thus constituting a long-term source of groundwater contamination and an important environmental concern.

Under anaerobic conditions PCE and TCE can experience natural sequential dehalogenation to *cis*-DCE, VC and non-toxic ethene and ethane. Frequently, however, incomplete reductive dechlorination with the accumulation of *cis*-DCE and VC can occur due to the lack of specialized degrader communities (Friis, *et al.*, 2006). The accumulation of these compounds is of great concern because of their potential or proven carcinogenicity (U.S. EPA, 2009) where VC is the most toxic product of the degradation chain. Regarding CF, it can be biodegraded through aerobic and anaerobic co-metabolic processes (Cappelletti *et al.*, 2012); however, some factors may affect the CF co-metabolism such as, the competition with the growth substrates, the need of a reducing agent to keep the activity of the enzymes, and the toxicity of the products formed, among others. Recently, CF dechlorination was linked to the growth of bacterial strains belonging to *Dehalobacter* genus (Grostern *et al.* 2010; Lee *et al.* 2012) through CF dehalorespiration. Due to the uncertainties of natural biodegradation, there has been an increasing interest in engineered abiotic degradation to remove these compounds in an efficient way.

Zero valent iron permeable reactive barrier (ZVI-PRB) treatment involves the placement of particulate ZVI in the flow path of a contaminated plume. As the plume moves through the barrier, ZVI is designed to sequentially degrade PCE and TCE by reductive dechlorination to form the non-toxic end compounds ethene and ethane (Arnold and Roberts, 2000). In contrast to biodegradation, which occurs exclusively by hydrogenolysis, ZVI is able to degrade the chlorinated compounds also through the β -dichloroelimination pathway, dominating over hydrogenolysis, then circumventing the production of VC. Concerning CF, its abiotic degradation with ZVI gives the toxic daughter product dichloromethane (DCM), which is not further degradable by this reactive material (ITRC, 2005).

In this thesis, the effect of a ZVI-PRB installed at a field site contaminated mainly with PCE, TCE and *cis*-DCE was evaluated. Moreover, a novel strategy to degrade the recalcitrant CF - alkaline hydrolysis induced by concrete-based recycled construction wastes- was proposed and developed at pilot field-scale in order to test its efficiency in degrading this pollutant. Compound specific isotope analysis (CSIA) is a valuable tool for monitoring an environmental

treatment in the field, based on the isotope fractionation of an element during transformation reactions. The stable isotopes approach permits the evaluation of the extent of a degradation reaction excluding the processes that do not involve contaminant destruction such as dilution, dispersion, volatilization, etc.

The general aim of this thesis is to use compound specific isotope analysis of ^{13}C , ^{37}Cl and ^2H as a tool to assess both induced attenuation processes 1) chlorinated ethenes degradation by a ZVI-PRB installed at the field sited; and, 2) the proposed new remediation technique based on the use of concrete-based recycled construction wastes to degrade chloroform (CF) by alkaline hydrolysis applied at a site contaminated by this pollutant.

Laboratory experiments were conducted to study both ZVI and concrete effects on the chlorinated ethenes and the chloroform, respectively. ZVI experiments yielded carbon isotope fractionation values of the chlorinated ethenes degradation by the specific ZVI used in the field application, as well as, the first chlorine isotope fractionation values of TCE and *cis*-DCE associated to this reaction (are ϵ_{Cl} of $-2.6\pm 0.1\%$ for TCE and of $-6.2\pm 0.8\%$ for *cis*-DCE). Two promising approaches to discriminate the abiotic ZVI degradation versus biotic degradation present at the field site were brought forward 1) the dual isotope ^{13}C - ^{37}Cl approach, which distinguished slopes 4 times lower than for biodegradation of *cis*-DCE by the reported commercially available *Dehalococcoides*-containing mixed culture KB-1 (Abe *et al.*, 2009); and 2) the product-specific carbon isotope fractionation that showed a 10‰ difference between those products coming from β -dichloroelimination and hydrogenolysis reactions. Concrete experiments with CF achieved a 95% CF degradation after 28 d, accompanied by a significant carbon isotope fractionation. The carbon isotopic fractionation associated with alkaline hydrolysis of CF was $-53\pm 3\%$. Moreover, the large difference between the obtained ϵ_{C} and the reported carbon isotopic fractionation of CF by a *Dehalobacter*-containing culture [ϵ_{C} of $-27.5\pm 0.9\%$ (Chan *et al.*, 2012)] implies a great potential for the use of $\delta^{13}\text{C}$ values for in situ monitoring of the degree of CF degradation by alkaline hydrolysis.

The obtained laboratory data permitted the assessment of the respective induced degradation treatments applied at the field site. At the site with the ZVI-PRB treatment, both occurrence of biodegradation and degradation by ZVI-PRB were evidenced by means of detected metabolites and ^{13}C data, with quantitative estimates of ZVI-PRB efficiency of less than 10% and 2% for PCE and *cis*-DCE, respectively. Dual element ^{13}C - ^{37}Cl isotope plots confirmed that the effect of the ZVI-PRB was masked by biodegradation. Based on carbon isotopes data, 49% and almost 100% of PCE and TCE, respectively, were estimated to be removed by biodegradation. Finally the combination of ^2H with ^{13}C and ^{37}Cl discriminated two different sources of contamination spilled from the same industry. This indicates the potential of $\delta^2\text{H}$ to discriminate if a compound

is of industrial origin, or whether it is formed as a daughter product during degradation. Regarding CF hydrolysis, field-scale pilot experiments were used to test the efficiency of the concrete-base recycled construction wastes to induce alkaline hydrolysis. The carbon isotopic fractionation obtained at the lab scale allowed the calculation of the percentage of chloroform degradation in the field-scale pilot experiments where alkaline conditions were induced in two recharge water interception trenches filled with concrete-based construction wastes. A maximum of approximately 30-40% of chloroform degradation was achieved during the two studied recharge periods. Although further research is required, the treatment of chloroform in groundwater through the use of concrete-based construction wastes is proposed. This strategy would also imply the recycling of construction and demolition wastes for use in value-added applications to increase economic and environmental benefits.

Overall, by combining C, Cl and H isotopes, this thesis provided new tools to discriminate ZVI versus biodegradation at the field site, as well as to identify industrial versus product-formation contaminant sources. Since hydrogen isotopes approach shows great potential, further research on this research line should be done. Moreover, the new proposed CF alkaline hydrolysis induced by concrete-based recycled construction wastes, was proved to efficiently degrade this pollutant, as well as to be working on a field-scale pilot experiment monitored by the use of carbon isotopes. Therefore, it is suggested that, the proposed strategy which would also imply the revalorization of construction and demolition wastes, merits evaluation.

Chapter 1.

General Introduction

1.1. CHLORINATED COMPOUNDS AND THEIR ENVIRONMENTAL IMPACT

During recent years, groundwater contamination by organic compounds from industrial activities has become a matter of great environmental concern. Large releases of contaminants into the environment due to poor waste management and the persistence of some compounds can result into the contamination of large groundwater volumes. The most common groundwater organic contaminants are volatile organic compounds (VOC), and among them the most frequently detected are chlorinated organic solvents, which usually reach levels in groundwater in the $\mu\text{g/L}$ to mg/L range (Pankow and Cherry, 1996).

The USGS carried out a study during 1985-2001 from 100 different aquifer studies in the U.S. and about 3500 water samples collected (Fig. 1.1). The most frequently found chlorinated organic solvents were chloroform (CF), tetrachloroethene (PCE) and trichloroethene (TCE), which were positioned in the first, second and fourth place respectively in the list of detected VOCs (Table 1.1). The chlorinated ethenes daughter products, *cis*-dichloroethene (*cis*-DCE) and vinyl chloride (VC) were also commonly detected (Fig. 1.1). The “Agència Catalana de l’Aigua de la Generalitat de Catalunya (ACA)” is actively working in the study and restoration of sites contaminated with these organic chlorinated compounds (ACA, 2002, 2003, 2007). The above-mentioned compounds will be the target of study of this thesis.

Table 1.1. VOCs found in about 1 percent or more of aquifer samples, at an assessment level of 0.2 µg/L (compounds listed by decreasing detection frequency) (Zogorski *et al.*, 2006).

Compound name	VOC group
Chloroform	trihalomethane
Perchloroethene	solvent
Methyl <i>tert</i> -butyl ether	gasoline oxygenate
Trichloroethene	solvent
Toluene	gasoline oxygenate
Dichlorodifluoromethane	refrigerant
1,1,1-Trichloroethane	solvent
Chloromethane	solvent
Bromodichloromethane	trihalomethane
Trichlorofluoromethane	refrigerant
Bromoform	trihalomethane
Dibromochloromethane	trihalomethane
<i>trans</i> -1,2-Dichloroethene	solvent
Methene chloride	solvent
1,1-Dichloroethane	solvent

Chlorinated ethenes have been produced commercially since the beginning of the 1900s. PCE and TCE have been used as degreasers and in dry cleaning processes (PCE was the main compound used for dry-cleaning purposes since TCE was limited for that use in the 1950s) (IARC, 1995). CF was used as a surgical anesthetic and in cough syrups and toothpastes until 1976 (when carcinogenicity effects were suspected); however, its use as an industrial solvent and for water and bleaching of paper was almost doubled from 1980 to 1990 (Capelletti *et al.*, 2012).

Human-health and environmental concerns resulted in the decline in chlorinated solvents production in the 1970s, however, hundreds of thousands of tons of these compounds are still used every year (Pankow and Cherry, 1996). Currently PCE and TCE are mainly used for dry cleaning, metal degreasing (80-90% of current TCE worldwide is used for metal degreasing) and as chemical intermediates. CF is presently used in the manufacture of the refrigerant chlorodifluoromethane (HCFC-22) and in the production of fluoropolymers. CF is also added in pesticides formulations and used as a cleaning agent (as solvent for fats, oils, waxes, varnishes, rubber, and resins), in fire extinguishers and in the rubber industry (Pankow and Cherry, 1996; Zogorski *et al.*, 2006; Cappelletti *et al.*, 2012).

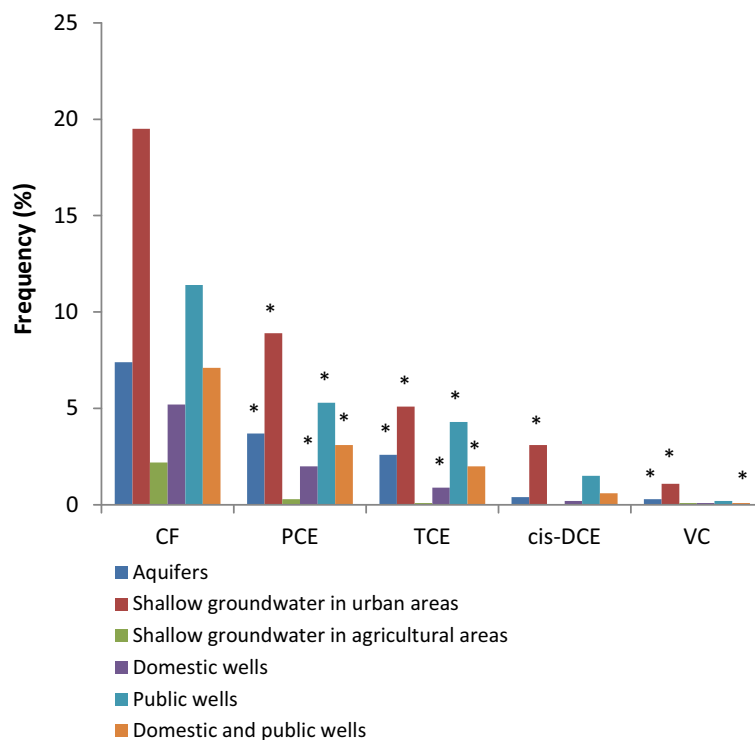


Figure 1.1. Frequency at which CF, PCE, TCE, *cis*-DCE and VC were found in one or more percent of 3500 water samples from the 100 different aquifer studies carried out by the USGS in concentration higher than 0.2 $\mu\text{g/L}$. * the concentration of contaminant was above the Maximum Contaminant Level (MCL). (MCL: 5 $\mu\text{g/L}$ for PCE and TCE, 2 $\mu\text{g/L}$ for VC and 70 $\mu\text{g/L}$ for *cis*-DCE and CF) [from Zogorski *et al.* (2006) data].

In 2012 the International Agency for Research on Cancer (IARC) classified TCE as carcinogenic compound to humans (Group 1) (Hansen *et al.*, 2013), while PCE and CF are considered probably carcinogenic to humans (Group 2A). The daughter product VC is also classified as carcinogenic by the IARC (IARC, 1995). Besides the carcinogenic effects, these VOCs may adversely affect the liver and the nervous, reproductive, and immunological systems. They can produce eye, skin, and throat irritation (Doherty, 2000; Zogorski *et al.*, 2006).

Chlorinated organic solvents are denser than water, for this reason they are commonly referred to as “dense non-aqueous phase liquids” (DNAPLs). Due to the high density, when DNAPLs are spilled into the subsurface, they can migrate below the water table providing long-term sources of contamination (Pankow and Cherry, 1996). DNAPLs low liquid viscosity let them move easily into the subsurface enabling their migration (Zogorski *et al.*, 2006). Moreover, their interfacial tension with water facilitates their entrance into water-wet fractures. Their low water solubility ($\approx 150\text{-}3500$ mg/L for chlorinated ethenes and 8000 mg/L for CF), together with their moderate volatility (between 13 and 121°C) make them diffuse rapidly into the unsaturated zone easily spreading the contamination. Despite their low absolute solubility, the solubility is high

when compared to the Maximum Concentration Limit (MCL) of TCE, PCE and CF (5 µg/L for both PCE and TCE; and 70 µg/L for CF) established by the U.S. Environmental Protection Agency (Zogorski *et al.*, 2006). The drinking water thresholds established by the Spanish Government are of 10 µg/L for the sum of both TCE and PCE; and 100 µg/L for the sum of trihalomethanes (THM) including CF (Real Decreto 140/2003).

1.2. REMEDIATION TECHNIQUES

Remediation techniques to degrade contaminants in the environment can be based on three main strategies that can be applied in conjunction or separately 1) contaminant destruction; 2) extraction of the contaminant from the contaminated groundwater; 3) immobilization of the contaminant (FRTR, 2007). Direct destruction strategies are preferred over non-destructive techniques because they aim at eliminating the target contaminant, avoiding the increase of contaminant volume, and/or the necessity to do a subsequent treatment.

Generally, remediation techniques for groundwater decontamination are classified into two principal categories, *ex-situ* and *in-situ* treatments. In *ex-situ* treatments, waters are extracted from the aquifer to be treated on the surface. This type of treatment is generally characterized by shorter time periods than in situ treatment, with more certainty about the uniformity of the treatment because of the capacity to homogenize and continuously mix the groundwater. Nevertheless, *ex-situ* treatment requires pumping of water to bring it to the surface, increasing the costs and the required engineering equipment (FRTR, 2007). *In-situ* treatments are directly applied into the aquifer (Reddy, 2008). The principal advantages of *in-situ* treatments are cost savings and minimization of potential cross-contamination since the non-contaminated surface is not exposed to the contaminated groundwater. However, higher uncertainty rises regarding homogeneity of the treatment (due to variability in aquifer characteristics); and treatments can take longer time to achieve the design goals (FRTR, 2007). Nevertheless, monitoring the applied treatment with proper tools may solve this main drawback of the *in-situ* treatment. This thesis will be focused on the *in-situ* treatments, which can be divided into natural and induced processes.

Monitored Natural Attenuation (MNA) is a natural *in-situ* treatment consisting on monitoring natural attenuation processes that, without human intervention, are capable to degrade contaminants or reduce their concentration in groundwater (FRTR, 2007; U.S. EPA, 2012). It may be used with other remediation processes as a finishing option or as the only remediation process if the rate of contaminant degradation is fast enough to protect human health and the

environment (U.S. EPA, 2012). Natural attenuation includes biodegradation but also a diversity of physical and chemical processes such as dispersion, dilution, sorption and volatilization that do not degrade the contaminants. Biodegradation consists of biological processes mediated by indigenous microorganisms that transform contaminants via enzymes that act as catalyst (Suthersan, 1999). For biotic degradation to take place, adequate microbial populations have to be present in the environment, as well as specific conditions that might affect their growth and metabolic activity, such as nutrients, temperature, pH, moisture content, and redox potential.

Induced attenuation can be grouped into biotic and abiotic processes. Biotic processes aim at achieving the best conditions for microorganisms development. These treatments include biostimulation and bioaugmentation. In biostimulation, nutrients, such as nitrogen and phosphorus, as well as oxygen and other electron acceptors are added to the microbial environment in order to stimulate the activity of microorganisms. Bioaugmentation involves the addition of exogenous microbes to the subsurface where organisms capable to degrade the target compounds are deficient (Suthersan, 1999).

Induced abiotic processes include several chemical and physical processes such as *in-situ* chemical oxidation (ISCO), thermal treatment and passive/reactive treatment barriers, which are the most used for chlorinated organic compounds. ISCO is a remedial technology that involves the introduction of a chemical oxidant (i.e. permanganate, Fenton's reagent, ozone, persulfate) into the subsurface, transforming the groundwater contaminant into less harmful chemical species (U.S. EPA, 2014). The thermal treatment consists of the vaporization of volatile and semivolatile contaminants from groundwater by the introduction of hot water or a steam flow through injection wells. Vaporized components rise to the unsaturated zone where they are removed by vacuum extraction and then are treated. Regarding permeable reactive barriers (PRBs), they are trenches filled with a reactive material installed across the flow path of a contaminant plume that allow the water to passively move through it while transforming or retaining the contaminants by the reactive material (U.S. EPA, 1998; Puls *et al.*, 1999); further information is found in section 1.3.

This thesis is focused on studying two induced *in-situ* degradation processes: 1) a permeable reactive barrier (PRB) of zero valent iron (ZVI) for the degradation of chlorinated ethenes; and 2) a proposed new technique based on induced alkaline hydrolysis of chloroform by using concrete-based recycled construction wastes.

1.3. PERMEABLE REACTIVE BARRIERS

Permeable reactive barriers were presented by the National Research Council, in 1994, as one of the most promising alternative technologies to the commonly used *ex-situ* pump-and-treat method, which was recognized to present limitations regarding the restoration of the groundwater to drinking water standards (U.S. EPA, 1998). According to the U.S. EPA (2008), the permeable reactive barrier (PRB) technology is accepted as an effective passive remediation technique to decontaminate groundwater of a diversity of chlorinated organic and inorganic contaminants (O'Hannesin and Gillham, 1998; Blowes *et al.*, 2000).

There are different types of configuration, depending on 1) if the contaminated flow naturally passes through the barrier containing the reactive material (continuous PRB); 2) if the flow is directed to a gate with the reactive material (Funnel and gate PRB); or 3) if the contaminated groundwater is directed to subsurface vessels containing the reactive media (*In-situ* vessels PRB) (U.S. EPA, 1998). The continuous PRB is the most commonly used configuration in USA (Birke *et al.*, 2007) and in consequence, worldwide, as in USA there are around 90 of the approximately 140 PRBs worldwide (ITRC, 2005). Only in Europe the Funnel and gate PRB (ITRC, 2005) is the most installed one.

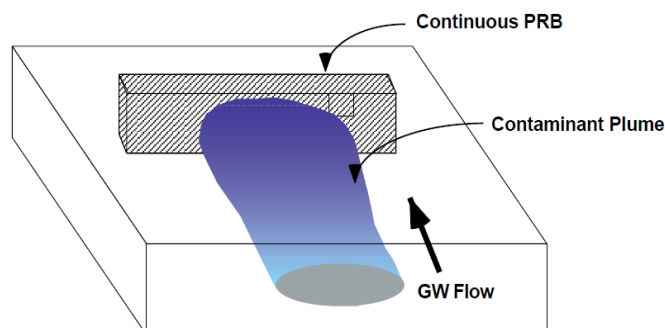


Figure 1.2. Continuous permeable reactive barrier, the most commonly used configuration (U.S. EPA, 1998).

The most widely used reactive material in PRBs is the Zero Valent Iron (Fe^0) (ZVI), owing its success the fact of being capable to treat common organic and inorganic contaminants in groundwater, such as chlorinated organic compounds (VOCs), petroleum hydrocarbons, chromium, and arsenic (ITRC, 2005). Other materials used in PRBs are 1) activated carbon, to which organic and heavy metal contaminants are adsorbed; 2) limestone, extensively used to treat the impact of acid mine drainage by increasing the pH and precipitating metal

contaminants as hydroxides or carbonates; 3) zeolite, an anionic mineral with high adsorbing, catalytic and ion-exchange capacities with a strong affinity for several toxic heavy metals; and 4) microorganisms that biodegrade toxic organic contaminants in the subsurface (Thiruvengkatachari *et al.*, 2008).

1.3.1. ZVI-PRB treatment

Lo *et al.*, (2002) summarizes the introduction of the use of ZVI to degrade chlorinated ethenes. According to Lo *et al.*, (2002) Sweeney's works from 1972 reported the first data on the use of zero-valent zinc to enhance the degradation of chlorinated pesticides. Later, in 1988 Senzaki and Kumagai, found the potential of electrolytic iron powder to degrade 1,1,2,2-tetrachloroethane (TeCA) and in 1989 revealed its effectiveness in degrading TCE (Lo *et al.*, 2002). In 1992 Gillham and O'Hanessin published the great capacity of ZVI in degrading a wide range of chlorinated compounds (Lo *et al.*, 2002). As a result, the first pilot-field application of a permeable reactive barrier of ZVI was installed in 1991 for in situ remediation of TCE and PCE of groundwater in the Canadian Force Base of Borden (Ontario), achieving degradations of 95 and 91 %, respectively (Gillham and O'Hanessin, 1992). After the success of the first ZVI-PRB field demonstration, the first commercial ZVI-PRB was installed in 1995 in Sunnyvale (Santa Clara, California) for the removal of chlorinated hydrocarbons in groundwater (Warner *et al.*, 2005). This PRB was proven to be working successfully even after 10 years of operation (Warner *et al.*, 2005). Since the first commercial ZVI-PRB and over the following 10 years ZVI-PRBs evolved from an innovative technology to an accepted standard practice. During that period of time, a total of 83 ZVI-PRB were installed worldwide, 67 of them were located only in the USA (ITRC, 2005; Warner *et al.*, 2005).

Granular ZVI is currently available in the market in large quantities to be used in PRB technology applications. The most common source of ZVI is from recycled scrap from the manufacturing of automotive pieces that is subjected to several processes to get the granular iron. Granular ZVI is also known as cast ZVI. Since dechlorination reactions happen in the surface of the iron, the surface has an important role in the resultant reaction efficiency. Thus, a higher surface area and purity that give a higher number of reactive sites on the surface, will result in greater reaction rates (Johnson *et al.*, 1996; Slater *et al.*, 2002). The specific surface area of cast iron from several providers (Fischer, Aldrich, Gotthart Maier, Peerless, Master Builders, Connelly) determined by the BET (Brunauer-Emmett-Teller) method in two studies (Su and Puls, 1999; Suk, *et al.*, 2009) goes from 0.091 to 1.38 m²/g. The granulometry in general is between 300 and 2000 µm of diameter. Purity of ZVI should be of more than 90% of metal iron, with a content of carbon lower than 3%, and nontoxic levels of leachable metal

impurities. ZVI granules must not present any surface coatings that would inhibit its reactivity, such as oils or grease (ITRC, 2011).

The oxidation of Fe^0 provides a source of electrons that can reduce chlorinated hydrocarbons, degrading them to final nontoxic products (Bhandari *et al.*, 2007). Among these degradable compounds are the chlorinated ethenes TCE, PCE, *cis*-DCE and VC and some chlorinated ethanes, chlorinated methanes (such as CF), chlorinated propanes between others indicated in Table 1.2 (ITRC, 2005). Some chlorinated organic compounds not treatable by ZVI are dichloromethane (DCM), chloromethane, 1,2-dichloroethane and chloroethane (ITRC, 2005). ZVI is capable of degrading other organic compounds such as benzene, toluene, ethyl-benzene and xylene (BTEX) and metals such as Cr, U, As, Hg (ITRC, 2005).

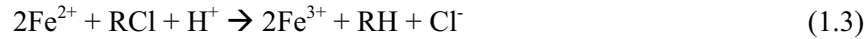
Table 1.2. Compounds degradable by ZVI (ITRC, 2005)

<i>Common name</i>	<i>Common abbreviation</i>
Ethenes	
Tetrachloroethene	PCE
Trichloroethene	TCE
<i>cis</i> -1,2-Dichloroethene	<i>cis</i> -1,2-DCE
<i>trans</i> -1,2-Dichloroethene	<i>trans</i> -1,2-DCE
1,1-Dichloroethene	1,1-DCE
Vinyl chloride	VC
Ethanes	
Hexachloroethane	HCA
1,1,1,2-Tetrachloroethane	1,1,1,2-TeCA
1,1,2,2-Tetrachloroethane	1,1,2,2-TeCA
1,1,1-Trichloroethane	1,1,1-TCA
1,1,2-Trichloroethane	1,1,2-TCA
1,1-Dichloroethane	1,1-DCA
1,2-Dibromoethane	1,2-DBA
Methanes	
Tetrachloromethane	CT
Chloroform	CF
Tribromomethane	TBM
Propanes	
1,2,3-Trichloropropane	1,2,3-TCP
1,2-Dichloropropane	1,2-DCP
Other Chlorinated	
N-Nitrosodimethylamine	NDMA
Dibromochloropropane	DBCP
Lindane	
1,1,2-Trichlorotrifluoroethane	
Trichlorofluoromethane	

The main reaction produced between the iron and the chlorinated compound takes place under anaerobic conditions and involves the release of two electrons that directly reduce the chlorinated compound (Matheson and Tratnyek, 1994):



However, the oxidation of Fe^0 by O_2 under aerobic conditions, and by water in an anaerobic environment, can also lead to the reduction of chlorinated compounds (Matheson and Tratnyek, 1994),



, where the Fe^{2+} obtained from Eq. 1.2 reduces the chlorinated compound (Eq. 1.3); and H_2 , from Fe^0 corrosion with water (Eq. 1.4), acts as the reducing agent of the chlorinated compound (Eq. 1.5). These reactions can contribute to longevity reduction (see section 3.1.1).

The reaction of chlorinated solvents in contact with highly pure Fe^0 in a closed, well-mixed and anaerobic batch system is described by a pseudo-first order rate model (Eq. 1.6) with respect to the aqueous phase concentration (Lin and Lo, 2005).

$$-\frac{dC_w}{dt} = K_{\text{obs}} \times C_w \quad (1.6)$$

Where C_w is the concentration of contaminants in the aqueous phase; t is reaction time (h), and K_{obs} is the observed rate constant (h^{-1}).

1.3.1.1. Longevity of the ZVI-PRBs

The rate of reduction reaction is influenced by ZVI surface characteristics, such as specific surface area, impurity, crystallinity and morphology (Lin and Lo, 2005). Moreover, it has also become evident that the performance of ZVI-PRBs progressively decreases with time, and that the lifetime of ZVI-PRBs is strongly affected, not only by the contaminant load but also, and perhaps even more importantly, by the local, site-specific hydrochemistry (Prommer *et al.*, 2008). With many ZVI-PRB working since more than 10-15 years ago, there is abundant field data from a longevity perspective. Henderson and Demond (2007) collected and analyzed data from 16 in situ PRB field applications with the objective to determine which parameters contribute to the reduction of the PRB longevity; being longevity defined as the length of time that a PRB continues treating groundwater to design levels (Henderson and Demond, 2007).

ZVI may be dissolved by the presence of oxygen in groundwater, which by following Eq. 1.3 produces a mixture of ferric oxide-hydroxide and ferric hydroxides that accumulate at the

upgradient interface of the PRB with the water (ITRC, 2011). ZVI is also dissolved due to its oxidation with water molecules, producing the consequent release of H_2 (Eq. 1.4) and leading to an increase in pH. The oxidized iron (Eq. 1.4) also results in the formation of ferrous oxides and hydroxides, as described by the reaction (Perebar, 2000):



Moreover, the reducing environment generated as a result of the excess of electrons that the ZVI brings to the system together with the indicated increase in pH, produces the precipitation of groundwater inorganic dissolved species such as calcium, carbonates, sulfates, and silicates (ITRC, 2011).

Overall, the compounds likely to precipitate in the ZVI include ferrous hydroxide, ($Fe(OH)_2$), magnetite (Fe_3O_4), maghemite (Fe_2O_3), iron carbonate hydroxide, calcite ($CaCO_3$), carbonate green rust $\{[Fe^{2+}_4Fe^{3+}_2(OH)_{12}]^{2+}[CO_3\ 2H_2O]^{2-}\}$, magnesite-siderite ($(Mg, Fe)CO_3$), mackinawite (FeS), goethite ($\alpha\text{-}FeOOH$), and pyrite (FeS_2) (ITRC, 2011). These precipitates can passivate the ZVI particles, and reduce their reactivity. If precipitates are deposited between particles of either the reactive or non-reactive media, they can produce cementation over time, with a loss of porosity and hydraulic conductivity.

However, although it is recognized that all PRBs show a gradual decrease in performance from the installation moment (ITRC, 2005), to date no PRB has failed due to loss of permeability and reactivity as a result of mineral precipitations (Henderson and Demond, 2007). Based on the past ZVI-PRB working experiences the most common potential reason of PRB failure are design flaws mainly caused by an improper hydraulic characterization of the site to treat (Henderson and Demond, 2007). Actually, among the literature described studies, it is rare to find a cause of PRB failure attributed to something different than a design flaw.

1.3.1.2. Microbial activity in the ZVI-PRB

H_2 generated due to corrosion of ZVI iron by groundwater (Eq. 1.4), is an excellent energy source for many anaerobic microbes, including methanogens, sulfate reducers, metal reducers, denitrifiers and halorespirers (Gu *et al.*, 2002). Therefore, accumulation of microbial biomass with a higher proportion of anaerobic metal reducers, sulfate reducers and denitrifiers has been found around PRBs (Gu *et al.*, 2002; ITRC, 2011). Within the iron zone, the greatest accumulation of biomass is at the upgradient aquifer/iron interface which has been attributed to the pH at this area that is not as high as in the downgradient aquifer/iron interface (ITRC, 2011). However Gu *et al.*, (2002) identified a varied microbial community (sulfate-reducing bacteria,

denitrifying bacteria, and methanogens) within the ZVI barrier at a pH of up to around 10 and found an increase of microbial population from upgradient to downgradient the barrier.

Microbial activity at the ZVI-PRB area can have positive and negative implications. Depending on the geochemistry of the specific groundwater, an enriched microbial activity can reduce the porosity and the hydraulic performance of the barrier caused by the accumulation of biomass, the production of gas bubbles and mineral precipitation (Scherer *et al.*, 2000; Gu *et al.*, 2002). Wilkin *et al.*, (2003) reported in their study a loss of porosity due to biomass and mineral precipitation that ranged only from 1-5% of the original porosity, although, biofouling has not been observed to be a concern at most ZVI-PRB sites (ITRC, 2011). Positively, microorganisms can contribute on the performance of the ZVI reactive barriers by enhancing the degradation of the chlorinated ethenes (Gu *et al.*, 2002). Indeed, Lampron (2001) showed through laboratory experiments that TCE half-life had drastically been reduced when ZVI was combined with a microbial culture. However, microbial activity can also have important implications on the chlorinated ethenes degradation pathway. Laboratory studies carried out by Lampron (2001) showed that TCE had its reduction pathways modified due to the presence of microbial cultures in combination with the ZVI; observing an accumulation of VC in quantities that wouldn't be expected in abiotic systems. Positively, Lampron (2001) concluded that aside from the negative implications of the microbial activity in the PRB, the presence of H₂ in the effluent groundwater can be used by microorganisms downstream of the ZVI-PRB in order to degrade residual chlorinated ethenes that still have not been eliminated through the barrier or that have bypassed it.

1.4. CHLORINATED COMPOUNDS DEGRADATION PATHWAYS

When a ZVI-PRB is applied at the field site to degrade chlorinated ethenes, natural biodegradation of these compounds can be occurring at the same time and, as observed in the previous section, can be even enhanced by the generated reductive environment. In order to assess the induced abiotic process installed at the field site, it is necessary to discriminate both kinds of degradation reactions in the environment. The knowledge of the degradation pathways involved in both processes is essential to distinguish the dechlorination of the chlorinated ethenes produced by both, 1) biodegradation due to the microbial population present in the field; and 2) the reaction with zero valent iron of a PRB.

1.4.1. Biotic degradation pathways

The metabolism of microbes is generally classified into aerobic and anaerobic. Aerobic transformation, also known as aerobic respiration, occurs in the presence of molecular oxygen that serves as electron acceptor (Suthersan, 1999); not all the chlorinated compounds are amenable to this type of degradation (Leeson, 2004). Anaerobic reactions occur only in the absence of molecular oxygen, and it may potentially degrade at least all the common chloroethenes and chloromethanes (Leeson, 2004) (Table 1.3).

Table 1.3. Processes that can degrade chloroethenes and chloromethanes. N: Not documented in the literature; Y: documented in the literature; P: Potential for reaction to occur but not well documented in the literature (CT, MC and CM are carbon tetrachloride, methylene chloride and chloromethane, respectively) (Leeson, 2004).

<i>Degradation process</i>	<i>Chloroethenes</i>				<i>Chloromethanes</i>			
	PCE	TCE	DCE	VC	CT	CF	MC	CM
Aerobic oxidation	N	N	P	Y	N	N	Y	P
Aerobic cometabolism	N	Y	Y	Y	N	Y	Y	Y
Anaerobic oxidation	N	N	P	Y	N	N	Y	P
Direct Anaerobic Reductive Dechlorination	Y	Y	Y	Y	Y	Y	Y	Y
Cometabolic anaerobic reduction	Y	Y	Y	Y	Y	Y	Y	P
Abiotic transformation	Y	Y	Y	Y	Y	Y	Y	Y

During biodegradation of an organic substrate, the aquifer is depleted of dissolved oxygen (DO). Once DO is consumed, anaerobic microorganisms use native electron acceptors in the following order (until available): nitrate, manganese and ferric iron hydroxides, sulfate, and finally carbon dioxide. Biotic anaerobic reductive dechlorination can be of two types:

- 1) Direct anaerobic reductive dechlorination, also referred to as halo-respiration or dehalorespiration, in which bacteria obtain energy and grow as chlorine atoms are replaced with hydrogen in an anaerobic environment. The chlorinated compound serves as electron acceptor, while hydrogen is the electron donor. Hydrogen in this reaction is generally supplied by fermentation of organic substrates (Suthersan, 1999; Leeson, 2004).
- 2) Cometabolic anaerobic reductive dechlorination, in which a chlorinated compound (considered a secondary substrate) is reduced fortuitously by a non-specific enzyme generated by microorganism growing at the expense of another substrate (the primary substrate) in an anaerobic environment (Suthersan, 1999; Leeson, 2004). This reaction does not produce any energy or growth benefit to the microorganisms that mediate the reaction (U.S. EPA, 2000). Only sufficient primary substrate is required to support growth of the microorganisms and sustain the cometabolic process.

Mainly, biotic anaerobic reductive dechlorination occurs by sequential removal of chloride ions. The most thoroughly studied anaerobic dechlorination pathway is the transformation of PCE and TCE to *cis*-DCE and VC, and finally to ethene and ethane (Leeson, 2004) (Fig.1.3). Among

the three possible DCE isomers formed, *cis*-1,2-DCE (generally called *cis*-DCE) predominates over *trans*-1,2-DCE, and 1,1-DCE is the least significant (Suthersan, 1999).

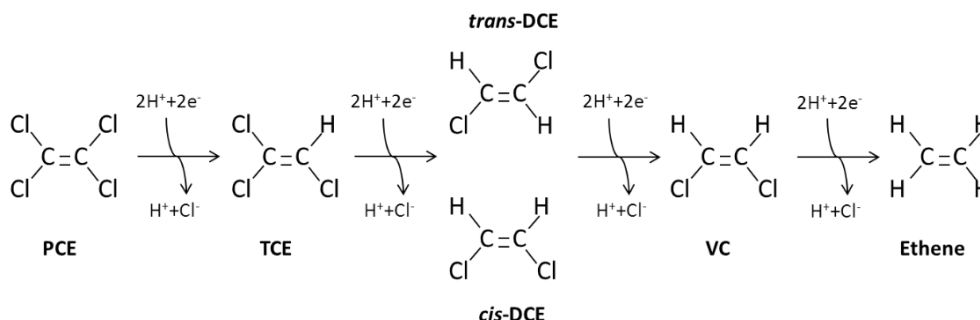


Figure 1.3. Sequential anaerobic reductive dechlorination of PCE to ethene (Leeson, 2004).

Highly chlorinated compounds (such as PCE and TCE) are more susceptible to reduction than the lesser chlorinated ones (such as *cis*-DCE and VC) due to their higher oxidation state; giving the first ones much greater anaerobic transformation rates (Suthersan, 1999; Leeson, 2004). Therefore, *cis*-DCE and VC, which are considered more toxic than their parent compounds, tend to accumulate and persist longer in the environment; making necessary that this transformation sequence is completed to innocuous end products.

The groups of bacteria responsible of anaerobic reductive dechlorination of chlorinated compounds are methanogens, sulfate-reducing bacteria and dechlorinating bacteria. In the case of PCE and TCE, microorganisms capable of their reduction to *cis*-DCE have been found to be ubiquitous in the environment, however to date only one bacterial pure culture, *Dehalococcoides ethenogenes*, has been found to completely dehalogenate PCE to ethane by itself (Hunkeler *et al.*, 2011). But in nature, mixed cultures typically carry out the complete anaerobic dechlorination. Some dechlorinators sequentially degrade PCE to TCE, others to *cis*-DCE and some others to VC (Leeson, 2004). Complete dechlorination of PCE to ethene with a mixed culture that did not contain *Dehalococcoides* sp. was demonstrated by Flynn *et al.*, (2000). Furthermore other degradation pathways exist for the less chlorinated compounds such as VC, *cis*-DCE and even TCE, through both aerobic and anaerobic environments, that achieve their total degradation (Table 1.3) (Leeson, 2004).

1.4.2. Abiotic zero valent iron degradation pathways

Complete reductive dechlorination of chlorinated ethenes by Fe^0 consists of multi-steps hydrogenolysis, reductive- β -elimination and hydrogenation reaction pathways through which chlorinated ethenes, such as PCE and TCE, are sequentially reduced to the lesser chlorinated ethenes *cis*-DCE, VC, dichloroacetylene, chloroacetylene, acetylene, and the

nontoxic final products ethene and ethane (Fig. 1.4) (Arnold and Roberts, 2000). Depending on the predominant pathway, daughter products will be produced in more or less quantity, becoming the type of reaction a crucial factor to obtain a higher or lower quantity of the toxic daughter products (*cis*-DCE and VC).

Hydrogenolysis is the replacement of a chlorine atom by hydrogen under anaerobic conditions. These reactions involve the typical reductive dechlorination sequence $\text{PCE} \rightarrow \text{TCE} \rightarrow \text{cis-DCE} \rightarrow \text{VC} \rightarrow \text{Ethene}$, which also corresponds to the microbial anaerobic reductive dechlorination (Fig. 1.4).

Reductive- β -elimination involves the removal of either two chlorine atoms or a chlorine and a hydrogen atom with simultaneous formation of a triple bond (Farrel *et al.*, 2000; Roberts *et al.*, 1996). It produces dichloroacetylene from PCE, chloroacetylene from TCE and acetylene from *cis*-DCE (Fig. 1.4). So it is an alternative pathway to the presence of the toxic VC intermediate. Degradations from dichloroacetylene to chloroacetylene and from chloroacetylene to acetylene are produced through hydrogenolysis reactions.

Hydrogenation is the reduction of triple bonds to double bonds by H_2 (Arnold and Roberts, 1998). It intervenes in the formation of *cis*-DCE and ethene from dichloroacetylene and acetylene, respectively (Fig 1.4).

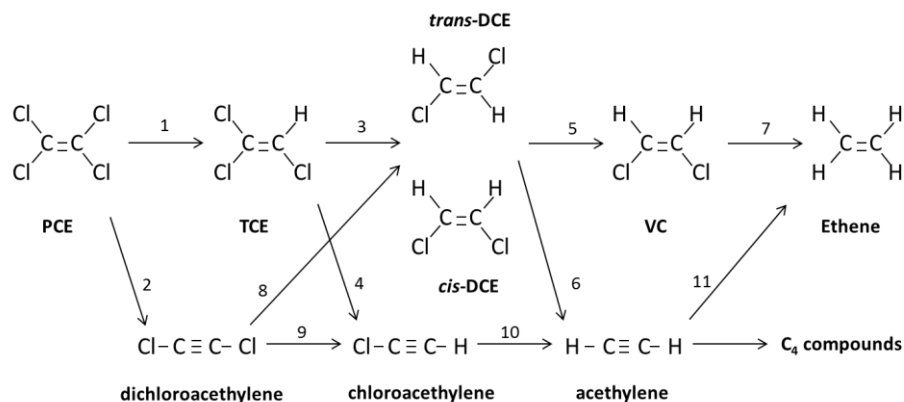


Fig. 1.4. Hypothesized reaction pathways for the chlorinated ethenes and other intermediates during reduction by Fe^0 . Reactions 1, 3, 5, 7, 9 and 10 correspond to hydrogenolysis reactions, while reactions 2, 4 and 6 are reductive β -elimination reactions and reactions 8 and 11 are hydrogenation reactions (adapted from Arnold and Roberts, 2000).

Arnold and Roberts (1998, 2000) proved through kinetic experiments that the dominant pathway involved in the reductive dechlorination of chlorinated ethenes by zero-valent iron was the reductive- β -elimination, accounting for 87% of PCE, 97% of TCE and 94% of *cis*-DCE reaction. Arnold and Roberts (1998, 2000) could also show that these reductive- β -elimination reactions are thermodynamically more favorable, showing that the transformation occurred via reductive- β -elimination increased as the two-electron reduction potential for these specific

reactions also increased. In Arnold and Roberts (2000) dichloro and chloroacetylene were degraded into lesser chlorinated daughter products through hydrogenolysis reaction in a 76 and 100%, respectively.

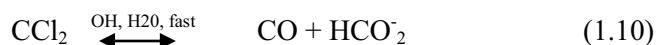
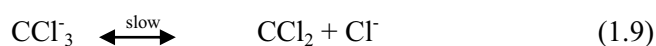
1.5. HYDROLYSIS AS A PROPOSED CHLOROFORM REMEDIATION TECHNIQUE

Chlorinated ethenes are effectively degraded by *in-situ* biodegradation and ZVI-PRB treatment, as explained in Section 1.4. In contrast, to our knowledge, *in situ* applications of CF biodegradation have not been reported to date. Although CF can be biodegraded through aerobic and anaerobic co-metabolic processes (Cappelletti *et al.*, 2012), some factors may affect the CF co-metabolism such as, the competition with the growth substrates, the need of a reducing agent to keep the activity of the enzymes, and the toxicity of the products formed, among others. However, CF dechlorination was recently linked to the growth of bacterial strains belonging to Dehalobacter genus (Grostern *et al.*, 2010; Lee *et al.*, 2012) through CF dehalorespiration; and bioremediation of CF by biostimulation and/or bioaugmentation strategies has been suggested (Shan *et al.*, 2010). Regarding CF abiotic degradation with ZVI, while CF is degradable by ZVI, its toxic daughter product, DCM, is not degradable by this reactive material (ITRC, 2005). Furthermore, even though many chlorinated hydrocarbons removal can be achieved by *in situ* chemical oxidation (ISCO), CF is poorly reactive with common oxidants, such as permanganate, iron-activated persulfate, ozone, hydrogen peroxide or Fenton's Reagent (Huling and Pivetz, 2006). Therefore novel remediation strategies should be developed in order to efficiently degrade this recalcitrant compound in the environment.

In this thesis the remediation of chloroform by alkaline hydrolysis induced by concrete-based recycled construction wastes is proposed. Alkaline hydrolysis has been already proposed as a remediation technology for other types of contaminants, such as explosives (Su and Christodoulatos, 1996; Emmrich, 2001; Hwang *et al.*, 2005; Karakaya *et al.*, 2005; Hwang *et al.*, 2006) organophosphorous insecticides (NorthPestClean, 2013), tert-butyl formate (Church *et al.*, 1999), and 1,2,3-trichloropropane (Sarathy, *et al.*, 2010). To our knowledge, until now, there is only one pilot-scale study where *in-situ* alkaline hydrolysis has been implemented at a site contaminated with pesticides (Bondgaard *et al.*, 2013). Nevertheless, with respect to chlorinated methanes alkaline hydrolysis has received little attention so far. Generally, hydrolysis is a reaction in which an organic molecule reacts with a molecule of water (or hydroxide ion) and one part of the organic molecule (i.e., the leaving group) is separated from the molecule (Schwarzenbach *et al.*, 2003). In the case of chlorinated hydrocarbons, the leaving

group is a halide ion, and hydrolysis of these compounds includes both elimination reaction and nucleophilic substitution mechanisms. The competition between elimination and nucleophilic substitution reactions depends on the substrate structure, the nature of the base and stereoelectronic factors. Strong nucleophiles favor elimination over nucleophilic substitution, therefore, alkaline hydrolysis reactions (i.e., reaction with OH^-) of polychlorinated aliphatic compounds are expected to be dominated by elimination reactions, whereas neutral hydrolysis (i.e., reaction with H_2O) is expected to occur mainly by nucleophilic substitution reactions (Bruckner, 2002). The pH at which the changeover from the dominance of neutral reactions to the dominance of alkaline reactions occurs, I_{NB} , is different for each compound, being 6.5 in the case of CF (Schwarzenbach *et al.*, 2003).

Hydrolysis of chlorinated compounds, including CF, has been well demonstrated in the literature (Hine, 1950; Mabey and Mill, 1978; Jeffers *et al.*, 1989; Vogel, 1994; Miyamoto and Urano, 1996). However, within the range of normal groundwater temperatures and pH values, reaction rates are often quite slow. For this reason, available reported rates of hydrolysis reactions involving chlorinated solvents are typically obtained from the extrapolation of experiments performed at higher temperatures. It is known that neutral hydrolysis of CF is very slow, with reported neutral first-order rate constants (K_{N}) at 25 °C and pH 7 ranging from 6.2×10^{-8} (extrapolated from Fells and Moelwyn-Hughes, 1959) to $2.8 \times 10^{-7} \text{ day}^{-1}$ (Jeffers *et al.*, 1989), which represents half-lives of approximately 30700 and 6900 years, respectively. Since OH^- cannot successfully compete with water in substitution reactions with chlorinated hydrocarbons at typical ambient conditions, the neutral hydrolysis reaction may be described by a first-order law, regardless of whether the reaction occurs by an SN_1 or SN_2 substitution mechanism or a mixture of both. Therefore, neutral hydrolysis of CF is first-order with respect to the concentration of CF and is independent of pH (Jeffers *et al.*, 1989). Regarding the alkaline hydrolysis of CF in an aqueous solution, experimental and theoretical approaches suggested that it proceeds through an E1_{CB} mechanism and that the SN_2 mechanism is unlikely to play a major role (Hine, 1950; Valiev *et al.*, 2007). The E1_{CB} mechanism is a type of elimination reaction, which, in general terms, consists of a rapid first step where a C-H bond is broken by deprotonation with a base, followed by a slow second step where the leaving group is expelled. In the case of CF, the E1_{CB} mechanism features the rapid, reversible, base-catalyzed deprotonation of the molecule with the formation of trichloromethyl carbanion (CCl_3^-), followed by the rate-determining unimolecular loss of a chloride ion to produce the reactive intermediate carbon dichloride, which is then rapidly transformed into the final products, carbon monoxide and formate ion.



The rate of the reaction has been suggested to be first order with respect to both OH^- and CF concentrations (Hine, 1950; Fells and Moelwyn-Hughes, 1959). Following this assumption and using the neutral and alkaline rate constants (k_N and k_B , respectively) of the hydrolysis of CF at 25 °C reported by Jeffers *et al.*, (1989) ($k_N = 2.8 \times 10^{-7} \text{ d}^{-1}$; $k_B = 7.5 \text{ M}^{-1} \text{ d}^{-1}$) and extrapolated from Fells and Moelwyn-Hughes (1959) ($k_N = 6.2 \times 10^{-8} \text{ d}^{-1}$; $k_B = 5.7 \text{ M}^{-1} \text{ d}^{-1}$), pseudo-first-order rate constant ($k'_{\text{obs}} = k_N + k_B C_{\text{OH}^-}$) values of 0.075 and 0.057 day^{-1} , respectively, can be calculated at constant pH 12 (Annex C; Table 1). This yields half-lives of approximately 9-12 days, implying an attractive potential use of CF remediation strategies based on alkaline hydrolysis. All the literature cited above determined the kinetics of CF hydrolysis in homogeneous solutions. In contrast, the effects of heterogeneity on the hydrolysis rates have received little attention so far (Amonette *et al.*, 2010). Amonette *et al.*, (2010 and 2012) studied the effect of various mineral phases (montmorillonite, kaolinite, albite, muscovite and smectite) on the hydrolysis rates of CF at 50 and 16°C, respectively. The authors observed a significant effect of the type of solid on the CF hydrolysis rates at both temperatures, which was attributed to the different pH values maintained by the solid phases in contact with the aqueous phase.

In this thesis, concrete is the agent proposed to maintain alkaline conditions and thus to induce alkaline hydrolysis of CF . Concrete is an artificial conglomerate stone made essentially of Portland cement, aggregates, water and supplementary cementitious materials. Portland cement is made by heating finely ground limestone and finely divided clay at high temperatures. Concrete has high pH buffering capacity due to the lime content of the cement. For these reasons, recycled concrete has been already used as a reactive material for neutralizing acidic groundwater (Golab *et al.*, 2006; Indraratna *et al.*, 2010; Regmi *et al.*, 2011). Moreover, cement-based stabilization/solidification (s/s) treatments have been proven to immobilize chlorinated solvents from contaminated soils and groundwater (Hawng and Batchelor, 2000; Hawng and Batchelor 2002; Hawng *et al.*, 2005). These s/s treatments have been used in combination with abiotic reductive dechlorination treatments with additions of Fe(II) , in which ferrous iron and cement are used as an electron donor and a catalyst, respectively. Therefore, it was considered that the feasibility of the use of concrete to induce alkaline hydrolysis and/or sorption of CF at contaminated sites should be evaluated.

1.6. COMPOUND SPECIFIC ISOTOPE ANALYSES (CSIA)

CSIA is an isotopic technique extensively used to monitor degradation processes occurring at the field site, that has greatly facilitated assessment of sources and transformation processes of organic pollutants. Stable isotope techniques are based on the presence of at least two stable isotopes in nature of elements such as carbon, hydrogen, chlorine, nitrogen, oxygen, and sulfur, which are present in different natural abundances (Table 1.4).

Table 1.4. Selected elements and relative abundance and mass differences of the international standards (Meckenstock *et al.*, 2004)

Element	Relative isotope abundance	Relative mass difference	Standard
H/D	99.9844/0.0156	2.00	V-SMOW
$^{12}\text{C}/^{13}\text{C}$	98.89/1.11	1.08	V-PDB
$^{14}\text{N}/^{15}\text{N}$	99.64/0.36	1.07	Air
$^{16}\text{O}/^{18}\text{O}$	99.76/0.02	1.13	V-SMOW
$^{32}\text{S}/^{34}\text{S}$	94.02/4.21	1.06	V-CTD
$^{35}\text{Cl}/^{37}\text{Cl}$	75.53/24.47	1.06	24.47

Compound-specific isotope analysis (CSIA) is capable to separate organic analytes from complex mixtures and to determine the individual stable isotope ratio of the target element at natural isotopic abundances (Elsner *et al.*, 2012). This development has been accomplished by direct coupling of a gas chromatograph (GC) that separates the different compounds, to an isotope ratio mass spectrometer (IRMS) through a combustion interface that converts carbon atoms to CO_2 (GC-C-IRMS) (Fig. 1.5). Details on the principles and technical aspects of this technique can be found, among others, in Hunkeler *et al.*, (2008) and in Palau *et al.*, (2007).

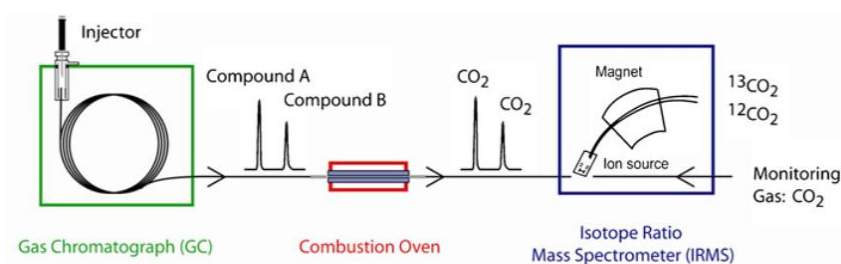


Figure 1.5. Instrumentation for carbon isotope analysis (GC-C-IRMS) by compound specific isotope analysis.

As a historical overview, stable isotope ratio measurements were first applied in the late 1930s when Nier and Gulbransen observed that carbon isotope composition varies in nature (Elsner *et*

al., 2012). Since that first observation, natural changes were readily attributed to isotope fractionation processes and this approach started to be used to trace complex geochemical and biological processes, as well as in climate change studies (Elsner *et al.*, 2012). Subsequent developments in the technique were introduced and in 1950 the delta notation was presented in order to standardize reported experimental data (Elsner *et al.*, 2012):

$$\delta^hE_{\text{comp}} = \frac{R(^hE/^lE)_{\text{comp}} - R(^hE/^lE)_{\text{std}}}{R(^hE/^lE)_{\text{std}}} = \frac{R(^hE/^lE)_{\text{comp}}}{R(^hE/^lE)_{\text{std}}} - 1 \quad (1.11)$$

δ^hE_{comp} represents the relative difference between the isotope ratio of a sample $R(^hE/^lE)_{\text{comp}}$ (i.e., $R(^{13}\text{C}/^{12}\text{C})$) and of an internationally accepted reference standard $R(^hE/^lE)_{\text{std}}$. Positive and negative δ values express enrichment and depletion of the heavier isotope in a sample relative to the reference material. The international standards for each element are indicated in Table 1.4.

It was in the late 1990s when the first studies in CSIA to assess organic contaminant sources and their transformation reactions in the environment were published (Hunkeler *et al.*, 1999; Meckenstock *et al.*, 1999; Sherwood Lollar *et al.*, 1999). Since those initial studies, this field has rapidly grown resulting in numerous studies (Elsner *et al.*, 2012 and references therein). Until recently, carbon isotopic composition (^{13}C) was the most commonly applied in organic compounds contamination studies. Recent developments in chlorine isotope analysis allowed the determination of Cl isotope fractionation. The continuous flow compound specific Cl isotope analysis method (GC-CF-IRMS) developed by Shouakar-Stash *et al.*, (2006) does not include the combustion step and the intact chlorinated ethene molecules are directly transferred to the IRMS, ionized and fragmented for their isotopic ratio measurement (Fig. 1.6A). New developments in hydrogen (^2H) isotopes analyses allowed starting using this isotope in chlorinated compounds studies through the use of a chromium reduction tube in a pyrolysis system coupled between the GC and the IRMS (GC-R-IRMS) (Shouakar-Stash and Drimmie, 2013) (Fig. 1.6B).

One of the applications of CSIA is to identify contaminant sources in the environment in cases when different sources present consistently different isotopic composition, and when this isotopic composition remains stable over spatial and time scale. Environmental forensics work has been extensively performed for hydrocarbons such as polycyclic aromatic hydrocarbons (PAHs), which depending on their formation process showed depleted or enriched ^{13}C values (Mazeas *et al.*, 2002; Guillon *et al.*, 2013). For chlorinated organic compounds, few studies of field sites with contaminated groundwater are published (Hunkeler *et al.*, 2004; Blessing *et al.*, 2009).

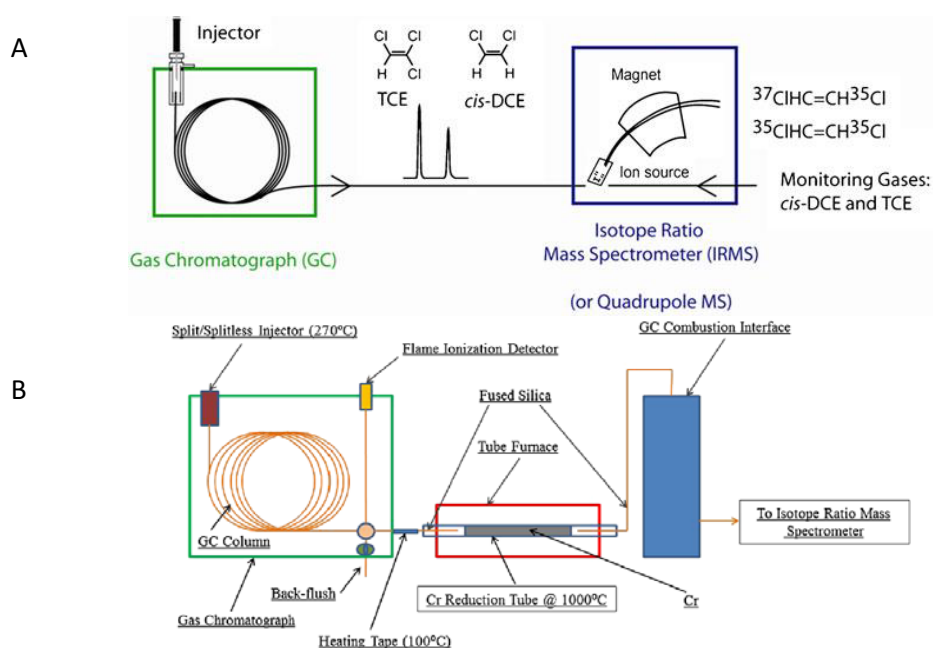


Figure 1.6. A) GC-CF-IRMS equipment for chlorine isotopes analysis; and B) GC-R-IRMS for hydrogen isotopes analyses (Elsner *et al.*, 2012, Shouakar and Drimmie, 2013).

Apart from source discrimination, CSIA can be applied to monitor abiotic or biotic degradation reactions and to quantify their extent. This use of CSIA is based on the evidence that during degradation reactions significant kinetic isotope effects (KIEs) occur. KIEs are governed by the different rates of reaction of the molecules containing heavier or lighter isotopes, which lead to an unequal isotopic distribution between substrates and reaction products. The different rates are due to the strength of the chemical bonds containing the heavier isotope, which have higher activation energy. Therefore, in a chemical reaction, the molecules with light isotopes will react faster because of the lower energy necessary to break them (Meckenstock *et al.*, 2004), leaving the residual substrate with a higher proportion of heavy isotopes. This increases the $\delta^{\text{H}}\text{E}$ according to Equation 1.11 (Fig. 1.7), while the new formed product has a lower $\delta^{\text{H}}\text{E}$ than the original substrate (Fig. 1.7). In a reductive dechlorination sequence of chlorinated ethenes by hydrogenolysis reactions, C atoms are transferred to the following compound, thus, products achieve the initial $\delta^{13}\text{C}$ of the precursor once it has been completely degraded (Fig. 1.7).

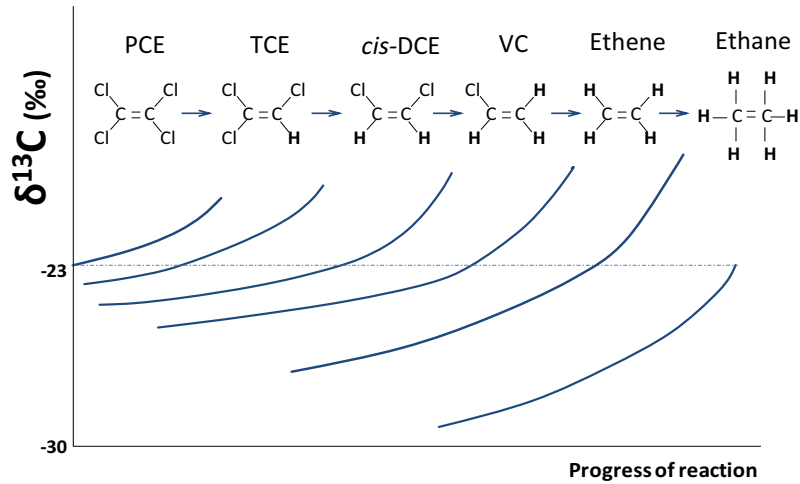


Figure 1.7. Evolution of the isotopic composition of an original PCE molecule and its daughter products along their transformation reactions.

The variation in the δ^{hE} is known as isotopic fractionation, and gives evidence of the occurrence of a transformation reaction. Other processes that decrease concentration, i.e. dispersion, dilution, diffusion, volatilization, but do not involve transformation reactions, do not produce significant isotope fractionation. Thus the isotopic approach, in contrast to concentration data alone, can discriminate transformation from non-transformation processes. In order to use the isotopic approach in field applications, it is necessary to determine the isotopic fractionation expressed as “ ϵ ” of a particular degradation mechanism, through the Rayleigh equation (Mariotti *et al.*, 1981)

$$\frac{R}{R_0} = \frac{(1000 + \delta^{\text{hE}})}{(1000 + \delta^{\text{hE}}_0)} = f^{(\epsilon_E)} \quad (1.12)$$

where R_0 and R are E (specific element) isotope ratios ($^{\text{hE}}/^{\text{lE}}$) at the beginning and at a given time (t) respectively, δ^{hE}_0 and δ^{hE} are the same values in delta notation and f is the fraction of substrate remaining at time “t”. According to the Rayleigh equation (Eq. 1.12) the ϵ_E reflects the extent of isotope fractionation per increment of transformation of the element. Once the isotope fractionation (ϵ_E) of an element is obtained in laboratory experiments for a specific transformation reaction of a compound, and with the measured field δ^{hE} and δ^{hE}_0 data, the real extent of the specific transformation reaction at field scale can be determined according to Equation 1.13.

$$D[\%] = \left[1 - \left(\frac{\delta^h E_t + 1000}{\delta^h E_0 + 1000} \right)^{\left(\frac{1000}{\epsilon E} \right)} \right] \cdot 100, \quad (1.13)$$

where, D represents the percentage of degraded fraction. Many studies reported the chlorinated ethenes carbon isotopic fractionation value (ϵ_C) from biodegradation experiments with mixed cultures (ranging from -2.6 to -7.1 ‰ for PCE, from -2.5 to -15.3 ‰ for TCE and from -14.1 to -25.5 ‰ for *cis*-DCE) (Sherwood Lollar *et al.*, 1999; Bloom *et al.*, 2000; Slater *et al.*, 2001; Liang *et al.*, 2007; Schmidt *et al.*, 2010; Fletcher *et al.*, 2011). Previous studies of reductive dechlorination with ZVI of chlorinated ethenes confirmed enrichment of ^{13}C during the progression of the reaction (Dayan *et al.*, 1999; Slater *et al.*, 2002, Prommer *et al.*, 2008). These studies reported a C isotopic fractionation value (ϵ_C) ranging from -5.7‰ to -25.3‰ for PCE; -8.6‰ to -27‰ for TCE; -6.9‰ to -23.1‰ for *cis*-DCE; and -6.9‰ to -20.1‰ for VC (Dayan *et al.*, 1999; Slater *et al.*, 2002; Vanstone *et al.*, 2004; Elsner *et al.*, 2008). Therefore, stable carbon isotopes were already suggested as a valuable tool to evaluate both, biodegradation and abiotic ZVI degradation, of chlorinated ethenes in field applications (Prommer *et al.*, 2008). Regarding CF alkaline hydrolysis induced by concrete wastes, no previous studies were available in the literature; therefore the carbon isotope fractionation should be determined at laboratory scale in order to evaluate its usefulness as a tool to quantify the induced alkaline hydrolysis of CF.

The specific isotope fractionation pattern of the byproducts can be expressed by determining the product-specific isotope fractionation ($\epsilon_{\text{substrate} \rightarrow \text{product}}$). According to Elsner *et al.*, (2008), it can be calculated through the following abbreviated equation:

$$\epsilon_{\text{substrate} \rightarrow \text{product}} = \delta^{13}\text{C}_{0,\text{product}} - \delta^{13}\text{C}_{0,\text{substrate}} = D(\delta^{13}\text{C}) + \epsilon_C \quad (1.14),$$

where $D(\delta^{13}\text{C})$ is the deviation that a product can experience from the weighted average of all products, expressed as $D(\delta^{13}\text{C}) = \delta^{13}\text{C}_{\text{product}} - \delta^{13}\text{C}_{\text{product, average}}$. Using Sigma Plot 12, the $D(\delta^{13}\text{C})$ can be obtained from iteration and graphical representation of the following (Elsner *et al.*, 2008):

$$(1000 + \delta^{13}\text{C}_{\text{product}}) / (1000 + \delta^{13}\text{C}_{0,\text{substrate}}) = (1 + (D(\delta^{13}\text{C})/1000)) \times ((1 - f^{\epsilon_C/(1000+1)}) / (1 - f)) \quad (1.15)$$

Equations 1.14 and 1.15 allow the determination of product-specific isotope fractionation even without knowledge of absolute reaction rates, product distribution, or molar balances, since they rely solely on isotope measurements of the substrate and a given product (Elsner *et al.*, 2008).

A challenge in the CSIA approach is the discrimination between several degradation processes that can occur at the field site. For example, the presence of a contaminant downgradient of a permeable reactive barrier (PRB) may result: 1) from an incomplete degradation within the PRB; 2) from bypassing under or around the PRB; 3) from contaminants already present before the installation of the PRB that could be experiencing biodegradation. Thus, unless the isotope fractionation values (ϵ) are very different it is difficult to identify the predominant process. In the case of ϵ_C for biodegradation and ZVI of chlorinated ethenes values seem to overlap. To give further insight distinguishing reaction pathways the use of the dual isotope approach has been proposed. The rationale of this approach is that the isotopic fractionation of the two elements implicated in the breakage of a bond can be different depending on the degradation process, due to, i.e., possible different chemical reaction mechanisms or different rate-limiting steps. In chlorinated ethenes, the combination of carbon isotope data with other elements (Cl or H) bears potential to provide additional insight into transformation mechanisms. In particular, dual isotope plots of the reacting contaminant have the potential to distinguish different transformation pathways (Elsner *et al.*, 2005; Abe *et al.*, 2009; Hunkeler *et al.*, 2011). Abe *et al.*, (2009) successfully used the dual isotope approach (^{13}C - ^{37}Cl) to distinguish between biotic aerobic oxidation and biotic reductive dechlorination reactions for *cis*-DCE and VC. The slopes ($\epsilon_C/\epsilon_{\text{Cl}}$) obtained for the reductive dechlorination biodegradation model with a mixed culture enriched with *Dehalococcoides ethenogenes* for *cis*-DCE and VC were 12.5 and 14, respectively. Hunkeler *et al.*, (2011), discriminated a slope of 2 ($\epsilon_C/\epsilon_{\text{Cl}}$) for *cis*-DCE degradation in the field site where *Dehalococcoides* sp. was detected.

Regarding the use of hydrogen isotope data together with carbon or chlorine isotopes, to the author's knowledge, no data had been reported before this thesis. Only hydrogen isotope data of commercial TCE and very few laboratory experiments were published up to date (Ertl *et al.*, 1998; Shouakar-Stash *et al.*, 2003). The $\delta^2\text{H}$ of manufactured TCE ranged from +466.9 to +681.9 ‰. This highly enrichment in ^2H of the manufactured TCE has been attributed to its production process (Ertl *et al.*, 1998; Shouakar-Stash *et al.*, 2003) where chlorination steps take place with the hydrogen substitution by chlorine. As the H-C bond with ^2H is stronger than the ^1H bond, TCE is enriched in the heavy isotope. In contrast to these very enriched in ^2H results, a very depleted in ^2H TCE ($\delta^2\text{H}$ of around -350 ‰) was obtained from PCE dechlorination in column experiments with ZVI. Evidences of fractionation of the surrounding water were also observed in this study (Shouakar-Stash *et al.*, 2003) suggesting a fractionation process during water- H_2 equilibrium. This finding has strong implications for distinguishing TCE coming from

PCE dechlorination from manufactured TCE. The recent analytical improvements (during the progression of the Thesis) of the CSIA technique for the analyses of $\delta^2\text{H}$ chlorinated ethenes (Shouakar-Stash and Drimmie, 2013) (Fig. 1.6B) have allowed the analysis of groundwater samples polluted with dissolved chlorinated compounds (not only the measurement of pure phases) and with accurate results ($\pm 10\%$). This permits to apply the dual isotope ^{13}C - ^2H or ^{37}Cl - ^2H approach and the use of hydrogen isotopes to distinguish among manufactured and non-manufactured TCE. During the progress of this thesis, Kuder *et al.*, (2013) published the first multi isotope results (C, Cl and H) from laboratory experiments, as well as, the first negative $\delta^2\text{H}$ values (up to -184%) of manufactured TCE. However, the depletion in ^2H during TCE formation in the environment might be so high that $\delta^2\text{H}$ may still be a potential way to discriminate the origin of TCE and, consequently, of the compounds produced during its degradation reaction sequence.

An alternative approach to distinguish biotic and abiotic transformations of chlorinated ethenes does not involve Cl isotope ratios, but relies instead on C isotope analysis of daughter compounds (Elsner *et al.*, 2008; Elsner *et al.*, 2010). The sequential fractionation sketched in Figure 1.7 for chlorinated ethenes hydrogenolysis reactions typical for biodegradation, differs in the case of the abiotic reactions where β -elimination and hydrogenation reactions are also involved as suggested by Elsner *et al.*, (2008) (Fig. 1.8).

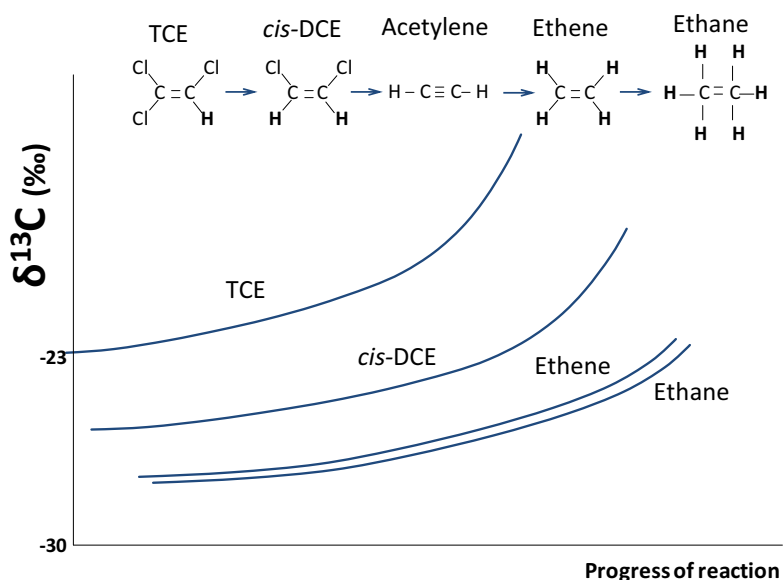


Figure 1.8. Evolution of the isotopic composition of an TCE over the degradation products in abiotic degradation reactions. Adapted from Elsner *et al.*, (2008).

Parallel isotope fractionation trends were observed between the daughter products formed during abiotic degradation by ZVI (Fig. 1.8). Therefore, if these products show different isotope trends depending on whether they come from either abiotic or biotic degradation, both pathways might be identified. Elsner *et al.*, (2008) showed that hydrogenolysis and β -dichloroelimination daughter products (i.e. *cis*-DCE and ethene, respectively) during transformation by nanoparticulate ZVI differed consistently by 10‰ in C isotope values. A follow-up field study used these results, to attempt for the first time, to discriminate between abiotic and biotic transformations in the field (Elsner *et al.*, 2010).

Therefore, two lines of evidence have recently been brought forward to discriminate between abiotic and biotic pathways: (i) evidence from dual isotope plots, (ii) evidence from product isotope ratios.

Finally, the kinetic isotope effect (KIE) might also distinguish different reaction mechanisms due to its specificity on the broken bond. Isotope fractionation of a compound reflects the average behavior of isotopes in the molecules, without reflecting the isotope specific effect in the reacting bond. In contrast, the parameter kinetic isotope effect (KIE) corresponds to the reaction rate at the specific site of the reaction due to the presence of the heavy isotope, which is represented by:

$$\text{KIE}_E = \frac{{}^l k}{{}^h k} \quad (1.16)$$

Where ${}^l k$ and ${}^h k$ are the rate constants for molecules with a light and heavy isotope, respectively, at the specific site of reaction (Wolfsberg *et al.*, 2010). Isotope fractionation values and kinetic isotope effects or apparent kinetic isotope effects (AKIE), are related by a mathematical approach (Elsner *et al.*, 2005), by taking into account that the heavy isotope may be present at positions that do not participate in the reaction and that multiple reacting positions may occur in a molecule but only one of them is the one that reacts (Elsner *et al.*, 2005). The following equation can be obtained:

$$(\text{A})\text{KIE}_E = \frac{1}{\left(\frac{\varepsilon_{\text{E,compound average}}}{1000}\right) + 1} \quad (1.17)$$

Where n is the number of atoms of element E in a molecule (Elsner *et al.*, 2005). Equation 1.17 shows that an increase in the number of atoms of the target element in a molecule decreases the observable isotope fractionation, thus, the isotope fractionation perceptible in a molecule is directly related to its size, in the case of C and H in organic molecules (or to the presence of the atom in the molecule). The KIE parameter is specific for determined bonds breakages (i.e. C-Cl,

C-H), thus obtaining a KIE value might give more evidence to identify degradation reactions (Elsner *et al.*, 2005).

1.7. STUDY SITES

1.7.1. ZVI-PRB study site

The study site is located at the industrial area of Granollers, 20 Km NW from Barcelona, Catalonia. An automotive industry that used PCE and TCE as degreasers operated in the area from 1965 to 1989. The site is bounded on its west side by the *Can Ninou* creek, which continues to the S-SW (Annex B; Fig. 1). The lithology of the site, based on 6 borehole wells interpretation, is mainly composed by an alternation of sand and silt Miocene sediments in a clayey matrix that extends from 4 m to a minimum of 14 m depth (Annex B; Fig. 1). In general, the presence of sand increases in depth. Above these materials, there are 4 m of quaternary glaciis formed by the eroded Miocene materials and mainly composed by poorly structured clays and silts. The Miocene sediments are positioned unconformably onto the Paleozoic base, which in this sector consists of Late-Hercynian granitoids. The water table of the aquifer is located at an average depth of 5.4 ± 2.1 m below ground surface (BGS). The deepest water table (around 8 m BGS) was measured at the base and at the top of the studied valley area (length of the studied area 900 m). While at around 300 m from the top of this area the water table was located closer to the surface (around 3 m BGS). The average water table variation due to seasonal changes was of -0.5 ± 0.9 m. The deepest studied well reached 20 m depth. The flow velocity was 0.16 m/day at the shallow quaternary clayey depths; and 0.84 m/day at the more sandy Miocene depths. Groundwater contamination with PCE and TCE was produced due to the discharge of industrial waters into a seepage pit located at the south of the plant (close to MW17 well, see Annex B; Fig. 1); this point is considered the contamination source area, where historical data from 2004 revealed concentrations of *cis*-DCE up to 160 mg/L and of its precursors PCE and TCE of 25 and 180 mg/L, respectively. Chlorinated ethenes could have infiltrated from the seepage pit of the industrial plant and lixiviated until the saturated zone where they probably reached the deeper aquifer depths crossing the clayey matrix, accumulating mainly in the more sandy units [between 8 and 20 m at least as detected in the field by a portable gas photoionization detector (PID, MiniRAE 3000, RAE Systems, Kastrup, Denmark)] and started moving following the NE to W-SW groundwater flow direction. During the period 2005-2010, a total of 12 wells were installed along the east bank of the creek, from the source area to 900 m downstream of the creek. A dual remediation strategy was performed at the studied site: the

removal of the contaminated soil from the source area in 2009 and the installation of a ZVI-PRB to treat the groundwater contaminant plume in 2010. The PRB was built approximately 320 m downstream the contaminated source, transverse to the creek, from NW to SE position (Annex B; Fig. 1). The top of the PRB was placed 4-5 m below ground surface and its size is 20 m long, 5 m high and 60 cm thick, with a 3% (v/v) of granular cast ZVI inside a sand matrix. Five multilevel wells were installed immediately upgradient and downgradient the barrier in March 2012.

1.7.2. CF alkaline hydrolysis study site

The site is located 50 km northwest from Barcelona (NE, Spain). The subsurface geological characterization is based on the lithological core interpretation of ten boreholes drilled in 2005. The aquifer is an unconfined fractured bedrock (approximately from 2.2 to 6.0 m BGS) composed of blue-grey limestone alternating with blue-grey marl and sandstone beds, which forms a low-permeability matrix with conductive fractures and fissures. Coarse sandstone and microconglomerate beds are also present in this unit, reaching a thickness of 4.3 m around the disposal lagoon area. The bedrock is overlaid, from base to top, with brown sandstone and altered yellow marl layers (approximately from 0.3 to 4.2 m BGS). Quaternary deposits of sandy-silt (only found in some boreholes with a thickness up to 3.4 m at the SE of the studied area), and soil and/or anthropogenic fill. The water table is located at depths ranging between 3.2 and 11.7 m below ground surface (BGS). The hydraulic conductivity, estimated with pumping tests at the site, is highly variable ranging from 1.44×10^{-3} to 0.6 m/day (Palau, *et al.*, 2014). The hydraulic gradient showed significant seasonal variation and an average value of approximately 10% (Palau, *et al.*, 2014). The aquifer is mainly contaminated by chlorinated ethenes (PCE, TCE, *cis*-DCE), ethanes, methanes (CF, CT) and chlorobenzenes, together with traces of BTEX and pesticides from a chemical plant located at the area. An underground wastewater tank and a disposal pit located outside of the factory building were identified as the main contaminant release sources. High volatile organic compounds concentrations were detected in the subsurface in the areas located around the main pollution sources. The main measures implemented for the mitigation of the contamination, performed in July 2006, were the removal of approximately 2000 t of contaminated soil in the vicinity of the pollution source areas and the installation of two interception trenches filled with concrete-based aggregates in the unsaturated zone where contaminated soil had been removed (pit trench and tank trench). The pit trench is 14 m long, 6 m wide and 6.5 m deep, whereas the tank trench is 28 m long, 6 m wide and 6.5 m deep [Annex C; Supporting Information (SI) Fig. S2]. The recycled concrete-based aggregates were 40-70 mm-sized from a construction and demolition waste recycling plant. These aggregates had a density of approximately 1.10 t m^{-3} . At 50 cm below the ground

surface, a geotextile sheet was placed, which was covered by a layer of compacted clays. Three and five monitoring wells were installed along the pit and tank trenches, respectively (Annex C; SI Fig. S2). Rainwater lixiviates contaminants retained in the unsaturated zone and infiltrates to the trenches, where CF alkaline hydrolysis can be induced. Trench water discharges to the unsaturated zone towards the SSE, following the main water flow direction until reaching a fracture connected to the underlying carbonate aquifer (Annex C; SI Fig. S3). The trenches discharge until a minimum level, and the water accumulated in both trenches is occasionally removed for its management.

1.8. OBJECTIVES

The general aim of this doctoral thesis is to use compound specific isotope analysis of ^{13}C , ^{37}Cl and ^2H as a tool to assess induced attenuation of organic contaminants in groundwater. Two induced attenuation processes were the object of evaluation, 1) a zero valent iron permeable reactive barrier (ZVI-PRB) installed at a site contaminated with the chlorinated ethenes PCE, TCE and *cis*-DCE; and, 2) a proposed new remediation technique based on the use of concrete-based recycled construction wastes to degrade chloroform (CF) by alkaline hydrolysis applied at a site contaminated by this pollutant.

In order to achieve the general aim of this Thesis, both target treatments were studied, first in the laboratory, and later, at field scale.

Laboratory experiments with 1) ZVI and chlorinated ethenes; and 2) slurry from the site where the ZVI-PRB was installed and chlorinated ethenes (microcosms); were performed, with the following objectives:

- To prove that the concurring pathways that should occur during chlorinated ethenes degradation with ZVI, were operative with the same iron used at the ZVI-PRB.
- To determine not only carbon but, for the first time, also Cl isotope fractionation values (ϵ_{C} , ϵ_{Cl}) during the abiotic degradation of the chlorinated ethenes by ZVI.
- To study the potential to discriminate at a field site, chlorinated ethenes biodegradation from their abiotic degradation with ZVI, from two different perspectives:
 - o Dual element isotope plot of both C and Cl isotope data.
 - o Carbon isotope values of daughter products.
- To study the possible occurrence of chlorinated ethenes biodegradation, from the microcosm experiments.

- To obtain the carbon fractionation values (ϵ_C) of the chlorinated ethenes biodegradation.

Once laboratory results were obtained, the multiisotope approach ^{13}C , ^{37}Cl with the addition of ^2H , was tested at field scale, at the site where the ZVI-PRB is installed, with the following objectives:

- To confirm through carbon isotopes data the occurrence of biodegradation at the site
- To quantify the extent of chlorinated ethenes degradation through the ZVI-PRB using the ϵ_C obtained in the laboratory.
- To discriminate through the dual ^{13}C - ^{37}Cl isotope approach biotic from abiotic degradation at the site.
- To choose the appropriate isotope fractionation value (the biotic or the abiotic) depending on the discriminated processes to quantify the global degradation at the field site.
- To combine ^{13}C , ^{37}Cl and ^2H to study the potential benefits of the use of the $\delta^2\text{H}$ approach to distinguish manufactured TCE from TCE coming from PCE degradation in order to use it later in source origin elucidation studies.

In parallel, laboratory batch experiments will be carried out to investigate the capacity of concrete to induce alkaline hydrolysis of the recalcitrant CF. The main objectives were:

- To evaluate CF consumption under alkaline conditions (pH 12.0-12.7) induced by a solution with crushed concrete, a filtered concrete solution, a filtered cement solution and a pH buffer solution.
- To use carbon isotopic tools to determine whether fractionation occurs in order to discriminate if a reduction in concentration is produced due to degradation or to non-transformation processes.
- To obtain the carbon isotope fractionation value and determine if its magnitude is high enough to assess and quantify the induced alkaline hydrolysis of CF.

Once the laboratory experiments were performed, field-scale pilot experiments for inducing CF alkaline hydrolysis by concrete-based recycled construction wastes were evaluated by following these specific objectives:

- By means of carbon isotope field data, to confirm CF degradation at field scale due to the alkaline hydrolysis induced by the concrete aggregates.
- Through the laboratory obtained carbon isotope fractionation value of chloroform, to quantify the extent of CF degradation by the induced treatment in order to evaluate its feasibility to be applied at contaminated sites.

1.9. PUBLICATIONS DERIVED FROM THIS THESIS

The objectives were fulfilled and results were published in peer-reviewed journals. This is the list of publications :

1. Audí-Miró, C; Cretnik, S; Otero, N; Palau, J; Shouakar-Stash, O; Soler, A; Elsner, M. Cl and C isotope analysis to assess the effectiveness of chlorinated ethene degradation by zero-valent iron: Evidence from dual element and product isotope values. *Applied Geochemistry*. 2013, 32, 175-183

Impact factor: 1.708 (2012)

Quartile and category: Q2. Geochemistry & geophysics

2. Audí-Miró, C; Cretnik, S; Torrentó, C; Rosell, M.; Shouakar-Stash, O; Otero, N; Palau, J; Elsner, M; Soler, A. C, Cl and H compound-specific isotope analysis to assess natural versus Fe (0) barrier-induced degradation of chlorinated ethenes at a contaminated site. Submitted to *Environmental Science and Technology* in March 2014.

Impact factor: 5.257 (2012)

Quartile and category: Q1. Engineering, environmental. Environmental sciences

3. Torrentó, C; Audí-Miró, C.; Bordeleau, G.; Marchesi, M.; Rosell, M.; Otero, N.; Soler, A. 2014. The use of alkaline hydrolysis as a novel strategy for chloroform remediation: feasibility of using construction wastes and evaluation of carbon isotopic fractionation. *Environmental Science and Technology*. 2014, 48, (3), 1869–1877

Impact factor: 5.257 (2012)

Quartile and category: Q1. Engineering, environmental. Environmental sciences

The first two papers are focused on ZVI-PRB treatment to degrade chlorinated ethenes. The third paper is focused on a new remediation technique to degrade CF, alkaline hydrolysis induced by concrete-based recycled construction wastes. The first paper represents the initial stage on the assessment of a real ZVI-PRB, which is the study at laboratory scale of the degradation processes of the compounds of study (TCE and *cis*-DCE) due to ZVI. Batch experiments of the three compounds mixed with granular ZVI were performed, and their concentration, and C and Cl isotope analyses were measured over time. Their daughter products were analyzed as well. These experiments were conducted partially at the “Facultat de Geologia” of the “Universitat de Barcelona (UB)” where the concentration and carbon isotope analyses were performed at the “Centres Científics i Tecnològics de la UB (CCiTUB)”; and the other part of experiments were performed in the *Institute of Groundwater Ecology* of the

“Helmholtz Zentrum München” during a stay of three months, where, apart from concentration and carbon isotope analyses, also chlorine isotopes and quantitative data from the daughter products were analysed.

The second paper represents the field scale application of the technique previously studied in the laboratory. A ZVI-PRB installed at the field site and the biodegradation occurrence at the site, as well as the contaminant source, were evaluated by means of the ^{13}C , ^{37}Cl and ^2H compound specific isotope analysis. Multilevel wells around the barrier were installed, and four surveys were conducted from 13 conventional wells and the 5 multilevel wells. From the different surveys concentration and carbon, chlorine and hydrogen isotopes data were obtained of all the chlorinated ethenes and daughter products present at the site in sufficient concentration. Moreover, laboratory microcosm experiments with slurry from the site, and a laboratory batch experiment with ZVI and PCE were performed. The concentration and isotope analyses of the daughter products (ethene, ethane and acetylene) were conducted in the Department of Earth Sciences of the University of Toronto during a stay of three months in Toronto, the hydrogen isotope analyses of TCE and *cis*-DCE were analyzed by the Isotope Tracer Technologies of Waterloo, after learning the technique during the stay in Toronto. To our knowledge, these have been the first $\delta^2\text{H}$ field data of chlorinated ethenes from field samples. The chlorine isotope analyses were done by the Environmental Isotope Chemistry laboratory from the Helmholtz Zentrum München”. The rest of the analyses were conducted at the “CCiTUB”.

Finally, in the third paper a new way to degrade CF that involves the recycling of construction wastes is proposed, with the motivation of degrading a common toxic and recalcitrant chlorinated compound that can even inhibit natural degradation of chlorinated ethenes. Therefore, alkaline hydrolysis of CF by concrete-based recycled construction wastes was evaluated through batch experiments with CF and different alkaline induced media (concrete, buffer and cement) performed in the “Facultat de Geologia” of the “Universitat de Barcelona”. From the batch experiments, carbon and concentration analyses were conducted. Field-scale pilot experiments consisting of the implementation of two interception trenches filled with concrete-based recycled construction wastes in the recharge waters of a CF polluted aquifer were assessed by concentration and carbon isotope data. All the concentration and carbon isotope analyses were conducted at the “CCiTUB”.

Chapter 2.

Results

2.1 ASSESSMENT OF ZVI-PRB INDUCED CHLORINATED ETHENES DEGRADATION

2.1.1 Laboratory ZVI batch experiments

Prior to the assessment of the ZVI-PRB at the field site, laboratory batch experiments with ZVI were performed. Degradation rates (K_{obs}) of the chlorinated ethenes were calculated according to Equation 1.6 and normalized to the iron surface area [K_{SA} , $K_{\text{SA}} = (k_{\text{obs}}/a_s \cdot \rho_m)$, where a_s is the specific surface area of ZVI (m^2/g) and ρ_m is the mass concentration of ZVI ($\text{g} \cdot \text{L}^{-1}$), (Johnson *et al.*, 1996)]. Since PCE experiments used different iron mass/water volume ratio (100 g/L) than the called dual element experiments of TCE, *cis*-DCE and VC (200 g/L), normalized transformation rates allow the comparison between the different experiments. A K_{SA} decrease from PCE to VC (PCE>TCE>*cis*-DCE>VC) was observed. Calculated K_{SA} s can be found in Table S1 in the SI of Annex A (except for PCE, from which its K_{SA} is $2.8 \cdot 10^{-3} \text{ d}^{-1} \text{ m}^{-2}$). Calculated half-lives of PCE, TCE, *cis*-DCE and VC, equivalent to the same conditions, were 2, 3, 50 and 80 days. The observed degradation rates trend was opposite to the one observed during additional TCE and *cis*-DCE experiments also conducted with the same iron, from which K_{SA} s are also indicated in Table S1 in the SI of Annex A.

TCE, *cis*-DCE and VC dual element experiments generated ethene, ethane and methane as final products of the degradation sequence, with small amounts of *cis*-DCE, acetylene and VC intermediates detected during TCE degradation (Fig. 3.1A-B); and acetylene and VC from *cis*-DCE degradation. Also, traces of longer-chain hydrocarbons were observed, as well as C3 (propene, propane) and C4 (n-butane). These detected daughter products confirmed degradation

of TCE and *cis*-DCE through both hydrogenolysis and β -dechloroelimination pathways during degradation of chlorinated ethenes with the ZVI. Complete products are listed in Table 1 of Annex A. Daughter products in PCE experiment were not evaluated.

Enrichment in ^{13}C over time was observed for all the compounds, confirming carbon isotope fractionation due to degradation of the chlorinated ethenes with ZVI. In control experiments neither concentration decrease nor carbon isotope fractionation were detected. According to the Rayleigh Equation (Eq. 1.12), the calculated ϵ_{C} for PCE degradation with ZVI was $-9.5 \pm 2.2\text{‰}$ (Annex B; SI Fig. S3). For TCE a ϵ_{C} of $-14.8 \pm 0.6\text{‰}$ was obtained, which, taking into account the 95% confidence interval, overlapped with the preliminary additional TCE experiments ($-12.0 \pm 2.8\text{‰}$) (Fig. 2.1A). The average ϵ_{C} for TCE degradation is $-13.4 \pm 1.7\text{‰}$. From *cis*-DCE experiments an ϵ_{C} of $-20.5 \pm 1.8\text{‰}$ was obtained, with the 95% confidence intervals almost overlapping with those of the additional *cis*-DCE experiment ($-16.8 \pm 1.2\text{‰}$) (Fig. 2.1C), resulting in an average of $-18.6 \pm 1.5\text{‰}$. Overall, the comparison with the additional experiments showed consistent carbon isotope fractionation with the type of iron used, despite the opposite reactivity trends. Therefore, these values will be used to assess the ZVI-PRB field application. Isotope fractionation value of VC was not evaluated, since it was hardly transformed.

TCE and *cis*-DCE ZVI transformation were also associated to a pronounced chlorine isotope fractionation, with calculated ϵ_{Cl} of $-2.6 \pm 0.1\text{‰}$ for TCE and of $-6.2 \pm 0.8\text{‰}$ for *cis*-DCE (Fig. 2.1B and 2.1D) according to Equation 1.12. Thus, chlorine isotope fractionation can be an additional line of evidence for monitoring degradation in the field. According to Equation 1.17, chlorine apparent kinetic isotope effects AKIE_{Cl} of TCE and *cis*-DCE resulted in values of 1.008 ± 0.001 and 1.012 ± 0.002 , respectively.

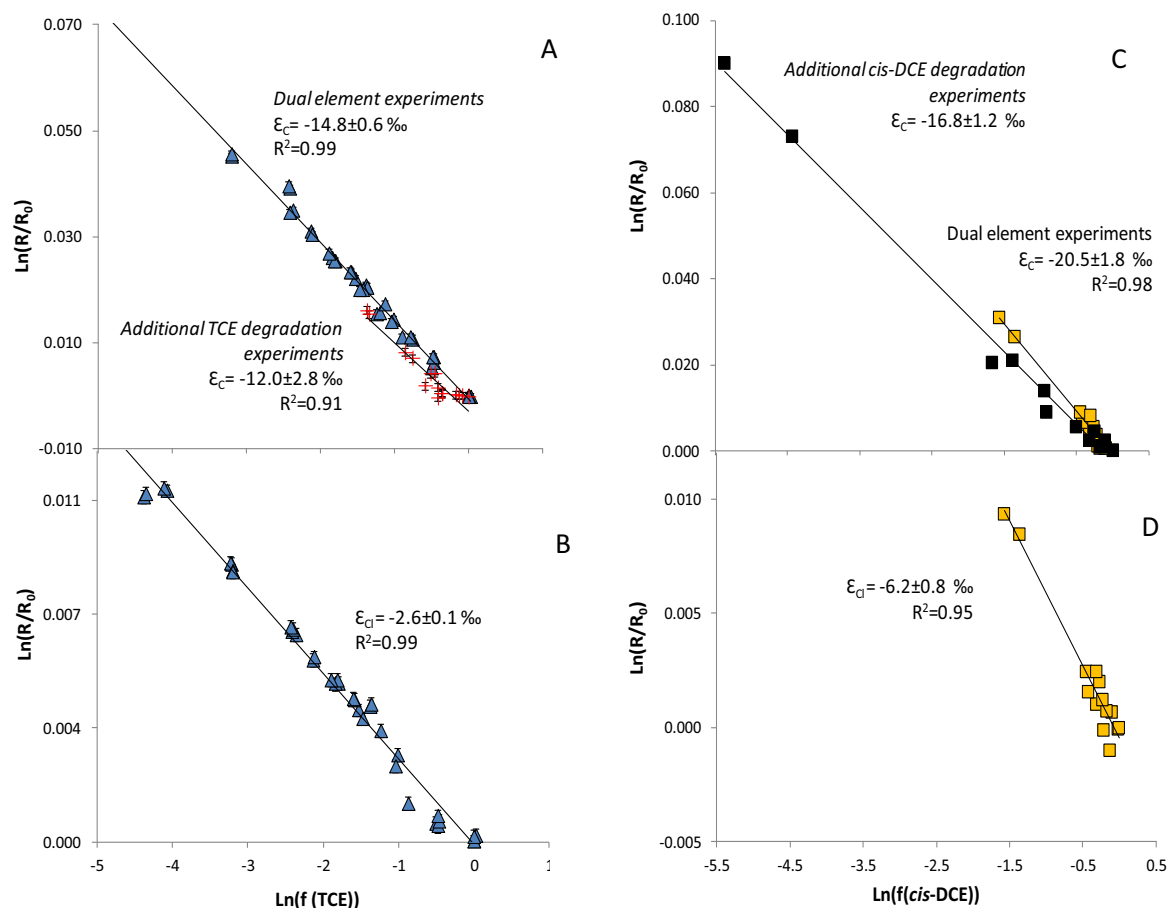


Figure 2.1. A and C) Carbon isotope values of residual TCE (A) and *cis*-DCE (C) fraction in a double logarithmic plot over the respective concentrations. The isotopic fractionation values ϵ_C are calculated from the slope of the regression line according to Equation 1.12. Triangles represent TCE dual element experiments and crosses represent TCE additional experiments (A); yellow squares represent *cis*-DCE dual element experiments and black squares represent *cis*-DCE additional experiments (C). B and D) Chlorine isotope values of residual TCE (B) and *cis*-DCE (D) fraction in a double logarithmic plot over the respective concentrations. The isotopic fractionation values ϵ_{Cl} has been obtained according to Equation 1.12. In A and C, error bars represent the calculated error due to a total instrumental uncertainty of 0.5‰ for compound-specific carbon isotope measurements, and in B and D of 0.2‰ for compound specific chlorine isotope measurements.

2.1.2. Laboratory microcosm experiments

Significant concentration decrease and an increase in $\delta^{13}\text{C}$ were observed in both PCE and TCE microcosm experiments. These results indicated not only that biodegradation occurred at both chlorinated ethenes experiments, but also that biodegradation could take place at the field site, since the microbiota of the slurry used in the experiment was able to biodegrade the contaminants. Daughter products formation (up to *cis*-DCE; VC was not detected and ethene and ethane were not evaluated after 500 days) also confirmed biodegradation of the chlorinated compounds towards reductive dechlorination products. The $\delta^{13}\text{C}$ of TCE and PCE remained constant in the control experiments (Annex B; SI Fig. S1) and no degradation products were detected along the incubation time. An $\epsilon_{C,PCE}$ of $-2.6 \pm 0.9\text{‰}$ (Annex B; SI Fig. S2A) was obtained. Regarding TCE experiments, an $\epsilon_{C,TCE}$ value of $-1.7 \pm 1.8\text{‰}$ was estimated (Annex B; SI Fig. S2B). Concerning *cis*-DCE microcosm experiments, no changes in both concentration

and isotope values were detected after 500 days. Additionally no VC was produced from *cis*-DCE.

2.1.3. ZVI-PRB field-scale application assessment

The redox conditions detected at the site were indicative of favorable biotic reductive dechlorination of chlorinated ethenes: 1) prevailing anaerobic conditions [dissolved oxygen (DO) below 2 mg/L]; 2) presence of dissolved Mn in concentration up to 1.36 mg/L; 3) dissolved Fe in concentrations up to 1.57 mg/L; 4) decreasing nitrate concentration at points where the highest Mn concentrations were detected; 5) decreasing sulfate concentrations in the MW17 well (from an average of 90 mg/L to 16.8 mg/L) (Annex B; SI Table S1). These redox conditions are also typical of abiotic chlorinated ethenes reductive dechlorination by ZVI, which would favor this process at the ZVI-PRB area. The pH analyzed all over the site was around 7.

Upgradient the ZVI-PRB, the main compounds detected were PCE, TCE (mainly in OMW6B and OMW7, see wells location in Annex B; Fig. 1) and *cis*-DCE (see concentrations in Table S2 in the SI of Annex B). VC was also detected (in MW17, OMW5 and Pz3), as well as ethene and ethane in MW17. These identified dechlorination products indicated that biodegradation was taking place at the site, achieving complete dechlorination of the chlorinated ethenes at the source area (MW17).

Carbon isotope shifts were observed at the site (Fig. 2.2), confirming biodegradation. PCE, TCE and *cis*-DCE most positive $\delta^{13}\text{C}$ values were detected right before the barrier (Fig. 2.2), indicating a higher degradation degree at these sampling points. A hypothesis of this effect could be an increased residence time due to a potential hydraulic barrier effect of the ZVI-PRB. PCE carbon isotope values in wells OMW5 and BR1-11 changed towards more positive values along the three years of study, indicating an increase of biodegradation extent over time (Fig. 2.3). The same trend was detected for *cis*-DCE in wells MW17 and BR1-9.5 m (Fig. 2.3). In well MW17, $\delta^{13}\text{C}$ of VC ($\delta^{13}\text{C}$ of -38.4‰) was depleted in ^{13}C compared to the parent compound ($\delta^{13}\text{C}_{\text{DCE}}$ of -15.7‰) as normally occurs during biodegradation reactions.

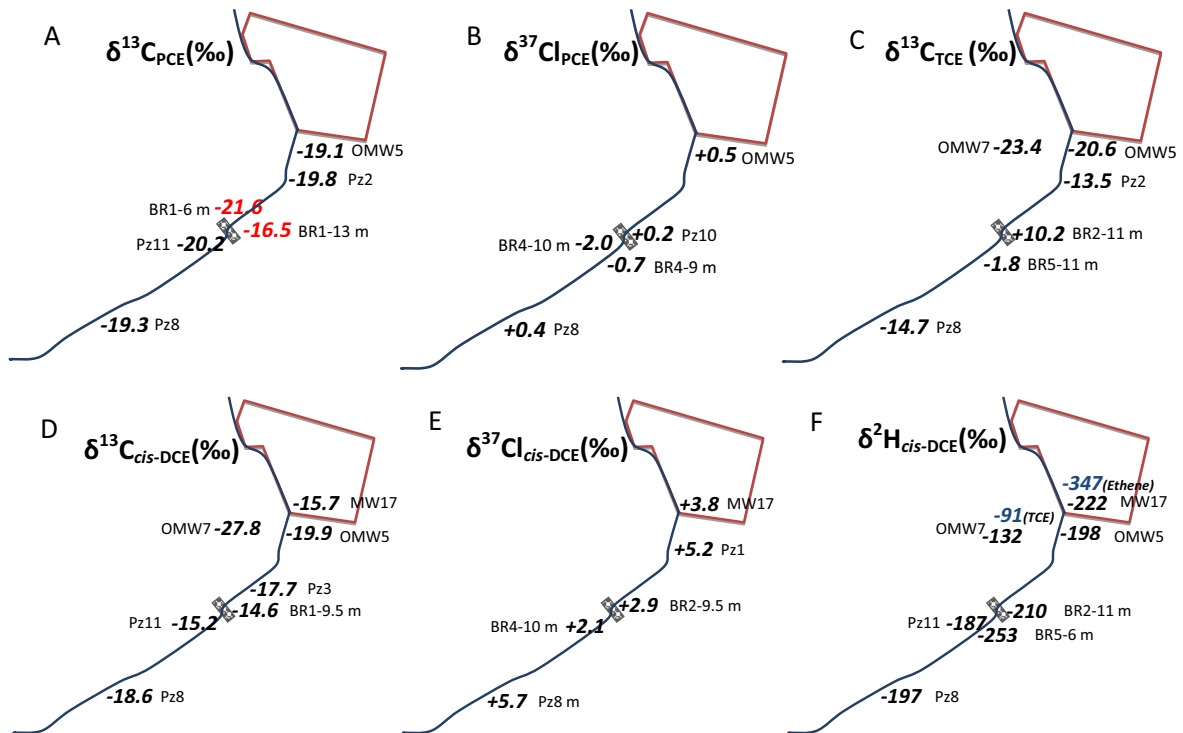


Figure 2.2. Isotope data of: $\delta^{13}\text{C}$ and $\delta^{37}\text{Cl}$ of PCE (A and B, respectively); $\delta^{13}\text{C}$ of TCE (C); and $\delta^{13}\text{C}$, $\delta^{37}\text{Cl}$ and $\delta^2\text{H}$ of *cis*-DCE (D, E and F, respectively). F also includes TCE and ethene data, indicated in blue. These isotopes data were obtained from the most representative wells from: 1) the last survey when $\delta^{13}\text{C}$ data was obtained (Mar-13) (except for the wells in red for $\delta^{13}\text{C}$ of PCE that are from Jun-12); and 2) the Oct-12 survey, when $\delta^2\text{H}$ and $\delta^{37}\text{Cl}$ were measured. OMW7 $\delta^{13}\text{C}$ and $\delta^2\text{H}$ data are from Sept-13. The ZVI-PRB is indicated by a rectangle crossing the creek.

Downgradient of the PRB chlorinated ethenes were still present, suggesting 1) that the barrier did not achieve complete degradation of the contaminants; 2) the presence of potential hydraulic bypasses. Lateral and underneath bypass effects were confirmed by the presence of PCE and *cis*-DCE in Pz4 and in the multilevel wells at 11 to 13 m depth, respectively, since Pz4 is located at the west side of the barrier and the barrier is positioned at around 10 m depth. The presence of acetylene at the central well BR4 (immediately after the barrier), gave evidence of abiotic degradation of the chlorinated ethenes through the ZVI-PRB, since acetylene was also detected in the laboratory experiments.

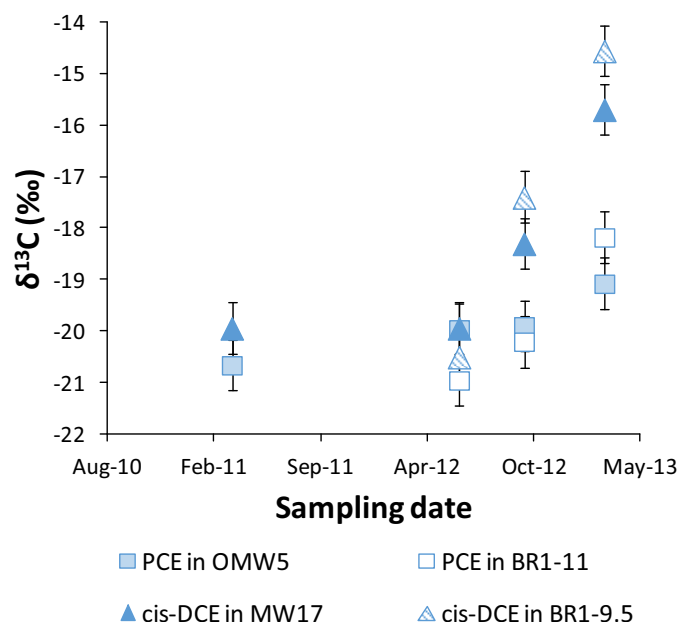


Figure 2.3. Changes in $\delta^{13}\text{C}$ over time of PCE and *cis*-DCE in wells OMW5 and BR1-11, and MW17 and BR1-9.5, respectively. Error bars represent $\delta^{13}\text{C}$ uncertainty of 0.5‰.

Carbon isotope results of the multilevel wells directly before (BR-1) and after (BR-3, BR-4) the ZVI-PRB exhibited, in June-12, a small but consistent enrichment of ^{13}C in both PCE and *cis*-DCE from upstream to downstream of the barrier (Fig. 2.4A), more visible at the central part of the barrier (BR4) where even formation of TCE was also observed. According to the ZVI laboratory results, these data confirm PCE and *cis*-DCE degradation by the ZVI-PRB. Since the average initial $\delta^{13}\text{C}$ (in BR-1) of *cis*-DCE was more positive than the one of PCE (-20 and -20.6‰, respectively) indicating degradation beyond *cis*-DCE, the extent of degradation could be estimated for the two compounds according to Equation 1.13 with the initial $\delta^{13}\text{C}$ values taken as the average from BR-1 of each compound; and the final $\delta^{13}\text{C}$ values as the average values from BR4 for each compound. The ϵ_{C} used was the carbon isotopic fractionation obtained in the PCE and *cis*-DCE degradation laboratory experiments with ZVI ($-9.5 \pm 2.2\%$ for PCE, and $-18.6 \pm 1.5\%$ for *cis*-DCE). The resultant calculated efficiency of the PRB in June-12 was less than 10 % and 2% for PCE and *cis*-DCE, respectively. In the following Oct-12 and Mar-13 surveys the effect of the PRB was not observed since several points upstream of the barrier were even enriched in ^{13}C regarding downstream values (Fig. 2.4B). These results suggested a strong biodegradation effect upstream of the barrier that could be masking the low ZVI-PRB effect, enhancing the hypothesis of a hydraulic barrier effect that might increase the residence time of the compounds and consequently their biodegradation.

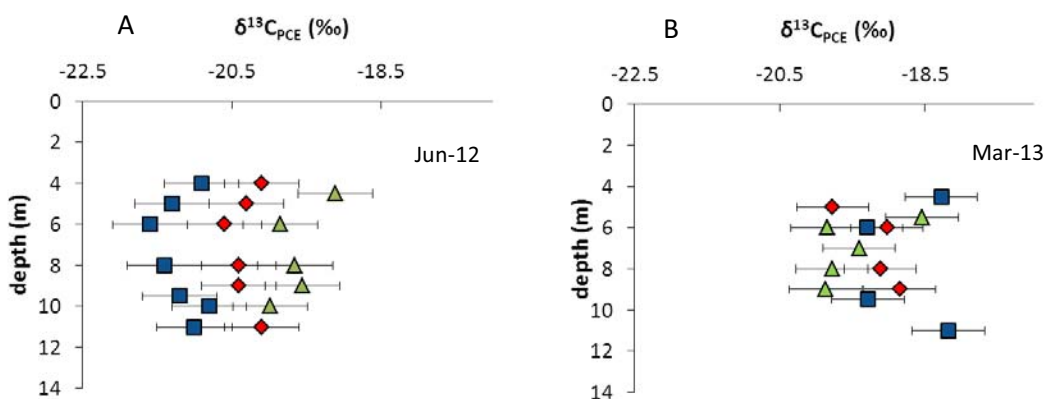


Figure 2.4A-B. $\delta^{13}\text{C}$ of PCE in BR1 (blue squares, directly in front of ZVI-PRB), BR3 (red diamonds) and BR4 (green triangles) (both directly behind ZVI-PRB) in depth from Jun-12 (A) and Mar-13 (B) campaigns. Error bars represent an uncertainty of 0.5‰ for $\delta^{13}\text{C}$ measurements (for location of wells, see Figure 1 of Annex B).

TCE concentration in well OMW7 (139 mg/L) differs in four orders of magnitude from TCE concentrations throughout the site, clearly suggesting a separate TCE source at this well, probably coming from a spillage of TCE. On the other hand, we would expect that TCE at the rest of the site could be formed from PCE. Since this hypothesis was clear, it enabled to check the potential of C, Cl and H isotope data to distinguish the different sources detected. Carbon isotopes data showed (Fig. 2.2) that the less degraded PCE ($\delta^{13}\text{C}$ of -21.6‰) was located at the ZVI-PRB area, so it had been transported to that point from the source in the direction of the creek. In contrast, the lowest $\delta^{13}\text{C}$ of TCE (-23.4‰) was found in OMW7 (Fig. 2.2), at the west of the site. Regarding chlorine isotope data, the most negative chlorine isotope values of both PCE and *cis*-DCE of the site were also detected at the ZVI-PRB area (BR4), as well as, in the case of hydrogen isotope data, the lowest $\delta^2\text{H}$ of *cis*-DCE was detected at the same area in BR5 (Fig. 2.2). These results confirm from carbon, chlorine and hydrogen isotope perspectives the presence of the less degraded PCE around the PRB. Moreover, the positive correlation (R^2 : 0.99) between the most depleted $\delta^{37}\text{Cl}$ values of PCE and *cis*-DCE at BR4, points to *cis*-DCE coming from PCE at this point (Annex B; SI Fig. S4).

2.2. ASSESSMENT OF THE CHLOROFORM ALKALINE HYDROLYSIS INDUCED BY CONCRETE-BASED CONSTRUCTION WASTES

2.2.1. Laboratory experiments of induced CF alkaline hydrolysis

In all the experiments consumption of CF was observed over time. In the control experiments concentrations remained unchanged up to 28 d (Fig. 2.5A) and chloride formation was not detected, ruling out possible losses of CF as a result of processes not induced by alkaline conditions. Under alkaline conditions, CF concentration decrease ranged from 72% (buffer experiments) to 99% (filtered cement experiments) after 28 d (Fig. 2.5A). In the four tested treatments, the pH remained constant over the duration of the experiments (12.33 ± 0.07 in the concrete experiments, 12.27 ± 0.04 in the filtered concrete experiments, 12.66 ± 0.02 in the filtered cement experiments and 11.92 ± 0.11 in the buffer experiments). As evidenced by the linear correlation relationship in $\ln(C/C_0)$ vs. time graphs (Annex C; SI Fig. S4), the hydrolysis of CF under alkaline conditions followed pseudo-first-order kinetics. Least-squares regression analysis showed $R^2 > 0.95$ (Annex C; Table 1). The rate of CF degradation generally increased as the pH of the alkaline solutions increased, with pseudo-first-order rate constant values, k'_{obs} , ranging from 0.047 to 0.201 d^{-1} . CF half-life was less than 15 d (Annex C; Table 1) for all tested alkaline pH values.

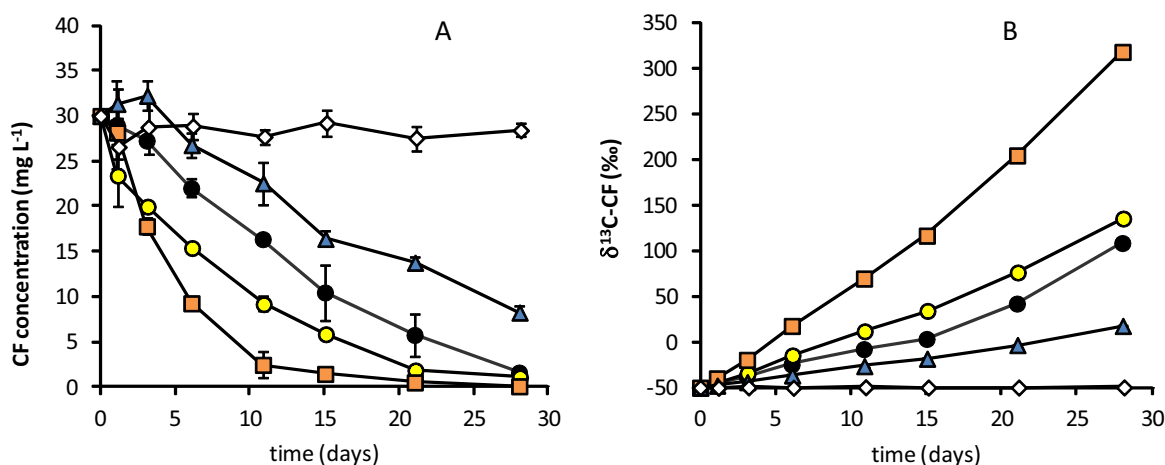


Figure 2.5. Changes in concentration (A) and $\delta^{13}\text{C}$ (B) of CF over time in the alkaline hydrolysis laboratory experiments: unfiltered concrete experiments (black circles), filtered concrete experiments (yellow circles), filtered cement experiments (orange squares), buffer experiments (blue triangles) and control experiments (white diamonds). The error bars show the standard deviation for duplicate experiments.

The initial concrete and cement solutions contained 2.1 and 15.8 mg L^{-1} of chloride, respectively. The chloride concentration related to CF dechlorination at each sampling time was determined by measuring the dissolved chloride concentrations in the samples subtracting the

background concentrations (initial measures in the concrete and cement solutions). The total molar mass balance of chlorine (chloride released + chlorine in the remaining CF) at each sampling time ranged from 81 to 127%, 91 to 105% and 92 to 112% of the initial chlorine mass throughout the experiments with concrete particles, filtered concrete solution, and filtered cement solution, respectively (Annex C; SI Fig. S6).

A considerable enrichment in ^{13}C in the remaining CF over the course of the experiments (Fig. 2.5B) was shown except in the control experiments. Carbon isotopic fractionations (ϵ_C) were evaluated by the linear regression of the data following the Rayleigh equation (Eq. 1.13). The resulting plots can be found in the SI of Annex 3 (Annex C; Fig. S7), and the experimental results are summarized in Table 2 of Annex C. Good fits (i.e., $R^2 > 0.96$) were obtained for all regressions. Carbon isotopic fractionation ranged from $-49 \pm 7\text{‰}$ to $-56 \pm 10\text{‰}$ for all experiments. The 95% confidence intervals of all ϵ_C values overlap. Therefore, an average ϵ_C value combining all data was determined to be $-53 \pm 3\text{‰}$ ($R^2 = 0.98$). The apparent kinetic carbon isotope effect (AKIE) obtained was 1.056 ± 0.003 (Eq. 1.17).

2.2.2 Field-scale experiments with concrete-based recycled construction wastes

Throughout the 35-month sampling period, the pH values of the water sampled from the two trenches remained constant (11.6 ± 0.3), confirming the high buffering capacity of the recycled construction wastes. It should be noted that groundwater collected in all the aquifer monitoring wells shown in Figure S2 in SI of Annex C, including the two wells located a few meters downgradient from the trenches, had neutral pH values, showing that alkaline conditions were restricted to the trenches. The water temperature of both trenches during the sampled period ranged between 14 and 17 °C (with mean values of 15.6 ± 1.0 °C and 15.3 ± 1.1 °C) according to seasonality, whereas the groundwater remained constant at a similar mean value of 15.4 ± 0.2 °C during the same studied period.

The water table elevation in the trenches ranged from approximately 431 to 434 meters above sea level (masl) (Annex 3; SI Fig. S9). Water table fluctuations occurred in response to rainfall. Between the precipitation events and the water level increases in the tank and pit trenches, a lag period of approximately 5-7 and 20-30 days was observed, respectively. The rapid recharge of the trenches can be seen after February 23rd 2011, when water of both trenches was removed for its management. Trench discharge after the high-intensity precipitation events proceeds according to Maillet's law. Under the four discharge conditions observed from May 2011 to March 2013 (Annex C; SI Fig. S9), the recession curves were used to calculate the average discharge flow rates for both trenches. The obtained average discharge flow rates were $0.18 \pm 0.03 \text{ m}^3\text{d}^{-1}$ and $0.23 \pm 0.06 \text{ m}^3\text{d}^{-1}$ for the pit and tank trenches, respectively. The mean

residence time of water in the trenches was calculated as the ratio of the effective trench volume to the average discharge flow rate. The obtained mean residence time was 513 ± 86 d and 730 ± 190 d for the pit and tank trenches, respectively. At the end of each of the four observed discharge cycles, discharge became zero and trench water remained at the minimum level (Annex C; SI Fig. S9). It should be noted that the first discharge cycle, lasting 90 days (see the period from June to October 2011 in Figure S9 in the SI of Annex C) is the only period without significant precipitation events and therefore corresponds to the maximum period without water entering the trenches.

Significant variations in the CF concentration were observed over time (Fig. 2.6) in both trenches. These fluctuations could be attributed not only to CF degradation, but also to other non-transformation processes such as dilution effects due to the entry of rainwater after short-duration high-intensity precipitation events, to the leaching of contaminants retained in the unsaturated zone by rainwater after long-duration low-intensity precipitation events, to sorption and/or desorption processes of the contaminants on the mineral micropores, etc. Considerable enrichments in ^{13}C of CF over time occurred in both trenches (Fig. 2.6), demonstrating CF transformation. In the two recharge periods, there was a general tendency of CF $\delta^{13}\text{C}$ values to increase in both trenches, with isotopic shifts of up to 20 and 28‰. Despite this general trend, certain CF $\delta^{13}\text{C}$ variability was observed due to the entry of non-degraded contaminant leaching from the subsoil after any precipitation event.

According to Equation 1.13 and with the isotopic fractionation value obtained from the laboratory experiments ($\epsilon_c = -53 \pm 3\%$), the extent of CF degradation in the trenches was estimated assuming that the alkaline hydrolysis induced by construction wastes was the only fractionation process. The $\delta^{13}\text{C}$ -CF values measured in both trenches at the start of the study period ($-23.0 \pm 0.1\%$ and $-29.5 \pm 0.2\%$, respectively) were used as the initial isotopic compositions of CF. This assumes that these isotopic compositions represent the contaminant that has been subjected to the least degradation before reaching the trenches. The calculated percentage of CF degradation in both trenches over time is shown in Fig. 2.7. The observed $\delta^{13}\text{C}$ enrichments in the tank trench allowed to calculate the maximum extent of degradation ($34 \pm 5\%$ and $39 \pm 9\%$) for the first and the second recharge periods, respectively. In the pit trench, the maximum estimated degradation was $32 \pm 5\%$ and $40 \pm 3\%$, respectively. The highest degrees of CF degradation occurred at the end of each observed discharge cycle, when discharge became zero and trench water was at the minimum level (Fig. 2.7 and Annex C; SI Fig. S9).

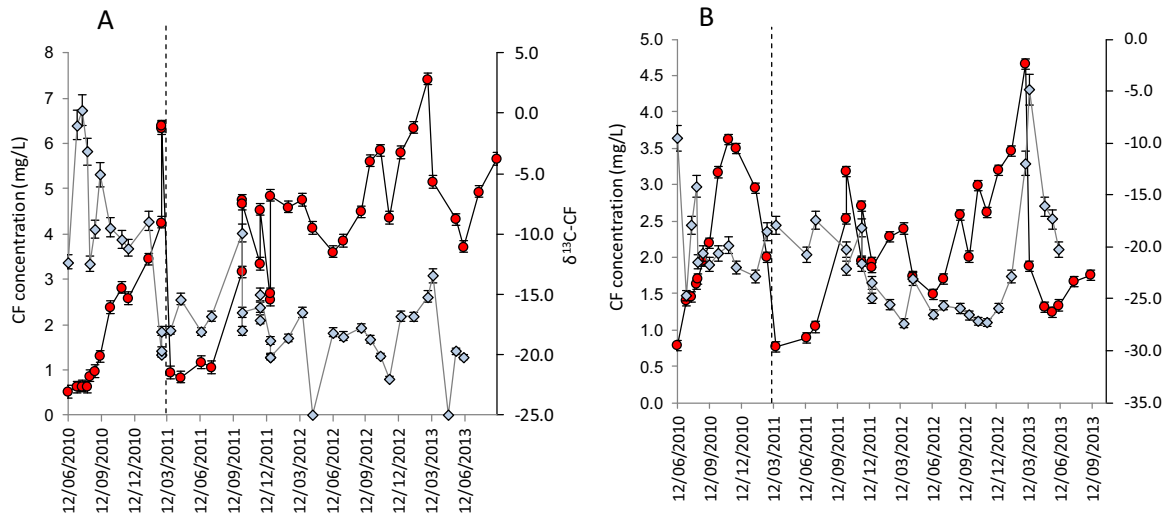


Figure 2.6. Variation over time of CF concentration (blue diamonds) and carbon isotope ratios ($\delta^{13}\text{C}\text{-CF}$, red circles) in the (A) tank trench and (B) pit trench during the studied period. The error bars show the standard deviation for replicate measurements of the concentration and isotopic data. Dashed lines indicate the day when the trenches were completely emptied for the management of the contaminated water.

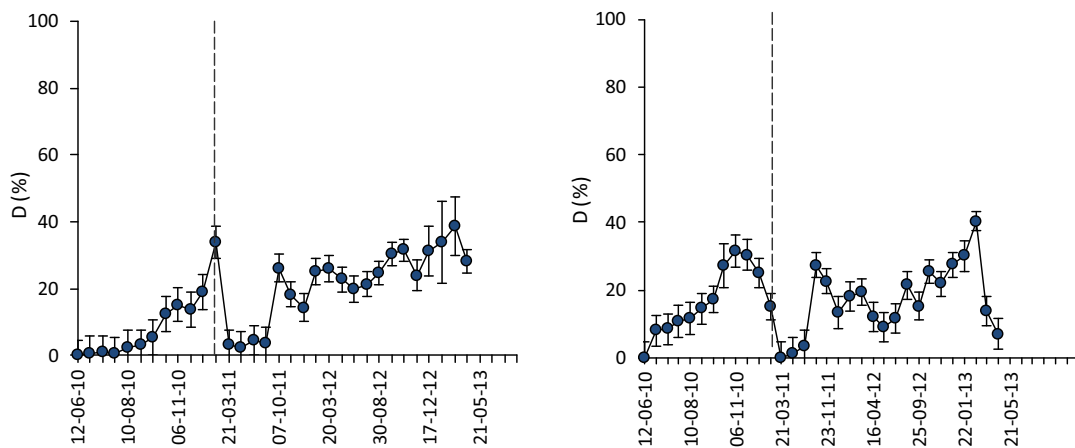


Figure 2.7. Estimation of the extent of chloroform degradation by alkaline hydrolysis induced by construction wastes in the (A) tank trench and the (B) pit trench using Equation 1.13. The uncertainty in the percentage of degradation was calculated by error propagation of the known total errors for $\delta^{13}\text{C}\text{-CF}$ measurements (the standard deviation of duplicated measurements) and ϵ_c estimation ($\pm 3\%$). Dashed lines indicate the day when the trenches were completely emptied for the management of the contaminated water.

Field-scale analyses revealed also variations in the concentration of other chlorinated volatile organic compounds in the two trenches (Annex C; SI Fig. S10), but the isotopic results showed negligible changes in $\delta^{13}\text{C}$ values of TCE and PCE (Annex C; SI Fig. S11). However, $\delta^{13}\text{C}$ values of carbon tetrachloride (CT) showed a significant enrichment during the two recharge periods in both trenches. In the tank trench, $\delta^{13}\text{C}\text{-CT}$ values increased from $-18.3\pm 0.2\%$ to $-13.2\pm 0.8\%$ in the first period and from $-19.0\pm 0.2\%$ to $-7.0\pm 0.1\%$ in the second period. In the pit trench, $\delta^{13}\text{C}\text{-CT}$ values increased from $-32.3\pm 1.3\%$ to $-20.4\pm 0.5\%$ and from $-29.2\pm 0.7\%$ to -

17.0±0.5%, in the first and second periods respectively. Therefore, CT transformation in the trenches is occurring, especially in the tank trench.

Chapter 3.

Discussion

3.1 ASSESSMENT OF ZVI-PRB INDUCED CHLORINATED ETHENES DEGRADATION

3.1.1. Laboratory ZVI batch experiments

Degradation of all the chlorinated ethenes occurred in the ZVI experiments, with calculated half-lives for PCE, TCE, *cis*-DCE and VC of 2, 3, 50 and 80 days, respectively. Detected degradation trends in the order PCE>TCE>*cis*-DCE>VC are consistent with earlier studies with ZVI by Gillham and O'Hannesin (1994); Dayan *et al.* (1999) and Elsner *et al.* (2008). Moreover, Leeson (2004) described that, the higher chlorinated compounds, are more susceptible to reduction than the lesser chlorinated ones, due to higher oxidation state, thus giving higher transformation rates. However, an opposite trend was observed (TCE<*cis*-DCE) in the additional studies, which is also consistent with other literature data (Arnold and Roberts, 2000; Elsner *et al.* 2008). At present, the reasons for these reactivity trends remain imperfectly understood.

According to Arnold and Roberts (2000) and Prommer *et al.* (2008), ethene can be produced either (i) from hydrogenation of acetylene, previously formed through the β -dichloroelimination pathway or (ii) through VC hydrogenolysis. VC and acetylene concentration profiles (Fig. 3.1B), suggested that in this process acetylene might be the main intermediate of ethene formation, (i) due to an extremely rapid acetylene concentration decrease while ethene appeared, and (ii) because VC concentrations, in contrast, accumulated over time (Fig. 3.1B). These observations point out that both hydrogenolysis and β -dichloroelimination pathways (Fig. 1.4) are occurring simultaneously as parallel reactions rather than as consecutive reactions and

that ethene and ethane are produced primarily through the β -dichloroelimination pathway. Only 20% of degraded TCE was transformed to *cis*-DCE, which, in turn was transformed at a much slower rate to VC.

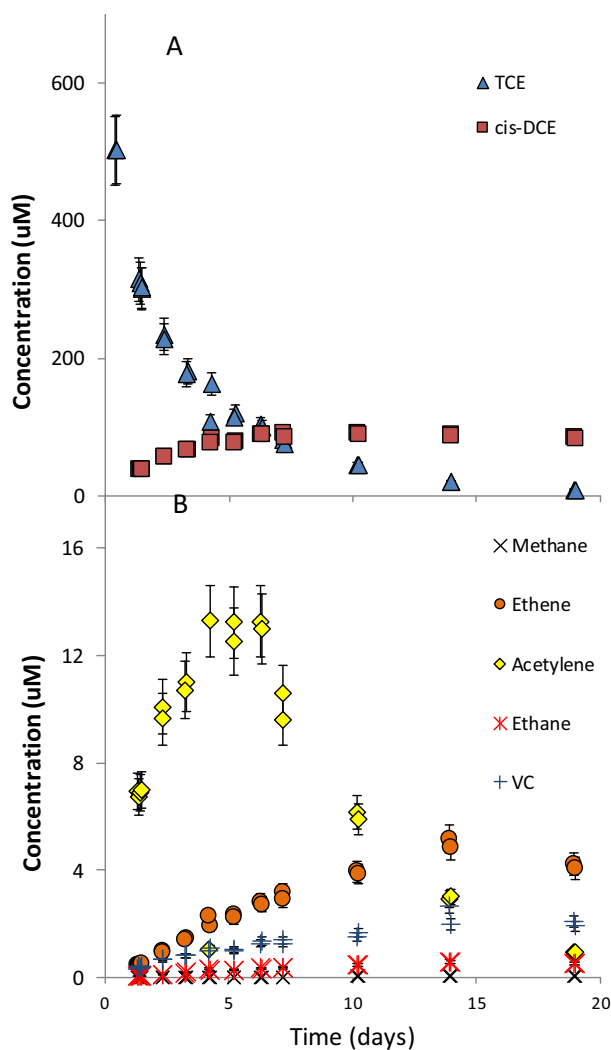


Figure 3.1. Changes in concentration of TCE (panel A), from Dual Element TCE experiments, and its byproducts over time (A and B). Panel B is a zoom of Panel A without TCE and *cis*-DCE to see by-products curve shape clearly. Error bars indicate total instrumental uncertainty of $\pm 10\%$.

Both carbon and chlorine isotope fractionation were observed in all the ZVI conducted experiments while chlorinated compounds concentration decreased. The obtained isotope fractionation was of $-9.5 \pm 2.2\%$ for PCE, $-13.4 \pm 1.7\%$ for TCE and $-20.5 \pm 1.8\%$ for *cis*-DCE. PCE and TCE ϵ_C values are within the wide literature ranges -5.7 to -25.3% for PCE (Dayan *et al.*, 1999; Vanstone *et al.*, 2004), and -7.5 to -27% for TCE (Dayan *et al.*, 1999; Slater *et al.*, 2002; Vanstone *et al.*, 2004; Elsner *et al.*, 2008). These wide ranges indicate that the ϵ_C depends on each specific ZVI material, reinforcing the necessity to accurately determine the characteristic ϵ_C prior to applying it at the field scale to evaluate the extent of the reductive dechlorination. Regarding *cis*-DCE, ϵ_C reported data varied from -6.9 to -16.0% (Dayan *et al.*,

1999; Vanstone *et al.*, 2004). The obtained value in the present experiment was lower, $-18.6 \pm 1.5\%$.

Compared to other studies (Dybala-Defratyka *et al.*, 2004; Hofstetter *et al.*, 2007; Dybala-Defratyka *et al.*, 2008; Wolfsberg *et al.*, 2010), the calculated TCE and *cis*-DCE apparent kinetic isotope effects $AKIE_{Cl}$ (1.008 ± 0.001 and 1.012 ± 0.002 , respectively) are typical, or even at the higher end of ranges reported for chlorine isotope effects. Therefore, they are clearly indicative of the presence of primary rather than secondary isotope effects meaning that (i) during the rate-determining step of the ZVI-catalyzed transformation, a C-Cl bond is cleaved; and (ii) this intrinsic isotope effect is not significantly masked by mass transfer, adsorption, etc. In particular, our estimated values are much higher than the $AKIE_{Cl} = 1.003$ calculated for biotransformation of *cis*-DCE by the mixed culture KB-1 (Abe *et al.*, 2009) suggesting potential differences in the underlying transformation mechanism.

The $\delta^{37}Cl$ in *cis*-DCE, as a TCE product, was slightly greater compared to its precursor TCE, which, in contrast to what Hunkeler *et al.* (2009) predicted, showed an initial enrichment in ^{37}Cl instead of ^{35}Cl of the product *cis*-DCE (Figure 3.2). The reason of this observation in the $\delta^{37}Cl$ values may be an inverse secondary isotope effect or an unequal distribution of isotope ratios in different positions of TCE so that the position containing more ^{37}Cl is preferably transferred to the product pool. These preliminary results indicate that chlorine isotope measurements might have potential to investigate the reaction chemistry of TCE and *cis*-DCE in future studies.

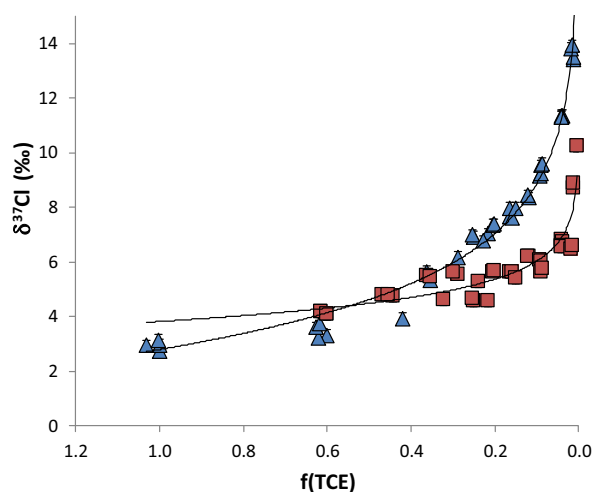


Figure 3.2. Changes in chlorine isotope values of TCE (triangles), as substrate, and *cis*-DCE (squares), as product, during TCE combined Dual Element experiments. Error bars represent the total instrumental uncertainty of 0.2% for compound-specific chlorine isotope measurements.

As a first approach to later distinguish ZVI degradation from biodegradation at the field site, dual ^{13}C - ^{37}Cl isotope data were plotted. TCE transformation experiment gave slopes of 5.2 ± 0.3 for TCE and 5.0 ± 0.6 for the daughter product *cis*-DCE (Fig. 3.3A); and for the *cis*-DCE

transformation experiment of 3.1 ± 0.2 (Fig. 3.3B). To our knowledge, the obtained dual (^{13}C - ^{37}Cl) isotope plots are the first ones reported for chlorinated ethenes transformation by ZVI. A parallel trend for TCE and its daughter product *cis*-DCE is observed when plotting dual ^{13}C - ^{37}Cl data (Figure 3.3A), something that is predicted for cases when further transformation of *cis*-DCE is very slow or even negligible (Hunkeler *et al.*, 2009).

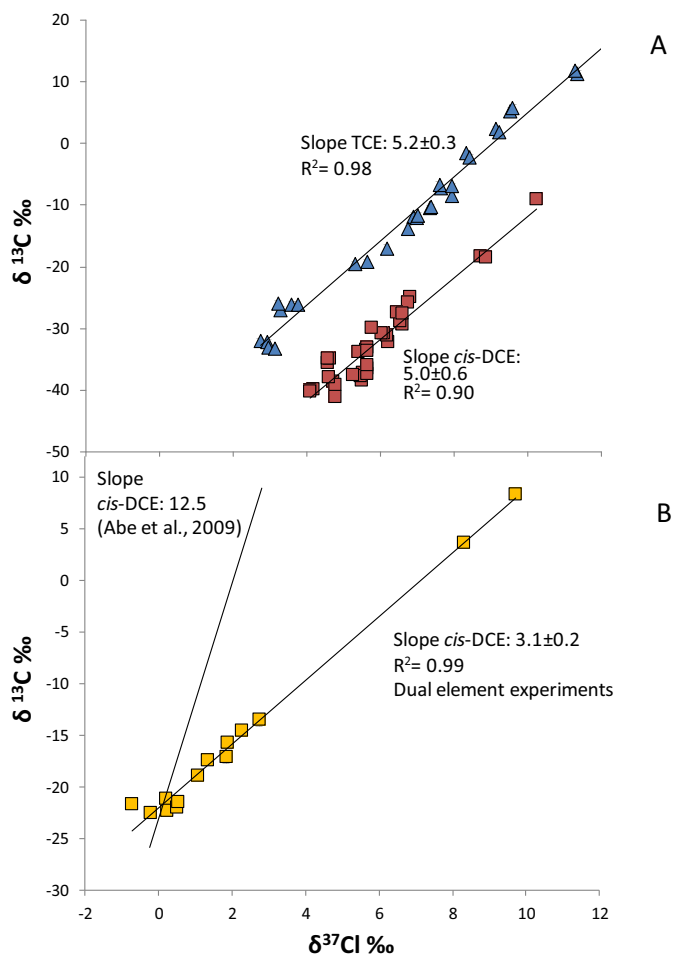


Figure 3.3. A) Dual isotope plot $\delta^{13}\text{C}$ versus $\delta^{37}\text{Cl}$ obtained from TCE Dual Element combined experiments. The slopes of TCE (blue triangles) and *cis*-DCE as a product (red squares) are represented. B) Dual isotope plot $\delta^{13}\text{C}$ versus $\delta^{37}\text{Cl}$ obtained from *cis*-DCE Dual Element combined experiments. The slope of the *cis*-DCE as a substrate, is represented and compared to the Abe *et al.* (2009) slope obtained for the same compound and degraded through reductive dechlorination by the mixed culture KB-1. Error bars in A and B represent the total instrumental uncertainty of 0.5‰ and 0.2‰ for compound-specific carbon and chlorine isotope measurements respectively.

In order to evaluate the potential use of the dual element isotope plot to discriminate between abiotic and biotic degradation reactions, a comparison of our data obtained with ZVI to literature dual element isotope data on biodegradation was attempted. Only *cis*-DCE data was available at the moment of publication of this work, thus, the dual element isotope plot could be compared to data of Abe *et al.* (2009) on reductive dechlorination by the mixed culture KB-1. The slope of 3.1 ± 0.2 observed in our experiments was 4 times smaller than that observed by

Abe *et al.* (2009) (12.5) (Figure 3.3B), giving potential to this technique as a way to discriminate biodegradation and abiotic reductive dechlorination from a PRB in the field.

A second approach to distinguish abiotic from biotic chlorinated ethenes degradation was studied from the carbon isotope ratios of *cis*-DCE, ethene and ethane as daughter products. Figure 3.4 shows that products initially had less ^{13}C compared to their parent compound, but subsequently showed a trend towards an increase in ^{13}C reflecting the enrichment trend of the precursor substrate. VC concentrations were too small for precise carbon isotope analysis. The product-specific isotope fractionation ($\epsilon_{\text{substrate} \rightarrow \text{product}}$) calculated according to Equation 1.14, revealed a remarkable difference of about 10‰ between β -dichloroelimination (ethene, ethane) and hydrogenolysis (*cis*-DCE) products (Figure 3.4 and Annex A; Table 1).

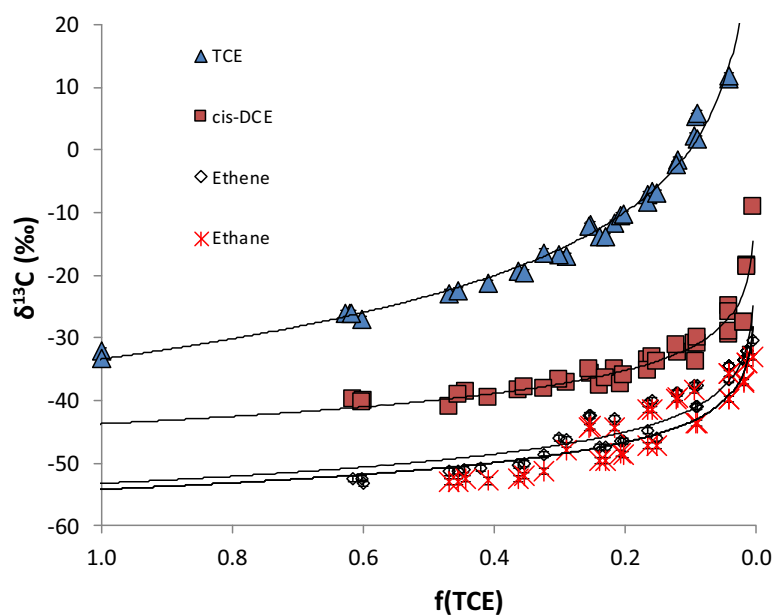


Figure 3.4. Isotope values of TCE and its by-products, with a 10‰ isotope difference between hydrogenolysis *cis*-DCE byproduct and β -dichloroelimination ethene and ethane by-products. Curves are fits of the data according to Equations 1.14 and 1.15. Error bars represent the total instrumental uncertainty of 0.5‰ for compound-specific carbon isotope measurements.

Previous studies (Elsner *et al.*, 2008) also observed a 10‰ difference in $\delta^{13}\text{C}$ of products formed with ZVI, therefore the pattern observed can be confirmed. Elsner *et al.*, (2008, 2010) already proposed that these parallel product curves may be considered characteristic of abiotic degradation, since they contrast with the sequential product generation trends during biodegradation (Elsner *et al.*, 2008). Our study, therefore, confirmed the potential of product isotope values to distinguish biotic from abiotic degradation with ZVI and to serve as an indicator of abiotic degradation processes in the field.

3.1.2 ZVI-PRB field-scale application assessment

Biodegradation was clearly evidenced at the site through carbon isotope shifts observed along the creek and the carbon isotope fractionation over time at some points (see Chapter 2; section 2.1.3). Moreover, the comparison of the lowest $\delta^{13}\text{C}$ of PCE and TCE values (-21.6 and -23.4‰, respectively) (Fig. 2.2) to the $\delta^{13}\text{C}$ literature data ranges for commercial products (from -35.3 to -23.2‰ for PCE; and from -33.5 to -25.8‰ for TCE) (van Warmerdam *et al.*, 1995; Jendrzewski *et al.*, 2001; Shouakar-Stash *et al.*, 2003) showed that both PCE and TCE were enriched in ^{13}C , confirming that PCE and TCE had undergone transformation compared to the original compounds. Proofs of a higher biodegradation occurring before the barrier were observed by the most enriched in ^{13}C PCE, TCE and *cis*-DCE values. Since results showed that the low or even inappreciable degradation effect of the ZVI-PRB might be masked by the strong biodegradation occurring before the barrier, a dual isotope slope was built with carbon and chlorine isotope data in order to confirm this hypothesis. A slope of $(\epsilon_{\text{C}}/\epsilon_{\text{Cl}})$ 1.5 ± 0.1 (Fig. 3.5) was obtained. The wells located before and after the barrier followed the same trend within the 95 % confidence interval indicating the occurrence of the same process upstream and downstream of the barrier. This unique slope suggested that there was only one main process at the site. Results were compared to literature data from laboratory experiments and field studies with biotic and abiotic degradation reactions (from our previous ZVI experiments) of *cis*-DCE either as substrate or intermediate product (Abe *et al.*, 2009; Hunkeler *et al.*, 2011; Audí-Miró *et al.*, 2013) (Fig. 3.5). The closer proximity of our results to the slope of 2 obtained from Hunkeler *et al.* (2011) in a field study with *cis*-DCE as intermediate, and where *Dehalococoides* sp. were detected, points to biodegradation as the main process occurring at the site, without distinguishing the low effect of the ZVI-PRB. It has to be taken into account that the direct implication of *Dehalococoides* sp. in *cis*-DCE degradation, could not be proven in Hunkeler *et al.* (2011) study. Moreover, the slope observed in these two studies (Hunkeler *et al.*, 2011 and ours) is far from the 12.5 value obtained by Abe *et al.* (2009) by the commercially available *Dehalococoides*-containing KB-1 culture, so biodegradation in both sites could be linked to many other anaerobic microorganisms.

The obtained $\delta^{37}\text{Cl}$ data gave further insight into the isotope fractionation effects. Isotope values of PCE were always more negative than $\delta^{37}\text{Cl}$ of *cis*-DCE (Fig. 2.2 and more detailed in Fig. S5 in SI of Annex B), an effect also observed by Lojkasek-Lima, *et al.* (2012) in a field study. Lojkasek-Lima, *et al.* (2012) attributed this effect to the parent compound (in this case PCE) degradation extending beyond *cis*-DCE with the production of VC and final degradation compounds. An alternative hypothesis is that an inverse secondary chlorine isotope effect is produced during reductive dechlorination, where the product might be preferably formed by

those molecules with more ^{37}Cl atoms in the non-reacting positions, with an enriched $\delta^{37}\text{Cl}$ compared to the parent compound. This effect was also observed in our previous laboratory experiments with ZVI, with an initial enrichment in ^{37}Cl of *cis*-DCE during TCE degradation to *cis*-DCE.

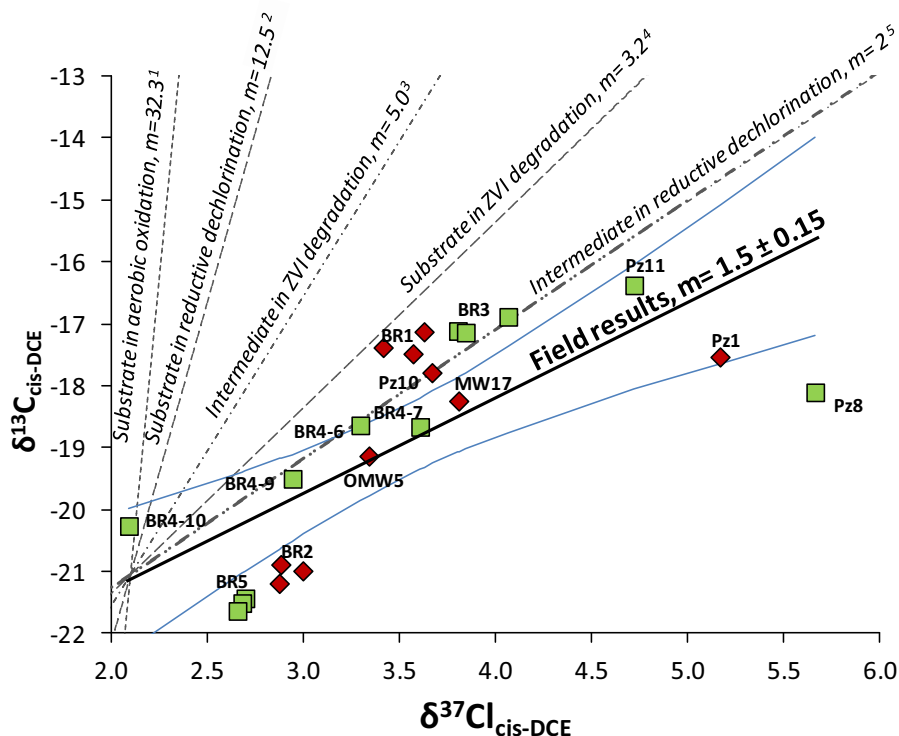


Figure 3.5. $\delta^{13}\text{C}$ versus $\delta^{37}\text{Cl}$ from Oct-12 campaign samples. A dual isotope slope ($\epsilon_{\text{C}}/\epsilon_{\text{Cl}}$) of 1.5 ± 0.1 was determined. Red diamonds represent wells upstream of the ZVI-PRB and green squares represent wells downstream the ZVI-PRB. Blue lines indicate the 95 % confidence intervals of the regression line. Dashed lines show the slopes obtained in previous studies: 1 *cis*-DCE substrate in Abe *et al.*, (2009) *β -Proteobacterium* spp. batch experiments; 2 *cis*-DCE substrate in Abe *et al.*, (2009) *Dehalococcoides* KB-1 batch experiments; 3 *cis*-DCE intermediate product in previous ZVI batch experiments (Audi-Miró, *et al.*, 2013); 4 *cis*-DCE substrate in previous ZVI degradation experiments (Audi-Miró, *et al.*, 2013); 5 *cis*-DCE intermediate in reductive dechlorination from Hunkeler *et al.*, (2011) field studies.

Since the added information from chlorine isotopes confirmed biodegradation as the main process occurring at the site, the carbon isotopic fractionation of biodegradation was chosen to determine the extent of PCE, TCE and *cis*-DCE average biodegradation of the site. To estimate the extent of the natural attenuation, the ϵ_{C} values obtained for PCE and TCE microcosm experiments ($-2.6 \pm 0.9\%$ and $-1.7 \pm 1.8\%$, respectively) were used, following Equation 1.13. Since the obtained ϵ_{C} for TCE was consistent with the literature ϵ_{C} range (-2.5 to -16%) (Bloom *et al.*, 2000; Slater *et al.*, 2001; Liang *et al.*, 2007; Abe *et al.*, 2009; Lee *et al.*, 2010), despite its high uncertainty, it was used for estimating biodegradation. As no *cis*-DCE degradation was observed in the microcosm experiments, the $\epsilon_{\text{C},\text{cis-DCE}}$ range reported in the literature (from -14.1 to -29.7%) was used (Bloom *et al.*, 2000; Slater *et al.*, 2001; Hunkeler *et al.*, 2002; Abe *et al.*, 2009; Lee *et al.*, 2010; Fletcher *et al.*, 2011). The lightest current ^{13}C signature of the parent compound PCE of the site was used as the initial isotopic composition also for TCE and *cis*-

DCE, taking into account isotopic balance of the target compounds during sequential reductive dechlorination. As the final isotopic composition, the average $\delta^{13}\text{C}$ data of all the samples was taken for each compound. The average calculated biodegradation was 48.7% for PCE, 99.9 % for TCE and between 9.2 and 18.3 % for *cis*-DCE.

Finally, since carbon, chlorine and hydrogen evidences pointed out the presence of two different sources at this site, hydrogen isotope data showed to have great potential to give further insight. By comparing the obtained $\delta^2\text{H}$ TCE value in the well OMW7 (-91‰) to available literature data, it was not as negative as expected from PCE dechlorination (-350‰) (Shouakar-Stash *et al.* 2003), neither as positive as reported manufactured TCEs (between +400 to +600‰) (Ertl *et al.*, 1998; Shouakar-Stash *et al.* 2003), thus a mixture of TCE coming from PCE dechlorination and manufactured TCE was suggested in OMW7.

TCE $\delta^2\text{H}$ was not available along the creek to compare it to OMW7 data due to low concentration, nevertheless, an approximation of $\delta^2\text{H}$ data could be calculated. First, it was necessary to calculate the $\delta^2\text{H}$ of the hydrogen added to TCE during its dechlorination to *cis*-DCE in OMW7 according to the equation proposed by Kuder *et al.* (2013)

$$\delta^2\text{H}_{\text{addition}} = (n \times \delta^2\text{H}_{\text{daughter-bulk}}) - ((n-1) \times \delta^2\text{H}_{\text{parent-bulk}}), \quad (3.1)$$

where “n” is the number of hydrogen atoms in the given daughter product, the “bulk” $\delta^2\text{H}$ refers to the average $\delta^2\text{H}$ of parent and daughter compounds, in this case, TCE and *cis*-DCE, respectively. Equation 3.1 assumes that the protonation conserves the isotope ratios of the hydrogen inherited from the parent compound, which do not undergo hydrogen isotope exchange while residing in the environment (Kuder *et al.*, 2013). Although the added hydrogen comes from the H_2 (generated from the oxidation of an organic substrate by microorganisms or abiotically at the ZVI barrier), its $\delta^2\text{H}$ is ultimately controlled by the $\delta^2\text{H}$ of the water medium since there is an equilibrium in the environment between water and this H_2 (Kuder *et al.*, 2013). The calculated value of -169‰ ($\delta^2\text{H}_{\text{addition}}$) allowed the estimation through the same equation 3.1, of the TCE $\delta^2\text{H}$ value in BR5-6 m where the *cis*-DCE $\delta^2\text{H}$ value was known, resulting in a $\delta^2\text{H}_{\text{TCE}}$ of -337‰. The presence around the barrier zone of a TCE with a very negative $\delta^2\text{H}$ confirms a different origin of this TCE and the TCE present in OMW7. Moreover, our estimated values are similar to the ones obtained by Shouakar-Stash *et al.* (2003) for a TCE from PCE dechlorination ($\delta^2\text{H}$ of around -350), suggesting that TCE is mainly coming from PCE degradation, in contrast to the TCE in OMW7.

Through Equation 3.1 the $\delta^2\text{H}$ added during *cis*-DCE transformation to ethene (with VC as intermediate) in MW17 was also calculated, resulting of -944‰. Since the measured $\delta^2\text{H}$ of our site groundwater was -37.5‰, the very depleted in ^2H hydrogen involved in the dechlorination processes, would confirm hydrogen isotope fractionation during water- H_2 equilibrium (Shouakar-Stash *et al.*, 2003; Kuder *et al.*, 2013). These $\delta^2\text{H}$ results are in the same order as the ones obtained in laboratory experiments by Kuder *et al.* (2013) (-150‰ for TCE to *cis*-DCE and -1420‰ for *cis*-DCE to ethene) for TCE biodegradation to *cis*-DCE with a mixed culture containing *Dehalococcoides* sp. and using a medium water with a quite similar $\delta^2\text{H}$ value (-42‰).

Moreover, the presented *cis*-DCE results, which to our knowledge are the first negative reported $\delta^2\text{H}$ *cis*-DCE values, contrast with the positive values (+200‰) of *cis*-DCE from reductive dechlorination of manufactured TCE in laboratory experiments (Kuder *et al.*, 2013), enhancing the evidence that *cis*-DCE comes mainly from the sequential reductive dechlorination from PCE at this site. When plotting $\delta^{13}\text{C}$ versus $\delta^2\text{H}$ of *cis*-DCE (Fig. 3.6), the difference in the TCE origin in OMW7 is evidenced again by the different trend revealed by its product *cis*-DCE regarding the rest of the wells. Although *cis*-DCE is predominantly coming from PCE, the $\delta^2\text{H}$ variability of *cis*-DCE at the wells along the creek might be the result of different contribution of certain ancient commercial TCE going also in this flow direction that provided a less negative $\delta^2\text{H}$ signature, because, according to the assumption of Equation 3.1, the $\delta^2\text{H}$ would be the same if all the *cis*-DCE came from the same parent (commercial TCE or dechlorinated PCE). This hypothesis also explains the more positive $\delta^2\text{H}$ of *cis*-DCE in comparison to TCE in BR5-6, since current TCE at this area is coming only from PCE dechlorination, and current *cis*-DCE may come from both new and ancient commercial TCE.

These results point to the significant potential of the use of $\delta^2\text{H}$ to assess the origin of industrial or degradation-derived chlorinated ethenes at contaminated sites with no other previous evidences. Despite the recently reported negative $\delta^2\text{H}$ values (up to -184‰) (Kuder *et al.*, 2013) of manufactured TCE, the high depletion in ^2H observed during TCE formation in the environment may still be a potential way to discriminate the origin of TCE and *cis*-DCE.

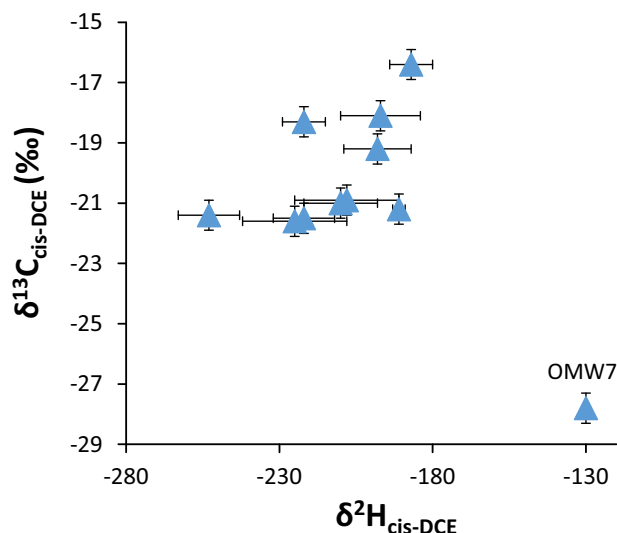


Figure 3.6. $\delta^{13}\text{C}$ versus $\delta^2\text{H}$ of *cis*-DCE in Oct-12 campaign all over the site showing a positive correlation between $\delta^2\text{H}$ and $\delta^{13}\text{C}$ shifts. Error bars represent an uncertainty of 0.5‰ for $\delta^{13}\text{C}$ and between 2 and 17‰ for $\delta^2\text{H}$ measurements. Sample from well OMW7 (-27.8 vs -130 ‰ of $\delta^{13}\text{C}$ and $\delta^2\text{H}$, respectively), does not follow the same trend as the others; see explanation in the text.

3.2. ASSESSMENT OF THE CHLOROFORM ALKALINE HYDROLYSIS INDUCED BY CONCRETE-BASED CONSTRUCTION WASTES

3.2.1 Laboratory experiments

The laboratory experiments showed that concrete particles immersed in water induced alkaline hydrolysis of CF, with 95% consumption after 28 d (Fig. 2.5). The other three alkaline treatments (chemical buffer, filtered cement and filtered concrete solutions) also showed degradation of CF, with half-lives below 15 days (Annex C; Table 1). Aside from CF, no other chlorinated volatile compounds were detected by GC-MS in scan mode. This result supports the E1_{CB} degradation mechanism of CF reported by Hine (1950), for which the final stable products were carbon monoxide (CO), formate (HCO_2^-), and chloride (Cl^-). Furthermore, excellent chlorine balances were achieved in the filtered experiments, indicating that CF was degraded without accumulation of chlorinated intermediates (Annex C; SI Fig. S6). Nevertheless, no special attempts were made to identify other potential products of CF degradation. In the experiments with concrete particles, dissimilar chlorine balances were achieved in the two duplicates (set A and set B), reflecting the variability in chloride leaching due to the heterogeneity of the concrete particles. The pseudo-first-order rate constants and half-lives obtained in this study of the hydrolysis of CF at room temperature are comparable to those calculated from the published values of Jeffers *et al.* (1989) and Fells and Fells and Moelwyn-

Hughes (1959) for pH values of 12 and 13 and a temperature range between 20 and 25 °C (Annex C; Table 1).

The lab-scale mean carbon isotopic fractionation associated with alkaline hydrolysis of CF was $-53\pm 3\%$ (Annex C; Table 2). To our knowledge, carbon isotopic fractionations associated with any abiotic CF degradation process have not been determined up to date. The AKIE obtained at the lab-scale experiments (1.056 ± 0.003) was consistent with the theoretical maximum carbon primary KIE for the C-Cl bond breakage [Streitwieser semiclassical upper limit of 1.057, Huskey (1991)]. The good correspondence between the theoretical KIE and the measured AKIE is consistent with an $E1_{CB}$ mechanism for CF alkaline hydrolysis where the C-Cl bond breakage is the rate determining step and, moreover, indicates that this type of abiotic reaction is not influenced by rate-limiting factors or masking effects due to mass transfer processes.

It is worth noting that microbial reductive dechlorination of CF by a *Dehalobacter*-containing culture resulted in a ϵ_C of $-27.5\pm 0.9\%$ (Chan *et al.*, 2012), which represents the only documented CF ϵ_C value until now. Therefore, the difference between the carbon fractionation associated with CF abiotic alkaline hydrolysis and that associated with CF anaerobic respiration might potentially be used to distinguish abiotic from biotic degradation processes at contaminated sites. The large carbon isotopic fractionation observed in the experiments implies a great potential for the use of $\delta^{13}C$ values for in situ monitoring of the degree of degradation of CF by alkaline hydrolysis. Even minor extents of degradation will result in significant carbon isotope shifts that can easily be detected by CSIA.

3.2.2 Field-scale experiments

During the entire study period (35 months), the concrete-based trenches installed in the field maintained a constant pH of 11.6 ± 0.3 in pore water confirming the longevity of concrete-based aggregates for inducing alkaline conditions. The results of the long-term field-scale pilot interception trenches, with significant ^{13}C enrichments, confirmed the capability of concrete-based construction wastes to induce alkaline hydrolysis of CF. Although the pH achieved in the field-scale experiments was slightly lower than the pH range studied in the lab-scale experiments, the independence observed between pH (from 12.0 to 12.7) and ϵ_C should allow us to estimate the extent of induced alkaline hydrolysis of CF in the field-scale experiments through the laboratory-obtained ϵ_C ($-53\pm 3\%$). However, further experiments at lower pH values should be performed to ensure this assumption. A maximum CF degradation percentage between 32 and 40% was achieved in both trenches during the two studied periods (Fig. 2.7). The efficiency in CF degradation depends on the precipitation regime. Any precipitation event could result in the entry of non-degraded contaminant leaching from the subsoil that would dilute the degradation effect. The alkaline conditions induced by the recycled

concrete-based construction wastes were restricted to the trenches and did not negatively affect the natural attenuation processes of chlorinated compounds in the aquifer below the trenches (Palau *et al.*, 2014). Actually, a concentration reduction of CF might be a key strategy for bioremediation purposes (Koenig *et al.*, 2012), because CF is a potent inhibitor of several microbial processes, such as methanogenesis or reductive dechlorination of chlorinated ethenes, the other major group of pollutants at the site (Maymó-Gatell *et al.*, 2001). Moreover, temperature has a substantial effect on the abiotic degradation rates of chlorinated compounds. The half-lives recalculated from published kinetic data at a typical groundwater temperature of 10 °C are approximately 15 times higher than those for 25 °C (Annex C; Table 1). At lower groundwater temperatures, for example 5 °C, alkaline hydrolysis of CF at pH 12 would yield a half-life of approximately 500 days (Annex C; Table 1). Therefore, temperature must be accounted for to predict the effectiveness of remediation strategies based on alkaline hydrolysis in the field. In the present field-scale experiments, the temperature remained approximately 15°C in both trenches, which was very similar to the underlying groundwater. The half-life calculated from the published values of Fells and Moelwyn-Hughes (1959) for pH 11.6 and 15 °C was 179 days, which is a promising result for the potential full implementation of this remediation approach at the site. For the mean calculated residence time of water in the trenches (513±86 and 730±190 d), a maximum theoretical percentage of degradation of approximately 90% would be achieved if there was no entry of new non-degraded contaminant leaching from the unsaturated zone by rainwater. Taking into account the maximum period without water entry into the trenches, and thus non-degraded contaminant entry (90 days, from June to October 2011, Annex C; SI Fig. S9), a maximum theoretical percentage of CF degradation of 30% can be estimated for both trenches, which is in agreement with the isotopic results. Therefore, the actual efficiency of the treatment depends on the precipitation regime and can easily be estimated by monitoring the CF isotopic composition.

Taking this into account, improvements in the design of the interception trenches can be proposed to increase the residence time in the system, such as the enlargement of the dimensions of the trenches or increasing the pH by choosing different concrete-based materials. The pH of leaching solutions of recycled concrete aggregates depends on the degree of carbonation. A study from Engelsen *et al.* (2009) on the alkaline capacity of several recycled concrete aggregates, including waste construction materials, found not only similar pH ranges as the ones observed in this study but also that a higher pH of 12.6 was reached with concrete material recycled from a highway pavement constructed in the beginning of 1980's. This material would result in a CF half-life of 18 days, which would translate into a maximum extent of degradation of 97% in the trenches during periods without the entrance of non-degraded contaminant. Monitoring of the isotopic composition would be required to estimate the actual efficiency of the treatment.

The observed carbon isotope fractionation of CT was investigated through additional laboratory batch experiments to verify the low capability of concrete to hydrolyze carbon tetrachloride since literature data pointed to extremely slow hydrolysis of CT (Jeffers *et al.*, 1989). A decrease in CT concentration over time was observed only in the experiments containing concrete particles (Annex C; SI Fig. S12), which was of 64 % after 28 d. The concentration decrease was not accompanied by any carbon isotope fractionation. Therefore, it is suggested that the heterogeneity in the specific surface area of concrete of recycled construction wastes produced CT immobilization by sorption onto the particles. Hence, the significant isotopic fractionation observed in the field-scale experiments, especially in the tank trench, could indicate the occurrence of other degradation processes distinct from alkaline hydrolysis, that may be linked to sorption or reactivity to iron minerals (Danielsen and Hayes, 2004; Elsner *et al.*, 2004; Zwank *et al.*, 2005; Lin and Liang, 2013). Further information on this is provided in the Supporting Information of Annex 3.

Chapter 4.

Conclusions

The general aim of this doctoral thesis was to use compound specific isotope analysis of ^{13}C , ^{37}Cl and ^2H to assess induced attenuation of organic contaminants in groundwater. Two induced attenuation processes were evaluated, 1) a zero valent iron permeable reactive barrier (ZVI-PRB) installed at a site contaminated with the chlorinated ethenes PCE, TCE and *cis*-DCE; and, 2) a proposed new remediation technique based on the use of concrete-based recycled construction wastes to degrade chloroform (CF) by alkaline hydrolysis.

The assessment of the efficacy of the zero valent iron permeable reactive barrier installed at the field site contaminated mainly with PCE, TCE and *cis*-DCE, was performed first at laboratory scale and the obtained results were applied at field scale.

The main conclusions derived from the initial stage of ZVI laboratory experiments were:

- Concurring hydrogenolysis and β -dichloroelimination pathways occurred as parallel reactions during chlorinated ethenes degradation by the ZVI.
- Carbon isotope fractionation values of PCE, TCE and *cis*-DCE were obtained for the specific ZVI used at the field site. Values of ϵ_{C} were of $-9.5 \pm 2.2\%$, $-13.4 \pm 1.7\%$ and $-20.5 \pm 1.8\%$, respectively.
- The first chlorine isotope fractionation data of TCE and *cis*-DCE during transformation with ZVI showed that Cl isotopes can be a new way to delineate ZVI degradation. Chlorine isotope fractionation values obtained were ϵ_{Cl} of $-2.6 \pm 0.1\%$ for TCE and of $-6.2 \pm 0.8\%$ for *cis*-DCE.

- Apparent kinetic isotope effects $AKIE_{Cl}$ of 1.008 ± 0.001 and 1.013 ± 0.002 for TCE and *cis*-DCE, respectively, indicated that (i) a C-Cl bond was broken in the rate-determining step, and (ii) the intrinsic effect was therefore not significantly masked by other processes. Hence, chlorine isotope analysis bears great potential to investigate reaction mechanisms of CAHs in future studies.
- The dual element (C, Cl) isotope plots of TCE and *cis*-DCE during degradation by ZVI, showed pronounced slope differences between our results and those of Abe *et al.* (2009) for biodegradation of *cis*-DCE by the commercially available *Dehalococcoides*-containing mixed culture KB-1. The biotic plot had a slope 4 times higher than the one from our *cis*-DCE abiotic pattern suggesting a promising new way to discriminate biodegradation and abiotic reductive dechlorination from a PRB in the field. TCE ZVI experiment gave slopes of 5.2 ± 0.3 for TCE and 5.0 ± 0.6 for *cis*-DCE as daughter product; and for the *cis*-DCE ZVI experiment of 3.1 ± 0.2 .
- Product-specific carbon isotope fractionation ($\epsilon_{\text{substrate} \rightarrow \text{product}}$) revealed a notable difference between the fractionation expressed in β -dichloroelimination (ethane, ethane) and in hydrogenolysis (*cis*-DCE) daughter products. The same difference (10‰) was observed in a previous work (Elsner *et al.*, 2008) suggesting that this product pattern is consistent and only occurs in the presence of β -dichloroelimination reactions, exclusive of abiotic degradation. Product-related carbon isotope fractionation may therefore provide a second, independent line of evidence to distinguish biotic from abiotic degradation with ZVI.
- $\delta^{13}C$ and products formation during PCE and TCE microcosms experiments revealed biodegradation at the site. ϵ_C associated to biodegradation were obtained, -2.6 ± 0.9 ‰ for PCE and -1.7 ± 1.8 ‰ for TCE. *cis*-DCE microcosm experiments, did not show any biodegradation after 500 days.

With regards to the field scale study of the ZVI-PRB the main conclusions were:

- Biodegradation was confirmed at the site using carbon isotope shifts at wells upgradient the barrier and biodegradation extent increased over time. $\delta^{13}C$ data revealed higher biodegradation occurring immediately before the barrier, suggesting a potential hydraulic barrier effect of the ZVI-PRB that could increase the compounds residence time.
- The efficiency of the barrier, calculated with the ϵ_C values obtained in the laboratory, was lower than 10 % and 2 % for PCE and *cis*-DCE, respectively. Following surveys did not show any effect of the ZVI-PRB, since the higher biodegradation detected before the barrier masked the ZVI-PRB effect.

- The dual (^{13}C - ^{37}Cl) approach ($\epsilon_{\text{C}}/\epsilon_{\text{Cl}}$ of 1.5 ± 0.1) suggested that there was only one main process at the site. The closer proximity of our results to the slope of 2 obtained from Hunkeler et al. (2011) in a field study with *cis*-DCE as intermediate and where *Dehalococcoides* sp. was detected, pointed to biodegradation as the main process occurring at the site, as expected from the low ZVI-PRB efficiency.
- Once the dominance of biodegradation at the site was confirmed, ϵ_{C} values from microcosms experiments allowed obtaining the percentage of PCE and TCE biodegradation at the site. Then, the average observed biodegradation was 48.7% for PCE, 99.9% for TCE and between 9.2 and 18.3% for *cis*-DCE [calculated from the ϵ_{C} literature data range (Bloom et al., 2000; Slater et al., 2001; Hunkeler et al., 2002; Abe et al., 2009; Lee et al., 2010; Fletcher et al., 2011)].
- Carbon, chlorine and hydrogen evidences pointed out the presence of two different sources at the site. Moreover, further insight into hydrogen isotopes data showed that, due to the high depletion in ^2H observed during TCE transformation in the environment, $\delta^2\text{H}$ has a great potential to assess the origin of industrial or degradation-derived chlorinated ethenes at contaminated sites with no other previous evidences.

The evaluation of the proposed CF alkaline hydrolysis treatment induced by concrete-based recycled construction wastes was also performed first at laboratory scale and then applied at field-scale pilot experiments.

The main conclusions of the CF degradation by alkaline hydrolysis laboratory experiments were:

- Concrete particles immersed in water induced alkaline hydrolysis of CF, with 95% consumption after 28 d. The other three alkaline treatments tested (pH 12.0-12.7) also showed degradation of CF, with half-lives below 15 days. Results indicated that no other chlorinated compounds were produced during the CF degradation.
- Carbon isotopic fractionation was detected during CF consumption, confirming CF degradation due to alkaline hydrolysis induced by concrete. The carbon isotopic fractionation associated with alkaline hydrolysis of CF was $-53 \pm 3\%$.
- To our knowledge, there are no published carbon isotopic fractionation values associated to any abiotic CF degradation processes. However, the only reported carbon isotopic fractionation of CF by a *Dehalobacter*-containing culture resulted in a ϵ_{C} of $-27.5 \pm 0.9\%$ (Chan et al., 2012). Therefore, the difference between the carbon isotopic fractionation

associated with CF abiotic alkaline hydrolysis and that associated with CF anaerobic respiration might potentially be used to distinguish abiotic from biotic degradation processes at contaminated sites.

- The large carbon isotopic fractionation observed in the experiments implies a great potential for the use of $\delta^{13}\text{C}$ values for in situ monitoring of the degree of degradation of CF by alkaline hydrolysis.
- The AKIE obtained at the lab-scale experiments (1.056 ± 0.003) is consistent with the theoretical maximum carbon primary KIE for the C-Cl bond breakage [Streitwieser semiclassical upper limit of 1.057, Huskey (1991)]. The good correspondence between the theoretical KIE and the measured AKIE is consistent with an E1_{CB} mechanism for CF alkaline hydrolysis where the C-Cl bond breakage is the rate determining step and, moreover, indicates that this type of abiotic reaction is not influenced by rate-limiting factors or masking effects due to mass transfer processes.

From the assessment of CF alkaline hydrolysis induced by concrete-based recycled construction wastes at the field-scale pilot experiments the main conclusions were:

- Significant ^{13}C enrichments confirmed the capability of concrete-based construction wastes to induce alkaline hydrolysis of CF.
- According to the obtained ϵ_{C} value ($-53\pm 3\%$), a maximum CF degradation percentage between 32 and 40% was achieved in both trenches during the two studied periods.
- At the trenches average conditions (pH 11.6 and 15°C), a CF half-life of 179 days was calculated from the published values of Fells and Moelwyn-Hughes (1959). This is a promising result for the potential full implementation of this remediation approach at the site.
- The efficiency of the CF treatment is subject to the precipitation regime, since any precipitation event could result in the entry of non-degraded contaminant leaching from the subsoil that would dilute the degradation effect. Therefore, taking into account the maximum period without water entry into the trenches (90 days), a maximum theoretical percentage of CF degradation of 30% could be estimated for both trenches, which is in agreement with the isotopic results.

Overall, by combining C, Cl and H isotopes, this thesis provided new tools to discriminate ZVI versus biodegradation at the field site, as well as to identify industrial versus product-formation contaminant sources, among other contributions. Moreover, the new proposed CF alkaline

hydrolysis induced by concrete-based recycled construction wastes, was proved to efficiently degrade this pollutant, as well as to be working on a field-scale pilot experiment monitored by the use of carbon isotopes.

These first analyses of hydrogen isotopes of chlorinated ethenes in field samples could represent the beginning of further investigation on this research line. More laboratory experiments would be necessary to better understand the protonation of the chlorinated ethenes including studies to investigate if hydrogen fractionation occurs during degradation of chlorinated compounds. On the other hand, to continue with the field study, investigation on the microbes present at the field site, responsible of the chlorinated compounds degradation would be also interesting in the sense that the obtained dual ^{13}C - ^{37}Cl isotope slope would be characteristic of that specific microbiota and could be therefore used in other sites with similar microbial population.

Finally, regarding CF hydrolysis induced by concrete-based recycled construction wastes, its application should be further developed in order to obtain its maximum benefit, by designing systems that increase compound residence time, or that reach higher pH. The use of concrete-based recycled construction wastes as the reactive material of permeable reactive barriers would be an interesting application in future studies.

Bibliography

Abe, Y.; Aravena, R.; Zopfi, J.; Shouakar-Stash, O.; Cox, E.; Roberts, J.D.; Hunkeler, D. Carbon and chlorine isotope fractionation during aerobic oxidation and reductive dechlorination of vinyl chloride and *cis*-1,2-dichloroethene. *Environ. Sci. Technol.* **2009**, 43, 101-107

Agència Catalana de l'Aigua. Àrea d'Inspecció i Control. Departament de Medi Ambient. Generalitat de Catalunya. Mostreig d'aigües subterrànies de la riera de Cal Jorba a Òdena. AIC-F-001. Barcelona, **2002**

Agència Catalana de l'Aigua. Departament de Medi Ambient. Generalitat de Catalunya. Estudi d'un episodi de contaminació per PCE als pous de la riera de Sant Pol. Sant Pol de Mar. Girona, **2003**

Agència de Residus de Catalunya. Departament de Medi Ambient. Generalitat de Catalunya. Tasques de mostreig i gestió de sòls contaminats a les instal·lacions de l'antiga HIGHTEX al terme municipal Òdena. Barcelona, **2007**

Amonette, J. E.; Jeffers, P. M.; Qafoku, O.; Russell, C. K.; Humphrys, D. R.; Wietsma, T. W.; Truex, M. J. Abiotic degradation rates for carbon tetrachloride and chloroform: Progress in FY 2010; PNNL-20044, Pacific Northwest National Laboratory: Richland, WA, **2010**

Amonette, J. E.; Jeffers, P. M.; Qafoku, O.; Russell, C. K.; Humphrys, D. R.; Wietsma, T. W.; Truex, M. J. Abiotic degradation rates for carbon tetrachloride and chloroform: Final report. PNNL-22062 RPT-DVZ-AFRI-012. Pacific Northwest National Laboratory: Richland, WA, **2012**

Arnold, W. A.; A. L. Roberts. Pathways of chlorinated ethylene and chlorinated acetylene reaction with Zn(0). *Environ. Sci. Technol.* **1998**, 32, 3017-3025

Arnold, W.A.; Roberts, A.L. Pathways and kinetics of chlorinated ethylene and chlorinated acetylene reaction with Fe(0) particles. *Environ. Sci. Technol.* **2000**, 34, 1794-1805

Audí-Miró, C.; Cretnik, S.; Otero, N.; Palau, J.; Shouakar-Stash, O.; Soler, A.; Elsner, M. Cl and C isotope analysis to assess the effectiveness of chlorinated ethene degradation by zero-valent iron: Evidence from dual element and product isotope values. *Appl. Geochem.* **2013**, 32, 175-183

Bhandari, A.; Surampalli, R.Y.; Champagne, P.; Ong, S.K.; Tyagi, R.D.; Lo, I.M.C. Remediation technologies for soils and groundwater. American Society of Civil Engineering (ASCE) publication. **2007**, ISBN-13: 978-0-7844-0894-0

Birke, V.; Burmeier, H.; Jefferis, S.; Gaboriau, H.; Touzé, S.; Chartier, R. Permeable reactive barriers in Europe (PRBs): Potentials and expectations. *Italian Journal of Engineering Geology and Environment.* **2007**. Special Issue 1 of the Trans-it kick-off meeting. Villa Vigoni, Lago di Como, 3-4 April 2006

Blessing, M.; Schmidt, T.C.; Dinkel, R.; Haderlein, S.B. Delineation of multiple chlorinated ethene sources in an industrialized area: A forensic field study using Compound-Specific Isotope Analysis. *Environ. Sci. Technol.* **2009**, 43 (8), 2701–2707

Bloom, Y.; Aravena, R.; Hunkeler, D.; Edwards, E.; Frape, S.K. Carbon isotope fractionation during microbial dechlorination of trichloroethene, *cis*-1,2-dichloroethene, and vinyl chloride: Implications for assessment of natural attenuation. *Environ. Sci. Technol.* **2000**, 34, 2768-2772

Blowes, D.W.; Ptacek, C.J.; Benner, S.G.; McRae, C.W.T.; Bennett, T.A.; Puls, R.W. Treatment of inorganic contaminants using permeable reactive barriers. *J. Contam. Hydrol.* **2000**, 45, 123-137

Bondgaard, M.; Hvidberg, B.; Melvej, A.; Ruegg, K.; Ernst, L.; Damgaard, T.; Fredborg, H.; Rügge, K.; Nissen, L.; Jorgensen, T.H.; Bennedsen, L.; Mackinnon, L.; Durant, N.; Thomas, M.; Petrovskis, E. "NorthPestClean". A large-scale demonstration project of in situ alkaline hydrolysis. In Book of abstracts of the 12th International UFZ-Deltares Conference on Groundwater-Soil-Systems and Water Resource Management, Barcelona. **2013**, 139

Bruckner, R. Advanced organic chemistry: Reaction mechanisms; Academic Press: New York, NY, **2002**

Cappelletti, M.; Frascari, D.; Zannoni, D.; Fedi, S. Microbial degradation of chloroform. *Appl. Microbiol. Biot.* **2012**, 96, 1395–1409

Chan, C. C. H.; Mundle, S. O. C.; Eckert, T.; Liang, X.; Tang, S.; Lacrampe-Couloume, G.; Edwards, E. A.; Sherwood-Lollar, B. Large carbon isotope fractionation during biodegradation of chloroform by *Dehalobacter* cultures. *Environ. Sci. Technol.* **2012**, 46, 10154-10160

Church, C.D.; Pankow, J.F.; Tratnyek, P.G. Hydrolysis of tert-butyl formate: Kinetics, products, and implications for the environmental impact of methyl tert-butyl ether. *Environ. Toxicol. Chem.* **1999**, 18 (12), 2789-2796

Danielsen, K. M.; Hayes, K. F. pH dependence of carbon tetrachloride reductive dechlorination by magnetite. *Environ. Sci. Technol.* **2004**, 38, 4745-4752

Dayan, H.; Abrajano, T.; Sturchio, N.C.; Winsor, L. Carbon isotopic fractionation during reductive dehalogenation of chlorinated ethenes by metallic iron. *Org Geochem.* **1999**, 30, 755-763

Doherty, R.E. A history of the production and use of carbon tetrachloride, tetrachloroethylene, trichloroethylene and 1,1,1-trichloroethane in the United States: Part 2 - trichloroethylene and 1,1,1-trichloroethane. *Journal of Environmental Forensics*, **2000**, 1, 83-93

Dybala-Defratyka, A., Rostkowski, M., Matsson, O., Westaway, K.C., Paneth, P. A new interpretation of chlorine leaving group kinetic isotope effects; a theoretical approach. *J. Org. Chem.* **2004**, 69, 4900-4905

Dybala-Defratyka, A., Szatkowski, L., Kaminski, R., Wujec, M., Siwek, A., Paneth, P. Kinetic isotope effects on dehalogenations at an aromatic carbon. *Environ. Sci. Technol.* **2008**, 42, 7744-7750

Elsner, M.; Haderlein, S. B.; Kellerhals, T.; Luzi, S.; Zwank, L.; Angst, W.; Schwarzenbach, R. P. Mechanisms and products of surface-mediated reductive dehalogenation of carbon tetrachloride by Fe(II) on goethite. *Environ. Sci. Technol.* **2004**, 38(7), 2058-2066

Elsner, M.; Zwank, L.; Hunkeler, D.; Schwarzenbach, R.P. A new concept linking observable stable isotope fractionation to transformation pathways of organic pollutants. *Environ. Sci. Technol.* **2005**, 39 (18), 6896-6916

Elsner, M.; Chartrand, M.; Vanstone, N.; Lacrampe-Couloume, G; Sherwood Lollar, B. Identifying abiotic chlorinated ethene degradation: characteristic isotope patterns in reaction products with nanoscale zero-valent iron. *Environ. Sci. Technol.* **2008**, 42, 5963-5970

Elsner, M. Stable isotope fractionation to investigate natural transformation mechanisms of organic contaminants: principles, prospects and limitations. *J. Environ. Monit.* **2010**, 12 (11), 2005-2031

Elsner, M; Jochmann, M.A.; Hofstetter, T.B.; Hunkeler, D.; Bernstein, A.; Schmidt, T.C.; Schimmelmann, A. Current challenges in compound-specific stable isotope analysis of environmental organic contaminants. *Anal. Bioanal. Chem.* **2012**, 403, 2471-2491

Emmrich, M. Kinetics of the alkaline hydrolysis of important nitroaromatic co-contaminants of 2,4,6-Trinitrotoluene in highly contaminated soils. *Environ. Sci. Technol.* **2001**, 35(5), 874-877

Engelsen, C.J.; van der Sloot, H.A.; Wibetoe, G.; Petkovic, G.; Stoltenberg-Hansson, E.; Lund, W. Release of major elements from recycled concrete aggregates and geochemical modeling. *Cement Concrete Res.* **2009**, 39, 446-459

Ertl, S.; Seibel, F.; Eichinger, L.; Frimmel, F. H.; Kettrup, A. The C-13/C-12 and H-2/H-1 ratios of trichloroethene, tetrachloroethene and their metabolites. *Isot. Environ. Health Stud.* **1998**, 34 (3), 245-253

España. Real Decreto 140/2003, de 7 febrero. Boletín Oficial del Estado, 21 de febrero **2003**, 45, 7228-7245

Farrel, J.; Kason, M.; Melitas, N.; Li, Tie. Investigation of the long-term performance of zero-valent iron for reductive dechlorination of trichloroethylene. *Environ. Sci. Technol.* **2000**, 34, 514-521

Fells, I.; Moelwyn-Hughes, E. A. The kinetics of the hydrolysis of the chlorinated methanes. *J. Chem. Soc.* **1959**, 398-409

Fletcher, K.E.; Nijenhuis, I.; Richnow; H-H.; Löffler, F.E. Stable carbon isotope enrichment factors for *cis*-1,2-dichloroethene and vinyl chloride reductive dechlorination by dehalococoides. *Environ. Sci. Technol.* **2011**, 45, 2951-2957

Flynn, S.; Löffler, F.; Tiedje, J. Microbial community changes associated with a shift from reductive dechlorination of PCE to reductive dechlorination of *cis*-DCE and VC. *Environ. Sci. Technol.* **2000**, 34(6), 1056-1061

Friis, A.K.; Albrechtsen, H.J.; Cox, E.; Bjerg, P.L. The need for bioaugmentation after thermal treatment of a TCE-contaminated aquifer: Laboratory experiments. *J Contam Hydrol.* **2006**, 88 (3-4), 235-48

FRTR. Federal Remediation Technologies Roundtable website. Federal Remediation Technologies Screening Matrix and Reference Guide, Version 4.0. <http://www.frtr.gov/scrntools.htm>. Updated in **2007**

Gillham, R. W.; O'Hannesin, S.F. Metal-catalysed abiotic degradation of halogenated organic compounds. Proceedings of the 1992 IAH Conference Modern Trends in Hydrogeology, May, Hamilton, Ontario, **1992**, 10-13

Gillham, R.W., O'Hannesin, S.F. Enhanced degradation of halogenated aliphatics by zero-valent iron. *Ground Water.* **1994**, 32, 958-967

Golab, A. N.; Peterson, M. A.; Indraratna, B. Selection of potential reactive materials for a permeable reactive barrier for remediating acidic groundwater in acid sulphate soil terrains. *Q. J. Eng. Geol. Hydroge.* **2006**, 39, 209-223

Grosterm, A.; Duhamel, M.; Dworatzek, S.; Edwards, E. Chloroform respiration to dichloromethane by a Dehalobacter population. *Environ. Microbiol.* **2010**, 12, 1053-1060

Gu, B.; Awatson, D.; Wu, L.; Phillips, D.; White, D.; Zhou, J. Microbiological characterization in a zero-valent-iron reactive barrier. *Environ. Monit. Assess.* **2002**, 77, 293-307

Guillon, A.; Ménach, K.L.; Flaud, P.-M.; Marchand, N.; Budzinski, H.; Villenave, E. Chemical characterization and stable carbon isotopic composition of particulate Polycyclic Aromatic Hydrocarbons issued from combustion of 10 Mediterranean woods. *Atmos. Chem. Phys.* **2013**, *13*, 2703-2719

Hansen, J.; Sallmén, M.; Seldén, A.I.; Anttila, A.; Pukkala, E.; Andersson, K.; Bryngelsson, I.-L. Risk of cancer among workers exposed to trichloroethylene: Analysis of three nordic cohort studies. Oxford University Press. DOI:10.1093/jnci/djt107. **2013**

Henderson, A.D.; Demond, A.H. Long-term performance of zero-valent iron permeable reactive barriers: A critical review. *Environ. Eng. Sci.* **2007**, *24*, 401-427

Hine, J. Carbon dichloride as an intermediate in the basic hydrolysis of chloroform. A mechanism for substitution reactions at a saturated carbon atom. *J. Am. Chem. Soc.* **1950**, *72*, 2438-2445

Hofstetter, T.B., Reddy, C.M., Heraty, L.J., Berg, M., Sturchio, N.C. Carbon and chlorine isotope effects during abiotic reductive dechlorination of polychlorinated ethanes. *Environ. Sci. Technol.* **2007**, *41*, 4662-4668

Huling, S. G.; Pivetz, B. E. In situ chemical oxidation-Engineering issue. EPA/600/R-06/072. U.S. Environmental Protection Agency Office of Research and Development, National Risk Management Research Laboratory: Cincinnati, OH, **2006**

Hunkeler, D.; Aravena, R.; Butler, B.J. Monitoring microbial dechlorination of tetrachloroethene (PCE) using compound- specific carbon isotope ratios: Microcosms and field experiments. *Environ. Sci. Technol.* **1999**, *33*(16), 2733-2738

Hunkeler, D.; Aravena, R.; Cox, E. Carbon isotopes as a tool to evaluate the origin and fate of vinyl chloride: Laboratory experiments and modeling of isotope evolution. *Environ. Sci. Technol.* **2002**, *36* (15), 3378-3384

Hunkeler, D.; Chollet, N.; Pittet, X.; Aravena, R.; Cherry, J.A.; Parker, B.L. Effect of source variability and transport processes on carbon isotope ratios of TCE and PCE in two sandy aquifers. *J. Contam. Hydrol.* **2004**, *74*(1-4), 265-282

Hunkeler, D.; Meckenstock, R.U.; Sherwood Lollar, B.; Schmidt, T.C.; Wilson, J.T. A guide for assessing biodegradation and source identification of organic ground water contaminants using Compound Specific Isotope Analysis (CSIA). Office of Research and Development. US EPA, Oklahoma, USA, **2008**

Hunkeler, D., Van Breukelen, B.M., Elsner, M. Modeling chlorine isotope trends during sequential transformation of chlorinated ethenes. *Environ. Sci. Technol.* **2009**, *43*, 6750-6756

Hunkeler, D.; Abe, Y.; Broholm, M.M.; Jeannotat, S.; Westergaard, C.; Jacobsen, C.S.; Aravena, R.; Bjerg, P.L. Assessing chlorinated ethene degradation in a large scale contaminant

plume by dual carbon–chlorine isotope analysis and quantitative PCR. *J. Contam. Hydrol.* **2011**, 119, 69–79

Huskey, W.P. Enzyme mechanism from isotope effects. In *Enzyme mechanism from isotope effects*; Cook, P. F., Ed.; CRC Press: Boca Raton, FL, **1991**; pp. 37-72

Hwang, I.; Batchelor, B. Reductive dechlorination of tetrachloroethylene by Fe(II) in cement slurries. *Environ. Sci. Technol.* **2000**, 34(23), 5017-5022

Hwang, I.; Batchelor, B. Reductive dechlorination of chlorinated methanes in cement slurries containing Fe(II). *Chemosphere.* **2002**, 48, 1019-1027

Hwang, S.; Ruff, T. J.; Bouwer, E. J.; Larson, S. L.; Davis, J.L. Applicability of alkaline hydrolysis for remediation of TNT-contaminated water. *Water Res.* **2005**, 39, 4503-4511

Hwang, S.; Felt, D. R.; Bouwer, E. J.; Brooks, M.C., Larson, S.L., Davis, J.L. Remediation of RDX-contaminated water using alkaline hydrolysis. *J. Environ. Eng.* **2006**, 132(2), 256-262

IARC. International agency for research on cancer. Monographs on the Evaluation of Carcinogenic Risks to Humans. Dry Cleaning, Some Chlorinated Solvents and Other Industrial Chemicals. **1995**, volume 63

Interstate technology Regulatory council (ITRC). Permeable reactive barriers: Lessons learned/new directions. **2005**

Interstate technology regulatory council (ITRC). Permeable reactive barrier: Technology update. **2011**

Jeffers, P. M.; Ward, L. M.; Woytowlitch, L. M.; Wolfe, N. L. Homogeneous hydrolysis rate constants for selected chlorinated methanes, ethanes, ethenes, and propanes. *Environ. Sci. Technol.* **1989**, 23(8), 965-969

Jendrzewski, N.; Eggenkamp, H.G.M.; Coleman, M.N. Characterization of chlorination hydrocarbons from chlorine and carbon isotopic compositions: scope of application to environmental problems. *Appl. Geochem.* **2001**, 16, 1021-1031

Johnson, T.L.; Sherer, M.M.; Tratnyek P.G. Kinetics of halogenated organic compound degradation by iron metal. *Environ. Sci. Technol.* **1996**, 30, 2634-2640

Karakaya, P.; Sidhoum, M.; Christodoulatos, C.; Nicolich, S.; Balas, W. Aqueous solubility and alkaline hydrolysis of the novel high explosive hexanitrohexaazaisowurtzitane (CL-20). *J. Hazard Mater.* **2005**, 120, 183-191

- Koenig, J. C.; Lee, M. J.; Manefield, M. Successful microcosm demonstration of a strategy for biodegradation of a mixture of carbon tetrachloride and perchloroethene harnessing sulfate reducing and dehalorespiring bacteria. *J. Hazard. Mater.* **2012**, 219-220, 169-175
- Kuder, T; van Breukelen, B.M.; Vanderford, M.; Philp, P. 3D-CSIA: Carbon, chlorine, and hydrogen isotope fractionation in transformation of tce to ethene by a dehalococcoides culture. *Environ. Sci. Technol.* **2013**, 47, 9668-9677
- Lampron, K.J.; Chiu, P.C.; Cha, D.K. Reductive dehalogenation of chlorinated ethenes with elemental iron: the role of microorganisms. *Water Res.* **2001**, 35 (13), 3077–3084
- Lee, J.W.; Cha, D.K.; Oh, Y.K.; Ko, K.B.; Jin, S.H. Wastewater screening method for evaluating applicability of zero-valent iron to industrial wastewater. *J. Hazard. Mater.* **2010**, 180, 354-360
- Lee, M.; Low, A.; Zemb, O.; Koenig, J.; Michaelsen, A.; Manefield, M. Complete chloroform dechlorination by organochlorine respiration and fermentation. *Environ. Microbiol.* **2012**, 14(4), 883-894
- Liang, X.; Dong, Y.; Kuder, T.; Krumholz, L. R.; Philp, R. P.; Butler, E. C. Distinguishing abiotic and biotic transformation of tetrachloroethylene and trichloroethylene by stable carbon isotope fractionation. *Environ. Sci. Technol.* **2007**, 41 (20), 7094-7100
- Lin, Y-T.; Liang, C. Carbon tetrachloride degradation by alkaline ascorbic acid solution. *Environ. Sci. Technol.* **2013**, 47, 3299-3307
- Lin, C.J.; Lo, S.L. Effects of iron surface pretreatment on sorption and reduction kinetics of trichloroethylene in a closed batch system. *Water Res.* **2005**, 39, 1037–1046
- Lo, I.; Surampalli, R.; Lai, K,C.K. Configuration and Construction of Zero-Valent Iron Reactive Barriers. Chapter 13 in: ASCE. Zero-valent iron reactive materials for hazardous waste and inorganics removal. Sponsored by Hazardous, Toxic, and Radioactive Waste Management Committee, Environmental and Water Resources Institute (EWRI) of the American Society of Civil Engineers. **2002**
- Lojkasek-Lima, P.; Aravena, R.; Parker, B.; Cherry, J.A. Fingerprinting TCE in a Bedrock Aquifer Using Compound-Specific Isotope Analysis. *Ground Water Monit. R.* **2012**, 32 (4), 53-62
- Mabey, W.; Mill, T. Critical review of hydrolysis of organic compounds in water under environmental conditions. *J. Phys. Chem. Ref. Data.* **1978**, 7(2), 383-415
- Mariotti, A.; Germon, J.C.; Hubert, P.; Kaiser,P.; Letolle,R.; Tardieux, A.; Tardieux, P. Experimental determination of nitrogen kinetic isotope fractionation: some principles; illustration for the denitrification and nitrification processes. *Plant Soil.* **1981**, 62, 413–430

Matheson, L.J.; Tratnyek, P.G.; Reductive dehalogenation of chlorinated methanes by iron metal. *Environ. Sci. Technol.* **1994**, 28, 2045–2053

Maymó-Gatell, X.; Nijenhuis, I.; Zinder, S. H. Reductive dechlorination of *cis*-1,2-dichloroethene and vinyl chloride by *Dehalococcoides ethenogenes*. *Environ. Sci. Technol.* **2001**, 35(3), 516-521

Mazeas, L.; Budzinski, H.; Raymond, N. Absence of stable carbon isotopic fractionation of saturated and polycyclic aromatic hydrocarbons during aerobic bacterial biodegradation. *Org. Geochem.* **2002**, 33, 1259-1272

Meckenstock, R.U.; Morasch, B.; Warthmann, R.; Schink, B.; Annweiler, E.; Michaelis, W.; Richnow, H.H. ¹³C/¹²C isotope fractionation of aromatic hydrocarbons during microbial degradation. *Environ. Microbiol.* **1999**, 1(5):409–414

Meckenstock, R.U.; Morasch, B.; Griebler, C.; Richnow, H.H. Stable isotope fractionation analysis as a tool to monitor biodegradation in contaminated aquifers. *J. Contam. Hydrol.* **2004**, 75(3– 4):215–255

Miyamoto, K.; Urano, K. Reaction rates and intermediates of chlorinated organic compounds in water and soil. *Chemosphere.* **1996**, 32(12), 2399-2408

NorthPestClean. Demonstration of in situ alkaline hydrolysis as a new technology for remediation of pesticide contaminated soil and groundwater. Technical pamphlet of the LIFE09 ENV/DK/000368 project. **2013**, 12

O'Hannesin, S. F.; Gillham, R.W. Long-term performance of an in situ "iron wall" for remediation of VOCs. *Ground Water.* **1998**, 36 (1), 164-170

Palau, J.; Soler, A.; Teixidor, P.; Aravena, R. Compound-specific carbon isotope analysis of volatile organic compounds in water using solid-phase micro-extraction. *J. Chromatogr.* **2007**, 1163, 260-268

Palau, J.; Marchesi, M.; Chambon, J.C.C.; Aravena, R.; Canals, À.; Binning, P.J.; Bjerg, P.L.; Otero, N.; Soler, A. Multi-isotope (Carbon and Chlorine) analysis for fingerprinting and site characterization at a fractured bedrock aquifer contaminated by chlorinated ethenes. *Sci. Total Environ.* **2014**, 475, 61-70

Pankow, J.F; Cherry, J.A. Dense chlorinated solvents and other DNAPLs in groundwater. 1st ed. Portland, Oregon. Waterloo Press., **1996**. ISBN: 0964801418

Lee, J.W.; Cha, D.K.; Oh, Y.K.; Ko, K.B.; Jin, S.H. Wastewater screening method for evaluating applicability of zero-valent iron to industrial wastewater. *J. Hazard. Mater.* **2010**, 180, 354-360

Leeson, A.; Beevar, E.; Henry, B.; Fortenberry, J.; Coyle, C. Principles and practices of enhanced anaerobic bioremediation of chlorinated solvents. Prepared for: Air Force Center for Environmental Excellence Brooks City-Base, Texas Naval Facilities Engineering Service Center Port Hueneme, California and Environmental Security Technology Certification Program Arlington, Virginia. **2004**

PEREBAR. Long-term performance of permeable reactive barriers used for the remediation of contaminated groundwater. Literature review: Reactive materials and attenuation processes for permeable reactive barriers. National Technical University of Athens Department of Mining and Metallurgical Engineering Laboratory of Metallurgy GR-157 80, Zografos, Athens, Greece. PEREBAR EVK1-CT-1999-00035. **2000**

Prommer, H.; Aziz, L.H.; Bolaño N.; Taubald, H.; Schüth, C. Modelling of geochemical and isotopic changes in a column experiment for degradation of TCE by zero-valent iron. *J. Contam. Hydrol.* **2008**, 97, 13–26

Puls, R.W.; Blowes, D.W.; Gillham, R.W. Long-term performance monitoring for a permeable reactive barrier at the U.S. Coast Guard Support Center, Elizabeth City, North Carolina. *J. Hazard. Mater.* **1999**, 68, 109–124

Reddy, K.R. Physical and chemical groundwater remediation technologies. In Darnault, C.G.J. Overexploitation and contamination of shared groundwater resources. ISBN: 978-1-4020-6983-3 (Print) 978-1-4020-6985-7 (Online). **2008**

Roberts, L.; Totten, L.A.; Arnold, W.; Burris, D.R.; Campbell, T.J. Reductive elimination of chlorinated ethylenes by zero-valent metals. *Environ. Sci. Technol.* **1996**, 30 (8) 2654-2659

Sarathy, V.; Salter, A.J.; Nurmi, J.T.; O'Brien Johnson, G.; Johnson, R.L.; Tratnyek, P.G. Degradation of 1,2,3-trichloropropane (TCP): hydrolysis, elimination, and reduction by iron and zinc. *Environ. Sci. Technol.* **2010**, 44(2), 787-93

Scherer, M.M.; Richter, S.; Valentine, R.L.; Alvarez, P.J.J. Chemistry and Microbiology of Permeable Reactive Barriers for In Situ Groundwater *Clean up. Cr. Cr. Rev. Microbiol.* **2000**, 26(4), 221–264

Schmidt, K.R.; Augenstein, T.; Heidinger, M.; Ertl, S.; Tiehm, A. Aerobic biodegradation of *cis*-1,2-dichloroethene as sole carbon source: Stable carbon isotope fractionation and growth characteristics. *Chemosphere.* **2010**, 78, 527-532

Schwarzenbach, R.P., Gschwend, P.M., Imboden, D.M. Environmental organic chemistry. 2nd edition; John Wiley & Sons: Hoboken, NJ, **2003**

Shan, H.; Kurtz, Jr, H. D.; Freedman, D. L. Evaluation of strategies for anaerobic bioremediation of high concentrations of halomethanes. *Water Res.* **2010**, 44, 1317-1328

- Sherwood-Lollar, B.; Slater, G.F.; Ahad, J.; Sleep, B.; Spivack, J.; Brennan, M.; MacKenzie, P. Contrasting carbon isotope fractionation during biodegradation of trichloroethylene and toluene: implications for intrinsic bioremediation. *Org. Geochem.* **1999**, 30(8), 813–820
- Shouakar-Stash, O.; Frappe, S.K.; Drimmie, R.J. Stable hydrogen, carbon and chlorine isotope measurements of selected chlorinated organic solvents. *J. Contam. Hydrol.* **2003**, 60, 211- 228
- Shouakar-Stash, O.; Drimmie, R.J.; Zhang, M.; Frappe, S.K. Compound-specific chlorine isotope ratios of TCE, PCE and DCE isomers by direct injection using CFIRMS. *Appl. Geochem.* **2006**, 21, 766-781
- Shouakar-Stash, O.; Drimmie, R.J. Online methodology for determining compound-specific hydrogen stable isotope ratios of trichloroethene and 1,2-*cis*-dichloroethene by continuous-flow isotope ratio mass spectrometry. *Rapid Commun. Mass Spectrom.* **2013**, 27, 1335-1344
- Slater, G.F.; Sherwood-Lollar, B.; Sleep, B.; Edwards, E. Variability in carbon isotopic fractionation during biodegradation of chlorinated ethenes: implications for field applications. *Environ. Sci. Technol.* **2001**, 35, 901-907
- Slater, G.F.; Sherwood-Lollar, B.; King, A.; O'Hannesin, S. Isotopic fractionation during reductive dechlorination of trichloroethene by zero-valent iron: influence of surface treatment. *Chemosphere.* **2002**, 49, 587-596
- Su, T.-L.; Christodoulatos, C. Destruction of nitrocellulose using alkaline hydrolysis. In Proceedings of the Tri-Service Environmental Technology Workshop, Hershey, PA. **1996**; 337-343
- Su, C.; Puls, R.W. Kinetics of trichloroethene reduction by zerovalent iron and tin: Pretreatment effect, apparent activation energy, and intermediate products. *Environ. Sci. Technol.* **1999**, 33, 163-168
- Suk, Jin.; Jeon, S.-W.; Gillham, R.W.; Gui, L. Effects of initial iron corrosion rate on long-term performance of iron permeable reactive barriers: column experimnts and numerical simulation. *J. Contam. Hydrol.* **2009**, 103, 145-156
- Suthersan, S.S. In situ bioremediation. Remediation engineering: Design concepts. Ed. Suthan S. Suthersan Boca Raton: CRC Press LLC. **1999**
- Thiruvengkatachari, R.; Vigneswaran, S.; Naidu, R. Permeable reactive barrier for groundwater remediation. *J. Ing. Eng. Chem.* **2008**, 14, 145-156
- U.S. EPA. Permeable reactive barrier technologies for contaminant remediation. Office of Solid Waste and Emergency Response Washington DC. **1998**. EPA/600/R-98/125

U.S. EPA. Engineered approaches to in situ bioremediation of chlorinated solvents: Fundamentals and field applications. Office of Solid Waste and Emergency Response. Division of Solid Waste and Emergency Response. **2000**. EPA 542-R-00-008

U.S. EPA. Field application of a permeable reactive barrier for treatment of arsenic in ground water. Environmental Protection Agency. Office of Research and Development National Risk Management Research Laboratory, Ada, OK. **2008**. EPA 600/R-08/093

U.S. EPA. Environmental Protection Agency. National primary drinking water regulations. EPA 816-F-09-004, **2009**. <http://water.epa.gov/drink/contaminants/upload/mcl.pdf>.

U.S. EPA. Environmental Protection Agency. Website: <http://www.epa.gov/oust/cat/mna.htm>. Consulted December **2012**

U.S. EPA. Ground water and ecosystems restoration research. Environmental Protection Agency. In situ chemical oxidation. Website: <http://www.epa.gov/ada/gw/isco.html>. Consulted February **2014**

Valiev, M.; Garrett, B. C.; Tsai, M. -K.; Kowalski, K.; Kathmann, S. M.; Schenter, G. K.; Dupuis, M. Hybrid approach for free energy calculations with high-level methods: Application to the SN₂ reaction of CHCl₃ and OH⁻ in water. *J. Chem. Phys.* **2007**, 127, 051102-1-4

Vanstone, N.A; Focht, R.M.; Mabury, S.A.; Sherwood-Lollar, B. Effect of iron type on kinetics and carbon isotopic enrichment of chlorinated ethylenes during abiotic reduction on Fe(0). *Ground Water*. **2004**, 42, 268–276

van Warmerdam, E.M.; Frappe, S.K.; Aravena, R.; Drimmie, R.J.; Flatt, H.; Cherry, J.A. Stable chlorine and carbon isotope measurements of selected chlorinated organic solvents. *Appl. Geochem.* **1995**, 10, 547-552

Vogel, T.M. Natural bioremediation of chlorinated solvents. In Handbook of Bioremediation; Norris, R.D., Hincee, R.E., Brown, R., McCarty, P.L., Semprini, L., Wilson, J.T., Kampbell, D.H., Reinhard, M., Bouwer, E.J., Borden, R.C., Vogel, T.M., Thomas, J.M., Ward, C.H., Eds.; Lewis Publishers: Boca Raton, Fla. **1994**, 201-222

Warner, S.; Longino, B.L.; Zhang, M.; Bennett, P.; Szerdy, F.S.; Hamilton, L.A. The first commercial permeable reactive barrier composed of granular iron: hydraulic and chemical performance at 10 years of operation. Permeable Reactive Barriers. Proceedings of the International Symposium held at Belfast, Northern Ireland, March 2004. IAHS. **2005**, 298

Wilkin, R. T.; Puls, W.; Sewell, G.W. Long-term performance of permeable reactive barriers using zero-valent iron: Geochemistry and microbiological effects. *Ground Water*. **2003**, 41(4), 493–503

Wolfsberg, M.; Van Hook, W.A.; Paneth, P. Isotope effects in the chemical, geological and bio sciences. Springer, Dordrecht, Heidelberg, London, New York. **2010**

Bibliography

Zogorski, J.S.; Carter, J.M.; Ivahnenko, T.; Lapham, W.W.; Moran, M.J.; Rowe, B.L.; Squillace, P.J.; Toccalino, P.L. Volatile Organic compounds in the nation's ground water and drinking-water supply wells. U.S. Geological Survey, Reston, Virginia. Circular 1292. **2006**

Zwank, L.; Elsner, M.; Aeberhard, A.; Schwarzenbach, R. P.; Haderlein, S. B. Carbon isotope fractionation in the reductive dehalogenation of carbon tetrachloride at iron (hydr)oxide and iron sulfide minerals. *Environ. Sci. Technol.* **2005**, 39(15), 5634-5641

Annex A

Audí-Miró, C; Cretnik, S; Otero, N; Palau, J; Shouakar-Stash, O; Soler, A; Elsner, M. Cl and C isotope analysis to assess the effectiveness of chlorinated ethene degradation by zero-valent iron: Evidence from dual element and product isotope values. *Applied Geochemistry*. 2013, 32, 175-183

Cl and C isotope analysis to assess the effectiveness of chlorinated ethene degradation by zero-valent iron: Evidence from dual element and product isotope values

Carme Audí-Miró^{a,°}, Stefan Cretnik^{b,°}, Neus Otero^a, Jordi Palau^{a,d}, Orfan Shouakar-Stash^c, Albert Soler^a, Martin Elsner^{b,*}

^aGrup de Mineralogia Aplicada i Medi Ambient. Departament de Cristal·lografia, Mineralogia i Dipòsits Minerals. Facultat de Geologia. Universitat de Barcelona. Martí Franquès s/n, 08028. Barcelona, Spain

^bInstitute of Groundwater Ecology, Helmholtz Zentrum München-National Research Center for Environmental Health, Ingolstädter Landstrasse 1, D-85764 Neuherberg, Germany.

^cDepartment of Earth Sciences, University of Waterloo, Waterloo, Ontario, Canada N2L 3G1

^dCentre for Hydrogeology and Geothermics, University of Neuchâtel, Rue Emile - Argand 11, CH-2000, Neuchâtel, Switzerland

This study investigated carbon and, for the first time, chlorine isotope fractionation of trichloroethene (TCE) and *cis*-dichloroethene (*cis*-DCE) during reductive dechlorination by cast zero-valent iron (ZVI). Hydrogenolysis and β -dichloroelimination pathways occurred as parallel reactions, with ethene and ethane deriving from the β -dichloroelimination pathway. Carbon isotope fractionation of TCE and *cis*-DCE was consistent for different batches of iron studied. Transformation of TCE and *cis*-DCE showed chlorine isotopic enrichment factors (ϵ_{Cl}) of $-2.6\text{‰} \pm 0.1\text{‰}$ (TCE) and $-6.2\text{‰} \pm 0.8\text{‰}$ (*cis*-DCE), with Apparent Kinetic Isotope Effects ($AKIE_{Cl}$) for chlorine of 1.008 ± 0.001 (TCE) and 1.013 ± 0.002 (*cis*-DCE). This indicates that a C-Cl bond breakage is rate-determining in TCE and *cis*-DCE transformation by ZVI. Two approaches were investigated to evaluate if isotope fractionation analysis can distinguish the effectiveness of transformation by ZVI as opposed to natural biodegradation. (i) Dual isotope plots. Our study reports the first dual (C, Cl) element isotope plots for TCE and *cis*-DCE degradation by ZVI. The pattern for *cis*-DCE differs markedly from that reported for biodegradation of the same compound by KB-1, a commercially available *Dehalococcoides*-containing culture. The different

trends suggest an expedient approach to distinguish abiotic and biotic transformation, but need to be confirmed in future studies. (ii) Product-related isotope fractionation. Carbon isotope ratios of the hydrogenolysis product *cis*-DCE differed consistently by 10‰ compared to the β -dichloroelimination products ethene and ethane providing a second line of evidence to differentiate abiotic or biotic degradation pathways.

1. Introduction

Chlorinated aliphatic hydrocarbons (CAHs) are used in a wide variety of applications as dry cleaning solvents and degreasers. Historical management of wastes containing CAHs has resulted in subsurface contamination, where the CAHs are often released as a mixture of dense non-aqueous phase liquids (DNAPL). Since DNAPLs have a higher density than water, they migrate downwards through the water table until they reach a confining layer forming pools (U.S. EPA, 2003). Moreover, within an aquifer, DNAPLs can be entrapped in fractures and matrix porosity constituting a long-term source of contamination of groundwater due to their low solubility (Dridi *et al.*, 2009).

Chlorinated solvents can have detrimental effects to both the environment and human health. Of particular relevance is trichloroethene (TCE). Although TCE may undergo natural or stimulated biodegradation, often intermediates such as *cis*-dichloroethene (*cis*-DCE) or vinyl chloride (VC) accumulate and they are more toxic than the parent compound (lower pathway in Figure 1, which shows the hydrogenolysis reactions, exclusive for biotic degradation sequences and concurring with a second pathway during abiotic reductive dehalogenation). Therefore, over the last couple of decades, various remediation techniques have been explored for clean-up (Clark *et al.*, 2003). In particular, in situ zero-valent iron (ZVI) permeable reactive barriers (PRB) have been implemented as a cost effective technology for treatment (Dries *et al.*, 2005; Liu *et al.*, 2006). ZVI is capable of effectively removing CAHs through reductive dechlorination. One of the most commonly used ZVI in field applications of PRBs is cast iron (Slater *et al.*, 2002). The virtue of transformation by ZVI is two-fold. On the one hand, in adequately designed barriers hydrogenolysis reactions (i.e., the lower pathway of Figure 1) tend to be more efficient than biodegradation so that toxic intermediates do not accumulate (Arnold & Roberts, 2000; Elsner *et al.*, 2008; Liu *et al.*, 2006). On the other hand, a second reductive dechlorination pathway that is operative with ZVI is vicinal β -dichloroelimination where two Cl substituents are cleaved off leading rapidly to harmless products such as ethene and ethane (upper pathway of Figure 1) (Arnold & Roberts, 2000; Elsner *et al.* 2008).

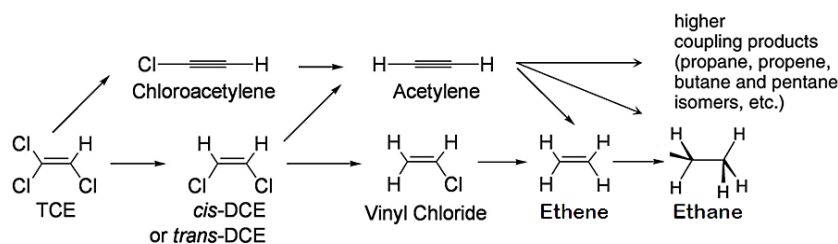


FIGURE 1. Concurring pathways proposed in chlorinated ethane dehalogenation (Elsner *et al.* 2008). Biodegradation generally involves sequential hydrogenolysis to ethene (lower pathway), while abiotic dehalogenation includes also β -dichloroelimination (upper pathway).

ZVI barriers are usually installed within existing contaminant plumes and elevated concentrations of contaminants are observed downgradient of PRBs, even long after the system has been installed. The presence of contaminants downgradient of a barrier hinders the monitoring of the PRB based on concentration data alone. In order to evaluate the PRB performance accurately, discrimination between (i) hydraulic bypasses around the barrier, (ii) incomplete abiotic degradation within the PRB, and (iii) biotic degradation stimulated by the resultant lower redox potential is necessary.

Compound Specific Isotope Analysis (CSIA) bears potential to provide precisely such discrimination. When a transformation process takes place -such as biotic or abiotic reductive dechlorination- a significant kinetic isotope effect (KIE) usually occurs, in contrast to non-degradative processes such as dilution, dispersion, and volatilization. As a consequence, reacting compounds become enriched in heavy isotopes, and the products formed are initially lighter than their parent compounds. Previous studies have determined carbon isotopic enrichment factors (ϵ_C) during CAHs reaction with ZVI ranging from -5.7 to -25.3‰ for tetrachloroethene (PCE); -8.6 to -27‰ for TCE; -6.9 to -23.1‰ for *cis*-DCE; and -6.9 to -20.1‰ for VC (Dayan *et al.*, 1999; Elsner *et al.*, 2008; Slater *et al.*, 2002; Vanstone *et al.*, 2004). The wide range of reported ϵ_C values limits the use of carbon isotopic enrichment on its own to assess the extent of degradation and to differentiate from biodegradation, since ranges of ϵ_C values overlap (Cichocka, *et al.*, 2008). In particular, it is unclear whether such variation is attributable to (i) fundamentally different chemical reaction mechanisms, (ii) the same mechanism, but different rate-limiting steps (i.e., mass transfer limitation) or (iii) mixed isotope fractionation of simultaneously ongoing degradation pathways. Combination with isotope analysis of other elements (chlorine or hydrogen) bears potential to provide additional insight into transformation mechanisms and is, therefore, expected to increase the insight from isotope data. In particular, dual isotope plots of the reacting contaminant have the potential to distinguish different transformation pathways (Abe *et al.*, 2009; Elsner *et al.*, 2005; Hunkeler *et al.*, 2011). The recent development of continuous flow compound specific chlorine isotope analysis (Shouakar-Stash *et al.*, 2006) has made such determinations of chlorine isotope fractionation and the use of dual carbon – chlorine isotope plots possible. Abe *et al.* (2009) successfully used the dual isotope approach (C/Cl) to distinguish between biotic aerobic

oxidation and biotic reductive dechlorination reactions for *cis*-DCE and VC. The slopes (i.e., ϵ_C/ϵ_{Cl}) obtained for the reductive dechlorination biodegradation model for *cis*-DCE and VC were 12.3 and 14, respectively. In contrast, chlorine isotope fractionation values for degradation of chlorinated ethenes by ZVI have not been reported so far.

Another approach to distinguish biotic and abiotic transformations of chlorinated ethenes does not involve chlorine isotope ratios, but relies instead on carbon isotope analysis of daughter compounds (Elsner *et al.*, 2010, 2008). As sketched in Figure 1, the same products that are formed in sequential order during biodegradation are formed in parallel during abiotic degradation by ZVI. If these products show different isotope trends depending on whether they are formed in parallel or in sequence, the type of pathway that produced them and consequently their abiotic or biotic origin may be identified. Elsner *et al.* (2008) obtained that hydrogenolysis and β -dichloroelimination byproducts during transformation by nanoparticulate ZVI differed consistently by 10‰ in carbon isotope values. A follow-up field study used these results, to attempt for the first time, to discriminate between abiotic and biotic transformations in the field (Elsner *et al.*, 2010). Therefore, two lines of evidence have recently been brought forward to discriminate between abiotic and biotic pathways: (i) evidence from dual isotope plots, (ii) evidence from product isotope ratios.

In this study TCE and *cis*-DCE batch experiments were carried out in order to investigate a) carbon and chlorine isotope fractionation and b) carbon isotope fractionation of parent compounds and daughter products during their transformation with cast ZVI. Our motivation was to evaluate the potential of both approaches for assessing the effectiveness of ZVI barrier treatment. Our main objectives were i) to evaluate whether the concurring pathways of Figure 1, hydrogenolysis and β -dichloroelimination were operative with this type of iron; ii) to determine not only carbon, but for the first time also chlorine isotope enrichment factors for abiotic transformation of TCE and *cis*-DCE by cast ZVI; (iii) to construct a Dual Element Isotope Plot of both carbon and chlorine isotope data and compare it to reported data on biodegradation, and iv) to investigate the potential of carbon isotope values of daughter products as an independent line of evidence to delineate their abiotic versus biotic origin.

2. Materials and methods

2.1 Experimental Procedure

2.1.1 Dual Element isotope study

Batch experiments were carried out in duplicate in closed 250 mL bottles equipped with Mininert valves (Supelco, Bellefonte, Pennsylvania, USA). Each bottle contained 20 ± 0.1 g of cast iron (92% purity, Gotthart Maier Metallpulver GmbH, Rheinfelden, Germany) and 100 mL of aqueous solutions containing 60 mg/L of either TCE or *cis*-DCE, or 12 mg/L of VC, leaving 150 mL of headspace. To this end, TCE (99%, Merck, Darmstadt, Germany), *cis*-DCE (97%, Sigma-Aldrich, St. Louis, Missouri, USA) and VC (2000 mg/L in Methanol, Supelco, Bellefonte,

Pennsylvania, USA) were used. Control bottles were filled with 100 mL of aqueous chloroethene solutions, without addition of cast iron.

The specific surface area of the cast iron determined by nitrogen gas adsorption (BET method) (Brunauer *et al.*, 1938) was $0.7038 \pm 0.0045 \text{ m}^2/\text{g}$. Prior to the experiment the iron was acid-cleaned and dried inside an anaerobic chamber operated with a gas mixture of 90% N₂ and 10% H₂. During acid cleaning, the iron was soaked in 1N degassed HCl for 1 h, then rinsed five times with degassed deionized water, and dried and stored in the anaerobic chamber (Dayan *et al.*, 1999; Matheson *et al.*, 1994; Slater *et al.*, 2002). The iron was weighed before and after the treatment to verify it was dry. Spike solutions of chlorinated ethenes were prepared by dissolving defined aliquots of pure compound in deionized water (Milli-Q Plus UV, Millipore™, Billerica, Massachusetts, USA), under vigorous stirring for 12 hours and in the absence of a headspace. Bottles were filled with the iron and deionized water inside the glovebox, closed, taken out and spiked outside with anoxic stock solutions of the chlorinated ethene by injection through the Mininert Valve.

After preparation, bottles were immediately covered with aluminum foil to avoid oxidation due to light and were rotated on a horizontal roller table (Wheaton, Millville, New Jersey, USA) at 60 rpm about their longitudinal axes to ensure rapid solid/water and water/air mass transfer. Samples were taken from the headspace of the reaction bottles through the Mininert valve by a Pressure-Lok® Analytical Syringe (VICI, Houston, Texas, USA) with sideport taper needle (1000 µL for compound concentration analysis, 250 to 2000 µL for carbon isotope analysis and 30 to 500 µL for chlorine isotope analysis). In order to keep reaction bottles over-pressurized during the experiments, an equal volume of argon gas was injected into the reaction bottles before samples were withdrawn. Headspace sampling from the same bottle for concentration, carbon and chlorine isotope measurements was performed sequentially, and samples were analyzed immediately to obtain values at the same time point. Duplicate experimental vials were sampled and analyzed right afterwards.

2.1.2 Additional *cis*-DCE and TCE Degradation Experiments

Prior to the Dual Element isotope study, additional *cis*-DCE and TCE degradation experiments were performed in two series of 25 mL vials and analyzed for carbon isotope fractionation. Vials were filled with $2.5 \pm 0.1 \text{ g}$ of iron and with a previously prepared solution of TCE and *cis*-DCE (one compound each series). They were covered with aluminum foil and put in a rotator (Heidolph, Schwabach, Germany) (23 rpm). Each pair of vials (duplicates) was prepared at different starting points, but all vials were sacrificed at the same time, assuring the same storage conditions, that they were analyzed on the same day, but at different degrees of conversion. Solutions were separated from the iron and split in two aliquots, one was kept at 4 °C without headspace for concentration analysis performed the day after, and the second one was frozen with headspace for isotopic analysis (Elsner *et al.*, 2006) which was performed 10 days later. Controls were assessed at three different time points along the experiments to ensure that other degradation mechanisms or losses were not affecting the TCE concentration.

2.2 Concentration and Isotope analysis

2.2.1 Dual Element isotope study

Analysis of compound concentrations was performed on a gas chromatograph with flame ionization detector (GC/FID, Hewlett Packard, Palo Alto, California, USA), equipped with a 60 m GS-Q (Agilent J&W, Santa Clara, California, USA) column, 0.32 mm inner diameter, using nitrogen as the carrier gas at 1.6 mL/min flow rate. The injector temperature was 200°C and the temperature program used was of 34°C (9 min), increasing at 15°C/min to 53°C (2.70 min), at 13°C/min to 134°C (3.30 min) and at 10°C/min to 190°C (23 min). This temperature program allowed separation of the chlorinated ethene byproducts, methane, ethane, ethene, acetylene, propene, n-propane, propyne, n-butane as well as of the chlorinated ethenes VC, *cis*-DCE and TCE. Before the start of the experiment a four point calibration for TCE, *cis*-DCE and VC was conducted, and one point calibrations were conducted daily during the experiment by injecting standard solutions of the three compounds. For methane, ethane, ethene, acetylene, propene, n-propane, propyne and n-butane an initial one point calibration was done before the start of the experiment and daily one-point calibrations were performed during the experiment by injecting gas mixtures of standards with 15 ppm of each compound in helium (Scotty® Analyzed Gases, Sigma-Aldrich, St. Louis, Missouri, USA). The resulting total relative error in concentrations is estimated as ± 10%.

Carbon isotope analysis of TCE, *cis*-DCE and their byproducts were conducted by Compound Specific Isotope Analysis (CSIA) by injection of headspace samples on a GC-C-IRMS system (Thermo Fisher Scientific, Waltham, Massachusetts, USA) consisting of a Trace GC coupled to a MAT 253 IRMS through a GC/C III combustion interface. The gas chromatograph was equipped with a 60 m GS-Q column (Agilent J&W, Santa Clara, California, USA), 0.32 mm inner diameter, and operated with He carrier gas at 1.4 mL/min. The temperature program was similar to the one used for concentration analysis, 34°C (9 min), increasing at 5°C/min to 53°C, at 13°C/min to 134°C (3.30 min) and at 10°C/min to 190°C (21 min). Carbon isotopic signatures ($\delta^{13}\text{C}$) of TCE and *cis*-DCE internal standards used were $-27.1\text{‰} \pm 0.2\text{‰}$ and $-25.5\text{‰} \pm 0.2\text{‰}$ respectively,

$$\delta^{13}\text{C} = \left(\frac{\left(\frac{^{13}\text{C}}{^{12}\text{C}} \right)_{\text{compound}} - \left(\frac{^{13}\text{C}}{^{12}\text{C}} \right)_{\text{VPDB}}}{\left(\frac{^{13}\text{C}}{^{12}\text{C}} \right)_{\text{VPDB}}} \right) \quad (1)$$

where VPDB is the Vienna Pee Dee Belemnite international reference standard. The analytical uncertainty 2σ of carbon isotopic measurements was ± 0.5‰ (Elsner *et al.*, 2012).

Chlorine isotope analyses of TCE and *cis*-DCE were determined according to a method adapted from Shouakar-Stash *et al.* (2006). This method is a new approach for GC/IRMS which does not include a combustion step; instead, intact chlorinated ethene molecules are directly transferred to the IRMS source through the He carrier stream, ionized and fragmented for the isotopic ratio measurement. In order to correct for instrument drifts, values are measured in comparison to reference peaks which are introduced via a dual inlet system consisting of the

same target analyte and converted to delta values relative to the international SMOC (Standard Mean Ocean Chloride) standard (Bernstein *et al.*, 2011).

In this study measurements were conducted on a GC-IRMS system (Thermo Scientific, Waltham, Massachusetts, USA) consisting of a Trace GC that was connected to a MAT 253 IRMS with dual inlet system *via* a heated transfer line. For the simultaneous determination of TCE and *cis*-DCE (product) a peak jump routine was performed, with *cis*-DCE monitoring gas peaks added at the beginning and TCE monitoring gas peaks added at the end of each analytical run. The gas chromatograph was equipped with a 30 m VOCOL column (Supelco, Bellefonte, Pennsylvania, USA) with a 0.25 mm inner diameter, with a film thickness of 1.5 μm and operated with He carrier gas at 1.4 mL/min. The GC program used was 50°C (7 min), increasing at 60°C/min to 70°C (2.70 min) and at 80°C/min to 140°C (0.10 min). External standards were measured daily for calibration of $\delta^{37}\text{Cl}$ values against the SMOC scale (Bernstein *et al.*, 2011). These standards had previously been characterized in the Department of Earth Sciences, University of Waterloo. TCE Eil-1 and Eil-2 internal standards (supplied by Orfan Shouakar-Stash, Canada) were +3.05‰ and -2.7‰ respectively,

$$\delta^{37}\text{Cl} = \left(\frac{\left(\frac{^{37}\text{Cl}}{^{35}\text{Cl}} \right)_{\text{compound}} - \left(\frac{^{37}\text{Cl}}{^{35}\text{Cl}} \right)_{\text{SMOC}}}{\left(\frac{^{37}\text{Cl}}{^{35}\text{Cl}} \right)_{\text{SMOC}}} \right) \quad (2)$$

where SMOC is the international reference standard Standard Mean Ocean Chloride. The chlorine isotopic signature ($\delta^{37}\text{Cl}$) of *cis*-DCE internal standards used, *cis*F and IS-63 (supplied by Orfan Shouakar-Stash, Canada), is -1.52‰ and +0.07‰ respectively. The analytical uncertainty of chlorine isotopic measurements was $\pm 0.2\%$ (Bernstein *et al.*, 2011).

2.2.2 Additional *cis*-DCE and TCE Degradation Experiments ($^{13}\text{C}/^{12}\text{C}$ analysis only)

Headspace (HS) concentration analysis was performed using a FOCUS gas chromatograph coupled with a DSQ II mass spectrometer (GC-MS) (Thermo Fisher Scientific, Waltham, Massachusetts, USA). The GC was equipped with a split/splitless injector and a 60 m, 0.32 mm inner diameter DB-624 capillary column (Agilent, Santa Clara, California, USA) with a film thickness of 1.8 μm and operated with He carrier gas at 1.8 mL/min. The following temperature program was used: 60 °C (2 min) and then increased at 8 °C/min to 220 °C (5 min). The injector was set at 220 °C. The compounds were identified in comparison to retention times and mass spectrum of calibration standards, and the concentrations were quantified using a set of multi-component external standards at different concentrations. Low molecular weight byproducts from *cis*-DCE degradation (ethene, ethane, methane) were semi-quantitatively determined by a gas chromatograph with a thermal conductivity detector (GC-TCD) (5890 Hewlett Packard, Palo Alto, California, USA). The following temperature program was used: 35 °C (5 min) and then increased at 25 °C/min to 220 °C (5 min). A headspace volume of 1 mL was manually injected with a gas tight syringe (Hamilton).

Carbon isotope ratios were determined using headspace solid-phase microextraction (HS-SPME) and a GC-C-IRMS system consisting of a Trace GC Ultra equipped with a splitless

injector, coupled to a Delta V Advantage isotope ratio mass spectrometer through a combustion interface. The method and equipment used are described in detail in Palau *et al.* (2007). A 60 m long column with 0.32 mm inner diameter and a film thickness of 1.8 μm (Supelco SPB-624, Bellefonte, Pennsylvania, USA) was used with He as carrier gas with a flow rate of 2.2 mL/min. The temperature program was: 60 $^{\circ}\text{C}$ (5 min), increase at 8 $^{\circ}\text{C}/\text{min}$ to 165 $^{\circ}\text{C}$ and then at 25 $^{\circ}\text{C}/\text{min}$ to 220 $^{\circ}\text{C}$ (1 min). The injector was set at 250 $^{\circ}\text{C}$ at a split ratio of 5:1.

Prior to extraction, samples were diluted to 20 $\mu\text{g}/\text{L}$ with Milli-Q water to a final volume of 100 mL. Then, the samples were put in agitation and the SPME fiber was introduced through the septum. The SPME fiber remained in the sample headspace during 15 minutes after which it was injected manually into the GC injector. Accuracy of isotope analysis was daily verified by measurements of laboratory standards characterized against international reference materials (referred to the VPDB international standard). The carbon isotopic signature ($\delta^{13}\text{C}$) of the TCE and *cis*-DCE laboratory standard are $-30.8 \pm 0.2\text{‰}$ and $-26.1 \pm 0.2\text{‰}$, respectively (Palau *et al.*, 2007).

2.3 Evaluation of carbon and chlorine isotope fractionation

Carbon isotopic enrichment factor (ϵ_c) was evaluated according to a Rayleigh regression not forced through the origin (Scott *et al.*, 2004):

$$R/R_0 = (1000 + \delta^{13}\text{C}) / (1000 + \delta^{13}\text{C}_0) = f^{\epsilon_c / (1000)} \quad (3)$$

where R_0 and R are carbon isotope ratios at the beginning and at a given time (t) respectively, $\delta^{13}\text{C}_0$ and $\delta^{13}\text{C}$ are the same values in delta notation and f is the fraction of substrate remaining at time t . According to Equation 3, if the ϵ_c has been obtained in laboratory experiments for a specific transformation, if the initial (= "source") $\delta^{13}\text{C}_0$ is known and if $\delta^{13}\text{C}$ is determined at a given time point without further knowledge of the extent of transformation, isotope data alone allows estimating the fraction of remaining reactant (f). This approach may be used to quantify the real extent of a specific transformation reaction in the field. The approach is independent of estimations based on concentration ratios of parent and daughter compounds, which are subject to sorption, dilution and further degradation so that these ratios may not show the actual extent of degradation.

The specific isotope fractionation pattern of the byproducts can be expressed by determining the product-specific isotope fractionation ($\epsilon_{\text{substrate} \rightarrow \text{product}}$). According to Elsner *et al.* (2008), it can be calculated through the following abbreviated equation:

$$\epsilon_{\text{substrate} \rightarrow \text{product}} = \delta^{13}\text{C}_{0,\text{product}} - \delta^{13}\text{C}_{0,\text{substrate}} = D(\delta^{13}\text{C}) + \epsilon_c \quad (4),$$

where $D(\delta^{13}\text{C})$ is the deviation that a product can experience from the weighted average of all products, expressed as $D(\delta^{13}\text{C}) = \delta^{13}\text{C}_{\text{product}} - \delta^{13}\text{C}_{\text{product, average}}$. Using Sigma Plot 12, the $D(\delta^{13}\text{C})$ has been obtained from iteration and graphical representation of the following (Elsner *et al.*, 2008):

$$(1000+\delta^{13}\text{C}_{\text{product}})/(1000+\delta^{13}\text{C}_{0,\text{substrate}}) = (1+(D(\delta^{13}\text{C})/1000)) \times ((1-f \epsilon_c/(1000+1))/(1-f)) \quad (5)$$

Equations 4 and 5 allow the determination of product-specific isotope fractionation even without knowledge of absolute reaction rates, product distribution, or molar balances, since they rely solely on isotope measurements of the substrate and a given product (Elsner *et al.*, 2008).

Elsner and Hunkeler (2008) demonstrated that chlorine isotope fractionation also follows a Rayleigh trend despite a high abundance of ^{37}Cl compared to ^{35}Cl . Thus, the Rayleigh equation was also used to evaluate the chlorine isotope data. An apparent kinetic chlorine isotope effect (AKIE) for chlorine may be estimated from the following equation (Elsner and Hunkeler, 2008):

$$\text{AKIE}_{\text{Cl}} = 1/(1+(n \cdot \epsilon_{\text{Cl}}/1000)) \quad (6),$$

where “n” is the total number of chlorine atoms which are considered to be located in the reactive positions, and assuming that secondary isotope effects are negligible.

Dual element isotope fractionation can be compared by (a) either considering the ratio of $\epsilon_c/\epsilon_{\text{Cl}}$ or, alternatively, (b) by plotting changes in isotope values $\delta^{13}\text{C}/\delta^{37}\text{Cl}$ (as shown exemplary for MTBE with $\delta^2\text{H}/\delta^{13}\text{C}$ in Elsner *et al.* (2007)).

3. Results and discussion

3.1 Reactivity Trends and product formation

Suspensions of 200 g/L of ZVI achieved 50% transformation of TCE leading to the formation of dehalogenated products in almost 3 days (Figure 2A). Under identical experimental conditions, observed half-lives for *cis*-DCE and VC were more than 50 and 80 days, respectively (Table S1). Figure 2 shows the kinetics for disappearance of TCE and simultaneous product formation in the dual element isotope experiment. Transformation rates decreased in the order TCE > *cis*-DCE > VC (Figure 2, Table S1). It can therefore be expected that isotope ratios of *cis*-DCE are primarily influenced by its formation from TCE, rather than by its further degradation to VC. While the observed trend in transformation rates is consistent with earlier studies by Dayan *et al.* (1999), Elsner *et al.* (2008), Gillham and O'Hannesin (1994) and Hunkeler *et al.* (2011), the opposite trend (TCE < *cis*-DCE) was observed in additional *cis*-DCE and TCE degradation experiments of this study (Table S1) and is consistent with previous studies by Arnold and Roberts (2000) and Elsner *et al.* (2008). At present, the reasons for these reactivity trends remain imperfectly understood.

Even though mass balances were typically not closed, the detection of several products allows conclusions about concurring transformation pathways. All experiments yielded ethene, ethane and methane as final products of the degradation sequence, with small amounts of *cis*-DCE, acetylene and VC intermediates produced during TCE degradation (Figure 2 A-B), and acetylene and VC from *cis*-DCE degradation. Complete products are listed in Table 1. According to Arnold and Roberts (2000) and Prommer *et al.* (2008), ethene may be produced either (i) from hydrogenation of acetylene, previously formed through the β -dichloroelimination

pathway or (ii) through VC hydrogenolysis. The evolution of VC and acetylene concentration profiles, however, suggests that acetylene is the main intermediate of ethene formation, (i) due to an extremely rapid acetylene concentration decrease while ethene appeared (Figure 2B), and (ii) because VC concentrations, in contrast, accumulated over time. These observations point out that both hydrogenolysis and β -dichloroelimination pathways (Figure 1) are occurring simultaneously as parallel reactions rather than as consecutive reactions and that ethene and ethane are produced primarily through the β -dichloroelimination pathway. As observed by Burris *et al.* (1995) traces of methane were formed. Also, traces of longer-chain hydrocarbons were observed, as C3 (propene, propane) and C4 (n-butane), probably coming from a concurrent acetylene degradation pathway (Arnold and Roberts, 2000; Elsner *et al.*, 2008) (Figure 1). Only 20% of degraded TCE was transformed to *cis*-DCE, which, in turn, was transformed at a much slower rate to VC (see reactivity trends above).

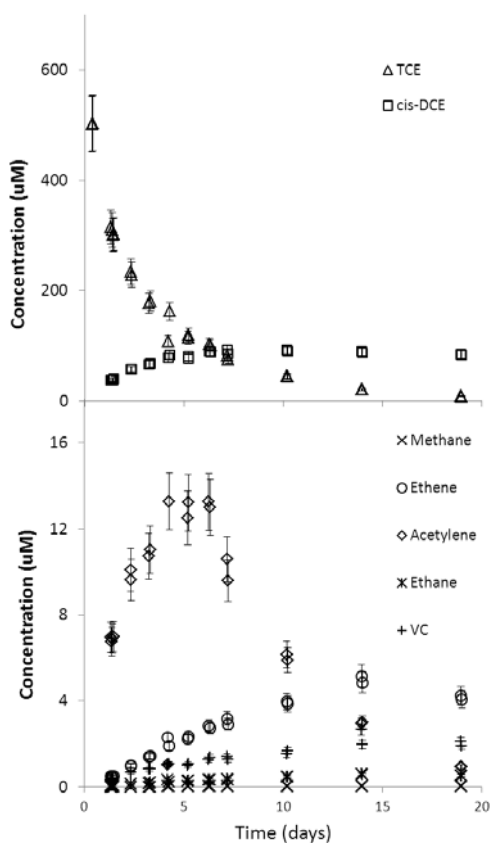


FIGURE 2. Changes in concentration of TCE and its byproducts over time in Dual Element TCE experiments (A and B). Panel B is a zoom of Panel A without TCE and *cis*-DCE to see the by-products concentration curve more clearly. Error bars indicate the uncertainty of the measurement of $\pm 10\%$.

3.2 Isotope fractionation according to the Rayleigh equation

Enrichment factors ϵ_C for TCE in the additional TCE degradation experiments versus dual element isotope experiments are indistinguishable, since their 95% confidence intervals overlap

(Table 1 and Figure 3A). In the case of *cis*-DCE, the 95% confidence intervals of ϵ_C are close to overlapping (Table 1 and Figure 4A). This indicates that the carbon isotope fractionation that we observed in this study is fairly consistent with this type of iron, even despite different reactivity trends (see above and Table S1). VC was not evaluated, since it was hardly transformed. Literature carbon isotopic enrichment factors for TCE exhibit a wide range of almost 20‰, depending on the type of ZVI-material used (-8.6 to -27‰) (Dayan *et al.*, 1999; Slater *et al.*, 2002; Elsner *et al.*, 2008). Therefore, prior to applying the ϵ_C at the field scale to evaluate the extent of the reductive dechlorination, the ϵ_C value produced by a specific ZVI-material should be accurately determined. For conservative estimates of degradation in the field according to a modified version of the Rayleigh equation (Eq. 1), the more negative value of epsilon (i.e., -15 ... -20 ...) should be chosen (Hunkeler *et al.*, 2008).

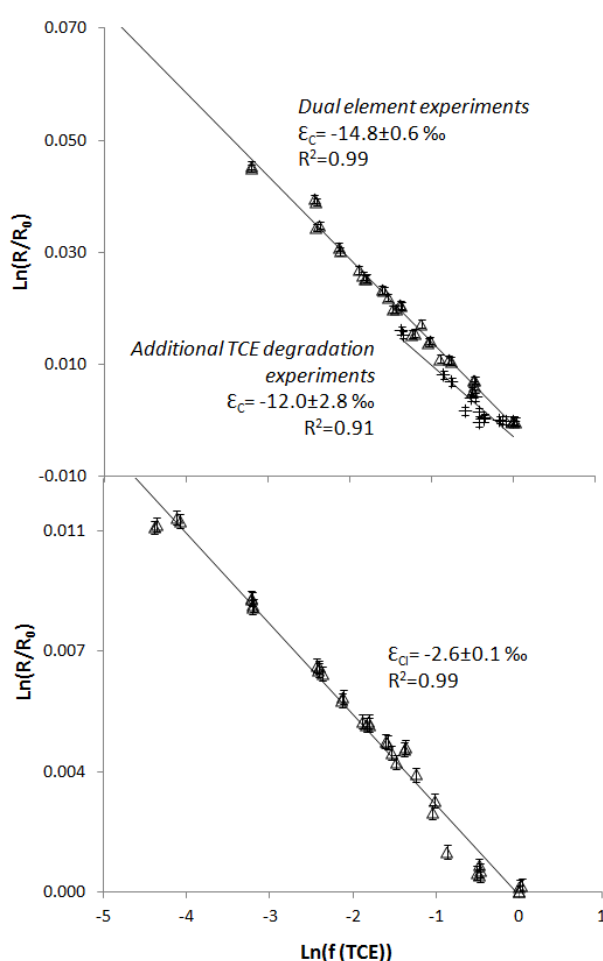


FIGURE 3. Carbon isotope values (3A) and chlorine isotope values (3B) of the residual TCE fraction in double logarithmic plots over the respective concentrations. The isotopic enrichment factors ϵ_C and ϵ_{Cl} can be calculated from the slope of the regression line according to Equation 3. Triangles represent combined TCE dual element experiments and crosses represent combined additional TCE degradation experiments. Error bars represent the total instrument uncertainty of 0.5‰ for compound-specific carbon isotope measurements, and of 0.2‰ for compound specific chlorine isotope measurements.

TABLE 1. Summary of the Rayleigh fractionation for carbon and chlorine, the carbon product-related fractionation, and all the byproducts detected for TCE and *cis*-DCE dual element and additional degradation experiments, and for VC dual element experiment.

Experiment	Substrate	Initial Conc. ^a (μM)	$\delta^{13}\text{C}$					$\delta^{37}\text{Cl}$			Detected products	
			$\epsilon_{\text{C}}(\text{‰}) \pm 95\% \text{ CI}^{\text{a,b}}$ Individual Experiments	$\epsilon_{\text{C}}(\text{‰}) \pm 95\% \text{ CI}^{\text{b}}$ Combined Data	$\epsilon_{\text{substrate} \rightarrow \text{product}}$ given for each particular product ^a	$D(\delta^{13}\text{C})^{\text{a,c}}$	R^2^{a}	$\epsilon_{\text{Cl}}(\text{‰})^{\text{a}}$ Individual Experiments	$\epsilon_{\text{Cl}}(\text{‰})$ Combined Data	AKIE_{Cl}		
Dual element experiments	TCE	441	-14.9 ± 0.9	-14.8 ± 0.6	<i>cis</i> -DCE: -7.9‰ Ethene: -18.2‰ Acetylene: -17.3‰ Ethane: -19.3‰	6.9 -3.4 -2.5 -4.5	0.55 0.71 0.34 0.69	-2.6 ± 0.2	-2.6 ± 0.1	$1,008 \pm 0.001$	<i>cis</i> -DCE Acetylene VC Ethene Ethane n-butane Propane Propene Methane	
		503	-14.8 ± 0.9		<i>cis</i> -DCE: -10.4‰ Ethene: -20.8‰ Acetylene: -14.7‰ Ethane: -22.9‰	4.4 -6.0 0.1 -8.1	0.87 0.72 0.60 0.73					-2.7 ± 0.1
	<i>cis</i> -DCE	787	-21.2 ± 2.1	-20.5 ± 1.8	VC: 1.8‰ Ethene: -25.4‰ Acetylene: -19.0‰ Ethane: -25.7‰	22.2 -5.0 1.4 -5.3	0.45 0.93 0.33 0.97	-6.6 ± 1.0	-6.2 ± 0.8	$1,013 \pm 0.002$	Acetylene VC Ethene Ethane n-butane Propane Propene Methane	
		852	-20.2 ± 4.2		VC:--- Ethene: -24.1‰ Acetylene: -23.5‰ Ethane: -23.3‰	n.q. -3.7 -3.2 -3.0	n.q. 0.78 0.34 0.95					-6.3 ± 0.7
	VC	VC	185	n.q.	n.q.	n.q.	n.q.	n.q.	n.q.	n.q.	n.q.	Acetylene Ethene Ethane Methane
			187	n.q.								
Additional <i>cis</i> - DCE and TCE degradation experiments	TCE	50	-14.3 ± 2.9	-12.0 ± 2.8	-----	-----	-----	-----	-----	-----	<i>cis</i> -DCE VC non chlorinated compounds not determined	
		50	-13.9 ± 4.8									
	<i>cis</i> -DCE	<i>cis</i> -DCE	186	-15.2 ± 2.7	-16.8 ± 1.2	-----	-----	-----	-----	-----	-----	VC Ethene ethane methane butane
			186	-12.0 ± 2.9								

^aNote that duplicates are listed separately so that each entry represents one experimental batch. ^b95% confidence interval. ^c $D(\delta^{13}\text{C})$: is the deviation that each product has experienced from the weighted average of all products. n.q. : not quantified

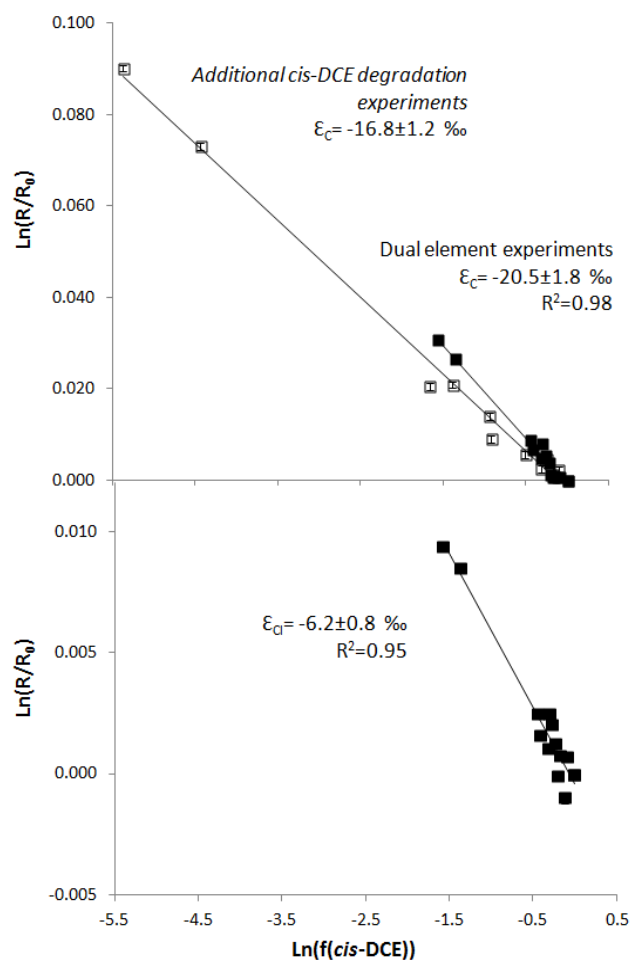


FIGURE 4. Carbon isotope values (4A) and chlorine isotope values (4B) of the residual *cis*-DCE fraction in a double logarithmic plots over the respective concentrations. The isotopic enrichment factor ϵ_C and ϵ_{Cl} can be calculated from the slope of the regression line according to Equation 3. Black squares represent combined *cis*-DCE dual element experiments and white squares represent combined additional *cis*-DCE degradation experiments. Error bars represent the total instrumental uncertainty of 0.5‰ for compound-specific carbon isotope measurements, and of 0.2‰ for compound specific chlorine isotope measurements.

Our study also reports the first chlorine isotope fractionation data associated with ZVI transformation. Results show that transformation of TCE and *cis*-DCE was associated with pronounced chlorine isotope fractionation, $\epsilon_{Cl} = -2.6 \pm 0.1 \text{ ‰}$ for TCE and $\epsilon_{Cl} = -6.2 \pm 0.8 \text{ ‰}$ for *cis*-DCE (see Table 1 and Figures 3B and 4B). This pronounced chlorine isotope fractionation may provide an additional line of evidence for degradation in the field.

Following Equation 6, it is possible to calculate tentative apparent kinetic isotope effects $AKIE_{Cl}$ from TCE and *cis*-DCE dual element isotope experiments resulting in values of 1.008 ± 0.001 and 1.012 ± 0.002 , respectively. Compared to other studies (Dybala-Defratyka *et al.*, 2008; Dybala-Defratyka *et al.*, 2004; Hofstetter *et al.*, 2007; Wolfsberg *et al.*, 2010) these $AKIE_{Cl}$ numbers are typical, or even at the higher end of ranges reported for chlorine isotope effects. They are, therefore, clearly indicative of the presence of primary rather than secondary isotope

effects meaning that (i) a C-Cl bond is cleaved in the rate-determining step of the ZVI-catalyzed transformation and (ii) this intrinsic isotope effect is not significantly masked by mass transfer, adsorption, etc. In particular, our estimated values are much higher than the $AKIE_{Cl} = 1.003$ calculated for biotransformation of *cis*-DCE by the mixed culture KB-1 (Abe *et al.*, 2009) suggesting potential differences in the underlying transformation mechanism.

In contrast to what Hunkeler *et al.* (2009) predicted, Cl in *cis*-DCE, as a TCE product, had a slightly greater $\delta^{37}Cl$ compared to TCE from which it was formed (Figure 5) showing an initial enrichment in ^{37}Cl instead of ^{35}Cl of the product *cis*-DCE. The reason of this observation in the $\delta^{37}Cl$ values may be an inverse secondary isotope effect or an unequal distribution of isotope ratios in different positions of TCE so that the position containing more ^{37}Cl is preferably transferred to the product pool. An inverse secondary isotope effect can occur, for instance, if an intermediate of the reaction has a more cramped coordination sphere, e.g. when the carbon changes from sp^2 to sp^3 hybridisation. In this case the positions adjacent to reactive bonds have stiffer vibrations and preferably contain heavy isotopes. These preliminary results give an exciting glimpse on the potential insight that can be obtained from chlorine isotope measurements to investigate the reaction chemistry of TCE and *cis*-DCE in future studies.

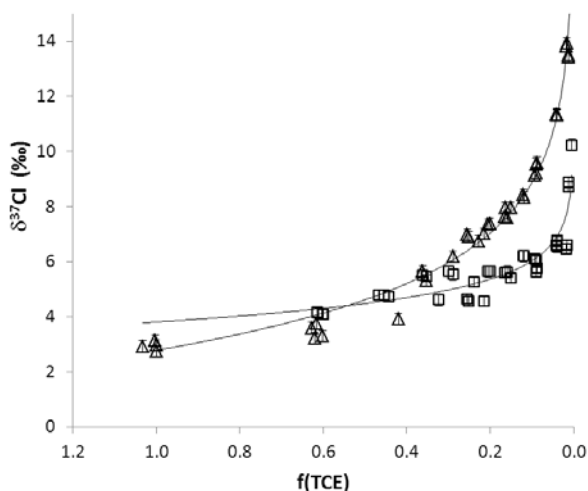


FIGURE 5. Changes in chlorine isotope values of TCE (triangles), as substrate, and *cis*-DCE (squares), as product, during TCE in the combined dual element experiments. Error bars represent the uncertainty of 0.2‰ for compound-specific chlorine isotope measurements.

3.3 Dual Isotope Approach

Figure 6 shows a dual element isotope plot of (a) the TCE transformation experiment with $\delta^{13}C$ and $\delta^{37}Cl$ values of TCE and one of its products, *cis*-DCE (Figure 6A); and (b) the analogous plot for transformation of *cis*-DCE (Figure 6B). To our knowledge, these are the first dual (C, Cl) isotope plots reported for chlorinated ethenes transformation by ZVI. Figure 6A shows that the graphs for TCE and *cis*-DCE show a parallel trend, as predicted for cases when further transformation of *cis*-DCE is very slow or even negligible (Hunkeler *et al.*, 2009)

To evaluate whether such a dual element isotope plot can discriminate between abiotic and biotic degradation reactions, a comparison to dual element isotope data on biodegradation was attempted. For TCE (Figure 6A), no such reference data is available yet. In the case of *cis*-DCE, however, the dual element isotope plot can be compared to data of Abe *et al.* (2009) on reductive dechlorination by the mixed culture KB-1. The slope of 3.1 ± 0.2 observed in our experiments is almost 4 times smaller than that observed by Abe *et al.* (2009) (11.4 ± 0.6) (Figure 6B). This observation provides further evidence that the small isotope fractionation observed with KB-1 by Abe *et al.* (2009) is not primarily attributable to masking / commitment to catalysis, but that fundamentally different chemical transformation mechanisms are at work. If this trend can be confirmed, then our results would delineate an expedient new way to discriminate biodegradation and abiotic reductive dechlorination from a PRB in the field. To this end, however, more data is necessary to substantiate these initial patterns.

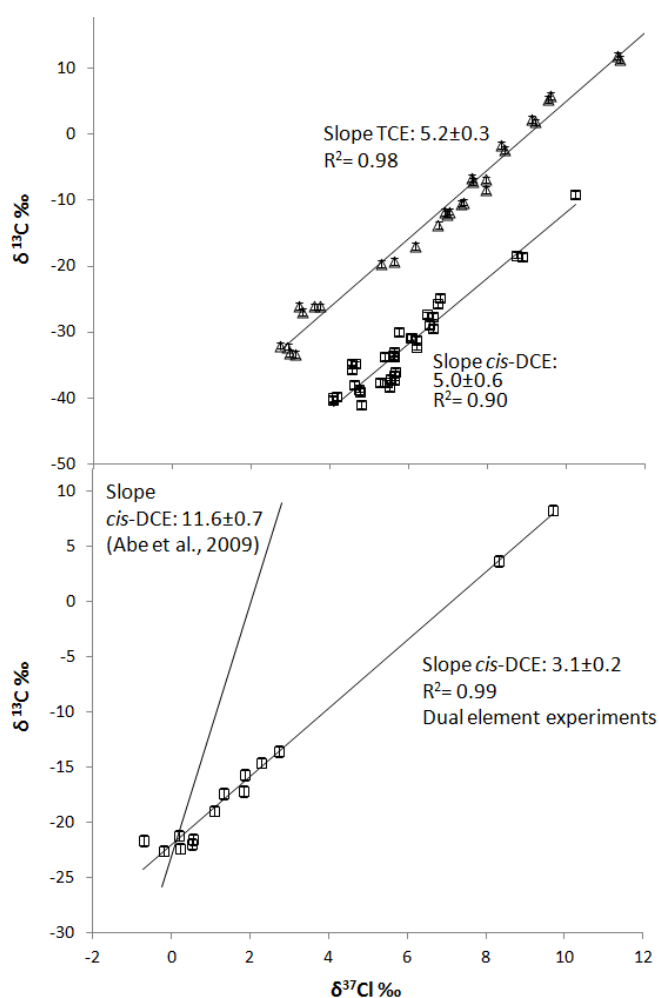


FIGURE 6. 6A) Dual element isotope plot of $\delta^{13}\text{C}$ versus $\delta^{37}\text{Cl}$ obtained from combined TCE dual element experiments. The slope of TCE (triangles) and *cis*-DCE as a product (squares) are given. 6B) Dual element isotope plot of $\delta^{13}\text{C}$ versus $\delta^{37}\text{Cl}$ from combined *cis*-DCE dual element experiments. The slope of *cis*-DCE as substrate is given and compared to the result of Abe *et al.* (2009) in reductive dechlorination by the mixed culture KB-1. Error bars in 6A and 6B represent the total instrumental uncertainty of 0.5‰ and 0.2‰ for compound-specific carbon and chlorine isotope measurements, respectively.

3.4 Product – Related isotopic fractionation

Carbon isotope ratios of *cis*-DCE, ethene and ethane were evaluated as a second, independent approach to distinguish abiotic from biotic chlorinated ethene degradation. Figure 7 shows that products initially had less ^{13}C compared to their parent compound, but subsequently showed a trend towards more ^{13}C reflecting the enrichment trend of the substance from which they were formed. VC concentrations were too small for precise carbon isotope analysis. The product-specific isotope fractionation ($\epsilon_{\text{substrate} \rightarrow \text{product}}$) revealed a notable difference of about 10‰ between β -dichloroelimination (ethene, ethane) and hydrogenolysis (*cis*-DCE) products (Figure 7 and Table 1). This 10‰ difference in $\delta^{13}\text{C}$ of products formed with ZVI confirms the pattern observed in previous studies (Elsner *et al.*, 2008). As proposed by Elsner *et al.*, (2008, 2010) these parallel product curves may be considered characteristic of abiotic degradation, since they contrast with trends during biodegradation, where products are generated in sequence and, therefore, different isotope patterns are obtained that vary in time and space (Elsner *et al.*, 2008). Our study, therefore, confirms the potential of product isotope values to distinguish biotic from abiotic degradation with ZVI and to serve as an indicator of abiotic degradation processes in the field.

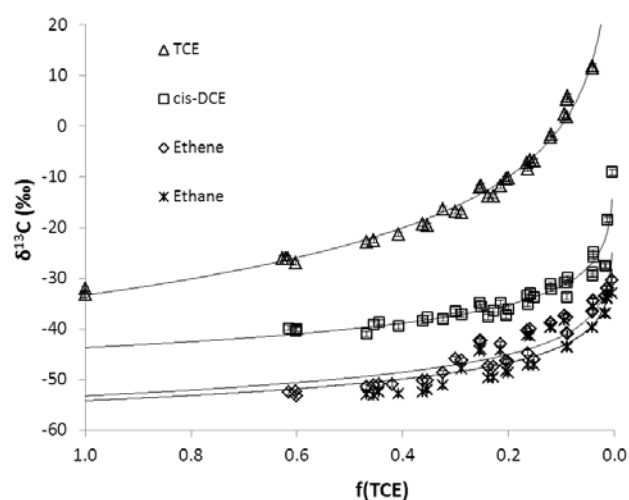


FIGURE 7. Isotope values of TCE and its by-products indicating a 10‰ isotopic difference between the hydrogenolysis byproduct *cis*-DCE and the β -dichloroelimination by-products ethene and ethane. Curves are fits of the data according to Equations 3 and 4. Error bars represent the total instrumental uncertainty of 0.5‰ for compound-specific carbon isotope measurements.

4. Conclusions

This study presents the first results on chlorine isotope fractionation of TCE and *cis*-DCE during transformation with ZVI. Apparent kinetic isotope effects AKIE_{Cl} of 1.008 ± 0.001 and 1.013 ± 0.002 for TCE and *cis*-DCE, respectively, indicate that (i) a C-Cl bond was broken in the rate-determining step, and (ii) the intrinsic effect was therefore not significantly masked by other

processes. Chlorine isotope analysis therefore bears great potential to investigate reaction mechanisms of CAHs in future studies.

This study also presents the first dual element (C, Cl) isotope plots of TCE and *cis*-DCE isotope ratios during degradation by cast ZVI. Pronounced differences in dual element (C, Cl) isotope slopes are observed between our results and those of Abe et al. (2009) for biodegradation of *cis*-DCE by the commercially available *Dehalococcoides*-containing culture mixed culture KB-1. The biotic plot had a slope 4 times higher than the one from our *cis*-DCE abiotic pattern suggesting a promising new way to discriminate biodegradation and abiotic reductive dechlorination from a PRB in the field. More data is necessary, however, to show whether these initial patterns can be reproduced in future studies with different organisms and different types of ZVI.

Product-specific carbon isotope fractionation ($\epsilon_{\text{substrate} \rightarrow \text{product}}$) revealed a notable difference between the fractionation expressed in β -dichloroelimination (ethane, ethane) and in hydrogenolysis (*cis*-DCE) daughter products. The same difference (10‰) was observed in recent work (Elsner *et al.*, 2008) suggesting that this product pattern is consistent. The pattern is indicative of abiotic transformation by ZVI, because the constant discrimination between products occurs only in the presence of β -dichloroelimination, which takes place only during abiotic transformation with ZVI. Product-related carbon isotope fractionation may therefore provide a second, independent line of evidence to distinguish biotic from abiotic degradation with ZVI.

Taken together, our study brings forward two promising approaches to distinguish biotic and abiotic transformation by ZVI and, therefore, to assess the effectiveness of ZVI treatment in field settings: (i) evidence from dual element isotope plots of chlorinated ethene parent compounds and (ii) evidence from carbon isotope ratios of their reaction products. We expect that these findings will increase the potential of carbon and chlorine isotopic data for monitoring a ZVI PRB treatment in the field.

5. Note added in proof

After submission of our manuscript, a study by Lojkasek-Lima *et al.*, 2012 has been published reporting chlorine isotope fractionation during TCE degradation by zero valent iron ($\epsilon_{\text{C}} = -12.4$ permil, $\epsilon_{\text{Cl}} = -2.98$ permil). The fact that experiments started with an initial mixture of PCE, TCE and *cis*-DCE makes interpretation of their enrichment factors and dual element isotope slopes more difficult. Several processes occurred simultaneously (formation of TCE from PCE, further degradation of TCE) which cannot be deconvolved from the available data. To compare the results directly, reported enrichment factors would therefore need to be confirmed in single compound experiments. Nonetheless, the reported dual isotope slope of TCE ($\epsilon_{\text{C}}/\epsilon_{\text{Cl}} = 4.2$)

agrees well with the one obtained in our experiments (5.2) providing a nice confirmation of the conclusions of our study.

6. Acknowledgements

Audí-Miró, C. and Cretnik, S., contributed equally to this work. This study was funded by the Spanish Government CICYT projects CGL2008-06373-C03-01/03-BTE and CGL2011-29975-C04-01 and by the Catalan Government project 2009 SGR 103. The authors would like to thank the Valles Business Park enterprise for providing the zero valent iron, the Catalan Water Agency for their support and the “Institute of Groundwater Ecology” from the “Helmholtz Zentrum München” together with the “Centres Científics i Tecnològics” of the “Universitat de Barcelona” for the chemical analyses. A special thanks also to the reviewers of this work and to Tom Bullen for their helpful contribution.

7. Supporting Information Available

Experimental conditions and calculated observed pseudo first order rate constants (K_{obs}) from Dual Element and additional cis-DCE and TCE Degradation experiments are indicated in Table S.1 from the Supporting Information, where they are compared to available literature data.

8. References

- Abe, Y., Aravena, R., Zopfi, J., Shouakar-Stash, O., Cox, E., Roberts, J.D., Hunkeler, D., 2009. Carbon and chlorine isotope fractionation during aerobic oxidation and reductive dechlorination of vinyl chloride and cis-1,2-dichloroethene. *Environ. Sci. Technol.* 43, 101–107.
- Arnold, W.A., Roberts, A.L., 2000. Pathways and kinetics of chlorinated ethylene and chlorinated acetylene reaction with Fe(0) particles. *Environ. Sci. Technol.* 34, 1794-1805
- Bernstein, A., Shouakar-Stash, O., Ebert, K., Laskov, C., Hunkeler, D., Jeannotat, S., Sakaguchi-Söder, K., Laaks, J., Jochmann, M.A., Cretnik, S., Jager, J., Haderlein, S.B., Schmidt, T.C., Aravena, R., Elsner, M., 2011. Compound-specific chlorine isotope analysis: a comparison of gas chromatography/isotope ratio mass spectrometry and gas chromatography/quadrupole mass spectrometry methods in an interlaboratory study. *Anal. Chem.* 83, 7624–7634
- Brunauer, S., Emmet, P.H., Teller, E., 1938. Adsorption of gases on multimolecular layers. *J. Am. Chem. Soc.* 60, 309–319.
- Burris, D.R., Campbell, T.J., Manoranjan, V.S., 1995. Sorption of trichloroethylene and tetrachloroethylene in a batch reactive metallic iron-water system. *Environ. Sci. Technol.* 29, 2850-2855

- Cichocka, D., Imfeld, G., Richnow, H.-H., Nijenhuis, I., 2008. Variability in microbial carbon isotope fractionation of tetra- and trichloroethene upon reductive dechlorination. *Chemosphere*. 71, 639-648
- Clark, C.J., Rao, P.S.C., Annable, M.D., 2003. Degradation of perchloroethylene in cosolvent solutions by zero-valent iron. *J. Hazard. Mater.* B96, 65-78
- Dayan, H., Abrajano, T., Sturchio, N.C., Winsor, L., 1999. Carbon isotopic fractionation during reductive dehalogenation of chlorinated ethenes by metallic iron. *Org. Geochem.* 30, 755-763
- Dridi, L., Pollet, I., Razakarisoa, O., Schäfer, G., 2009. Characterisation of a DNAPL source zone in a porous aquifer using the partitioning interwell tracer test and an inverse modelling approach. *J. Contam. Hydrol.* 107, 22-44
- Dries, J., Bastiens, L., Springael, D., Agathos, S.N., Diels, L., 2005. Combined removal of chlorinated ethenes and heavy metals by zerovalent iron in batch and continuous flow column systems. *Environ. Sci. Technol.* 39, 8460-8465
- Dybala-Defratyka, A., Rostkowski, M., Matsson, O., Westaway, K.C., Paneth, P., 2004. A new interpretation of chlorine leaving group kinetic isotope effects; a theoretical approach. *J. Org. Chem.* 69, 4900-4905
- Dybala-Defratyka, A., Szatkowski, L., Kaminski, R., Wujec, M., Siwek, A., Paneth, P., 2008. Kinetic isotope effects on dehalogenations at an aromatic carbon. *Environ. Sci. Technol.* 42, 7744-7750
- Elsner, M., Chartrand, M., Vanstone, N., Lacrampe-Couloume, G., Sherwood Lollar, B., 2008. Identifying abiotic chlorinated ethene degradation: characteristic isotope patterns in reaction products with nanoscale zero-valent iron. *Environ. Sci. Technol.* 42, 5963-5970
- Elsner, M., Hunkeler, D., 2008. Evaluating chlorine isotope effects from isotope ratios and mass spectra of polychlorinated molecules. *Anal. Chem.* 80, 4731-4740
- Elsner, M., Jochmann, M.A., Hofstetter, T.B., Hunkeler, D., Bernstein, A., Schmidt, T.C., Schimmelmann, A., 2012. Current challenges in compound-specific stable isotope analysis of environmental organic contaminants. *Anal. Bioanal. Chem.* In press.
- Elsner, M., Lacrampe Coulome, G., Mancini, S.A., Burns, L., Sherwood Lollar, B., 2010. Carbon isotope analysis to evaluate nanoscale Fe(0) treatment at a chlorohydrocarbon contaminated site. *Ground Water Monit. Rem.* 30, 79-85.
- Elsner, M., Lacrampe-Coulome, G., Sherwood Lollar, B., 2006. Freezing to preserve groundwater samples and improve headspace quantification limits of water-soluble organic contaminants for carbon isotope analysis. *Anal. Chem.* 78, 7528-7534
- Elsner, M., Mckelvie, J., Lacrampe-Couloume, G., Sherwood Lollar, B., 2007. Insight into methyl tert-butyl ether (MTBE) stable isotope fractionation from abiotic reference experiments. *Environ. Sci. Technol.* 41, 5693-5700

- Elsner, M., Zwank, L., Hunkeler, D., Schwarzenbach, A.P., 2005. A new concept linking observable stable isotope fractionation to transformation pathways of organic pollutants. *Environ. Sci. Technol.* 39, 6896-6916
- Gillham, R.W., O'Hannesin, S.F., 1994. Enhanced degradation of halogenated aliphatics by zero-valent iron. *Ground Water.* 32, 958-967
- Hofstetter, T.B., Reddy, C.M., Heraty, L.J., Berg, M., Sturchio, N.C., 2007. Carbon and chlorine isotope effects during abiotic reductive dechlorination of polychlorinated ethanes. *Environ. Sci. Technol.* 41, 4662-4668
- Hunkeler, D., Abe, Y., Broholm, M.M., Jeannotat, S., Westergaard, C., Jacobsen C.S., Aravena, R., Bjerg, P.L., 2011. Assessing chlorinated ethene degradation in a large scale contaminant plume by dual carbon-chlorine isotope analysis and quantitative PCR. *J. Contam. Hydrol.* 119, 69-79
- Hunkeler, D., Meckenstock, R.U., Sherwood Lollar, B., Schmidt, T., Wilson, J., 2008. A guide for assessing biodegradation and source identification of organic ground water contaminants using Compound Specific Isotope Analysis (CSIA). US EPA. EPA 600/R-08/148, Oklahoma.
- Hunkeler, D., Van Breukelen, B.M., Elsner, M., 2009. Modeling chlorine isotope trends during sequential transformation of chlorinated ethenes. *Environ. Sci. Technol.* 43, 6750-6756
- Liu, C.-C., Tseng, D.-H., Wang, C.-Y., 2006. Effects of ferrous ions on the reductive dechlorination of trichloroethylene by zero-valent iron. *J. Hazard. Mater.* B136, 706-713.
- Matheson, L.J., Tratnyek, P.G., 1994. Reductive dehalogenation of chlorinated methanes by iron metal. *Environ. Sci. Technol.* 28, 2045-2053
- Palau, J., Soler, A., Teixidor, P., Aravena, R., 2007. Compound-specific carbon isotope analysis of volatile organic compounds in water using solid-phase microextraction. *J. Chromatogr. A.* 1163, 260-268
- Prommer, H., Aziz, L.H., Bolaño, N., Taubald, H., Schüth, C., 2008. Modelling of geochemical and isotopic changes in a column experiment for degradation of TCE by zero-valent iron. *J. Contam. Hydrol.* 97, 13-26.
- Scott, K.M., Lu, X., Cavanaugh, C.M., Liu, J.S., 2004. Optimal methods for estimating kinetic isotope effects from different forms of the Rayleigh distillation equation. *Geochim. Cosmochim. Acta.* 68, 433-442
- Shouakar-Stash, O., Drimmie, R.J., Zhang, M., Frapce, S.K., 2006. Compound-specific chlorine isotope ratios of TCE, PCE and DCE isomers by direct injection using CF-IRMS. *Appl. Geochem.* 21, 766-781.
- Slater, G.F., Lollar, B.S., King, A., O'Hannesin, S., 2002. Isotopic fractionation during reductive dechlorination of trichloroethene by zero-valent iron: influence of surface treatment. *Chemosphere.* 49, 587-596

U.S. Environmental Protection Agency's Technology Innovation Office, 2003. Engineered approaches to in situ bioremediation of chlorinated solvents: fundamentals and field applications. EPA 542-R-00-008

Vanstone, N.A., Focht, R.M., Mabury, S.A., Sherwood Lollar, B., 2004. Effect of iron type on kinetics and carbon isotopic enrichment of chlorinated ethylenes during abiotic reduction on Fe(0). *Ground Water*. 42, 268-276

Wolfsberg, M., Van Hook, W.A., Paneth, P., 2010. *Isotope effects in the chemical, geological and bio sciences*. Dordrecht, Heidelberg, London, New York

TABLE S.1. Summary of observed pseudo first order rate constants (K_{obs}) for dechlorination of TCE and *cis*-DCE dual element and additional degradation experiments, for VC experiments and from literature by different ZVI types and surface treatments.

	Substrate	Concentration ^a (μM)	Iron type ^a	Surface treatment ^a	$a_s^{a,c}$ (m^2/g)	$\rho_m^{a,d}$ (g/L)	K_{obs}^a (d^{-1})	95% CI ^{a,b}	$R^{2,a}$	K_{obs} (d^{-1}) Combined exp.	95% CI ^b	K_{SA}^e ($\text{h}^{-1}\cdot\text{m}^{-2}\cdot\text{L}$)	95% CI ^b	Half-Life ^a (d)
TCE dual element experiment	TCE	441	Cast	Acid cleaned	0.70	200	0.28	± 0.015	0.98	0.24	± 0.018	$1.7\cdot 10^{-3}$	$\pm 1.3\cdot 10^{-4}$	2.5
		503	Cast	Acid cleaned	0.70	200	0.21	± 0.011	0.98					3.3
TCE additional degradation experiment	TCE	50	Cast	Acid cleaned	0.70	100	0.15	± 0.051	0.94	0.15	± 0.044	$2.1\cdot 10^{-3}$	$\pm 6.2\cdot 10^{-4}$	4.5
		50	Cast	Acid cleaned	0.70	100	0.15	± 0.060	0.91					4.6
<i>cis</i> -DCE dual element experiment	<i>cis</i> -DCE	787	Cast	Acid cleaned	0.70	200	0.013	± 0.001	0.99	0.01	± 0.001	$7.1\cdot 10^{-5}$	$\pm 8.5\cdot 10^{-6}$	51.7
		852	Cast	Acid cleaned	0.70	200	0.012	± 0.001	0.99					57.8
<i>cis</i> -DCE additional degradation experiment	<i>cis</i> -DCE	186	Cast	Acid cleaned	0.70	100	0.25	± 0.043	0.97	0.28	± 0.028	$4.0\cdot 10^{-3}$	$\pm 3.4\cdot 10^{-4}$	2.7
		186	Cast	Acid cleaned	0.70	100	0.31	± 0.034	0.98					2.2
VC dual element experiment	VC	185	Cast	Acid cleaned	0.70	200	0.009	± 0.005	0.64	0.007	± 0.003	$5.0\cdot 10^{-5}$	$\pm 2.1\cdot 10^{-5}$	80.6
		185	Cast	Acid cleaned	0.70	200	0.003	± 0.004	0.42					195.3
Slater et al., 2002	TCE	152	Cast	Autoclaved	-	100	0.09	-	0.94	-	-	-	-	7.6
	TCE	152	Cast	Autoclaved	-	50	0.07	-	0.86	-	-	-	-	10.3
	TCE	152	Cast	Autoclaved	-	25	0.05	-	0.98	-	-	-	-	13.8
	TCE	152	Cast	Acid cleaned	0.38	100	0.22	-	0.96	-	$5.8\cdot 10^{-3}$	-	-	3.2
	TCE	152	Cast	Autoclaved	0.35	100	0.03	-	0.96	-	$8.2\cdot 10^{-4}$	-	-	24.1
	TCE	152	Electrolytic 1	Acid cleaned	0.06	250	2.88	-	0.82	-	$2.0\cdot 10^{-1}$	-	-	0.2
	TCE	152	Electrolytic 1	Autoclaved	0.24	250	10.80	-	0.99	-	$1.8\cdot 10^{-1}$	-	-	0.1
	TCE	152	Electrolytic 2	Acid cleaned	-	250	2.64	-	0.95	-	-	-	-	0.3
	TCE	152	Electrolytic 2	Autoclaved	-	250	0.07	-	0.99	-	-	-	-	10.3
Dayan et al., 1999	TCE	91	Electrolytic	Acid cleaned	4.17	80	0.21	-	-	-	$6.2\cdot 10^{-4}$	-	-	3.4
	<i>cis</i> -DCE	784	Electrolytic	Acid cleaned	4.17	80	0.13	-	-	-	$1.3\cdot 10^{-5}$	-	-	5.5

^aNote that duplicates are listed separately so that each entry represents one experimental batch. ^b95% confidence interval. ^c a_s : specific surface area. ^d ρ : mass concentration of ZVI in solution. ^e K_{SA} : surface normalized rate constant

Annex B

Audí-Miró, C; Cretnik, S; Torrentó, C; Rosell, M.; Shouakar-Stash, O; Otero, N; Palau, J; Elsner, M; Soler, A. C, Cl and H compound-specific isotope analysis to assess natural versus Fe (0) barrier-induced degradation of chlorinated ethenes at a contaminated site. Submitted to *Environmental Science and Technology* in March 2014.

C, Cl and H compound-specific isotope analysis
to assess natural versus Fe (0) barrier-induced
degradation of chlorinated ethenes at a
contaminated site

Carme Audí-Miró^{†}, Stefan Cretnik[‡], Clara Torrentó[†], Mònica Rosell[†], Orfan Shouakar-Stash[§],
Neus Otero[†], Jordi Palau^ϕ, Martin Elsner[‡], Albert Soler[†]*

[†]Grup de Mineralogia Aplicada i Medi Ambient. Departament de Cristal·lografia, Mineralogia i Dipòsits Minerals. Facultat de Geologia. Universitat de Barcelona. Martí Franquès s/n, 08028. Barcelona, Spain

[‡]Institute of Groundwater Ecology, Helmholtz Zentrum München-National Research Center for Environmental Health, Ingolstädter Landstrasse 1, D-85764 Neuherberg, Germany.

[§]Department of Earth & Environmental Sciences, 200 University Ave. W, N2L 3G1 Waterloo, Ontario, Canada

^ϕUniversité de Neuchâtel. CHYN - Centre d'hydrogéologie. Rue Emile-Argand 11, CH – 2000, Neuchâtel, Switzerland.

Corresponding Author.

*Carme Audí-Miró. Phone: +34 934021343; Fax: +34 934021340, e-mail: carmeaudi@ub.edu

ABSTRACT

Compound specific isotope analysis of multiple elements (C, Cl, H) was tested to better assess the effect of a zero valent iron - permeable reactive barrier (ZVI-PRB) installation at a site contaminated with tetrachloroethene (PCE) and trichloroethene (TCE). The focus was on 1) using ^{13}C to evaluate natural chlorinated ethenes biodegradation and ZVI-PRB efficiency. 2) using dual element ^{13}C - ^{37}Cl isotope analysis to distinguish biotic from abiotic degradation of *cis*-DCE, 3) using triple element ^{13}C - ^{37}Cl - ^2H isotope analysis of *cis*-DCE and TCE to elucidate different contaminant sources. Both, biodegradation and degradation by ZVI-PRB, were evidenced by means of detected metabolites and ^{13}C data, with quantitative estimates of ZVI-PRB efficiency of less than 10% and 2% for PCE and *cis*-DCE, respectively. Dual element ^{13}C - ^{37}Cl isotope plots confirmed that the effect of the ZVI-PRB was masked by biodegradation. Based on carbon isotopes data, 49% and almost 100% of PCE and TCE, respectively, were estimated to be removed by biodegradation. ^2H combined with ^{13}C and ^{37}Cl discriminated two different sources of contamination spilled from the same industry. This indicates the potential of $\delta^2\text{H}$ to discriminate if a compound is of industrial origin, or whether it is formed as a daughter product during degradation.

Keywords: chlorinated ethenes, carbon, chlorine, hydrogen, isotopic fractionation, zero valent iron, permeable reactive barrier

INTRODUCTION

Tetrachloroethene (PCE) and trichloroethene (TCE) are dense chloro-aliphatic hydrocarbons (CAH) that have been used in large scale as metal and textile cleaners and degreasers. Due to spills and accidents, these CAHs have been extensively released to groundwater. In the aquifer, because they are denser than water, they migrate downwards through the saturated zone until they reach a confining layer, forming pools, thus constituting a long term source of groundwater contamination and an important environmental concern. PCE and TCE are among the most frequently detected volatile organic compounds (VOCs) in urban areas wells, e.g., in a survey of 3500 water samples from 100 different aquifer studies carried out by the USGS, PCE and TCE were detected in more than 2 % of the samples in concentrations higher than 0.2 $\mu\text{g/L}$.¹

Under reducing conditions, PCE and TCE can experience microbial sequential dechlorination to *cis*-DCE, VC and non-toxic ethene and ethane. Frequently, however, incomplete reductive dechlorination with the accumulation of *cis*-DCE and VC can occur due to the lack of

specialized degrader communities.² The accumulation of these compounds is of great concern because of their potential or proven carcinogenicity,³ where VC is the most toxic product of the degradation chain. Therefore, there has been an increasing interest in engineered abiotic degradation to remove these compounds in an efficient way, without the uncertainties of natural biodegradation.

Zero valent iron permeable reactive barrier (ZVI-PRB) treatment involves the placement of particulate cast ZVI in the flow path of a contaminated plume. As the plume moves through the barrier, ZVI is designed to sequentially degrade PCE by reductive dechlorination to form the non-toxic compounds ethene and ethane.⁴ In contrast to biodegradation, which occurs exclusively by hydrogenolysis, ZVI is able to degrade the chlorinated compounds also through the β -dichloroelimination pathway. The β -dichloroelimination pathway dominated over hydrogenolysis for some types of iron^{5, 6, 7} meaning that it can circumvent the production of VC, where acetylene and longer chain hydrocarbons (C3 to C6) are produced instead, as well as ethene and ethane.⁵

The potential high reactivity of the ZVI with chlorinated ethenes together with the prospect of long-term operation with low or even no need of maintenance, have made PRBs an attractive option for the remediation of contaminant plumes. Nevertheless, some aspects can affect the performance or the longevity of a barrier, such as 1) design flaws, including improper hydraulic characterization⁸ that can result in bypass and inadequate ZVI/sand ratios;⁹ 2) the alteration of the ZVI by geochemical factors that can induce minerals precipitation at the iron surface reducing its reactivity and hydraulic conductivity.¹⁰⁻¹⁵

When a ZVI-PRB is applied at a field site to degrade chlorinated ethenes, natural biodegradation of these compounds can occur at the same time. Therefore, it is necessary to discriminate both kinds of degradation reactions to determine the relevance of each process on the target compounds degradation. Overall, in order to accurately evaluate the PRB performance, it is important to investigate downgradient of the barrier (i) the occurrence of hydraulic bypasses; (ii) the presence of incomplete ZVI abiotic degradation products; and (iii) the relevance of the transformation due to ZVI compared to ongoing biodegradation.

Compound Specific Isotope Analysis (CSIA) bears potential to obtain such discrimination and to estimate the extent of either type of degradation. The approach is based on the Kinetic Isotope Effect (KIE) during a transformation process, whereas non-degradative processes entail much smaller isotope effects. As a result of the KIE, an enrichment of heavy isotopes in the reacting compound occurs while the product contains initially more lighter isotopes. This effect is

known as isotopic fractionation. The isotopic composition of a compound for a specific element (i.e. C, Cl, H) is expressed in the δ notation,

$$\delta^{13}\text{C} = \left(\frac{(^{13}\text{C}/^{12}\text{C})_{\text{compound}} - (^{13}\text{C}/^{12}\text{C})_{\text{VPDB}}}{(^{13}\text{C}/^{12}\text{C})_{\text{VPDB}}} \right), \quad (1)$$

where, for carbon, the international reference is the Vienna Pee Dee Belemnite (VPDB). In order to use the isotopic approach in field applications, it is necessary to determine the isotopic enrichment factor ϵ of a particular degradation mechanism.¹⁶ The isotopic enrichment factor is measured by the Rayleigh equation,¹⁷

$$\frac{R}{R_0} = \frac{(1000 + \delta^{13}\text{C})}{(1000 + \delta^{13}\text{C}_0)} = f^{(\epsilon_C)}, \quad (2)$$

where R_0 and R are C isotope ratios ($^{13}\text{C}/^{12}\text{C}$) at the beginning and at a given time (t) respectively, $\delta^{13}\text{C}_0$ and $\delta^{13}\text{C}$ are the same values in delta notation and f is the fraction of substrate remaining at time t . If the ϵ_C has been obtained in laboratory experiments for a specific transformation reaction, it can subsequently be applied to the field where the target process was identified, to estimate, according to Equation 3 the real extent of the specific transformation reaction at field scale.

$$D[\%] = \left[1 - \left(\frac{\delta^{13}\text{C}_t + 1000}{\delta^{13}\text{C}_0 + 1000} \right)^{\left(\frac{1000}{\epsilon_C} \right)} \right] \cdot 100, \quad (3)$$

where, D represents the percentage of degraded fraction. Numerous studies reported isotopic enrichment factors for carbon ϵ_C of chlorinated ethenes from biodegradation experiments with mixed cultures (ranging from -2.6 to -7.1 ‰ for PCE, from -2.5 to -15.3 ‰ for TCE and from -14.1 to -25.5 ‰ for *cis*-DCE¹⁸⁻²³) and for abiotic ZVI degradation (-5.7‰ to -25.3‰ for PCE, -8.6‰ to -27‰ for TCE, -6.9‰ to -23.1‰ for *cis*-DCE and from -6.9‰ to -20.1‰ for VC).^{6,7,24-26} Since ranges of ϵ_C for the two types of degradation overlap, it is not possible to discriminate between biodegradation and abiotic ZVI degradation. The combination of other elements (Cl or H), however, has the potential to obtain precisely such discrimination and to distinguish between the different transformation pathways.²⁷⁻²⁹ The reason is that the two elements implicated in the breakage of a bond might experience distinct isotopic fractionation during different degradation processes due to, i.e., possible different chemical reaction mechanisms or different rate-limiting step. Therefore, the combination of carbon isotope data with other elements (Cl or H), bears potential to provide additional insight into transformation mechanisms, thus to distinguish different degradation processes.²⁷⁻²⁹ The recent improvement of analytical methods for measuring chlorine isotope ratios of chlorinated ethenes enabled the

application of the dual ^{13}C - ^{37}Cl approach in field studies.³⁰ Our previous laboratory studies for TCE degradation with ZVI⁷ reported a dual isotope slope ($\epsilon_{\text{C}}/\epsilon_{\text{Cl}}$, i.e. ratio between C and Cl fractionations) of 5.2. While this value is distinguishable from those reported by Wiegert et al.³¹ ($\epsilon_{\text{C}}/\epsilon_{\text{Cl}}$ of 2.7) for a microbial culture enriched in *Desulfitobacteria*, and of Cretnik et al.³² ($\epsilon_{\text{C}}/\epsilon_{\text{Cl}}$ between 3.4 and 3.8) for *Geobacter lovleyi* and *Desulfitobacterium hafniense*, it overlaps significantly with values reported by Kuder et al.³³ for a Bio-Dechlor Inoculum (BDI) culture enriched in *Dehalococcoides* sp. ($\epsilon_{\text{C}}/\epsilon_{\text{Cl}}$: 4.7). Available data suggests that a better distinction may be possible for *cis*-DCE. Abe et al.²⁹ reported slopes ($\epsilon_{\text{C}}/\epsilon_{\text{Cl}}$) for reductive dechlorination by a mixed culture enriched with *Dehalococcoides ethenogenes* for *cis*-DCE and VC of 12.5 and 14, respectively. These values clearly fall in a different range compared to the slope of 3.1 obtained in our previous studies⁷ for *cis*-DCE-ZVI reductive dechlorination. However, since *cis*-DCE is also a product in the TCE dechlorination sequence there is a more complex picture to solve.

To tackle an even more difficult aspect - to disentangle a different origin of *cis*-DCE (as metabolite vs. original industrial product) - this study employs for the first time also compound-specific hydrogen isotope analysis on field samples. Earlier studies already proposed $\delta^2\text{H}$ as a useful tool to distinguish the origin of TCE, reporting that manufactured TCE presented very positive $\delta^2\text{H}$ values (between +400 to +600 ‰),^{34,35} in contrast to the TCE produced from PCE reductive dechlorination, with more negative $\delta^2\text{H}$ values (-350 ‰)³⁴. Although negative $\delta^2\text{H}$ values (up to -184 ‰) of manufactured TCE were recently reported³³, the expected high depletion in ^2H during TCE formation in the environment may still be a potential way to discriminate the origin of TCE and, consequently, of the compounds occurred during its degradation reaction sequence.

Therefore, the main goal of this work was to test the compound specific isotope analysis of multiple elements (C, Cl, H) to assess a ZVI-PRB treatment by 1) using ^{13}C analysis, to evaluate the occurrence of natural chlorinated ethenes biodegradation, to obtain their ϵ_{C} of biodegradation from microcosms experiments and to quantify the ZVI-PRB efficiency; 2) using dual element ^{13}C - ^{37}Cl isotope approach, to discriminate biotic from abiotic degradation of *cis*-DCE; 3) according to results of point 2, to choose the appropriate ϵ_{C} (the biotic or the abiotic one) in order to quantify the real degradation at the field site; and 4) using triple element ^{13}C - ^{37}Cl - ^2H isotope analysis of *cis*-DCE and TCE to elucidate different contaminant sources, in order to see the potential of the $\delta^2\text{H}$ approach to distinguish TCE of industrial origin.

SITE DESCRIPTION

The study site is located at the industrial area of Granollers, 20 Km NW from Barcelona, Catalonia. An automotive industry that used PCE and TCE as degreasers operated in the area from 1965 to 1989. The site is bounded on its west side by the *Can Ninou* creek, which continues to the S-SW (Figure 1). The lithology of the site is mainly composed by an alternation of sand and silt Miocene sediments in a clayey matrix that extends from 4 m to a minimum of 14 m depth (Fig.1). The water table of the aquifer is located at an average depth of 5.4 ± 2.1 m. The deepest water table (around 8 m) was measured at the base and at the top of the studied valley area (length of the studied area 900 m). While at around 300 m from the top of this area the water table was located closer to the surface (around 3 m depth). The average water table variation due to seasonal changes was of -0.5 ± 0.9 m. The deepest studied well reached 20 m depth. The direction of the flow is NE to W-SW. Details of the hydrogeological characterization of the study site are provided in the Supporting Information (SI).

Groundwater contamination with PCE and TCE was produced due to the discharge of industrial waters into a seepage pit located at the south of the plant (close to MW17); this point is considered the contamination source area, where historical data from 2004 revealed concentrations of *cis*-DCE up to 160 mg/L and of its precursors PCE and TCE of 25 and 180 mg/L, respectively. Before starting the present work, a dual remediation strategy was performed at the studied site: the removal of the contaminated soil from the source area in 2009 and the installation of a ZVI-PRB to treat the groundwater contaminant plume in 2010. The PRB was built approximately 320 m downstream the contaminated source, transverse to the creek, from NW to SE position (Fig. 1). The top of the PRB was placed 4-5 m below ground surface and its size is 20 m long, 5 m high and 60 cm thick, with a 3% (v/v) of granular cast ZVI inside a sand matrix.

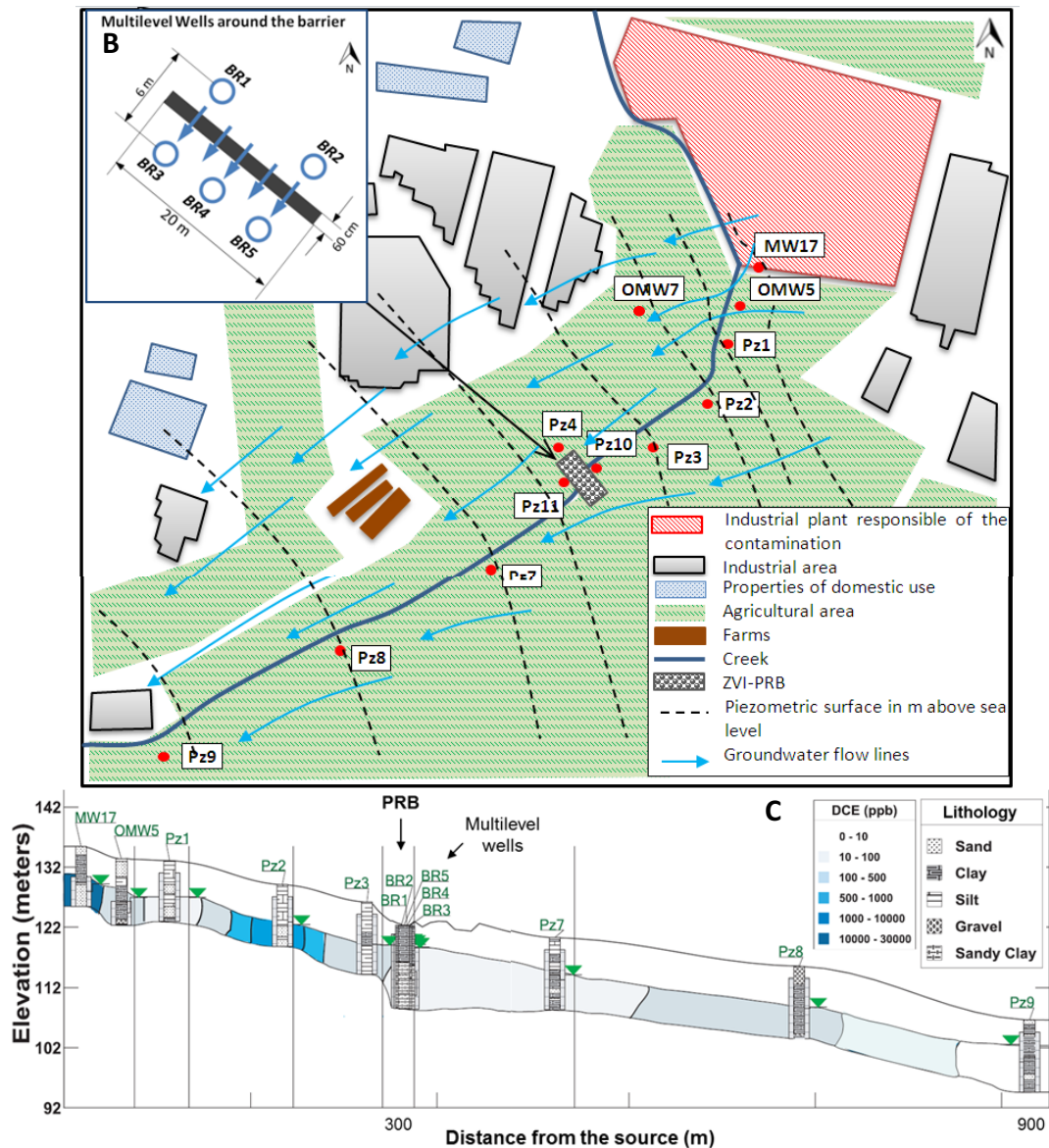


Figure 1. A) Map of the study site. The location of the wells installed along the *Can Ninou* Creek and the location of the ZVI PRB, as well as the piezometric surfaces and groundwater flow lines are represented. B) Distribution of the multilevel wells around the ZVI-PRB. C) Cross section along the creek from the source area to 900 m downstream. The lithology of each well is exposed, as well as the water table indicated by the green triangles. *cis*-DCE concentration contours are also shown.

METHODOLOGY

From April 2011 to March 2013, four sampling surveys were carried out (April 2011, June 2012, October 2012 and March 2013) from both conventional and multilevel wells (see SI for details). In all surveys, concentration and $\delta^{13}\text{C}$ of chlorinated ethenes were measured, whereas in the Oct-12 survey $\delta^{37}\text{Cl}$ of PCE and *cis*-DCE and $\delta^2\text{H}$ of *cis*-DCE and TCE were also determined.

Redox sensitive species were analyzed by standard analytical techniques as in Torrentó et al.³⁶ Concentrations of chlorinated ethenes were determined by headspace analysis using a FOCUS Gas Chromatograph coupled with a DSQ II mass spectrometer (GC-MS) (Thermo Fisher Scientific, Waltham, Massachusetts, USA). Carbon isotope composition of PCE, TCE and *cis*-DCE was analyzed using a gas chromatography-combustion-isotope ratio mass spectrometry system (GC-C-IRMS) consisting of a Trace GC Ultra equipped with a split/splitless injector, coupled to a Delta V Advantage IRMS (Thermo Scientific GmbH, Bremen, Germany) through a combustion interface. Chlorine isotopic measurements of PCE and *cis*-DCE were conducted on a GC-IRMS system (Thermo Scientific, Waltham, Massachusetts, USA) consisting of a Trace GC connected to a MAT 253 IRMS with dual inlet system via a heated transfer line.³² Hydrogen isotopic analyses of TCE and *cis*-DCE were determined following the method developed by Shouakar-Stash and Drimmie³⁷ using a Deltaplus XL CF-IRMS (ThermoFinnigan, Bremen, Germany) coupled with an Agilent 6890 GC (Agilent Technologies Inc., Santa Clara, CA, USA) and a chromium reduction (R) system.

Ethene, ethane and acetylene concentrations were measured in a Varian 3400 GC (Scientific Equipment Source, Oshawa, Ontario, Canada) coupled to a flame-ionization detector (FID). Carbon isotope measurement of ethene, was accomplished by using a purge and trap Teledyne-Tekmar XPT concentrator coupled to a Varian 3400 GC and a Finnigan MAT 252 IRMS via a combustion interface. Continuous flow $\delta^2\text{H}$ analysis of ethene, was conducted using the same purge and trap (Teledyne-Tekmar XPT concentrator) coupled to a HP 6890 GC system online with a micropyrolysis oven and a Finnigan Mat (Bremen Germany) Delta Plus XL IRMS (GC-TC-IRMS). Additional details of all methodologies are provided in the SI.

RESULTS AND DISCUSSION

Evidences of biodegradation and ZVI-PRB mediated degradation

From a geochemical perspective, the redox conditions of the site were conducive to biotic reductive dechlorination of chlorinated ethenes. Specifically 1) reducing conditions prevailed in all wells (dissolved oxygen (DO) below 2 mg/L); 2) dissolved Mn was present in concentration up to 1.36 mg/L and dissolved Fe in concentrations up to 1.57 mg/L; 3) nitrate concentration decreased from an average of 63 mg/L to below detection limit (<5 mg/L) in samples where the highest Mn concentrations were detected; 4) sulfate concentrations decreased in the MW17 well (from an average of 90 mg/L to 16.8 mg/L) (Table S1). These redox conditions are also characteristic of abiotic chlorinated ethenes reductive dechlorination by ZVI, which would

favor this process at the ZVI-PRB area. Nevertheless, the pH analyzed downgradient the barrier (approximately 7) did not correspond to the common increase of pH (up to pH of 8 - 10) that usually occurs after the corrosion of iron with water.³⁸

Dechlorination products identified upgradient the ZVI-PRB indicated that biodegradation occurred at the site. The main compounds detected were PCE, TCE (mainly in OMW6B and OMW7) and cis-DCE (Table S2). The presence of cis-DCE gave evidence of the reductive dechlorination of TCE. TCE, at the same time, could derive from PCE degradation and/or be one of the original commercial products. VC was also detected (in MW17, OMW5 and Pz3), confirming that cis-DCE was further degraded. The detection of ethene and ethane in MW17 (Table S3) indicated ongoing complete dechlorination of the chlorinated ethenes at the source area. The two most contaminated wells were OMW7 with 22 mg/L of cis-DCE and 139 mg/L of TCE and MW17 with 16 mg/L of cis-DCE. In general, at the rest of the wells concentrations of all target compounds were in the order of tens to hundreds of $\mu\text{g/L}$ (Table S2).

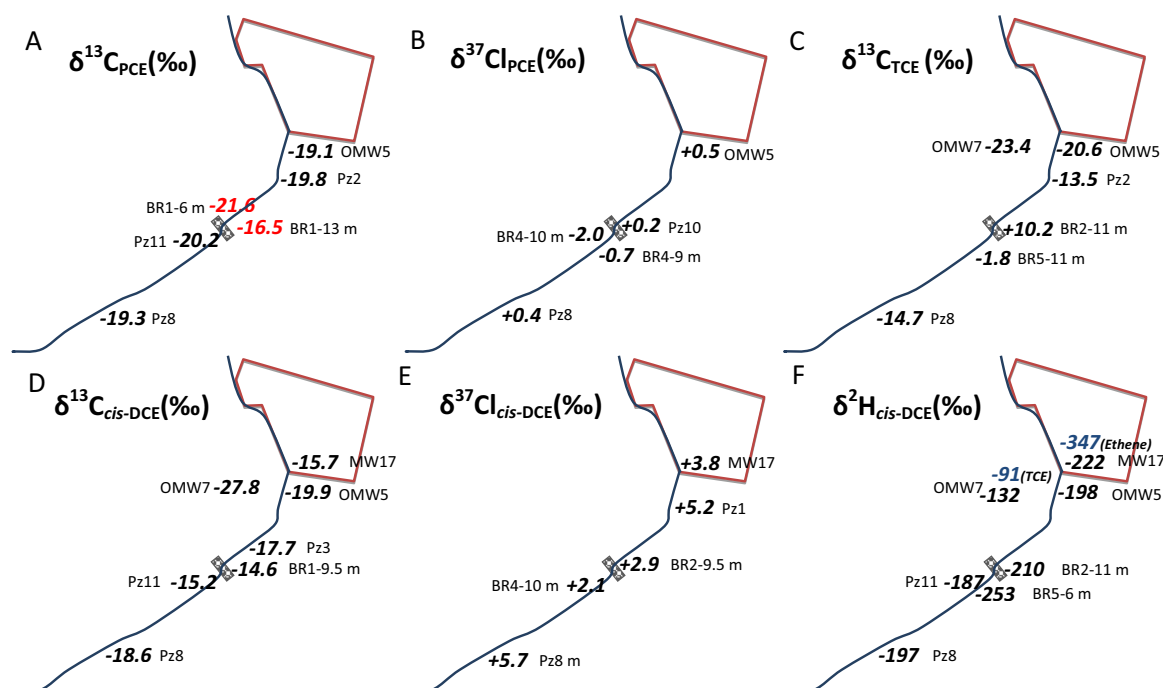


Figure 2. Isotope data of: $\delta^{13}\text{C}$ and $\delta^{37}\text{Cl}$ of PCE (A and B, respectively); $\delta^{13}\text{C}$ of TCE (C); and $\delta^{13}\text{C}$, $\delta^{37}\text{Cl}$ and $\delta^2\text{H}$ of cis-DCE (D, E and F, respectively). F also include TCE and ethene data, indicated in blue. These isotope data have been obtained from the most representative wells from: 1) the last survey when $\delta^{13}\text{C}$ data was obtained (Mar-13) (except for the wells in red for $\delta^{13}\text{C}$ of PCE that are from Jun-12); and from 2) the only survey when $\delta^2\text{H}$ and $\delta^{37}\text{Cl}$ were measured, Oct-12. OMW7 $\delta^{13}\text{C}$ and $\delta^2\text{H}$ data are from Sept-13.

Carbon isotope shifts observed in Figure 2 confirmed the occurrence of biodegradation at the site. The comparison of the lowest $\delta^{13}\text{C}$ of PCE and TCE values detected in the field (-21.6 and -

23.4 ‰, respectively) (Fig. 2) to the literature $\delta^{13}\text{C}$ ranges for commercial products (from -35.3 to -23.2 ‰ for PCE; and from -33.5 to -25.8 ‰ for TCE),^{34,39,40} shows that both PCE and TCE might be enriched in ^{13}C and therefore had been already degraded compared to the commercial compounds originating the contamination at this site. The most enriched in ^{13}C values of PCE, TCE and *cis*-DCE were detected right before the barrier (Fig.2), indicating a higher degradation degree which might be due to an increased residence time as a result of a possible hydraulic barrier effect of the ZVI-PRB. In addition, PCE carbon isotope values in wells OMW5 and BR1-11 changed towards more positive values along the three years of study, indicating not only biodegradation, but also an increase of the biodegradation extent over time (Fig. 3). The same trend was observed for *cis*-DCE in wells MW17 and BR1-9.5 (Fig. 3). In well MW17, $\delta^{13}\text{C}$ of VC ($\delta^{13}\text{C}$ of -38.4 ‰) was depleted in ^{13}C compared to the parent compound ($\delta^{13}\text{C}_{\text{DCE}}$ of -15.7 ‰), as typically occurs during biodegradation (Table S2). Complementary microcosm experiments with material from Pz1 and Pz3 wells (location in Fig. 1) verified the occurrence of biodegradation upgradient of the barrier (experiments detailed in the SI).

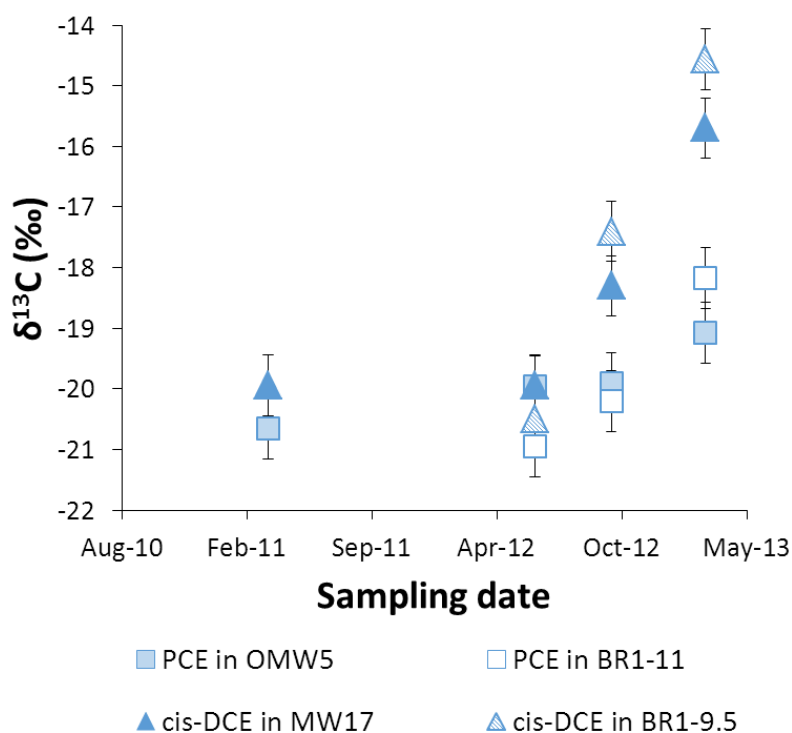


Figure 3. Changes in $\delta^{13}\text{C}$ over time of PCE and *cis*-DCE in wells OMW5 and BR1-11, and MW17 and BR1-9.5, respectively. Error bars represent $\delta^{13}\text{C}$ uncertainty of 0.5 ‰.

Downgradient of the PRB the presence of chlorinated ethenes suggested that the barrier did not achieve complete degradation of the contaminants and/or that hydraulic bypass was occurring. Lateral and underneath hydraulic bypass was suggested by the presence of PCE and *cis*-DCE in Pz4 and in the multilevel wells at 11 to 13 m depth (taking into account that the barrier is located at around 10 m depth). Acetylene was present in BR4, with the highest concentration (20 µg/L) at 8 m depth (Table S3), coinciding with the point located right at the central part of the barrier. This would give evidence of abiotic degradation due to the reaction of the chlorinated ethenes through the ZVI-PRB.^{5,6,7}

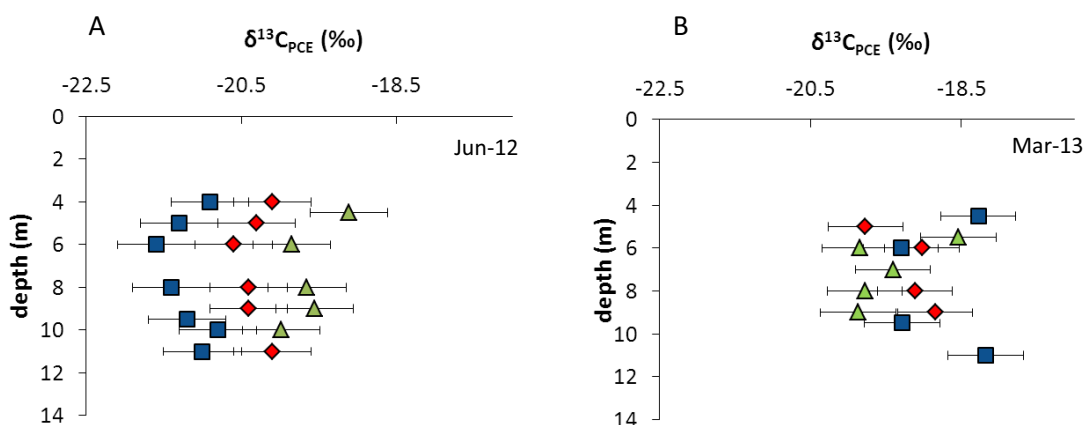


Figure 4. $\delta^{13}\text{C}$ of PCE in BR1 (blue squares, directly in front of ZVI-PRB), BR3 (red diamonds) and BR4 (green triangles) (both directly behind ZVI-PRB) in depth from Jun-12 (A) and Mar-13 (B) campaigns. Error bars represent an uncertainty of 0.5 ‰ for $\delta^{13}\text{C}$ measurements (for location of wells, see Figure 1).

The June-12 carbon isotope results of the multilevel wells directly before (BR-1) and directly after (BR-3, BR-4) the ZVI-PRB exhibited a small but consistent enrichment of ^{13}C in both PCE and *cis*-DCE from upstream to downstream of the barrier (Fig. 4A), more visible at the central part of the barrier (BR4) where significant formation of TCE was also observed (from almost not detected to 46 µg/L in BR4-10 m). These results confirmed PCE and *cis*-DCE degradation by the ZVI-PRB. Since *cis*-DCE initially contains less ^{13}C than the PCE from which it is formed, it can have more positive values only if it is further degraded. Then, the average value in BR1 $\delta^{13}\text{C}$ of -20‰ of *cis*-DCE compared to -20.6‰ of PCE indicates such degradation beyond *cis*-DCE. Therefore, the extent of degradation can be estimated for each of the two compounds according to Equation 3. $\delta^{13}\text{C}_0$ and $\delta^{13}\text{C}_t$ were taken as the average $\delta^{13}\text{C}$ values from before (BR-1) and after the barrier (here, only BR4 was considered due to less influence of bypass)

and the carbon enrichment factor ϵ_c obtained in previous PCE and *cis*-DCE degradation laboratory experiments with ZVI (-9.5 ‰ for PCE, see SI, and -18.6 ‰ for *cis*-DCE⁷) were used. The calculated efficiency of the PRB in June-12 was less than 10 % and 2% for PCE and *cis*-DCE, respectively. The effect of the PRB observed in June-12 was not detected in Oct-12 and Mar-13 surveys, when several points upstream of the barrier were even more enriched in ¹³C than downstream values (Fig. 4B). These results suggested that biodegradation upstream of the barrier might be masking the low ZVI-PRB effect, enhancing the hypothesis of a hydraulic barrier effect that might increase the residence time of the compounds, and thus, their biodegradation.

Evidences of biodegradation vs. ZVI-PRB mediated degradation from dual C-Cl isotope approach

In order to confirm the predominance of biodegradation versus the low effect of the barrier, the dual ¹³C-³⁷Cl isotope approach was used. The dual ¹³C-³⁷Cl isotope plots obtained from Oct-12 data from both the upstream and downstream barrier wells, yielded a dual isotope slope (ϵ_c/ϵ_{Cl}) of 1.5 ± 0.1 (Fig. 5). The positive ³⁷Cl versus ¹³C isotopes shifts correlation confirmed degradation processes also from a chlorine isotopes perspective. The wells located before and after the barrier (MW17, OMW5, Pz1 from upstream and BR4-6, 7, 9, 10 m and Pz11 from downstream) follow the same trend within the 95 % confidence interval. The slope obtained in this study, was compared to the literature data from laboratory experiments and field studies with biotic or abiotic degradation reactions of *cis*-DCE either as substrate or intermediate product^{7,27,29} (Fig. 5). The closer proximity of our results to the slope of 2 obtained from Hunkeler et al.²⁷ in a field study with *cis*-DCE as intermediate and where *Dehalococcoides* sp. were detected, points to anaerobic biodegradation as the main process occurring at the site, without distinguishing the low effect of the ZVI-PRB. It has to be taken into account, that the direct implication of *Dehalococcoides* sp. in *cis*-DCE degradation could not be proven in Hunkeler et al.²⁷ study. Moreover, the slope observed in these two studies (Hunkeler et al.²⁷ and ours) is far from the 12.5 value obtained by Abe et al. by the commercially available *Dehalococcoides*-containing KB-1 culture²⁹, so biodegradation in both sites could be linked to many other anaerobic microorganisms.

Observation of $\delta^{37}\text{Cl}$ data gave further insight into the isotope fractionation effects. Isotope values of PCE were always more negative than $\delta^{37}\text{Cl}$ values of *cis*-DCE (Fig. 2 and more detailed in Fig. S5), an effect that was also observed by Lojkasek-Lima et al.⁴³ in a field study. Lojkasek-

Lima et al.⁴³ attributed this effect to the parent compound (in this case PCE) degradation extending beyond *cis*-DCE with the production of VC and final degradation compounds. An alternative hypothesis is that an inverse secondary chlorine isotope effect is produced during reductive dechlorination, where the product might be preferably formed by those molecules with more ³⁷Cl atoms in the non-reacting positions, with an enriched $\delta^{37}\text{Cl}$ compared to the parent compound. This effect was early suggested in previous laboratory experiments with ZVI,⁷ where an initial enrichment in ³⁷Cl of *cis*-DCE was observed during TCE degradation.

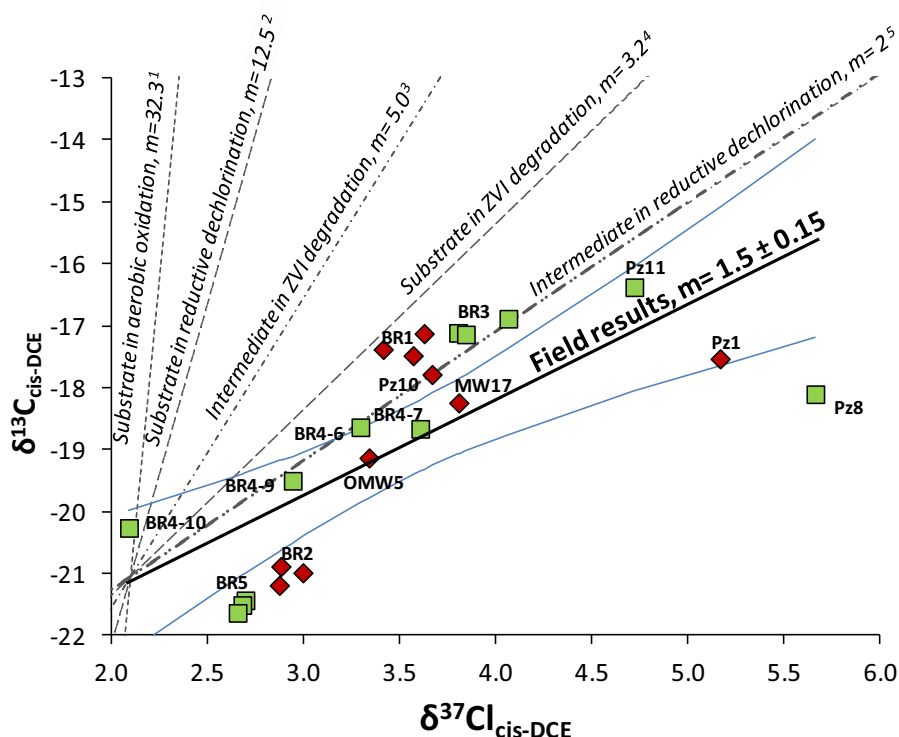


Figure 5. $\delta^{13}\text{C}$ versus $\delta^{37}\text{Cl}$ from Oct-12 campaign samples. A dual isotope slope (ϵ_C/ϵ_{Cl}) of 1.5 ± 0.1 was determined. Red diamonds represent wells upstream of the ZVI-PRB and green squares represent wells downstream the ZVI-PRB. Blue lines indicate the 95 % confidence intervals of the regression line. Dashed lines show the slopes obtained in previous studies: ¹ *cis*-DCE substrate in Abe et al.,²⁹ *β-Proteobacterium* spp. batch experiments; ² *cis*-DCE substrate in Abe et al.,²⁹ *Dehalococcoides* KB-1 batch experiments; ³ *cis*-DCE intermediate product in previous ZVI batch experiments ⁷; ⁴ *cis*-DCE substrate in previous ZVI degradation experiments ⁷; ⁵ *cis*-DCE intermediate in reductive dechlorination from Hunkeler et al.,²⁷ field studies.

Extent of the natural attenuation processes

Given that the added information from chlorine isotopes confirmed biodegradation as the main process occurring at the site, the most site-specific carbon isotopic enrichment factors could be chosen to determine the extent of PCE, TCE and *cis*-DCE average biodegradation in the field. The ϵ_C values obtained for PCE and TCE from the microcosm experiments (-2.6 ± 0.9 ‰ and -1.7 ± 1.8 ‰, respectively, see details in the SI) were used to estimate the extent of natural attenuation, following Equation 1. Despite the high uncertainty of the ϵ_C for TCE, this value was

used to estimate the degradation since it is consistent with the literature ϵ_c range (-2.5 to -16 ‰).^{19,20,21,29,41} However, as no *cis*-DCE degradation was observed in the microcosm experiments after 500 days of incubation, the $\epsilon_{c,cis\text{-DCE}}$ range reported in the literature (from -14.1 to -29.7 ‰) was used.^{19,20,23,29,41,42} The lightest current ^{13}C signature of the parent compound PCE of the site was used as the initial isotopic composition also for TCE and *cis*-DCE, taking into account isotopic balance of the target compounds during sequential reductive dechlorination. The average observed biodegradation was 48.7% for PCE, 99.9 % for TCE and between 9.2 and 18.3 % for *cis*-DCE.

Use of $\delta^{13}\text{C}$, $\delta^{37}\text{Cl}$ and $\delta^2\text{H}$ for chlorinated solvents source identification

Based on concentration data alone, the extremely high TCE concentrations at OMW7 (139 mg/L) together with the low concentrations of TCE throughout the site clearly suggested the presence of a separate TCE source in OMW7 groundwater flow direction. Based on our considerations, we would expect, on the other hand, that TCE close to the barrier should be formed from PCE. This clear hypothesis enabled us to test in the field whether these different sources would also be distinguishable from isotope analysis alone. Carbon isotopes showed that the less degraded PCE ($\delta^{13}\text{C}$ of -21.6‰) was transported downstream to the ZVI-PRB area (Fig. 2). Differently, the lowest $\delta^{13}\text{C}$ of TCE (-23.4 ‰) was detected in OMW7 (Fig. 2) west of the site. An initial approximation of chlorine and hydrogen isotope data, showed that the most negative chlorine isotope values of both PCE and *cis*-DCE of the site were also detected at the ZVI-PRB area (BR4), as well as, the lowest $\delta^2\text{H}$ of *cis*-DCE, detected in BR5 (Fig. 2). This would confirm that rests of the less degraded PCE are present around the PRB. The positive correlation (R^2 : 0.99) between the most depleted $\delta^{37}\text{Cl}$ values of PCE and *cis*-DCE at BR4 (Fig. S4), points to a *cis*-DCE coming from PCE at this point. Finally, regarding hydrogen isotope results, $\delta^2\text{H}$ TCE value in the well OMW7 (-91 ‰) was not as negative as expected from PCE dechlorination (-350‰),³⁴ neither as positive as reported manufactured TCEs (between +400 to +600 ‰),^{34,35} thus suggesting a mixture of TCE coming from PCE dechlorination and manufactured TCE.

Although the TCE concentration along the creek was too low to analyze the $\delta^2\text{H}$, an approximation of $\delta^2\text{H}$ data could be estimated. Previously, it was necessary to calculate the $\delta^2\text{H}$ of the hydrogen added to TCE during its dechlorination to *cis*-DCE in OMW7 according to the equation proposed by Kuder et al.³³

$$\delta^2\text{H}_{\text{addition}} = (n \times \delta^2\text{H}_{\text{daughter-bulk}}) - ((n-1) \times \delta^2\text{H}_{\text{parent-bulk}}), \quad (4)$$

where “n” is the number of hydrogen atoms in the given daughter product, the “bulk” $\delta^2\text{H}$ refers to the average $\delta^2\text{H}$ of parent and daughter compounds, in this case, TCE and cDCE, respectively. Equation 4 assumes that the protonation conserves the isotope ratios of the hydrogen inherited from the parent compound, which do not undergo hydrogen isotope exchange while residing in the environment.³³ Although the added hydrogen comes from the H_2 (generated from the oxidation of an organic substrate by microorganisms or abiotically at the ZVI barrier), its $\delta^2\text{H}$ is ultimately controlled by the $\delta^2\text{H}$ of the water medium since there is an equilibrium in the environment between water and this H_2 .³³ The calculated value of -169 ‰ ($\delta^2\text{H}_{\text{addition}}$) allowed the estimation through the same equation 4, of the TCE $\delta^2\text{H}$ value in BR5-6 m where the *cis*-DCE $\delta^2\text{H}$ value was known, resulting in a $\delta^2\text{H}_{\text{TCE}}$ of -337 ‰. The presence around the barrier zone of a TCE with a very negative $\delta^2\text{H}$ confirms a different origin of this TCE and the TCE present in OMW7. Moreover, our estimated values are similar to the ones obtained by Shoukar Stash et al.³⁴ for a TCE from PCE dechlorination ($\delta^2\text{H}$ of around -350), suggesting that TCE is mainly coming from PCE degradation, in contrast to the TCE in OMW7.

Through Equation 4 the $\delta^2\text{H}$ added during *cis*-DCE transformation to ethene (with VC as intermediate) in MW17 was also calculated, resulting of -944 ‰. Since the measured $\delta^2\text{H}$ of our site groundwater was -37.5 ‰, the very depleted in ^2H hydrogen involved in the dechlorination processes, would confirm hydrogen isotope fractionation during water- H_2 equilibrium.^{33,34} These $\delta^2\text{H}$ results are in the same order as the ones obtained in laboratory experiments by Kuder et al.³³ (-150 ‰ for TCE to *cis*-DCE and -1420 ‰ for *cis*-DCE to ethene) for TCE biodegradation to *cis*-DCE with a mixed culture containing *Dehalococcoides* sp. and using a medium water with a quite similar $\delta^2\text{H}$ value (-42‰).

Moreover, the presented *cis*-DCE results, which to our knowledge are the first negative reported $\delta^2\text{H}$ *cis*-DCE values, contrast with the positive values (+200 ‰) of *cis*-DCE from reductive dechlorination of manufactured TCE in laboratory experiments,³³ enhancing the evidence that *cis*-DCE comes mainly from the sequential reductive dechlorination from PCE at this site. When plotting $\delta^{13}\text{C}$ versus $\delta^2\text{H}$ of *cis*-DCE (Fig. 6), the difference in the TCE origin in OMW7 is evidenced again by the different trend revealed by its product *cis*-DCE regarding the rest of the wells. Although *cis*-DCE is predominantly coming from PCE, the $\delta^2\text{H}$ variability of *cis*-DCE at the wells along the creek might be the result of different contribution of certain ancient commercial TCE going also in this flow direction that provided a less negative $\delta^2\text{H}$ signature, because, according to the assumption of Equation 4, the $\delta^2\text{H}$ would be the same if all the *cis*-DCE came from the same parent (commercial TCE or dechlorinated PCE). This hypothesis also explains the more positive $\delta^2\text{H}$ of *cis*-DCE in comparison to TCE in BR5-6, since current TCE at

this area is coming only from PCE dechlorination, and current *cis*-DCE may come from both new and ancient commercial TCE.

Overall, the multi-isotope combination (C, Cl, H) by itself has elucidated two different TCE sources at the site, one composed by a mixture of manufactured TCE and TCE from PCE dechlorination travelling to the west (OMW7), and a second one mainly produced from PCE flowing in the creek direction. These results indicate significant potential of the use of $\delta^2\text{H}$ to assess the origin of industrial or degradation-derived chlorinated ethenes at contaminated sites with no other previous evidences. Despite the recently reported negative $\delta^2\text{H}$ values (up to -184 ‰)³³ of manufactured TCE, the high depletion in ^2H observed during TCE formation in the environment may still be a potential way to discriminate the origin of TCE and *cis*-DCE.

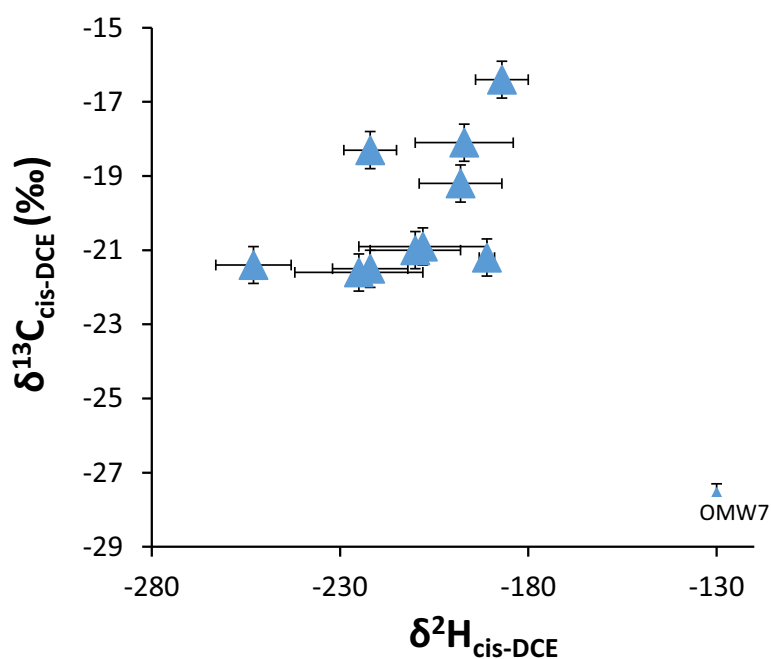


Figure 6. $\delta^{13}\text{C}$ versus $\delta^2\text{H}$ of *cis*-DCE in Oct-12 campaign all over the site showing a positive correlation between $\delta^2\text{H}$ and $\delta^{13}\text{C}$ shifts. Error bars represent an uncertainty of 0.5 ‰ for $\delta^{13}\text{C}$ and between 2 and 17 ‰ for $\delta^2\text{H}$ measurements. Sample from well OMW7 (-27.8 vs -130 ‰ of $\delta^{13}\text{C}$ and $\delta^2\text{H}$, respectively), does not follow the same trend as the others; see explanation in the text.

SUPPORTING INFORMATION

Site study extension, groundwater sampling extension, chlorinated ethenes analyses description, analyses of the most volatile compounds, complementary microcosm experiments and experiment of PCE degradation with ZVI are included in the Supporting Information. As well as complementary figures and tables commented in the main text.

ACKNOWLEDGMENTS

This study was funded by the Spanish Government CICYT projects CGL2008-06373-C03-01/03-BTE and CGL2011-29975-C04-01, by the Catalan Government project 2009SGR-00103 and a Marie Curie Career Integration Grant in the framework of the IMOTEC-BOX project (PCIG9-GA-2011-293808) within the European Union 7th Framework Programme. The authors would like to thank Clapé Group for providing us with the used zero valent iron, financing the installation of the multilevel wells and contracting us to study the ZVI-PRB efficiency as well as allowing this publication. We would also like to thank the Catalan Water Agency for their support, and the *Institute of Groundwater Ecology* from the “Helmholtz Zentrum München”, the *Isotope Trace Technologies* from Waterloo, the *Stable Isotope Laboratory* from the University of Toronto, and the “Centres Científics i Tecnològics de la Universitat de Barcelona” for the chemical analyses. We want to thank Daniel Sancho, Roberto Espinola, Adriana Rossi, Diana Rodríguez, Alba Grau, Mercè de Olamendi and Raul Carrey for helping in the field surveys. Special thanks to Joan Martínez from “GEOMAR Ingeniería del Terreny”, for the installation of the well OMW7.

REFERENCES

1. Zogorski, J.S.; Carter, J.M.; Ivahnenko, T.; Lapham, W.W.; Moran, M.J.; Rowe, B.L.; Squillace, P.J.; Toccalino, P.L. Volatile Organic Compounds in the Nation's Ground Water and Drinking-Water Supply Wells. **2006**. U.S. Geological Survey, Reston, Virginia. Circular 1292.
2. Friis, A.K.; Albrechtsen, H.J.; Cox, E.; Bjerg, P.L. The need for bioaugmentation after thermal treatment of a TCE-contaminated aquifer: Laboratory experiments. *J Contam Hydrol.* **2006**, 88 (3-4), 235-48
3. United States Environmental Protection Agency, National primary drinking water regulations. EPA 816-F-09-004 **2009**.
<http://water.epa.gov/drink/contaminants/upload/mcl.pdf>.
4. Scherer, M.M.; Richter, S.; Valentine, R.L.; Alvarez, P.J.J. Chemistry and Microbiology of Permeable Reactive Barriers for In Situ Groundwater Clean up. *Environ. Sci. Technol.* **2000**, 30 (3), 363-411
5. Arnold, W.A.; Roberts, A.L. Pathways and kinetics of chlorinated ethylene and chlorinated acetylene reaction with Fe(0) particles. *Environ. Sci. Technol.* **2000**, 34, 1794–1805.

6. Elsner, M.; Chartrand, M.; Vanstone, N.; Lacrampe-Couloume, G; Sherwood Lollar, B. Identifying abiotic chlorinated ethene degradation: characteristic isotope patterns in reaction products with nanoscale zero-valent iron. *Environ. Sci. Technol.* **2008**, 42, 5963-5970.
7. Audí-Miró, C.; Cretnik, S.; Otero, N.; Palau, J.; Shouakar-Stash, O.; Soler, A.; Elsner, M. Cl and C isotope analysis to assess the effectiveness of chlorinated ethene degradation by zero-valent iron: Evidence from dual element and product isotope values. *Appl. Geochem.* **2013**, 32, 175-183
8. Henderson, A.D.; Demond, A.H. Long-Term Performance of Zero-Valent Iron Permeable Reactive Barriers: A Critical Review. *Environ Eng Sci.* **2007**, 24, 401-427
9. O'Hannesin, S. F.; Gillham, R.W. Long-term performance of an in situ "iron wall" for remediation of VOCs. *Ground Water.* **1998**, 36 (1), 164-170.
10. Yabusaki S.; Centrell, K.; Sass, B.; Steefel, C. Multicomponent Reactive Transport in an In Situ Zero-Valent Iron Cell. *Environ. Sci. Technol.* **2001**, 36 (7), 1493-1503.
11. Kohn, T.; Livi, K.J.T.; Roberts, A.L.; Vikesland, P.J. Longevity of Granular Iron in Groundwater Treatment Processes: Corrosion Product Development. *Environ. Sci. Technol.* **2005**, 39 (8), 2867-79.
12. Johnson, R. L.; Thoms, R.B.; Johnson, R.O.; Nurmi, J.T.; Tratnyek, P.G. Mineral Precipitation Upgradient from a Zero-Valent Iron Permeable Reactive Barrier. *Ground Water Monit. R.* **2008**, 28 (3) 56-64.
13. Wilkin, R. T.; Puls, R.W. Capstone Report on the Application, Monitoring, and Performance of Permeable Reactive Barriers for Ground-Water Remediation: Vol. 1. Performance Evaluations at Two Sites. EPA/600/R-03/045a. U.S. Environmental Protection Agency, National Risk Management Research Laboratory, Ground Water and Ecosystems Restoration Division. **2003**
14. Sass, B.; Gavaskar, A.; Yoon, W.; Reeter, C.; Drescher, E. Geochemical Factors Affecting Performance and Longevity of Permeable Reactive Barriers. Proceedings, Third International Conference on Remediation of Chlorinated and Recalcitrant Compounds, Monterey, Calif. Columbus, Ohio: Battelle. **2002**
15. Phillips, D. H.; Watson, D.B.; Roh, Y.; Gu B. Mineralogical Characteristics and Transformations during Long-Term Operation of a Zero-Valent Iron Reactive Barrier. *J. Environ. Qual.* **2003**, 32 (6), 2033-45.

16. Clingenpeel, S.C.; Moan, J.L.; McGrath, D.N.; Hungate, B.A.; Watwood, M.E. Stable carbon isotope fractionation in chlorinated ethene degradation by bacteria expressing three toluene oxygenases. *Front Microbiol.* **2012**, 3 (63), 1-7.
17. Mariotti, A.; Germon, J.C.; Hubert, P.; Kaiser, P.; Letolle, R.; Tardieux, A.; Tardieux, P. Experimental determination of nitrogen kinetic isotope fractionation: some principles; illustration for the denitrification and nitrification processes. *Plant Soil.* **1981**, 62, 413–430.
18. Sherwood-Lollar, B.; Slater, G.F.; Ahad, J.; Sleep, B., Spivack, J., Brennan, M.; Mackenzie, P. Contrasting carbon isotope fractionation during biodegradation of trichloroethylene and toluene: Implications for intrinsic bioremediation. *Org. Geochem.* **1999**, 30, 813-820
19. Bloom, Y.; Aravena, R.; Hunkeler, D.; Edwards, E.; Frape, S.K. Carbon Isotope Fractionation during Microbial Dechlorination of Trichloroethene, *cis*-1,2-Dichloroethene, and Vinyl Chloride: Implications for Assessment of Natural Attenuation. *Environ. Sci. Technol.* **2000**, 34, 2768-2772
20. Slater, G.F.; Sherwood-Lollar, B.; Sleep, B.; Edwards, E. Variability in Carbon Isotopic Fractionation during Biodegradation of Chlorinated Ethenes: Implications for Field Applications. *Environ. Sci. Technol.* **2001**, 35, 901-907
21. Liang, X.; Dong, Y.; Kuder, T.; Krumholz, L. R.; Philp, R. P.; Butler, E. C. Distinguishing abiotic and biotic transformation of tetrachloroethylene and trichloroethylene by stable carbon isotope fractionation. *Environ. Sci. Technol.* **2007**, 41 (20), 7094-7100.
22. Schmidt, K.R.; Augenstein, T.; Heidinger, M.; Ertl, S.; Tiehm, A. Aerobic biodegradation of *cis*-1,2-dichloroethene as sole carbon source: Stable carbon isotope fractionation and growth characteristics. *Chemosphere.* **2010**, 78, 527-532
23. Fletcher, K.E.; Nijenhuis, I.; Richnow; H-H.; Löffler, F.E. Stable Carbon Isotope Enrichment Factors for *cis*-1,2-Dichloroethene and Vinyl Chloride Reductive Dechlorination by Dehalococcoides. *Environ. Sci. Technol.* **2011**, 45, 2951-2957
24. Dayan, H.; Abrajano, T.; Sturchio, N.C.; Winsor, L. Carbon isotopic fractionation during reductive dehalogenation of chlorinated ethenes by metallic iron. *Org. Geochem.* **1999**, 30, 755-763.
25. Slater, G.F.; Lollar, B.S.; King, A.; O'Hannesin, S. Isotopic fractionation during reductive dechlorination of trichloroethene by zero-valent iron: influence of surface treatment. *Chemosphere.* **2002**, 49, 587-596.

26. Vanstone, N.A.; Focht, R.M.; Mabury, S.A.; Sherwood Lollar, B. Effect of iron type on kinetics and carbon isotopic enrichment of chlorinated ethylenes during abiotic reduction on Fe(0). *Ground Water*. **2004**, 42, 268-276.

27. Hunkeler, D.; Abe, Y.; Broholm, M.M.; Jeannotat, S.; Westergaard, C.; Jacobsen, C.S.; Aravena, R.; Bjerg, P.L. Assessing chlorinated ethene degradation in a large scale contaminant plume by dual carbon–chlorine isotope analysis and quantitative PCR. *J. Contam. Hydrol.* **2011**, 119, 69–79.

28. Elsner, M.; Zwank, L.; Hunkeler, D.; Schwarzenbach, A.P. A new concept linking observable stable isotope fractionation to transformation pathways of organic pollutants. *Environ. Sci. Technol.* **2005**, 39, 6896-6916.

29. Abe, Y.; Aravena, R.; Zopfi, J.; Shouakar-Stash, O.; Cox, E.; Roberts, J.D.; Hunkeler, D. Carbon and chlorine isotope fractionation during aerobic oxidation and reductive dechlorination of vinyl chloride and *cis*-1,2-dichloroethene. *Environ. Sci. Technol.* **2009**, 43, 101-107.

30. Shouakar-Stash, O.; Drimmie, R.J.; Zhang, M.; Frape, S.K. Compound-specific chlorine isotope ratios of TCE, PCE and DCE isomers by direct injection using CFIRMS. *Appl. Geochem.* **2006**, 21, 766-781.

31. Wiegert, C.; Mandalakis, M.; Knowles, T.; Polymenakou, P.N.; Aeppli, C.; Macháčková, J.; Holmstrand, H.; Evershed, R.; Pancost, R.D.; Gustafsson, O. Carbon and Chlorine Isotope Fractionation During Microbial Degradation of Tetra- and Trichloroethene. *Environ. Sci. Technol.* **2013**, 47, 6449-6456

32. Cretnik, S.; Thoreson, K.A.; Bernstein, A.; Ebert, K.; Buchner, D.; Laskov, C.; Haderlein, S.; Shouakar-Stash, O.; Kliegman, S.; McNeill, K.; Elsner, M. Reductive dechlorination of TCE by chemical model systems in comparison to dehalogenating bacteria: Insights from dual element isotope analysis ($^{13}\text{C}/^{12}\text{C}$, $^{37}\text{Cl}/^{35}\text{Cl}$). *Environ. Sci. Technol.* **2013**, 47, 6855-6863.

33. Kuder, T.; van Breukelen, B.M.; Vanderford, M.; Philp, P. 3D-CSIA: Carbon, Chlorine, and Hydrogen Isotope Fractionation in Transformation of TCE to Ethene by a *Dehalococcoides* Culture. *Environ. Sci. Technol.* **2013**, 47, 9668-9677

34. Shouakar-Stash, O.; Frape, S.K.; Drimmie, R.J. Stable hydrogen, carbon and chlorine isotope measurements of selected chlorinated organic solvents. *J. Contam. Hydrol.* **2003**, 60, 211- 228

35. Ertl, S.; Seibel, F.; Eichinger, L.; Frimmel, F. H.; Kettrup, A. The C-13/C-12 and H-2/H-1 ratios of trichloroethene, tetrachloroethene and their metabolites. *Isot. Environ. Health Stud.* **1998**, 34 (3), 245-253.
36. Torrentó, C.; Audí-Miró, C.; Bordeleau, G.; Marchesi, M.; Rosell, M.; Otero, N.; Soler, A. The use of alkaline hydrolysis as a novel strategy for chloroform remediation: feasibility of using urban construction wastes and evaluation of carbon isotopic fractionation. *Environ. Sci. Technol.* **2014**, 48(3): 1869–1877
37. Shouakar-Stash, O.; Drimmie, R.J. Online methodology for determining compound-specific hydrogen stable isotope ratios of trichloroethene and 1,2-*cis*-dichloroethene by continuous-flow isotope ratio mass spectrometry. *Rapid Commun. Mass Spectrom.* **2013**, 27, 1335-1344
38. Suponik, T. Groundwater treatment with the use of ze-ro-valent iron in the permeable reactive barrier technology. *Physicochem. Probl. Min. Process.* **2013**, 49 (1), 13-23
39. van Warmerdam, E.M.; Frape, S.K.; Aravena, R.; Drimmie, R.J.; Flatt, H.; Cherry, J.A. Stable chlorine and carbon isotope measurements of selected chlorinated organic solvents. *Appl. Geochem.* **1995**, 10, 547-552
40. Jendrzewski, N.; Eggenkamp, H.G.M.; Coleman, M.N. Characterization of chlorination hydrocarbons from chlorine and carbon isotopic compositions: scope of application to environmental problems. *Appl. Geochem.* **2001**, 16, 1021-1031
41. Lee, J.W.; Cha, D.K.; Oh, Y.K.; Ko, K.B.; Jin, S.H. Wastewater screening method for evaluating applicability of zero-valent iron to industrial wastewater. *J. Hazard. Mater.* **2010**, 180, 354-360
42. Hunkeler, D.; Aravena, R.; Cox, E. Carbon isotopes as a tool to evaluate the origin and fate of vinyl chloride: Laboratory experiments and modeling of isotope evolution. *Environ. Sci. Technol.* **2002**, 36 (15), 3378-3384
43. Lojkasek-Lima, P.; Aravena, R.; Parker, B.; Cherry, J.A. Fingerprinting TCE in a Bedrock Aquifer Using Compound-Specific Isotope Analysis. *Ground Water Monit. R.* **2012**, 32 (4), 53-62

Supporting Information

C, Cl and H compound specific isotope analysis to assess natural attenuation and ZVI-PRB induced degradation in a chlorinated ethenes contaminated site

Carme Audí-Miró^{†}, Stefan Cretnik[‡], Clara Torrentó[†], Mònica Rosell[†], Orfan Shouakar-Stash[§],
Neus Otero[†], Jordi Palau^φ, Martin Elsner[‡], Albert Soler[†]*

[†]Grup de Mineralogia Aplicada i Medi Ambient. Departament de Cristal·lografia, Mineralogia i Dipòsits Minerals. Facultat de Geologia. Universitat de Barcelona. Martí Franquès s/n, 08028. Barcelona, Spain

[‡]Institute of Groundwater Ecology, Helmholtz Zentrum München-National Research Center for Environmental Health, Ingolstädter Landstrasse 1, D-85764 Neuherberg, Germany.

[§]Department of Earth & Environmental Sciences, 200 University Ave. W, N2L 3G1 Waterloo, Ontario, Canada

^φUniversité de Neuchâtel. CHYN - Centre d'hydrogéologie. Rue Emile-Argand 11, CH – 2000, Neuchâtel, Switzerland.

Corresponding Author.

*Carme Audí-Miró. Phone: +34 934021343; Fax: +34 934021340, e-mail: carmeaudi@ub.edu

Total number of pages (including cover): 14

Figures: 5

Tables: 3

STUDY SITE EXTENSION

The lithology of the site, studied through the observation of the wells drilling cores, is mainly composed by an alternation of sand and silt Miocene sediments in a clayey matrix that extends from 4 m to a minimum of 14 m depth (Fig.1 in the manuscript). In general, the presence of sand increases in depth. Above these materials, there are 4 m of quaternary glaciis formed by the eroded Miocene materials and mainly composed by poorly structured clays and silts. The Miocene sediments are positioned unconformably on the Paleozoic base, which in this sector consists of Late-Hercynian granitoids. The water table of the aquifer is located at an average depth of 5.4 ± 2.1 m. The deepest water table (around 8 m) was measured at the base and at the top of the studied valley area (length of the studied area 900 m). While at around 300 m from the top of this area the water table was located closer to the surface (around 3 m depth). The average water table variation due to seasonal changes was of -0.5 ± 0.9 m. The deepest studied well reached 20 m depth. Chlorinated ethenes could have infiltrated from the seepage pit of the industrial plant and lixiviated until the saturated zone where they probably reached the deeper aquifer depths crossing the clayey matrix, accumulating mainly in the more sandy units [between 8 and 20 m at least as detected in the field by a portable gas photoionization detector (PID, MiniRAE 3000, RAE Systems, Kastrup, Denmark)] and started moving following the NE to W-SW groundwater flow direction.

During the period 2005-2010, a total of 12 wells were installed along the east bank of the creek (expected direction of the groundwater flow), from the source area to 900 m downstream of the creek. The groundwater flow velocity was estimated around 0.16 m/day at the shallow quaternary clayey depths; and 0.84 m/day at the more sandy Miocene depths.

GROUNDWATER SAMPLING EXTENSION

Groundwater samples were collected from 12 conventional wells with PVC tubing of 50 mm inner diameter. Five additional wells were installed under our supervision and decision-making in March 2012 surrounding the barrier, two immediately before the PRB and three immediately after it due to this study (Fig. 1B in the manuscript). These five wells have a multilevel sampling system installed, consisting of small diameter PTFE tubes (5x3 mm diameter) placed around the PVC tube and positioned at different depths. An additional well (OMW7) was installed in September 2013 in order to evaluate the possible contaminant migration to the west side of the creek, where the only available well, OMW6B, was destroyed by agricultural tasks after the Apr-11 survey.

Groundwater piezometric level was measured in every survey and physico-chemical parameters (pH, temperature, dissolved oxygen, Eh and conductivity) were determined using a flow through cell (Eijkelkamp, Netherlands) to avoid contact with the atmosphere and measured with a Multi3410 multi-parameter meter (WTW, Weilheim, Germany). Samples were collected and preserved following standard sampling and storage techniques.

CHLORINATED ETHENES ANALYSES DESCRIPTION

Concentration and carbon isotope composition of the chlorinated ethenes were carried out at the “Centres Científics i Tecnològics de la Universitat de Barcelona (CCiTUB)”. Concentration was determined by headspace (HS) analysis using a FOCUS gas chromatograph coupled with a DSQ II mass spectrometer (HS-GC/MS) (Thermo Fisher Scientific, Waltham, Massachusetts, USA). The GC was equipped with a split/splitless injector and a DB-624 capillary column (60 m, 0.32 mm i.d., 1.8 μm film thickness, Agilent, Santa Clara, California, USA) operating with He carrier gas at 1.8 mL/min. The injector was set at 220 $^{\circ}\text{C}$ and the following oven temperature program was used: 60 $^{\circ}\text{C}$ (2 min) and then increased at 8 $^{\circ}\text{C}/\text{min}$ to 220 $^{\circ}\text{C}$ (5 min). The volume of injection was 0.75 mL in split mode (split ratio of 22:1) at 220 $^{\circ}\text{C}$ and 40 mL/min of helium as the carrier gas. The error based on replicate measurements was 5%. Compounds identification and concentration calculation were obtained by standard techniques.

Carbon isotope composition of PCE, TCE and cis-DCE was performed using a gas chromatography-combustion-isotope ratio mass spectrometry system (GC-C-IRMS) consisting of a Trace GC Ultra equipped with a split/splitless injector, coupled to a Delta V Advantage IRMS (Thermo Scientific GmbH, Bremen, Germany) through a combustion interface. The system was equipped with a Supelco SPB-624 column (60 m \times 0.32 mm, 1.8 μm film thickness, Bellefonte, PA, USA). The injector was set at 250 $^{\circ}\text{C}$ at a split ratio of 5:1 and the following temperature program was used: 60 $^{\circ}\text{C}$ (5 min), increase at 8 $^{\circ}\text{C}/\text{min}$ to 165 $^{\circ}\text{C}$ and then at 25 $^{\circ}\text{C}/\text{min}$ to 220 $^{\circ}\text{C}$ (1 min). Helium was used as a carrier gas with a flow rate of 2.2 mL min^{-1} . The chlorinated compounds were extracted from the aqueous samples by automated headspace solid-phase micro-extraction (HS-SPME) using a 75- μm Carboxen-PDMS fiber (Supelco, Bellefonte, PA, USA) (Palau et al., 2007). The 20 mL-vials filled with 10 mL-aqueous samples (diluted in Milli-Q water to a concentration similar to the standards) were placed in the TriPlusTM Autosampler equipped with a SPME holder (Thermo Fisher Scientific, Waltham, USA). The extraction of the analytes was done at 40 $^{\circ}\text{C}$ during 20 minutes at constant agitation (600 rpm). All the measurements were run in duplicate as a quality control and the standard deviations of the $\delta^{13}\text{C}$ values obtained were below $\pm 0.5\text{‰}$ (Sherwood Lollar et al., 2007). The analytical system was verified daily using in-house control standards of chlorinated solvents with known carbon isotope ratios (-23.1 ‰ for cis-DCE, -30.6 ‰ for TCE and -31.2 ‰ for PCE) which were determined previously using a Flash EA1112 (Carlo-Erba, Milano, Italy) elemental analyser (EA) coupled to a Delta C isotope ratio mass spectrometer (Thermo Fisher Scientific, Bremen, Germany) through a Conflo III interface (ThermoFinnigan, Bremen, Germany) using four international reference materials (USGS 40, IAEA 600, IAEA CH6, IAEA CH7) with respect to the Vienna PeeDee Belemnite (VPDB) standard according to Coplen et al. (2006).

Chlorine isotopic measurements were conducted at the Environmental Isotope chemistry laboratory of the Institute of Groundwater Ecology at the “Helmholtz Zentrum München” on a GC-IRMS system (Thermo Scientific, Waltham, Massachusetts, USA) consisting of a Trace GC connected to a MAT 253 IRMS with dual inlet system via a heated transfer line. For the simultaneous determination of PCE and cis-DCE a peak jump routine was performed, with cis-DCE monitoring gas peaks added at the beginning and PCE monitoring gas peaks added at the end of each analytical run. Samples were prepared in triplicates, each of them with 3 mL of liquid volume in headspace-vials with a total volume of 10 mL, which were crimped with Teflon coated silicon Septa. Sampling was performed after 3 min of agitating at 40 $^{\circ}\text{C}$ using SPME with an equilibration time of the fiber in the headspace of 10 min. The fiber used in this

procedure was a Supelco® CAR/PDMS StableFlex 57335-U with 85 µm and 24 gauge. Preconditioning and injection of the fiber occurred at 280 °C, with a carrier flow of He at 1.4 ml/min and a split flow of 14 ml/min. The GC was equipped with a 30 m VOCOL column (Supelco, Bellefonte, Pennsylvania, USA) with a 0.25 mm inner diameter, with a film thickness of 1.5 µm. The GC program used was 50 °C (7 min), increasing at 60 °C/min to 70 °C (2.70 min) and at 80 °C/min to 140 °C (0.10 min). External standards were measured daily for calibration of $\delta^{37}\text{Cl}$ values against the SMOC scale (Bernstein et al., 2011). These standards had previously been characterized in the Department of Earth Sciences, University of Waterloo. For *cis*-DCE the respective standards have $\delta^{37}\text{Cl}$ values of $+0.07 \pm 0.1\text{‰}$ and $-1.52 \pm 0.1\text{‰}$; for PCE the standards have $\delta^{37}\text{Cl}$ values of $+0.29 \pm 0.1\text{‰}$ and $-2.52 \pm 0.1\text{‰}$ respectively to the SMOC standard. The measurements were conducted at masses $m/z = 94, 96$ for PCE and $m/z = 96, 98$ for *cis*-DCE. .

Hydrogen isotopic analyses of TCE and *cis*-DCE were carried out at the *Isotope Tracer Technologies laboratories* of Waterloo (Canada) following the method developed by Shouakar-Stash and Drimmie (2013). Isotope ratios for hydrogen were measured using a CF-IRMS coupled with a GC and a chromium reduction (R) system. The IRMS system was a Deltaplus XL CF-IRMS (ThermoFinnigan, Bremen, Germany). The GC was an Agilent 6890 gas chromatograph (Agilent Technologies Inc., Santa Clara, CA, USA) equipped with a split/splitless injector and a DB-5 capillary column. The GC temperature program was: 35 °C (4 min), increase at 50°C/min to 125 °C and then increase at 80°C/min to 285 °C (4 min). Purified helium (UHP Grade 5.0) was used as a carrier gas and the flow rate was constant at 2.5 mL/min. A high temperature (Max T: 1200 °C) tube furnace (Thermcraft, model XST-3-0-12-10, Winston-Salem, NC, USA) was used to heat the Cr reduction tube to 1000 °C and produce the hydrogen gas during the analyses. The samples analyses consisted of an initial extraction with a SPME fiber (75-µm Carboxen-PDMS fiber 57344U, Supelco, Bellefonte, PA, USA) of the organic compounds from the 5 mL headspace of a 60 mL VOA vial during 20 min, and then the fiber was injected in the split/splitless injection inlet at 270°C. Every daily run included a set of two internal standard of each compound, TCE and *cis*-DCE, with distinct isotope ratios. The two standards were prepared at different concentrations in order to correct for any possible linearity effect. The ^2H values for the two TCE standards were 467 and $682\text{‰} \pm 10\text{‰}$, and for the two *cis*-DCE 434 and $646\text{‰} \pm 10\text{‰}$.

ANALYSES OF THE MOST VOLATILE COMPOUNDS

Low molecular weight byproducts from the chlorinated ethenes degradation (ethene, ethane, acetylene) were measured at the Stable Isotope Laboratory of the University of Toronto (Canada) by headspace (HS) analysis as described by Slater et al. (1999). Using a 500 µL pressure-lock gastight syringe, 300 µL out of 10 mL headspace were withdrawn from the 40 mL VOA vials and after pressure compensation, 200 µL were injected for the concentration analysis to a Varian 3400 GC (Scientific Equipment Source, Oshawa, Ontario, Canada) fitted with a 90 m × 0.32 mm ID GS-Q (Agilent J & W Scientific) column and a flame-ionization detector (FID). Before each sample extraction, an equivalent volume of air was injected into the VOA vial to restore pressure. The injector temperature was set at 110 °C and the temperature program was of 25 °C (2 min), increasing at 2 °C/min to 70 °C, increasing at 20 °C/min to 210 °C (2 min). This temperature program allowed successful separation of ethene, ethane and acetylene. The helium carrier gas flow through the column was 2.2 mL/min. Before

the start of sample analyses, a three point calibration curve for ethene and ethane, and two point calibration curve for acetylene were conducted, checking a reproducibility of $\pm 5\%$ (relative error) at concentrations higher than 16.8, 15.6 and 18 $\mu\text{g/L}$ for ethene, acetylene and ethane, respectively. A quality control standard for each compound was injected daily to check the linearity of the instrument. .

Carbon and hydrogen isotope measurement of ethene were also accomplished in Toronto. For carbon, by using a purge and trap Teledyne-Tekmar XPT concentrator coupled to a Varian 3400 GC and a Finnigan MAT 252 IRMS via a combustion interface. The GC was fitted with a 90 m \times 0.32 mm ID GS-Q (Agilent J & W Scientific) column, the injector temperature was set at 200 $^{\circ}\text{C}$ at a split ratio of 6:1 and the temperature program was of 30 $^{\circ}\text{C}$ (2 min), increasing at 2 $^{\circ}\text{C}/\text{min}$ to 70 $^{\circ}\text{C}$, increasing at 20 $^{\circ}\text{C}/\text{min}$ to 210 $^{\circ}\text{C}$ (2 min). 25 mL of aqueous sample was injected into the purge and trap concentrator using a 50 mL gastight syringe. The sample was purged for 11 minutes with a helium flow of 40 mL/min. The trap was then purged with dry helium for 1 minute, followed by heating the trap to 220 $^{\circ}\text{C}$. The desorbed compounds were injected over the course of 4 minutes into the GC through a heated line (225 $^{\circ}\text{C}$) with a flow rate of 6.25 mL/min. Total uncertainty on $\delta^{13}\text{C}$ values is $\pm 0.5\text{‰}$, incorporating both the accuracy of the measurement with respect to international standards (V-PDB) and the reproducibility on replicate measurements of the sample (Sherwood Lollar et al., 2007). For continuous flow $\delta^2\text{H}$ analyses of ethene, the same purge and trap was coupled to a HP 6890 GC system online with a micropyrolysis oven and a Finningan Mat (Bremen Germany) Delta Plus XL IRMS (GC-TC-IRMS). The volume, purge and trap and GC methods were equal to the analysis of carbon isotope ratios. The micropyrolysis oven consisted of an empty 0.5 mm i.d. ceramic tube heated to 1460 $^{\circ}\text{C}$ to achieve thermoconversion of H to H_2 . Total uncertainty on $\delta^2\text{H}$ values is $\pm 5\text{‰}$ (Chartrand et al., 2007), incorporating both the accuracy of the measurement with respect to international standards (V-SMOW) and the reproducibility on replicate measurements of the sample.

COMPLEMENTARY MICROCOSM EXPERIMENTS

In order to check the potential biodegradation occurring at the field site, and to obtain the site-specific carbon isotopic enrichment factor associated to this biodegradation, microcosm experiments with material from Pz1 and Pz3 wells were performed.

Materials and methods

Two and a half liters of slurry (groundwater with sediment) were collected from the bottom of wells Pz1 and Pz3. Prior to the beginning of the experiment, samples were purged with a N_2 gas stream sterilized through a 0.2 μm filter during 30 minutes inside an anaerobic chamber, in order to remove all the volatile organic compounds. The oxygen partial pressure in the glove box was maintained between 0.1 and 0.2% O_2 and was continuously monitored by an oxygen partial pressure detector with an accuracy of $\pm 0.1\%$ O_2 . Each experiment series consisted of four triplicates of 125mL bottles one for each target compound (PCE, TCE and cis-DCE). Bottles were filled with 100 mL of homogeneous slurry leaving an initial headspace of 25 mL. After being filled, bottles of one of the series of each well were autoclaved for 45 min at 121 $^{\circ}\text{C}$ on three consecutive days in order to control potential abiotic contaminants losses in the presence of the sediment (called Killed Control). A fifth series of bottles was prepared with

sterilized distilled water (sterilized with a 0.2 μm filter) for the three compounds and in triplicates as well, thus constituting another control experiment for volatile losses along the incubation time (called Control). Appropriate volumes of the pure contaminant were injected to each bottle by a 10 μL syringe to provide an initial concentration of 60 mg/L of PCE, TCE or cis-DCE depending on each case. The bottles were incubated statically, in the dark at room temperature (controlled between 20 and 25°C). Over a total incubation time of almost 500 days, 6 samplings took place (time 0, 29, 68, 120, 174, 494 days). In each sampling time, 2 mL samples were taken from the solution of the reaction bottles through the Teflon septa by a sterile disposable 5-mL plastic syringe with a sterile disposable stainless steel needle. Samples were filtered with a 0.2- μm syringe filter into a 4 mL vials and stored at -20°C to avoid any further microbial degradation until analysis. Concentration and isotope analyses were performed as explained above.

Results and discussion

Significant PCE and TCE concentration decrease and $\delta^{13}\text{C}$ enrichment were observed in both microcosms series, confirming that indigenous bacteria in the slurry had the ability to degrade PCE and TCE. Moreover, byproducts were formed (up to cis-DCE; VC was not detected and ethene and ethane were not evaluated after 500 days). The formed TCE experienced at the same time further reductive dechlorination, as it is shown by the higher enrichment in ^{13}C than its parental PCE and the formation of lighter cis-DCE over time (Figure S1). In controls and killed controls, the $\delta^{13}\text{C}$ remained constant (Figure S1) and no degradation products were detected along the incubation time, showing that the effects observed in live bottles were exclusively related to biotic reductive dechlorination. $\epsilon_{\text{C,PCE}}$ was obtained for both wells of study, Pz1 and Pz3. Taking into account the 95% confidence interval (CI), both wells presented the same $\epsilon_{\text{C,PCE}}$ value ($-2.1 \pm 1.2\text{‰}$ for Pz1 and $-2.8 \pm 1.6\text{‰}$ for Pz3), indicating that probably the same degradation mechanism is taking place. Combining data for both wells, the $\epsilon_{\text{C,PCE}}$ obtained was $-2.6 \pm 0.9\text{‰}$ (Figure S2A). Regarding TCE experiments, after 120 days TCE had disappeared in the Pz3 experiment, and taking into account some concentration analytical issues an approximated Pz1 and Pz3 combined $\epsilon_{\text{C,TCE}}$ value of $-1.7 \pm 1.8\text{‰}$ was estimated (Figure S2B). New microcosm experiments should be performed in order to confirm the TCE carbon isotopic fractionation. Concerning cis-DCE, no changes in concentration or isotopic composition were detected indicating that biodegradation was not taking place after 500 days. Additionally, no VC was produced. The lack of cis-DCE degradation in the microcosm experiments contrasts with its proven degradation observed at the field site suggesting that conditions provided at the microcosms might not be reproducing the environmental field conditions.

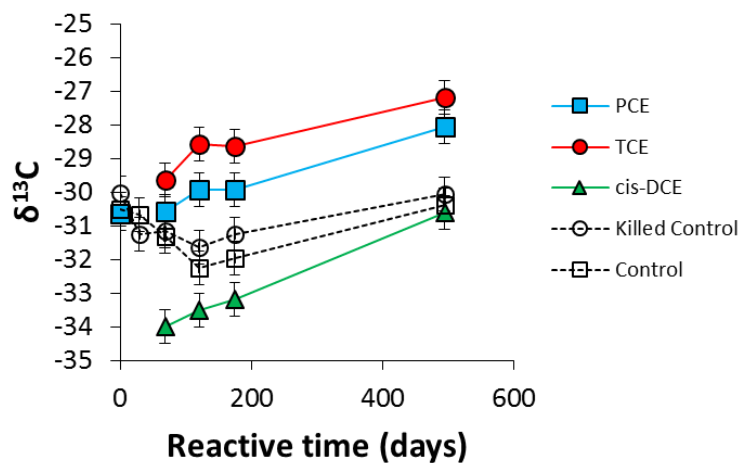


Figure S1. $\delta^{13}\text{C}$ variation of PCE and its byproducts TCE and cis-DCE during the PCE Pz1 microcosm experiment over the reaction course. The controls and killed controls are represented. Error bars represent an uncertainty of 0.5 ‰ for $\delta^{13}\text{C}$ measurements.

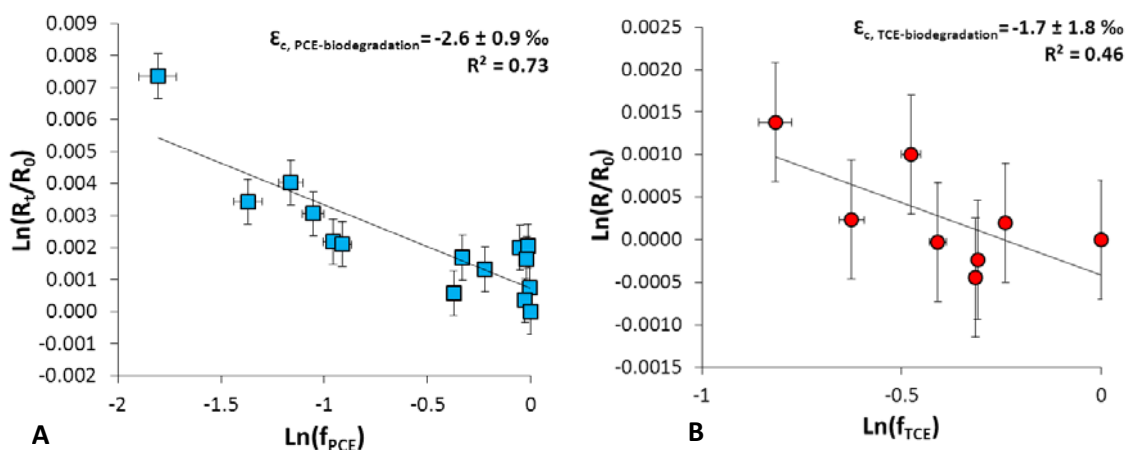


Figure S2. Carbon isotope values of PCE (A) and TCE (B) from the PCE and TCE microcosms experiments, respectively in double logarithmic plots over the respective concentrations. The isotopic fractionation ϵ_c has been calculated from the slope of the regression line according to Eq. (3). Error bars represent the total instrument uncertainty of 0.5‰ for compound-specific C isotope measurements, and of 5‰ for HS concentrations analyses.

EXPERIMENT OF PCE DEGRADATION WITH ZVI

Materials and methods

Laboratory batch experiments with PCE and ZVI were performed to obtain the carbon isotopic fractionation associated to the degradation of PCE with ZVI. PCE degradation experiments were performed in two series (duplicates) of eight 25 mL vials filled with 2.5 ± 0.1 g of ZVI and with a previously prepared PCE solution (60 mg/L) in distilled deoxygenated water. The vials were covered with Al foil in order to avoid photolytic oxidation of PCE and were put in a rotator (Heidolph, Schwabach, Germany) (23 rpm) to ensure maximum contact between all the PCE solution and the ZVI. Each pair of vials (duplicates) was prepared at different starting points, and all of them were sacrificed at the same time, assuring the same storage conditions and the analyses of all of them on the same day, but at different conversion degrees (stopped at 8 different time points, up to 196 hours of reaction). Solutions were separated from the Fe and were split in two aliquots, one was kept at 4 °C without headspace for concentrations analysis the day after, and the second one was frozen with headspace for isotopic analysis (Elsner et al., 2006), which was performed within the following 10 days. Controls were assessed at three different time points along the experiments to ensure that other degradation mechanisms or losses were not affecting the PCE concentration. Concentration and isotope analyses were performed as explained above.

Results and discussion

A PCE concentration reduction of 93% was achieved after 196 hours of experiment and a pseudo first order rate constant (K_{obs}) of 0.0081 h^{-1} was obtained. Carbon isotopic composition of PCE showed a significant enrichment in ^{13}C during the course of the reaction (from -31.62 to -13.4 ‰). However, two points at the beginning of the experiments showed no carbon isotope fractionation although there was a high concentration decrease, an effect also observed by other authors (Burris, et al., 1995; Dayan et al., 1999; Slater et al., 2002) who associated this unfit to sorption processes onto the iron surface, thus indicating a non-equilibrium partitioning of PCE between iron and water at the early stages of the reaction. Having foreseen this lack of equilibrium at the beginning of the experiment, Burris et al. (1995) started collecting samples after 19 hours of reaction. Accordingly, in this experiment, samples after 18 hours of reaction have been used to estimate the ϵ_c value of PCE in reaction with ZVI (Figure S3). The estimated ϵ_c (-9.5 ± 2.2 ‰) is inside the range obtained by Vanstone et al. (2004) (-5.7 to -15.5 ‰). Contrarily, Dayan et al. (1999) obtained a very different ϵ_c value (-25.3 ‰) in electrolytic iron PCE degradation experiments. The variation in ϵ_c values corresponds to the use of different types of iron, even due to differences on the zero valent iron provider. Thus, it is important to use the specific value obtained (-9.5 ± 2.2 ‰) to calculate the real extend of PCE degradation at the field site with the used type of iron.

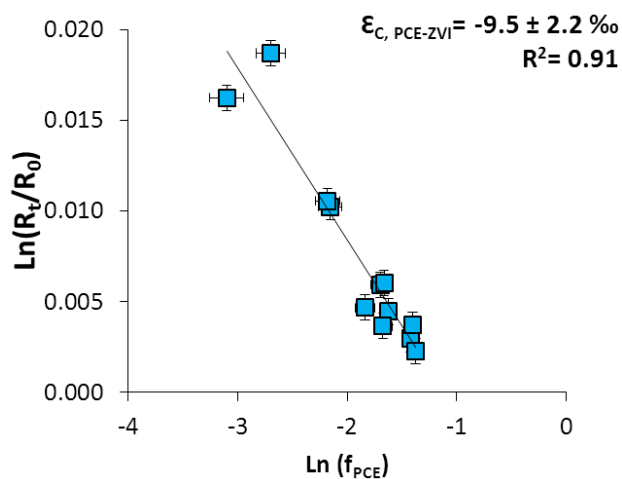


Figure S3. Carbon isotope values of PCE from the experiment of PCE degradation with ZVI in a double logarithmic plot over the respective concentration. The isotopic fractionation ϵ_C has been calculated from the slope of the regression line according to Eq. (3). Error bars represent the total instrument uncertainty of 0.5‰ for compound-specific C isotope measurements, and of 5‰ for HS concentrations analyses.

Figure S4

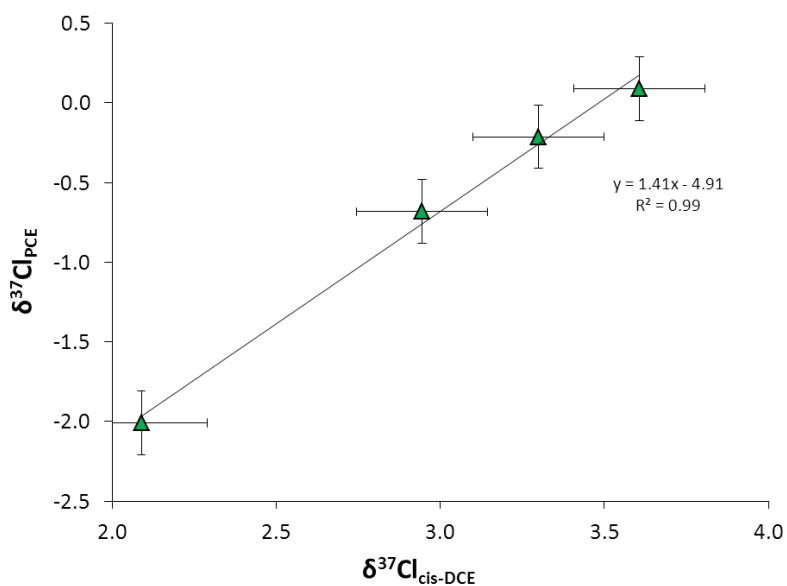


Figure S4. $\delta^{37}\text{Cl}$ of PCE versus $\delta^{37}\text{Cl}$ of cis-DCE in Oct-12 campaign showing a correlation of 0.99. Error bars represent an uncertainty of 0.2 ‰ for $\delta^{37}\text{Cl}$ measurements.

Figure S5

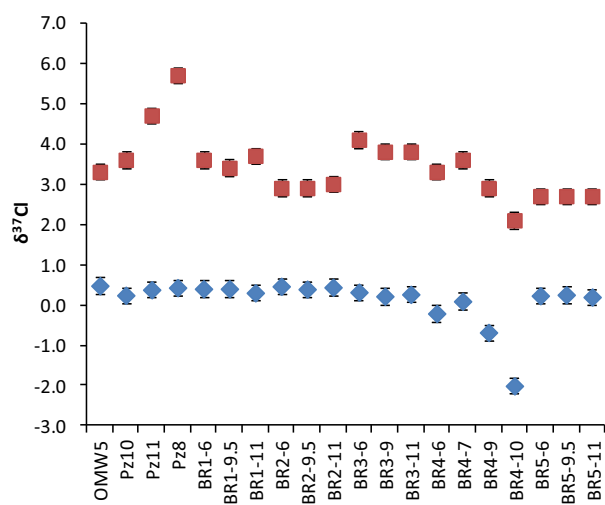


Figure S5. $\delta^{37}\text{Cl}$ of PCE (blue diamonds) and cis-DCE (red squares) at the wells analyzed in Oct-12 survey. Error bars represent an uncertainty of 0.2 ‰ for $\delta^{37}\text{Cl}$ and of 0.5 ‰ for $\delta^{13}\text{C}$ measurements

Table S1. Average from the four sampling campaigns of the main redox parameters measured. - below detection limit. Detection limit is: 0.02 mg/L or Mn²⁺ and Fe²⁺ and 5 mg/L for NO₃⁻ and SO₄²⁻

	Mn ²⁺ (mg/L)	Fe ²⁺ (mg/L)	NO ₃ ⁻ (mg/L)	SO ₄ ²⁻ (mg/L)
MW17	1.21	0.94	-	16.8
OMW5	0.32	-	18.5	83.8
MW10B	-	-	-	59.5
PZ1	0.12	0.27	-	82.5
PZ2	0.11	-	18.8	95.6
PZ3	0.17	-	15.1	67.2
Pz4	-	-	213.9	99.9
Pz10	-	-	130.8	93.0
Pz11	0.51	-	32.7	96.1
PZ7	0.06	-	23.4	125.6
Pz8	-	-	28.2	86.8
Pz9	-	-	79.1	89.4
BR1	-	-	76.8	89.1
BR1 - 4 m	-	-	84.4	86.4
BR1-4.5	-	0.06	200.5	135.9
BR1 - 5 m	-	-	84.6	92.6
BR1 - 6 m	-	-	154.6	102.6
BR1 - 8 m	-	-	86.2	89.3
BR1 - 9.5 m	-	-	164.5	110.5
BR1 - 10 m	-	-	85.2	91.0
BR1 - 11 m	-	-	164.9	109.5
BR1 - 13 m	0.30	-	-	97.0
BR2	-	-	24.7	80.1
BR2 - 4 m	-	-	24.8	77.6
BR2 - 5 m	-	-	71.8	94.0
BR2 - 6 m	-	0.99	73.7	100.1
BR2 - 7 m	-	-	29.1	88.7
BR2 - 8 m	-	-	26.7	23.0
BR2 - 9.5 m	-	-	72.2	91.6
BR2 - 10.5 m	-	-	26.5	81.7
BR2 - 11 m	-	-	72.0	91.8
BR2 - 11.5 m	-	-	27.6	92.3
BR3	-	-	69.1	91.0
BR3 - 4 m	0.51	-	62.9	85.9
BR3 - 5 m	0.25	-	97.9	113.0
BR3 - 6 m	0.11	-	124.0	101.5
BR3 - 7 m	0.24	-	79.2	86.5
BR3 - 8 m	0.23	-	107.2	105.0
BR3 - 9 m	0.17	-	129.9	109.3
BR3 - 11 m	0.21	-	123.4	96.7
BR4	0.14	-	20.6	90.7
BR4 - 4 m	1.18	1.57	-	52.8
BR4 - 5 m	0.99	0.15	81.8	105.2
BR4 - 5.5 m	0.70	0.18	59.9	88.8
BR4 - 6.5 m	0.13	-	160.1	113.7
BR4 - 7.5 m	0.12	-	68.4	96.4
BR4 - 8.5 m	0.19	-	55.3	108.7
BR4 - 9.5 m	0.30	-	-	100.1
BR4 - 13 m	1.36	0.09	-	93.3
BR5	0.56	-	18.3	76.9
BR5 - 4 m	0.33	0.08	-	63.8
BR5 - 5 m	0.42	-	87.5	81.3
BR5 - 6 m	0.17	0.06	56.8	95.1
BR5 - 8 m	0.66	0.12	-	81.7
BR5 - 9.5 m	0.26	0.12	51.1	95.9
BR5 - 10 m	0.59	0.23	-	79.6
BR5 - 11 m	0.07	-	49.5	93.4

Table S2. Concentration and isotope data of the main compounds of the site obtained from the groundwater sampling campaigns conducted from April 2011 to March 2013. ¹distance from the source, n.a. not analyzed, n.d. not detected. $\delta^{13}\text{C}$ values uncertainty is 0.5 ‰, for $\delta^{37}\text{Cl}$ is 0.2 ‰ and for $\delta^2\text{H}$ measurements it has been between 2 and 26 ‰. Concentration uncertainty is 10%.

	Upgradient the ZVI-PRB																								W from the ZVI-PRB				Downgradient the ZVI-PRB											
	MW17. 23 m ³				OMW5. 60 m ³				OMW6B. 7 m ³	OMW7. 13 m ³		Pz1. 100 m ³				Pz2. 200 m ³				Pz3. 280 m ³				Pz10. 320 m ³				Pz4. 330 m ³				Pz11. 326 m ³				Pz7. 500 m ³				
	Apr-11	June-12	Oct-12	Mar-13	Apr-11	June-12	Oct-12	Mar-13	Apr-11	Apr-11	June-12	Oct-12	Mar-13	Apr-11	June-12	Oct-12	Mar-13	Apr-11	June-12	Oct-12	Mar-13	Apr-11	June-12	Oct-12	Mar-13	Apr-11	June-12	Oct-12	Mar-13	Apr-11	June-12	Oct-12	Mar-13	Apr-11	June-12	Oct-12	Mar-13			
PCE	µg/L	<2.6	<2.6	<2.6	28	38	58	127	246	178	<2.6	<2.6	<2.6	27	123	90	n.a.	517	329	253	n.a.	11	48	703	917	145	7	391	n.a.	49	80	209	158	27	<2.6	5	3	5		
	$\delta^{13}\text{C}$ (‰)	n.d.	n.d.	n.d.	n.d.	-20.7	-20.0	-19.9	-19.1	-19.6	n.d.	n.d.	n.d.	-19.9	-19.6	-19.7	n.a.	-19.8	-20.0	-19.6	n.a.	n.d.	-19.8	-20.3	-20.1	-19.2	n.d.	-19.9	n.a.	-20.4	-19.9	-19.5	-19.3	-20.2	n.d.	-20.6	n.d.	n.d.		
	$\delta^{37}\text{Cl}$ (‰)	n.a.	n.a.	n.a.	n.a.	n.a.	0.5	n.a.	n.a.	n.a.	n.a.	n.a.	n.a.	n.a.	n.a.	n.a.	n.a.	n.a.	n.a.	n.a.	n.a.	n.a.	n.a.	0.2	n.a.	n.a.	n.d.	n.a.	n.a.	n.a.	0.4	n.a.	n.a.	0.4	n.a.	n.a.	n.a.	n.a.		
TCE	µg/L	<2.6	<2.6	<2.6	26	17	<2.6	74	4072	139336	11	<2.6	<2.6	8	24	11	n.a.	44	3	15	n.a.	56	<2.6	7	<2.6	<2.6	<2.6	<2.6	n.a.	<2.6	<2.6	7	3	<2.6	<2.6	<2.6	<2.6	<2.6		
	$\delta^{13}\text{C}$ (‰)	n.d.	n.d.	n.d.	n.d.	-19.9	n.d.	n.d.	-20.6	-19.9	-20.0	n.d.	n.d.	n.d.	-16.0	-13.5	n.a.	n.d.	n.d.	-12.2	n.a.	n.d.	n.d.	n.d.	n.d.	n.d.	n.d.	n.d.	n.a.	n.d.	n.d.	n.d.	n.d.	n.d.	n.d.	n.d.	n.d.	n.d.		
	$\delta^2\text{H}$ (‰)	n.a.	n.a.	n.a.	n.a.	n.a.	n.a.	n.a.	n.a.	n.a.	n.a.	n.a.	n.a.	n.a.	n.a.	n.a.	n.a.	n.a.	n.a.	n.a.	n.a.	n.a.	n.a.	n.a.	n.a.	n.a.	n.a.	n.a.	n.a.	n.a.	n.a.	n.a.	n.a.	n.a.	n.a.	n.a.	n.a.	n.a.		
DCE	µg/L	45735	16745	18010	28681	104	166	266	188	<2.6	21740	13	54	530	33	861	720	n.a.	1328	88	479	n.a.	218	17	191	154	15	<2.6	21	n.a.	3	7	99	251	27	5	3	3	18	
	$\delta^{13}\text{C}$ (‰)	-19.9	-19.9	-18.3	-15.7	-22.0	-20.0	-19.2	-19.9	n.d.	-27.8	-17.9	-16.8	-17.5	-15.2	-14.7	-19.7	n.a.	-20.2	-17.4	-21.2	n.a.	-17.7	-15.5	-20.9	-17.5	-16.6	n.d.	-11.3	n.a.	-14.8	-11.6	-18.2	-16.4	-15.2	n.d.	n.d.	n.d.	-15.8	
	$\delta^{37}\text{Cl}$ (‰)	n.a.	n.a.	3.8	n.a.	n.a.	n.a.	3.3	n.a.	n.a.	n.a.	n.a.	n.a.	5.2	n.a.	n.a.	n.a.	n.a.	n.a.	n.a.	n.a.	n.a.	n.a.	n.a.	n.a.	3.6	n.a.	n.a.	n.a.	n.a.	n.a.	n.a.	n.a.	4.7	n.a.	n.a.	n.a.	n.a.	n.a.	n.a.
VC	µg/L	n.a.	7886	247	1280	n.a.	5	<2.6	<2.6	n.a.	<2.6	<2.6	<2.6	<2.6	<2.6	<2.6	<2.6	<2.6	<2.6	<2.6	<2.6	114	n.a.	<2.6	<2.6	<2.6	<2.6	<2.6	n.a.	<2.6	n.a.	7	<2.6	<2.6	<2.6	<2.6	<2.6	<2.6	<2.6	<2.6
	$\delta^{13}\text{C}$ (‰)	n.a.	n.a.	n.a.	-38.4	n.a.	n.a.	n.d.	n.d.	n.a.	n.a.	n.d.	n.d.	n.d.	n.a.	n.a.	n.a.	n.a.	n.a.	n.a.	n.a.	n.a.	-20.4	n.a.	n.a.	n.d.	n.d.	n.a.	n.a.	n.a.	n.a.	n.a.	n.d.	n.d.	n.d.	n.d.	n.a.	n.a.	n.d.	n.d.

	Downgradient the ZVI-PRB												Multilevel Wells BR1. Upgradient the ZVI-PRB												Multilevel Wells BR2. Upgradient the ZVI-PRB																					
	Pz8. 750 m ³				Pz9. 900 m ³				BR1-4	BR1-4.5	BR1-5	BR1-6			BR1-8	BR1-9.5			BR1-10	BR1-11			BR1-13		BR2-4	BR2-5		BR2-6			BR2-7	BR2-8		BR2-9.5			BR2-10.5		BR2-11			BR2-11.5				
	Apr-11	June-12	Oct-12	Mar-13	Apr-11	June-12	Oct-12	Mar-13	June-12	Mar-13	June-12	June-12	Oct-12	Mar-13	June-12	June-12	Oct-12	Mar-13	June-12	June-12	Oct-12	Mar-13	June-12	Mar-13	June-12	June-12	Mar-13	June-12	Oct-12	Mar-13	June-12	June-12	June-12	Oct-12	Mar-13	June-12	June-12	June-12	Oct-12	Mar-13	June-12	June-12	Oct-12	Mar-13	June-12	
PCE	µg/L	132	100	207	205	<2.6	<2.6	<2.6	<2.6	646	184	519	604	521	161	541	484	503	157	463	416	296	156	23	55	383	258	498	372	758	466	322	329	346	615	397	297	335	714	453	333					
	$\delta^{13}\text{C}$ (‰)	-19.4	-19.8	-19.2	-19.3	n.d.	n.d.	n.d.	n.d.	-20.9	-18.3	-21.3	-21.6	-20.2	-19.3	-21.4	-21.2	-20.0	-19.3	-20.8	-21.0	-20.2	-18.2	-16.5	n.d.	-20.4	-20.4	-20.1	-20.3	-20.0	-19.8	-20.5	-20.3	-20.6	-20.2	-19.8	-20.6	-20.5	-19.7	-19.5	-20.4					
	$\delta^{37}\text{Cl}$ (‰)	n.a.	n.a.	0.4	n.a.	n.a.	n.a.	n.a.	n.a.	n.a.	n.a.	n.a.	n.a.	0.4	n.a.	n.a.	n.a.	0.4	n.a.	n.a.	n.a.	0.3	n.a.	n.a.	n.a.	n.a.	n.a.	n.a.	n.a.	n.a.	0.5	n.a.	n.a.	0.4	n.a.	n.a.	n.a.	n.a.	0.4	n.a.	n.a.	n.a.	n.a.			
TCE	µg/L	16	8	9	5	<2.6	<2.6	<2.6	<2.6	4	7	4	4	<2.6	5	5	4	<2.6	6	3	4	<2.6	6	<2.6	<2.6	<2.6	<2.6	8	3	52	7	3	3	3	<2.6	6	<2.6	<2.6	<2.6	3	6	7	3			
	$\delta^{13}\text{C}$ (‰)	-15.4	-14.7	n.d.	-12.1	n.d.	n.d.	n.d.	n.d.	n.d.	n.d.	n.d.	n.d.	n.d.	n.d.	n.d.	n.d.	n.d.	n.d.	n.d.	n.d.	n.d.	n.d.	n.d.	n.d.	n.d.	n.d.	n.d.	n.d.	n.d.	n.d.	n.d.	n.d.	n.d.	n.d.	n.d.	n.d.	n.d.	n.d.	n.d.	n.d.	n.d.	n.d.	n.d.		
	$\delta^2\text{H}$ (‰)	n.a.	n.a.	n.a.	n.a.	n.a.	n.a.	n.a.	n.a.	n.a.	n.a.	n.a.	n.a.	n.a.	n.a.	n.a.	n.a.	n.a.	n.a.	n.a.	n.a.	n.a.	n.a.	n.a.	n.a.	n.a.	n.a.	n.a.	n.a.	n.a.	n.a.	n.a.	n.a.	n.a.	n.a.	n.a.	n.a.	n.a.	n.a.	n.a.	n.a.	n.a.	n.a.	n.a.	n.a.	
DCE	µg/L	762	204	741	273	<2.6	<2.6	<2.6	<2.6	155	20	137	139	83	16	127	136	68	19	133	138	73	20	35	42	186	169	124	173	257	112	144	164	172	196	136	155	154	259	114	147					
	$\delta^{13}\text{C}$ (‰)	-19.2	-19.0	-18.1	-18.6	n.d.	n.d.	n.d.	n.d.	-20.4	-16.5	-20.5	-20.6	-17.1	-15.7	-20.4	-20.5	-17.4	-14.6	-20.5	-20.4	-17.8	-15.7	-16.8	-16.6	-21.3	-21.5	-19.1	-21.3	-20.9	-19.1	-21.3	-21.6	-21.3	-21.2	-18.7	-21.3	-21.2	-21.0	-18.8	-21.2	-21.0	-18.8			
	$\delta^{37}\text{Cl}$ (‰)	n.a.	n.a.	5.7	n.a.	n.a.	n.a.	n.a.	n.a.	n.a.	n.a.	n.a.	n.a.	3.6	n.a.	n.a.	n.a.	3.4	n.a.	n.a.	n.a.	3.7	n.a.	n.a.	n.a.	n.a.	n.a.	n.a.	n.a.	n.a.	2.9	n.a.	n.a.	2.9	n.a.	2.9	n.a.	n.a.	3.0	n.a.	n.a.	n.a.	n.a.	n.a.		
VC	µg/L	n.a.	<2.6	<2.6	<2.6	n.a.	<2.6	<2.6	<2.6	n.a.	<2.6	<2.6	<2.6	<2.6	<2.6	<2.6	<2.6	<2.6	<2.6	<2.6	<2.6	<2.6	<2.6	<2.6	<2.6	<2.6	<2.6	<2.6	<2.6	<2.6	<2.6	<2.6	<2.6	<2.6	<2.6	<2.6	<2.6	<2.6	<2.6	<2.6	<2.6	<2.6	<2.6	<2.6		
	$\delta^{13}\text{C}$ (‰)	n.a.	n.a.	n.d.	n.d.	n.a.	n.a.	n.d.	n.d.	n.a.	n.a.	n.d.	n.d.	n.d.	n.d.	n.a.	n.a.	n.a.	n.a.	n.a.	n.a.	n.a.	n.a.	n.a.	n.a.	n.a.	n.a.	n.a.	n.a.	n.a.	n.a.	n.a.	n.a.	n.a.	n.a.	n.a.	n.a.	n.a.	n.a.	n.a.	n.a.	n.a.	n.a.	n.a.	n.a.	n.a.

	Multilevel Wells BR3. Downgradient the ZVI-PRB											Multilevel Wells BR4. Downgradient the ZVI-PRB											Multilevel Wells BR5. Downgradient the ZVI-PRB																									
	BR3-4			BR3-5		BR3-6		BR3-7		BR3-8		BR3-9		BR3-11		BR4-4.5		BR4-5.5		BR4-6		BR4-7		BR4-8			BR4-9		BR4-10		BR4-13.5		BR5-4	BR5-5		BR5-6			BR5-8		BR5-9.5			BR5-10	BR5-11			
	June-12	June-12	Mar-13	June-12	Oct-12	Mar-13	June-12	June-12	Mar-13	June-12	Oct-12	Mar-13	June-12	Oct-12	June-12	Mar-13	June-12	Mar-13	June-12	Oct-12	Mar-13	June-12	Oct-12	Mar-13	June-12	Oct-12	Mar-13	June-12	Oct-12	June-12	Oct-12	June-12	June-12	Mar-13	June-12	June-12	Oct-12	Mar-13	June-12	June-12	Oct-12	Mar-13	June-12	June-12	Oct-12	Mar-13		
PCE	µg/L	243	392	77	446	425	80	484	349	85	337	406	114	342	361	18	63	127	191	84	368	114	73	41	89	90	52	110	20	50	<2.6	190	407	612	293	457	663	344	255	437	729	190	188	393	680			
	$\delta^{13}\text{C}$ (‰)	-20.1	-20.3	-19.8	-20.6	-20.3	-19.0	n.a.	-20.4	-19.1	-20.4	-19.9	-18.8	-20.1	-20.3	-19.1	-18.5	-19.8	-20.4	-19.8	-20.3	-19.4	-19.7	-20.0	-19.8	-19.6	-20.0	-19.9	-20.0	-20.3	n.d.	-19.5	-19.9	-19.9	-19.9	-20.4	-19.7	-20.2	-19.8	-20.3	-19.9	-19.4	-19.6	-20.7	-19.8			
	$\delta^{37}\text{Cl}$ (‰)	n.a.	n.a.	n.a.	n.a.	0.3	n.a.	n.a.	n.a.	n.a.	0.2	n.a.	n.a.	0.3	n.a.	n.a.	n.a.	n.a.	-0.4	n.a.	0.1	n.a.	n.a.	n.a.	n.a.	n.a.	n.a.	n.a.	n.a.	-2.0	n.a.	n.a.	n.a.	n.a.	n.a.	n.a.	n.a.	0.2	n.a.	0.3	n.a.	n.a.	n.a.	n.a.	n.a.	n.a.	n.a.	n.a.
TCE	µg/L	4	6	5	5	3	6	6	5	6	5	3	5	5	3	<2.6	5	3	<2.6	5	<2.6	6	4	<2.6	5	4	<2.6	5	46	3	<2.6	7	8	12	7	6	12	10	8	6	12	8	8	6	14			
	$\delta^{13}\text{C}$ (‰)	n.d.	n.d.	n.d.	n.d.	n.d.	n.d.	n.d.	n.d.	n.d.	n.d.	n.d.	n.d.	n.d.	n.d.	n.d.	n.d.	n.d.	n.d.	n.d.	n.d.	n.d.	n.d.	n.d.	n.d.	n.d.	n.d.	n.d.	n.d.	n.d.	n.d.	n.d.	n.d.	n.d.	n.d.	n.d.	n.d.	n.d.	n.d.	n.d.	n.d.	n.d.	n.d.	n.d.	n.d.	n.d.	n.d.	n.d.
	$\delta^2\text{H}$ (‰)	n.a.	n.a.	n.a.	n.a.	n.a.	n.a.	n.a.	n.a.	n.a.	n.a.	n.a.	n.a.	n.a.	n.a.	n.a.	n.a.	n.a.	n.a.	n.a.	n.a.	n.a.	n.a.	n.a.	n.a.	n.a.	n.a.	n.a.	n.a.	n.a.	n.a.	n.a.	n.a.	n.a.	n.a.	n.a.	n.a.	n.a.	n.a.	n.a.	n.a.	n.a.	n.a.	n.a.	n.a.	n.a.	n.a.	n.a.
DCE	µg/L	77	105	13	115	53	13	119	106	16	100	52	19	100	50	12	13	51	34	14	38	21	31	9	17	61	14	25	22	23	<2.6	205	320	355	293	212	387	289	328	220	374	240	276	206	416			
	$\delta^{13}\text{C}$ (‰)	-19.5	-19.5	-13.9	-19.1	-16.9	-15.0	n.a.	-19.4	-14.1	-19.5	-17.1	-14.6	-19.4	-17.1	-18.1	n.d.	-19.5	-18.6	-15.8	-18.7	-15.2	-19.5	-18.9	-16.9	-19.8	-19.5	-15.7	-20.																			

Table S3. Concentration and $\delta^{13}\text{C}$ and $\delta^2\text{H}$ of the non-chlorinated products at those wells where their presence has been found. q.l.d. is qualitatively detected. $\delta^{13}\text{C}$ values uncertainty is 0.5 ‰, and $\delta^2\text{H}$ of 5 ‰. Concentration uncertainty is 10%.

	Acetylene	Ethene		Ethane	
	$\mu\text{g/L}$	$\mu\text{g/L}$	$\delta^{13}\text{C}$ (‰)	$\delta^2\text{H}$ (‰)	Conc. ($\mu\text{g/L}$)
MW17		163.9	-40.0	-347.0	92.2
Pz11		q.l.d.			q.l.d.
BR3-9	q.l.d.	q.l.d.			q.l.d.
BR4-6	q.l.d.	q.l.d.			q.l.d.
BR4-7	q.l.d.	q.l.d.			q.l.d.
BR4-8	20	q.l.d.			q.l.d.
BR4-9	q.l.d.	q.l.d.			q.l.d.
BR5-6	q.l.d.	q.l.d.			q.l.d.
BR5-9.5	q.l.d.	q.l.d.			q.l.d.

REFERENCES

Bernstein, A., Shouakar-Stash, O., Ebert, K., Laskov, C., Hunkeler, D., Jeannotat, S., Sakaguchi-Söder, K., Laaks, J., Jochmann, M.A., Cretnik, S., Jager, J., Haderlein, S.B., Schmidt, T.C., Aravena, R., Elsner, M. Compound-specific chlorine isotope analysis: a comparison of gas chromatography/isotope ratio mass spectrometry and gas chromatography/quadrupole mass spectrometry methods in an interlaboratory study. *Anal. Chem.* **2007**, 83, 7624–7634.

Burris, D.R.; Campbell, T.J., Manoranjan, V. S. Sorption of trichloroethylene and tetrachloroethylene in a batch reactive metallic iron- water System. *Environ. Sci. Technol.* **1995**, 29, 2850-2855.

Coplen, T.B.; Brand, W.A.; Gehre, M.; Gröning, M.; Meijer, H.A.J.; Toman, B.; Verkouteren, R.M. After two decades a second anchor for the VPDB $\delta^{13}\text{C}$ scale. 2006. *Rapid Commun. Mass Spectrom.* **2006**, 20: 3165–3166

Chartrand, M.M.G.; Hirschorn, S.K.; Lacrampe-Couloume, G.; Sherwood Lollar, B. Compound-specific hydrogen isotope analysis of 1,2-dichloroethane: potential for delineating source and fate of chlorinated hydrocarbon contaminants in groundwater. *Rapid Commun. Mass Spectrom.* **2007**. 21 (12), 1841–1847

Dayan, H.; Abrajano, T.; Sturchio, N.C.; Winsor, L. Carbon isotopic fractionation during reductive dehalogenation of chlorinated ethenes by metallic iron. *Org Geochem.* **1999**, 30, 755-763

Elsner, M.; Coulome, G.L.; Lollar, B.S. Freezing To Preserve Groundwater Samples and Improve Headspace Quantification Limits of Water-Soluble Organic Contaminants for Carbon Isotope Analysis. *Anal. Chem.* **2006**, 78, 7528-7534

Palau, J., Soler, A., Teixidor, P., Aravena, R. Compound-specific carbon isotope analysis of volatile organic compounds in water using solid-phase microextraction. *J. Chromatog. A.* **2007**, 1163, 260–268.

Sherwood Lollar, B.; Hirschorn, S.K.; Chartrand, M.M.G.; and Lacrampe-Couloume, G. An approach for assessing total instrumental uncertainty in compound- specific carbon isotope analysis: Implications for environmental remediation studies. *Anal. Chem.* 2007, 79(9), 3469-3475.

Shouakar-Stash, O.; Drimmie, R.J. Online methodology for determining compound-specific hydrogen stable isotope ratios of trichloroethene and 1,2-cis-dichloroethene by continuous-flow isotope ratio mass spectrometry. *Rapid Commun. Mass Spectrom.* **2013**, 27, 1335-1344

Slater, G.F.; Dempster, H.S.; Sherwood Lollar, B.; Ahad, J. Headspace analysis: a new application for isotopic characterization of dissolved organic contaminants. *Environ. Sci. Technol.*, **1999**, 33, pp 190–194.

Slater, G.F.; Lollar, B.S.; King, A.; O'Hannesin, S. Isotopic fractionation during reductive dechlorination of trichloroethene by zero-valent iron: influence of surface treatment. *Chemosphere.* **2002**, 49, 587–596

Vanstone, N.A.; Focht, R.M.; Mabury, S.A.; Sherwood Lollar, B. Effect of iron type on kinetics and carbon isotopic enrichment of chlorinated ethylenes during abiotic reduction on Fe(0). *Ground Water.* **2004**, 42, 268-276.

Annex C

Torrentó, C; Audí-Miró, C.; Bordeleau, G.; Marchesi, M.; Rosell, M.; Otero, N.; Soler, A. The use of alkaline hydrolysis as a novel strategy for chloroform remediation: feasibility of using construction wastes and evaluation of carbon isotopic fractionation. *Environmental Science and Technology*. 2014, 48, (3), 1869–1877

The use of alkaline hydrolysis as a novel strategy for chloroform remediation: the feasibility of using construction wastes and evaluation of carbon isotopic fractionation

Clara Torrentó†, Carme Audi-Miró†, Geneviève Bordeleau‡, Massimo Marchesi†§, Mònica
Rosell†, Neus Otero† and Albert Soler†*

†Grup de Mineralogia Aplicada i Medi Ambient, Departament de Cristal·lografia, Mineralogia i Dipòsits
Minerals, Facultat de Geologia, Universitat de Barcelona (UB), Martí Franquès s/n, 08028. Barcelona,
Spain. clara.torrento@ub.edu, carneaudi@ub.edu, monica.rosell@ub.edu, notero@ub.edu,
albertsolergil@ub.edu

‡National Scientific Research Institute (INRS-ETE), 490 de la Couronne, G1K 9A9 Quebec, QC,
Canada. hazufelle@yahoo.ca

§Department of Earth & Environmental Sciences, University of Waterloo, 200 University Ave. W, N2L
3G1 Waterloo, Ontario, Canada. m2marchesi@uwaterloo.ca

Abstract

Laboratory and field-scale pilot experiments were performed to evaluate the feasibility of chloroform degradation by alkaline hydrolysis and the potential of $\delta^{13}\text{C}$ values to assess this induced reaction process at contaminated sites. In batch experiments, alkaline conditions were induced by adding crushed concrete (pH 12.33 ± 0.07), a filtered concrete solution (pH 12.27 ± 0.04), a filtered cement solution (pH 12.66 ± 0.02) and a pH 12 buffer solution (pH 11.92 ± 0.11). The resulting chloroform degradation after 28 days was 94, 96, 99 and 72%, respectively. The experimental data were described using a pseudo-first-order kinetic model, resulting in pseudo-first-order rate constant values of 0.10, 0.12, 0.20 and 0.05 d^{-1} , respectively. Furthermore, the significant chloroform carbon isotopic fractionation associated with alkaline hydrolysis of chloroform ($-53 \pm 3\%$) and its independence from pH in the admittedly limited tested pH range imply a great potential for the use of $\delta^{13}\text{C}$ values for in situ monitoring of the efficacy of remediation approaches based on alkaline hydrolysis. The carbon isotopic fractionation obtained at the lab scale allowed the calculation of the percentage of chloroform degradation in field-scale pilot experiments where alkaline conditions were induced in two recharge water interception trenches filled with concrete-based construction wastes. A maximum of approximately 30-40% of chloroform degradation was achieved during the two studied recharge periods. Although further research is required, the treatment of chloroform in groundwater through the use of concrete-based construction wastes is proposed. This strategy would also imply the recycling of construction and demolition wastes for use in value-added applications to increase economic and environmental benefits.

Keywords: alkaline hydrolysis, remediation, chlorinated methanes, isotopic fractionation.

1. Introduction

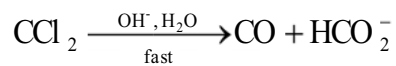
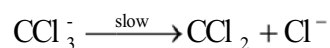
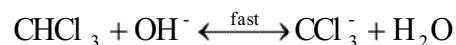
Halogenated volatile organic compounds are some of the most prevalent contaminants in groundwater.¹ Chloroform (CF) is one of the highest ranked halogenated volatile organic compounds on the Agency for Toxic Substances and Disease Registry (ATSDR) priority list of hazardous substances. This list compiles the compounds found at sites on the National Priorities List (NPL) in the United States that pose the most significant potential threat to human health.² In Europe, an environmental quality standard of 2.5 µg/L for CF has been established in the framework of water policy (Directive 2008/105/EC).

CF aerobic and anaerobic microbial cometabolic processes have been described.⁴ However, apart from recent reports describing CF as a terminal electron acceptor during growth of *Dehalobacter*-containing cultures^{5,6}, CF cometabolic degradation is restricted by several environmental factors (inhibition by the presence of growth substrates such as other chlorinated compounds, toxicity of derived metabolites, etc.).⁴ Bioremediation of CF by biostimulation and/or bioaugmentation strategies has been suggested.^{3,7} Nevertheless, to our knowledge, in situ bioremediation of these compounds has not been reported to date. Furthermore, although removal of many halogenated hydrocarbons from groundwater can be achieved by in situ chemical oxidation (ISCO), CF is poorly reactive with common oxidants, such as permanganate, iron-activated persulfate, ozone, hydrogen peroxide or Fenton's Reagent.⁸ New remediation strategies, that are efficient for this recalcitrant compound, should therefore be developed. Alkaline hydrolysis has been proposed as a remediation technology for other types of contaminants, such as explosives⁹⁻¹³, organophosphorous insecticides¹⁴, tert-butyl formate¹⁵, and 1,2,3-trichloropropane¹⁶. To our knowledge the Bondgaard et al.¹⁷ study is the only pilot-scale experiment for in situ alkaline hydrolysis-based groundwater remediation implemented in a

contaminated site until now. However, alkaline hydrolysis has received little attention so far with respect to chlorinated methanes. In general terms, hydrolysis is a reaction in which an organic molecule reacts with a water molecule (or hydroxide ion) and one part of the organic molecule (i.e., the leaving group) is split off from the molecule.¹⁸ In the halogenated hydrocarbons, the leaving group is a halide ion, and hydrolysis of these compounds includes both nucleophilic substitution and elimination reaction mechanisms. The competition between elimination and nucleophilic substitution reactions depends on the structure of the substrate, the nature of the base and stereoelectronic factors. Because strong nucleophiles favor elimination over nucleophilic substitution, alkaline hydrolysis reactions (i.e., reaction with OH⁻) of polyhalogenated aliphatic compounds are expected to be dominated by elimination reactions, whereas neutral hydrolysis (i.e., reaction with H₂O) is expected to occur primarily by nucleophilic substitution reactions.¹⁹ The pH at which the changeover from the dominance of neutral reactions to the dominance of alkaline reactions occurs, I_{NB}, is different for each compound, being 6.5 in the case of CF.¹⁸

Hydrolysis of chlorinated compounds has been well demonstrated in the literature.²⁰⁻²⁴ However, reaction rates are often quite slow within the range of normal groundwater temperatures and pH values. For this reason, reported rates of hydrolysis reactions involving chlorinated solvents are typically the result of extrapolation from experiments performed at higher temperatures. Neutral hydrolysis of CF is very slow, with reported neutral first-order rate constants (K_N) at 25 °C and pH 7 ranging from 6.2×10^{-8} (extrapolated from Fells and Moelwyn-Hughes²⁵) to $2.8 \times 10^{-7} \text{ day}^{-1}$,²² which would translate into half-lives of approximately 30700 and 6900 years, respectively. Because OH⁻ cannot compete successfully with water in substitution reactions with simple halogenated hydrocarbons at typical ambient conditions, the neutral

hydrolysis reaction may be described by a first-order law, regardless of whether the reaction occurs by an SN₁ or SN₂ substitution mechanism or a mixture of both. Neutral hydrolysis of CF is therefore first-order with respect to the concentration of CF and is independent of pH.²² Regarding the alkaline hydrolysis of CF in an aqueous solution, experimental and theoretical approaches suggested that it proceeds through an E1_{CB} mechanism and that the SN₂ mechanism is unlikely to play a major role.^{20,26} The E1_{CB} mechanism is a type of elimination reaction, which, in general terms, consists of a first step where a C-H bond is broken by deprotonation with a base, followed by a second step where the leaving group is expelled. In the case of CF, the E1_{CB} mechanism features the rapid, reversible, base-catalyzed deprotonation of the molecule with the formation of trichloromethyl carbanion (CCl₃⁻), followed by the rate-determining unimolecular loss of a chloride ion to produce the reactive intermediate carbon dichloride, which is then rapidly transformed into the final products, carbon monoxide and formate ion.



The rate of the reaction has been suggested to be first order with respect to both OH⁻ and CF concentrations.^{20,25} Following this assumption and using the neutral and alkaline rate constants (k_N and k_B, respectively) of the hydrolysis of CF at 25 °C reported by Jeffers et al.²² (k_N= 2.8×10⁻⁷ d⁻¹; k_B=7.5 M⁻¹d⁻¹) and extrapolated from Fells and Moelwyn-Hughes²⁵ (k_N= 6.2×10⁻⁸ d⁻¹; k_B=5.7 M⁻¹d⁻¹), pseudo-first-order rate constant (k'_{obs}= k_N + k_B C_{OH⁻}) values of 0.075 and 0.057 day⁻¹, respectively, can be calculated at constant pH 12 (Table 1). This yields half-lives of approximately 9-12 days, which implies an attractive potential use of CF remediation strategies based on alkaline hydrolysis. All the literature cited above determined the kinetics of CF

hydrolysis in homogeneous solutions. In contrast, the effects of heterogeneity on the hydrolysis rates have received little attention so far.²⁷ Amonette et al.²⁷ studied the effect of various mineral phases (montmorillonite, kaolinite, albite and muscovite) on the hydrolysis rates of CF. The authors observed a significant effect of the type of solid on the CF hydrolysis rates at 50 °C, which was attributed to the different pH values maintained by the solid phases in contact with the aqueous phase.

Table 1. Summary of the kinetics of CF degradation by hydrolysis under alkaline conditions. Pseudo-first-order rate constant (k'_{obs}) errors are given as the standard deviation (sd) calculated on the regression of the pseudo-first-order kinetic model. Half-life ($t_{1/2}$) uncertainties were calculated by propagation of the first-order rate constant errors. Pseudo-first-order rate constants and half-lives calculated from the published data of Jeffers et al.²² and Fells and Moelwyn-Hughes²⁵ for pH values of 12 and 13 and for temperatures (T) of 5, 10, 20 and 25 °C are also shown. The empirical temperature dependence relationships reported by Fells and Moelwyn-Hughes²⁵ (SI Equations 12 and 13) were used to extrapolate rate constants to the selected temperatures.

Observed pseudo-first-order rate constants and half-lives for CF degradation by hydrolysis at the experiments					
experiments	pH	T (°C)	k'_{obs} (d ⁻¹) ± sd	R ²	$t_{1/2}$ (d) ± sd
Filtered cement	12.7	23±2	0.20±0.01	0.994	3.4±0.1
Filtered concrete	12.4	23±2	0.12±0.01	0.987	5.8±0.3
Unfiltered concrete	12.4	23±2	0.10±0.01	0.950	7.1±0.7
pH 12 buffer	12.0	23±2	0.05±0.00	0.967	14.7±1.3

Kinetic parameters of CF hydrolysis calculated from published data for selected pH and temperature conditions				
reference	pH	T (°C)	k'_{obs} (d ⁻¹)	$t_{1/2}$ (d)
Modified from Jeffers et al. ²²	12.0	25	0.08	9.2
	13.0	25	0.75	0.9
Modified from Fells and Moelwyn-Hughes ²⁵	12.0	25	0.06	12.2
	12.0	20	0.02	28.8
	12.0	10	0.004	186.2
	12.0	5	0.001	513.8
	13.0	25	0.57	1.2
	13.0	20	0.24	2.9
	13.0	10	0.04	18.6
	13.0	5	0.01	51.4

In the present study, we propose that concrete might be used to maintain alkaline conditions and thus to induce alkaline hydrolysis of CF. Concrete is an artificial conglomerate stone made essentially of Portland cement, aggregates, water and supplementary cementitious materials. Portland cement is made by heating finely ground limestone and finely divided clay at high temperatures. Concrete has high pH buffering capacity due to the lime content of the cement. For these reasons, recycled concrete has been used as a reactive material for neutralizing acidic groundwater.²⁸⁻³⁰ Furthermore, cement-based stabilization/solidification (s/s) treatments have been proven to immobilize chlorinated solvents from contaminated soils and groundwater.³¹⁻³³ These s/s treatments have been used in combination with abiotic reductive dechlorination treatments with additions of Fe(II), in which ferrous iron and cement are used as an electron donor and a catalyst, respectively. The feasibility of the use of concrete to induce alkaline hydrolysis and/or sorption of CF at contaminated sites merits evaluation.

To assess the efficiency of remediation strategies at contaminated sites, the interpretation of concentration data alone is often insufficient; therefore, isotopic data are required. For example, the presence of a contaminant downgradient of a permeable reactive barrier (PRB) may result from incomplete degradation within the PRB, from bypassing under or around the PRB or from contaminants already present before the installation of the PRB. To distinguish these origins, compound specific isotope analysis (CSIA) can be used. The fundamentals of this approach imply that biological and chemical degradation reactions, which involve the cleavage of chemical bonds, usually cause isotopic fractionation. The result is generally an enrichment in heavy isotopes in the remaining substrate because light isotopomers (e.g., ^{12}C , ^1H and ^{35}Cl) typically react faster than heavy isotopomers (e.g., ^{13}C , ^2H and ^{37}Cl).³⁴ In contrast, non-destructive abiotic natural processes, such as dispersion, sorption or volatilization, generally do

not cause significant isotopic fractionation.³⁵⁻³⁹ Therefore, significant changes in isotope ratios over time and space can be used to monitor the success of remediation strategies at contaminated sites.³⁰ Quantification of the extent of contaminant transformation based on stable isotopes requires the experimental determination of the isotopic fractionation associated with the reaction under consideration.

In this study, laboratory batch experiments and field-scale pilot experiments were performed. The batch experiments were carried out to investigate the capacity of concrete to induce alkaline hydrolysis of CF. Additionally, the field-scale pilot experiments were performed to evaluate the feasibility of inducing alkaline hydrolysis of CF in the recharge water of a highly polluted fractured bedrock aquifer by implementing two interception trenches filled with construction wastes (recycled concrete aggregates). The main objectives of this study were i) to evaluate, through the batch experiments, CF consumption under alkaline conditions (pH 12.0-12.7) induced by a solution with crushed concrete, a filtered concrete solution, a filtered cement solution and a pH buffer solution; ii) to use carbon isotopic tools to determine whether fractionation occurs in both batch and field experiments in order to discriminate if a reduction in concentration is produced due to degradation or to non-transformation processes; and iii) to determine if the magnitude of the lab-obtained carbon isotopic fractionation is high enough to assess and quantify the induced alkaline hydrolysis of CF, first, at the pilot field experiment and, later, at contaminated field sites. Because tetrachloromethane (CT), commonly found together with CF, is considered a recalcitrant compound listed on the ATSDR priority list as well, additional laboratory batch experiments and field-scale pilot experiments were also conducted to assess the behavior of CT under induced alkaline conditions. Concentration and isotope results and a discussion about CT are found in the Supporting Information (SI).

2. Materials and methods

2.1. Laboratory-scale experiments

Batch experiments were performed to assess the induced alkaline hydrolysis of CF and to determine the magnitude of carbon isotopic fractionation associated with this process. The materials and solutions used in the experiments are detailed in the SI. Alkaline conditions were induced by adding concrete particles (achieving a pH value of 12.37 ± 0.03) or by using the three different alkaline solutions described in the SI. The experiments with the filtered concrete solution and with the concrete particles were performed to distinguish the effects of degradation versus sorption. Glass vials (26 mL) were used as reaction vessels for the filtered concrete, filtered cement, chemical buffer and control experiments. These vials were filled with the corresponding alkaline solutions or, in the case of the control experiments, with distilled water (pH 5.5 ± 0.2). For the experiments with concrete particles, 39-mL glass vials were filled with 20 g of crushed concrete and approximately 30 mL of distilled water. In all vials, the reaction was started by adding an appropriate volume of the contaminant stock solution described in the SI to provide an initial CF concentration of 30 mg L^{-1} . The vials were completely filled without any headspace to avoid partitioning of chlorinated compounds between the aqueous and gas phases and were closed with PTFE-lined caps. Furthermore, the vials were covered with aluminum foil to avoid photochemical effects. Duplicates (labeled A and B) were performed and all the experiments were conducted at a room temperature of $23 \pm 2 \text{ }^\circ\text{C}$. The experiments were started at different times to achieve reaction times varying from 0 to 28 d. After 28 d from the earliest prepared vials, all the vials were sacrificed at the same time, ensuring that from the stop of the reactions until the analyses, which would be on the same day for all the reactors, all the samples underwent the same storage conditions. Appropriate volumes of the pH 6 buffer solution were

added to the vials to neutralize the solution to pH 6 and quench the alkaline hydrolysis reaction (i.e., 2.1 mL for the 26-mL vials). Preliminary experiments proved that no catalyst effect was induced by the added quenching solution (data not shown). In the experiments with concrete particles, the particles were discarded and the solution was filtered with a 0.45- μm syringe nylon filter (Uptidisc 25 mm, Interchim, France) before neutralization. Samples were held at 4 °C in darkness until analysis (within one week).

2.2. Field-scale pilot experiments

Two field-scale pilot interception trenches were installed in the unsaturated zone of a contaminated fractured bedrock aquifer to induce alkaline hydrolysis of CF in the contaminated recharge water accumulated in the trenches before the water reaches the aquifer. The aquifer is unconfined fractured bedrock, consisting mainly of an Eocene blue-gray limestone bed, which forms a low-permeability matrix with conductive fractures and fissures.⁴⁰ The aquifer is mainly contaminated by chlorinated ethenes, ethanes, methanes and chlorobenzenes, together with traces of BTEX and pesticides. An underground wastewater tank and a disposal pit located outside of the factory building were identified as the main contaminant release sources. High volatile organic compounds concentrations were detected in the subsurface in the areas located around the main pollution sources (SI Fig. S1). The main measures implemented for the mitigation of the contamination, performed in July 2006, were the removal of approximately 2000 t of contaminated soil in the vicinity of the pollution source areas and the installation of the two interception trenches in the unsaturated zone where contaminated soil had been removed (pit trench and tank trench). The pit trench is 14 m long, 6 m wide and 6.5 m deep, whereas the tank trench is 28 m long, 6 m wide and 6.5 m deep (SI Fig. S2). The trenches were filled with 40-70

mm-sized recycled concrete-based aggregates from a construction and demolition waste recycling plant. These aggregates had a density of approximately 1.10 t m^{-3} . Finally, at 50 cm below the ground surface, a geotextile sheet was placed, which was covered by a layer of compacted clays. Three and five monitoring wells were installed along the pit and tank trenches, respectively (SI Fig. S2). Rainwater lixiviates contaminants retained in the unsaturated zone and infiltrates to the trenches, where CF alkaline hydrolysis can be induced. Trench water discharges to the unsaturated zone towards the SSE, following the main water flow direction until reaching a fracture connected to the underlying carbonate aquifer (SI Fig. S3). The trenches discharge until a minimum level, and the water accumulated in both trenches is occasionally removed for its management.

Sampling of the water accumulated in the trenches through one of the monitoring wells of each trench was performed monthly from June 2010 until April 2013. This periodical sampling started 15 days after the trenches were emptied. The collected data are divided into two different periods, henceforth called the first (9 months, from June 12th 2010 to February 23rd 2011) and the second (26 months, March 21st 2011 to April 29th 2013) recharge periods, following water removals on May 26th 2010 and February 23rd 2011, respectively. Physicochemical parameters (pH, temperature, conductivity, Eh and dissolved oxygen) were measured in situ using a flow-through cell (Eijkelkamp, Netherlands) to avoid contact with the atmosphere. Additional details are provided in the SI. Water samples for concentration measurements and isotopic analyses of chlorinated volatile organic compounds were collected in 125-mL amber glass bottles, completely filled and closed with PTFE-lined caps. Samples were held at 4 °C in darkness until analysis. The water level in the trenches and groundwater level in two wells downgradient from

both trenches were continuously recorded using Cera- and Mini-Divers® (Schlumberger Water Service, Postbus, Netherlands), respectively.

2.3. Analytical methods

Chlorinated compound concentrations were determined by headspace (HS) analysis using a FOCUS Gas Chromatograph coupled with a DSQ II Mass Spectrometer (Thermo Fisher Scientific, Waltham, MA, USA). Concentrations in the batch experiments were corrected for the dilution induced by the addition of the quenching solution. Carbon isotope analyses of chlorinated compounds were performed using a Thermo Finnigan Trace GC Ultra instrument coupled via a GC-Isolink interface to a Delta V Advantage isotope ratio mass spectrometer (Thermo Scientific GmbH, Bremen, Germany). Additional details are provided in the SI.

Aliquots of samples were preserved in nitric acid to measure concentrations of cations by inductively coupled plasma-optical emission spectrometry (ICP-OES) and inductively coupled plasma mass spectrometry (ICP-MS). Dissolved chloride concentration was measured in duplicate by titration with a AgNO_3 0.0125 N solution using a 702 SM Titrino automatic titrator. The error based on replicate measurements was 5%. Solution pH was measured with a calibrated WTW pH Meter at room temperature (23 ± 2 °C). The pH error was 0.02 pH units. Alkalinity (as HCO_3^-) was analyzed by automatic titration using unfiltered samples.

3. Results

3.1. Laboratory experiments

Consumption of CF was observed over time in all the experiments, except in the controls, in which concentrations remained unchanged up to 28 d (Fig. 1A) and chloride formation was not detected (data not shown). The results of the control experiments rule out possible losses of CF as a result of processes not induced by alkaline conditions. Under alkaline conditions, contaminant degradation ranged from 72% (buffer experiments) to 99% (filtered cement experiments) after 28 d (Fig. 1A). In each treatment, the pH remained constant over the duration of the experiments (12.33 ± 0.07 in the concrete experiments, 12.27 ± 0.04 in the filtered concrete experiments, 12.66 ± 0.02 in the filtered cement experiments and 11.92 ± 0.11 in the buffer experiments). The hydrolysis of CF under alkaline conditions followed pseudo-first-order kinetics, as evidenced by the linear correlation relationship in $\ln(C/C_0)$ vs. time graphs (SI Fig. S4). Least-squares regression analysis showed $R^2 > 0.95$ (Table 1). The rate of CF degradation generally increased as the pH of the alkaline solutions increased, with pseudo-first-order rate constant values, k'_{obs} , ranging from 0.047 to 0.201 d^{-1} . For all tested alkaline pH values, the half-life was less than 15 d (Table 1). The obtained second-order rate constant was 4.6 ± 2.4 (95% confidence interval) $\text{M}^{-1} \text{d}^{-1}$ (see SI for calculation details and Fig. S5). The order of the reaction was obtained as the slope of the same logarithm plot, and was 1.1 ± 0.5 . Hydroxide concentrations were not directly measured but were estimated from pH values and ionic strength data using the code PHREEQC and the thermodynamic database MINTEQ.v4.⁴¹

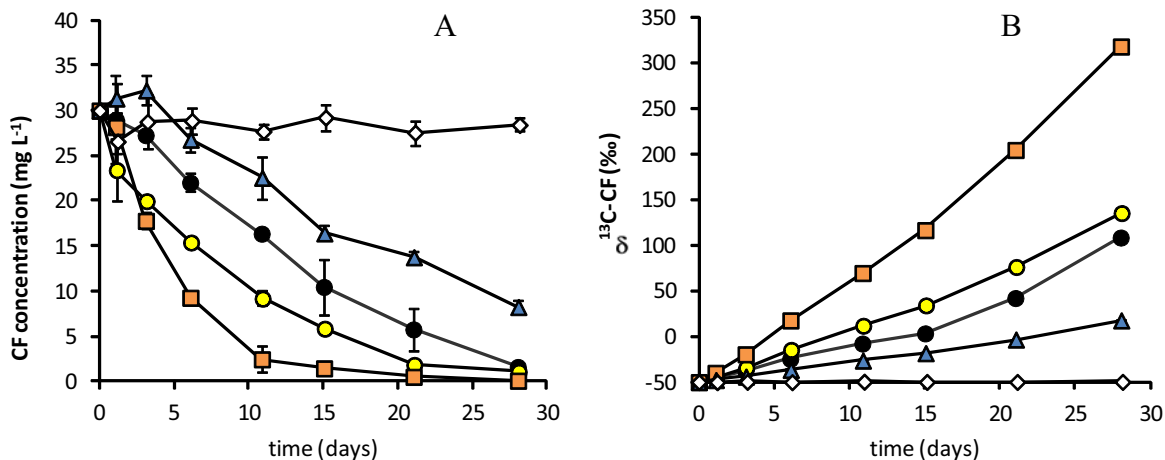


Figure 2.5. Changes in concentration (A) and $\delta^{13}\text{C}$ (B) of CF over time in the alkaline hydrolysis laboratory experiments: unfiltered concrete experiments (black circles), filtered concrete experiments (yellow circles), filtered cement experiments (orange squares), buffer experiments (blue triangles) and control experiments (white diamonds). The error bars show the standard deviation for duplicate experiments.

The initial concrete and cement solutions contained 2.1 and 15.8 mg L^{-1} of chloride, respectively. The chloride concentration related to CF dechlorination at each sampling time was determined by subtracting the background concentrations (measured in the initial concrete and cement solutions) from the measured dissolved chloride concentrations in the samples. The total molar mass balance of chlorine (chloride released + chlorine in the remaining CF) at each sampling time ranged from 81 to 127%, 91 to 105% and 92 to 112% of the initial chlorine mass throughout the experiments with concrete particles, filtered concrete solution, and filtered cement solution, respectively (SI Fig. S6). In addition to chloride, the experiments with concrete particles released Ca, K, S, Sr, Ba, Li, Al and Zn into solution, with concentrations after 28 d of approximately 240, 80, 6.0, 1.5, 1.0, 0.15, 0.1 and 0.05 mg L^{-1} , respectively (SI Table S1). Other measured cations (Cd, As, Cu, Ni, Pb, Cr, Hg, Fe and Mg) were below detection limits.

All of the CF experiments, except the control experiments, show a considerable enrichment in ^{13}C in the remaining CF over the course of the experiments (Fig. 1B). Carbon isotopic fractionations (ϵ_c) were evaluated by a linear regression of the data following the Rayleigh

equation (more details are shown in the SI). The resulting plots can be found in the SI (Fig. S7), and the experimental results are summarized in Table 2. Good fits (i.e., $R^2 > 0.96$) were obtained for all regressions. Carbon isotopic fractionation ranged from $-49 \pm 7\%$ to $-56 \pm 10\%$ for all experiments. The 95% confidence intervals of all ϵ_C values overlap. Consequently, an average ϵ_C value combining all data was determined to be $-53 \pm 3\%$ ($R^2 = 0.98$). The apparent kinetic carbon isotope effect (AKIE) obtained was 1.056 ± 0.003 (see SI for calculation details).

Table 2. Carbon isotope fractionation (ϵ_C) and 95% confidence interval (95% CI) of the regression lines for hydrolysis of CF under the alkaline conditions reported for the experiments, as well as total combined data.

experiments	ϵ_C (‰) \pm 95% CI	n	R^2
Filtered cement	-56 ± 10	8	0.968
Filtered concrete	-53 ± 5	11	0.985
Unfiltered concrete	-51 ± 4	16	0.983
pH 12 buffer	-49 ± 7	11	0.964
Total combined data	-53 ± 3	46	0.977

n : number of analyzed data points

3.2. Field-scale experiments

The pH values of the water sampled from the two trenches remained constant (11.6 ± 0.3) throughout the 35-month sampling period. These results confirm the high buffering capacity of the recycled construction wastes. It should be noted that groundwater collected in all the aquifer monitoring wells shown in Fig. S2 (SI), including the two wells located a few meters downgradient from the trenches, had neutral pH values, showing that alkaline conditions are restricted to the trenches. The results of additional lab experiments evaluating the interaction

between alkaline water and the carbonate aquifer confirmed the high buffering capacity of the aquifer and the restriction of the alkaline conditions to the trenches (see SI for details). Table S1 (SI) shows the concentrations of cations in water collected on May 2008 from both trenches. The temperatures of the water collected from both trenches during the sampled period ranged between 14 and 17 °C (with mean values of 15.6 ± 1.0 °C and 15.3 ± 1.1 °C for both trenches) according to seasonality, whereas the groundwater remained constant at a similar mean value of 15.4 ± 0.2 °C during the same studied period.

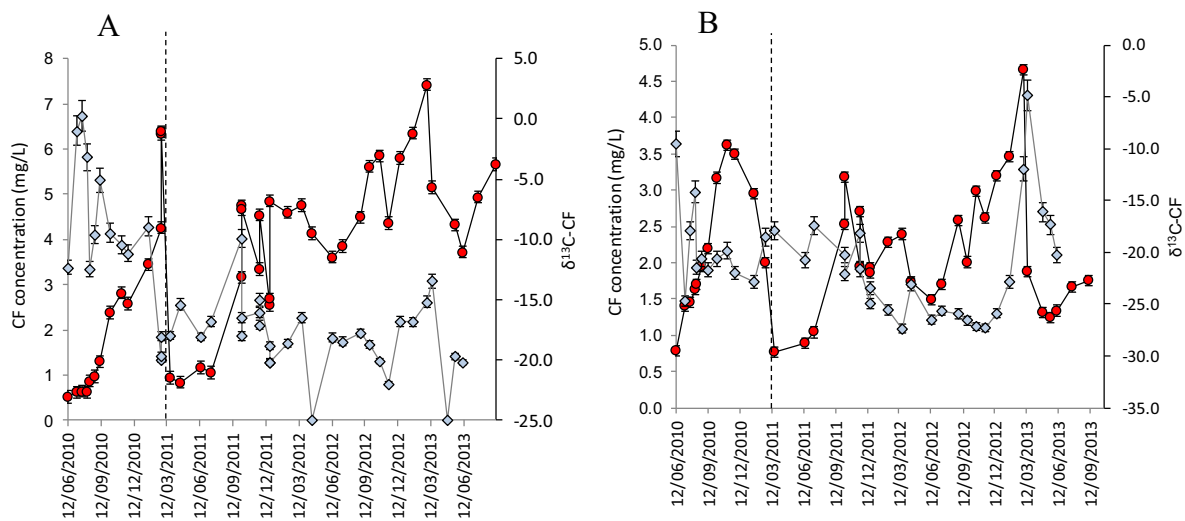


Figure 2.6. Variation over time of CF concentration (blue diamonds) and carbon isotope ratios ($\delta^{13}\text{C-CF}$, red circles) in the (A) tank trench and (B) pit trench during the studied period. The error bars show the standard deviation for replicate measurements of the concentration and isotopic data. Dashed lines indicate the day when the trenches were completely emptied for the management of the contaminated water.

During the study period, the water table elevation in the trenches ranged from approximately 431 to 434 meters above sea level (masl) (SI Fig. S9). Water table fluctuations occurred in response to rainfall. A lag period of approximately 5-7 and 20-30 days was observed between the

precipitation events and the water level increases in the tank and pit trenches, respectively. The rapid recharge of the trenches can be seen after February 23rd 2011, when water of both trenches was removed for its management. Trench discharge after the high-intensity precipitation events proceeds according to Maillet's law. Under the four discharge conditions observed from May 2011 to March 2013 (Fig. S9), the recession curves were used to calculate the average discharge flow rates for both trenches. The obtained average discharge flow rates were $0.18 \pm 0.03 \text{ m}^3 \text{ d}^{-1}$ and $0.23 \pm 0.06 \text{ m}^3 \text{ d}^{-1}$ for the pit and tank trenches, respectively. The mean residence time of water in the trenches was calculated as the ratio of the effective trench volume to the average discharge flow rate. The obtained mean residence time was $513 \pm 86 \text{ d}$ and $730 \pm 190 \text{ d}$ for the pit and tank trenches, respectively. At the end of each of the four observed discharge cycles, discharge becomes zero and trench water remains at the minimum level (Fig. S9). It should be noted that the first discharge cycle, with a duration of 90 days (see the period from June to October 2011 in Fig. S9), is the only period without significant precipitation events and therefore corresponds to the maximum period without water entering the trenches.

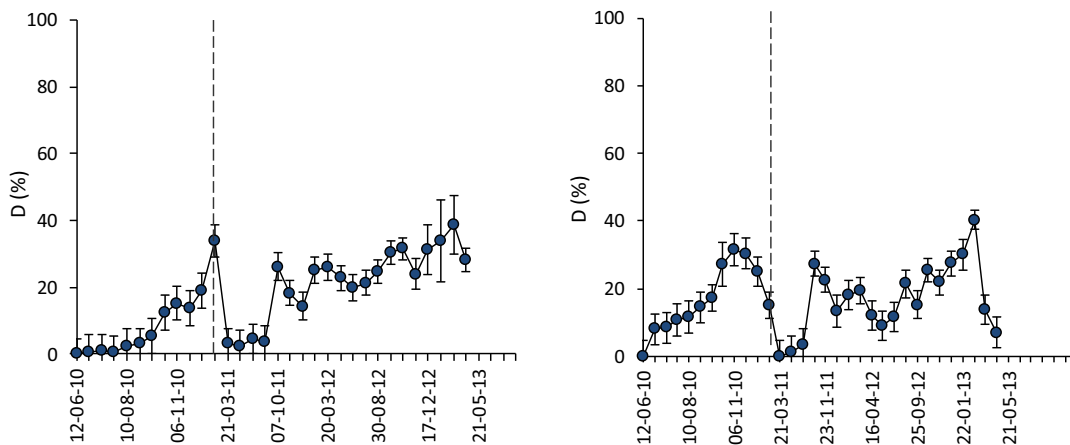


Figure 2.7. Estimation of the extent of chloroform degradation by alkaline hydrolysis induced by construction wastes in the (A) tank trench and the (B) pit trench using Equation 1.13. The uncertainty in the percentage of degradation was calculated by error propagation of the known total errors for $\delta^{13}\text{C-CF}$ measurements (the standard deviation of duplicated measurements) and ϵ_c estimation ($\pm 3\%$). Dashed lines indicate the day when the trenches were completely emptied for the management of the contaminated water.

In both trenches, significant variations in the CF concentration were observed over time (Fig. 2). These fluctuations could be attributed not only to CF degradation but also to dilution effects due to the entry of rainwater after short-duration high-intensity precipitation events, to the leaching of contaminants retained in the unsaturated zone by rainwater after long-duration low-intensity precipitation events, to sorption and/or desorption processes of the contaminants on the mineral micropores, etc. Substantial enrichments in ^{13}C of CF over time occurred in both trenches (Fig. 2), demonstrating CF transformation. In the two recharge periods, there was a general tendency of CF $\delta^{13}\text{C}$ values to increase in both trenches, with isotopic shifts of up to 20 and 28‰. Despite this general trend, certain CF $\delta^{13}\text{C}$ variability was observed due to the entry of non-degraded contaminant leaching from the subsoil after any precipitation event. Using the isotopic fractionation obtained from laboratory experiments ($\epsilon_c = -53 \pm 3\%$), the extent of CF degradation in the trenches (D) was estimated assuming that the alkaline hydrolysis induced by construction wastes was the only degradation fractionation process and fitted to the following expression derived from the Rayleigh distillation equation:

$$D(\%) = \left[1 - \left(\frac{\delta^{13}\text{C}_t + 1000}{\delta^{13}\text{C}_0 + 1000} \right)^{\frac{1000}{\epsilon_c}} \right] \times 100 \quad (1)$$

where $\delta^{13}\text{C}_t$ and $\delta^{13}\text{C}_0$ are the current and initial isotopic compositions (‰) of CF, respectively. The $\delta^{13}\text{C}$ -CF values measured in both trenches at the start of the study period ($-23.0 \pm 0.1\%$ and $-29.5 \pm 0.2\%$), which correspond to the lightest values measured, were used as the initial isotopic compositions of CF for the tank and pit trenches, respectively. This assumes that these isotopic compositions represent the contaminant that has been subjected to the least degradation before reaching the trenches. The calculated percentage of CF degradation in both trenches is shown in Fig. 3. The observed $\delta^{13}\text{C}$ enrichments in the tank trench translate to maximum estimated extents

of degradation of $34\pm 5\%$ and $39\pm 9\%$ for the first and the second recharge periods, respectively. In the pit trench, the two enrichment periods translate to maximum estimated extents of degradation of $32\pm 5\%$ and $40\pm 3\%$. The highest degrees of CF degradation occurred at the end of each observed discharge cycle, when discharge becomes zero and trench water was at the minimum level (Fig. 3 and Fig. S9).

The evolution over time of the concentration and carbon isotopic composition of the other major chlorinated volatile organic compounds present in the trench water (CT, perchloroethylene and trichloroethylene) is shown in the SI.

4. Discussion

The laboratory experiments show that concrete particles immersed in water induced alkaline hydrolysis of CF, with 95% consumption after 28 d (Fig. 1). Degradation of CF was also observed in the other three alkaline treatments (chemical buffer, filtered cement and filtered concrete solutions), with half-lives below 15 days (Table 1). Aside from CF, no other chlorinated volatile compounds were detected by GC-MS in scan mode. This result supports the $E1_{CB}$ degradation mechanism of CF reported by Hine¹⁶, for which the final stable products were carbon monoxide (CO), formate (HCO_2^-), and chloride (Cl^-). Furthermore, excellent chlorine balances were achieved in the filtered experiments, indicating that CF was degraded without accumulation of chlorinated intermediates (SI Fig. S6). Nevertheless, no special attempts were made to identify other potential products of CF degradation. In the experiments with concrete particles, dissimilar chlorine balances were achieved in the two duplicates (set A and set B), reflecting the variability in chloride leaching due to the heterogeneity of the concrete particles. This heterogeneity could also be responsible for the poorer linear correlation between the CF

concentration data and time and for the slightly lower degradation rate observed in the experiment with concrete particles compared to the filtered concrete experiment (Table 1 and SI Fig. S4). Further research on the solid phase is required to confirm this assumption. The pseudo-first-order rate constants and half-lives obtained in this study of the hydrolysis of CF at room temperature are comparable to those calculated from the published values of Jeffers et al.²² and Fells and Moelwyn-Hughes²⁵ for pH values of 12 and 13 and a temperature range between 20 and 25 °C (Table 1).

The lab-scale mean carbon isotopic fractionation associated with alkaline hydrolysis of CF was $-53\pm 3\text{‰}$ (Table 2). To our knowledge, carbon isotopic fractionations associated with any abiotic CF degradation process have not been determined to date. The AKIE obtained at the lab-scale experiments (1.056 ± 0.003) is consistent with the theoretical maximum carbon primary KIE for the C-Cl bond breakage (Streitwieser semiclassical upper limit of 1.057, Huskey⁴²). The good correspondence between the theoretical KIE and the measured AKIE is consistent with an E1_{CB} mechanism for CF alkaline hydrolysis where the C-Cl bond breakage is the rate determining step and, moreover, indicates that this type of abiotic reaction is not influenced by rate-limiting factors or masking effects due to mass transfer processes.

It is worth noting that microbial reductive dechlorination of CF by a *Dehalobacter*-containing culture resulted in a ϵ_C of $-27.5\pm 0.9\text{‰}$ ⁴³, which represents the only documented CF ϵ_C value until now. Therefore, the difference between the carbon fractionation associated with CF abiotic alkaline hydrolysis and that associated with CF anaerobic respiration might potentially be used to distinguish abiotic from biotic degradation processes at contaminated sites.

The large carbon isotopic fractionation observed in the experiments implies a great potential for the use of $\delta^{13}\text{C}$ values for in situ monitoring of the degree of degradation of CF by alkaline

hydrolysis. Even minor extents of degradation will result in significant carbon isotope shifts that can easily be detected by CSIA. For example, considering a carbon fractionation of $-53\pm 3\%$, a 5% degradation will involve a change in $\delta^{13}\text{C}$ values of $+2.7\pm 0.1\%$, which is significantly larger than the analytical uncertainty of $\pm 0.5\%$.

The real concrete-based construction wastes used in the field-scale experiments maintained a constant pH of 11.6 ± 0.3 in pore water during the entire study period (35 months), confirming the longevity of concrete-based aggregates for inducing alkaline conditions. The results of the long-term field-scale pilot interception trenches, with significant ^{13}C enrichments, confirmed the capability of concrete-based construction wastes to induce alkaline hydrolysis of CF. Although the pH achieved by the used construction wastes in the field-scale experiments was slightly lower than the pH range studied in the lab-scale experiments, the independence observed between pH (from 12.0 to 12.7) and ϵ_{C} should allow us to estimate the extent of induced alkaline hydrolysis of CF in the field-scale experiments through the laboratory-obtained ϵ_{C} ($-53\pm 3\%$). However, further experiments at lower pH values should be done to ensure this assumption. A maximum CF degradation percentage between 32 and 40% was achieved in both trenches during the two studied periods (Fig. 3). The efficiency in CF degradation depends on the precipitation regime. Any precipitation event could result in the entry of non-degraded contaminant leaching from the subsoil that would dilute the degradation effect. The alkaline conditions induced by the recycled concrete-based construction wastes were restricted to the trenches and did not negatively affect the natural attenuation processes of chlorinated compounds in the aquifer below the trenches⁴⁰. Actually, a concentration reduction of CF might be a key strategy for bioremediation purposes⁴⁴ because CF is a potent inhibitor of several microbial processes, such as methanogenesis or reductive dechlorination of chlorinated ethenes, the other major group of

pollutants at the site.⁴⁵ Moreover, temperature has a substantial effect on the abiotic degradation rates of chlorinated compounds. The half-lives recalculated from published kinetic data at a typical groundwater temperature of 10 °C are approximately 15 times higher than those for 25 °C (Table 1). At lower groundwater temperatures, for example 5 °C, alkaline hydrolysis of CF at pH 12 would yield a half-life of approximately 500 days (Table 1). Therefore, temperature must be accounted for to predict the effectiveness of remediation strategies based on alkaline hydrolysis in the field. In the present field-scale experiments, the temperature remained approximately 15°C in both trenches, which was very similar to the underlying groundwater. The half-life calculated from the published values of Fells and Moelwyn-Hughes²⁵ for pH 11.6 and 15 °C was 179 days, which is a promising result for the potential full implementation of this remediation approach at the site. For the mean calculated residence time of water in the trenches (513±86 and 730±190 d), a maximum theoretical percentage of degradation of approximately 90% would be achieved if there was no entry of new non-degraded contaminant leaching from the unsaturated zone by rainwater. Taking into account the maximum period without water entry into the trenches, and thus non-degraded contaminant entry (90 days, from June to October 2011, Fig. S9), a maximum theoretical percentage of CF degradation of 30% can be estimated for both trenches, which is in agreement with the isotopic results. Therefore, the actual efficiency of the treatment depends on the precipitation regime and can easily be estimated by monitoring the CF isotopic composition.

Taking this into account, improvements in the design of the interception trenches can be proposed to increase the residence time in the system, such as the enlargement of the dimensions of the trenches or increasing the pH by choosing different concrete-based materials. The pH of leaching solutions of recycled concrete aggregates depends on the degree of carbonation. A study from Engelsen et al.⁴⁶ on the alkaline capacity of several recycled concrete aggregates, including

waste construction materials, found not only similar pH ranges as the ones observed in this study but also that a higher pH of 12.6 was reached with concrete material recycled from a highway pavement constructed in the beginning of 1980's. This material would result in a CF half-life of 18 days, which would translate into a maximum extent of degradation of 97% in the trenches during periods without the entrance of non-degraded contaminant. Monitoring of the isotopic composition would be required to estimate the actual efficiency of the treatment.

Overall, these results indicate that alkaline hydrolysis induced by concrete-based construction wastes seems to represent a potential alternative remediation strategy for CF-contaminated recharge water before the water reaches fractured aquifers. Furthermore, it is proposed that construction wastes could be implemented as a permeable reactive barrier (PRB) system to degrade CF by alkaline hydrolysis in combination with ISCO, which would be able to remove the rest of the accompanying pollutants (usually perchloroethylene, trichloroethylene and cis-1,2-dichloroethylene). Thus, the combination of the two methods, neither of which alone could achieve the degradation of all the compounds, might achieve an efficient decontamination of the groundwater. The usefulness of carbon isotope analyses to evaluate the effectiveness of these types of remediation approaches is also verified in this study. Recycling and reusing construction wastes would furthermore result in environmental and economic benefits.

Supporting Information. Experimental details, the approach for the quantification of isotopic fractionation and the kinetics of alkaline hydrolysis, the field-scale pilot experiment layout with compound concentrations and piezometric information, a schematic representation of the proposed hydrogeological performance of the trenches, the $\ln(C/C_0)$ vs. time plot for the lab-scale experiments, the correlation between the OH^- concentrations and pseudo-first-order rate

constants of the lab experiments, the chlorine mass balance in selected lab experiments, plots for the calculation of ϵC during CF degradation by alkaline hydrolysis for selected lab experiments, additional lab experiments of alkaline water and carbonated aquifer interaction, the evolution of the water table elevation over time in the field-scale experiments, a discussion of cation release, the evolution of the concentration and carbon isotopic composition of other chlorinated volatile organic compounds over time in the field-scale experiments and a discussion of CT behavior. This information is available free of charge via the Internet at <http://pubs.acs.org/>.

Acknowledgments. This work has been carried out with the economical support of the projects CGL2011-29975-C04-01 from the Spanish Government and 2009SGR-00103 from the Catalan Government and a Marie Curie Career Integration Grant in the framework of the IMOTEC-BOX project (PCIG9-GA-2011-293808) within the European Union 7th Framework Programme. We want to thank Albert Folch from the “Universitat Politècnica de Catalunya” for helping in the interpretation of hydrogeological data; Arnau Follia, Ignasi Hernández, Oriol Diaz, Pol Pla, Adriana Rossi and Diana Rodriguez-Fernandez for helping with the field-scale experiment; and the “Centres Científics i Tecnològics” of the “Universitat de Barcelona” for their services. We are grateful to Dr. Jennifer A. Field and three anonymous reviewers for the beneficial comments that increased the quality of the manuscript.

References

1. Carter, J. M.; Lapham, W. W.; Zogorski, J. S. Occurrence of volatile organic compounds in aquifers of the United States. *J. Am. Water Resour. As.* **2008**, 44(2), 399-416

2. ATSDR. Priority list of hazardous substances. Agency for Toxic Substances and Disease Registry Website, <http://www.atsdr.cdc.gov/spl/>
3. Penny, C.; Vuilleumier, S.; Bringel, F. Microbial degradation of tetrachloromethane: mechanisms and perspectives for bioremediation. *FEMS Microbiol. Ecol.* **2010**, 74, 257-275
4. Cappelletti, M.; Frascari, D.; Zannoni, D.; Fedi, S. Microbial degradation of chloroform. *Appl. Microbiol. Biot.* **2012**, 96, 1395-1409
5. Grostern, A.; Duhamel, M.; Dworatzek, S.; Edwards, E. Chloroform respiration to dichloromethane by a *Dehalobacter* population. *Environ. Microbiol.* **2010**, 12, 1053-1060
6. Lee, M.; Low, A.; Zemb, O.; Koenig, J.; Michaelsen, A.; Manefield, M. Complete chloroform dechlorination by organochlorine respiration and fermentation. *Environ. Microbiol.* **2012**, 14(4), 883-894
7. Shan, H.; Kurtz, Jr, H. D.; Freedman, D. L. Evaluation of strategies for anaerobic bioremediation of high concentrations of halomethanes. *Water Research* **2010**, 44, 1317-1328
8. Huling, S. G.; Pivetz, B. E. *In situ chemical oxidation-Engineering issue*. EPA/600/R-06/072. U.S. Environmental Protection Agency Office of Research and Development, National Risk Management Research Laboratory: Cincinnati, OH, **2006**;
http://www.epa.gov/ada/gw/pdfs/insituchemicaloxidation_engineering_issue.pdf
9. Su, T.-L.; Christodoulatos, C. Destruction of nitrocellulose using alkaline hydrolysis. In *Proceedings of the Tri-Service Environmental Technology Workshop*, Hershey, PA. **1996**; pp 337-343

10. Emmrich, M. Kinetics of the alkaline hydrolysis of important nitroaromatic co-contaminants of 2,4,6-Trinitrotoluene in highly contaminated soils. *Environ. Sci. Technol.* **2001**, 35(5), 874-877
11. Hwang, S.; Felt, D. R.; Bouwer, E. J.; Brooks, M.C., Larson, S.L., Davis, J.L. Remediation of RDX-contaminated water using alkaline hydrolysis. *J. Environ. Eng.* **2006**, 132(2), 256-262
12. Hwang, S.; Ruff, T. J.; Bouwer, E. J.; Larson, S. L.; Davis, J.L. Applicability of alkaline hydrolysis for remediation of TNT-contaminated water. *Water Research* **2005**, 39, 4503-4511
13. Karakaya, P.; Sidhoum, M.; Christodoulatos, C.; Nicolich, S.; Balas, W. Aqueous solubility and alkaline hydrolysis of the novel high explosive hexanitrohexaazaisowurtzitane (CL-20). *J. Hazard Mater.* **2005**, 120, 183-191
14. NorthPestClean. Demonstration of in situ alkaline hydrolysis as a new technology for remediation of pesticide contaminated soil and groundwater. Technical pamphlet of the LIFE09 ENV/DK/000368 project. **2013**, 12 pp
15. Church, C.D.; Pankow, J.F.; Tratnyek, P.G. Hydrolysis of tert-butyl formate: Kinetics, products, and implications for the environmental impact of methyl tert-butyl ether. *Environ. Toxicol. Chem.* **1999**, 18(12), 2789-2796
16. Sarathy, V.; Salter, A.J.; Nurmi, J.T.; O'Brien Johnson, G.; Johnson, R.L.; Tratnyek, P.G. Degradation of 1,2,3-trichloropropane (TCP): hydrolysis, elimination, and reduction by iron and zinc. *Environ. Sci. Technol.* **2010**, 44(2),787-93

17. Bondgaard, M.; Hvidberg, B.; Melvej, A.; Ruegg, K.; Ernst, L.; Damgaard, T.; Fredborg, H.; Rügge, K.; Nissen, L.; Jorgensen, T.H.; Bennedsen, L.; Mackinnon, L.; Durant, N.; Thomas, M.; Petrovskis, E. "NorthPestClean" – A large-scale demonstration project of in situ alkaline hydrolysis. In *Book of abstracts of the 12th International UFZ-Deltares Conference on Groundwater-Soil-Systems and Water Resource Management*, Barcelona. **2013**; pp 139

18. Schwarzenbach, R.P., Gschwend, P.M., Imboden, D.M. *Environmental organic chemistry*. 2nd edition; John Wiley & Sons: Hoboken, NJ, **2003**

19. Bruckner, R. *Advanced Organic Chemistry: Reaction Mechanisms*; Academic Press: New York, NY, **2002**

20. Hine, J. Carbon dichloride as an intermediate in the basic hydrolysis of chloroform. A mechanism for substitution reactions at a saturated carbon atom. *J. Am. Chem. Soc.* **1950**, 72, 2438-2445

21. Mabey, W.; Mill, T. Critical review of hydrolysis of organic compounds in water under environmental conditions. *J. Phys. Chem. Ref. Data* **1978**, 7(2), 383-415

22. Jeffers, P. M.; Ward, L. M.; Woytowlitch, L. M.; Wolfe, N. L. Homogeneous hydrolysis rate constants for selected chlorinated methanes, ethanes, ethenes, and propanes. *Environ. Sci. Technol.* **1989**, 23(8), 965-969

23. Vogel, T.M. Natural bioremediation of chlorinated solvents. In *Handbook of bioremediation*; Norris, R.D., Hinchee, R.E., Brown, R., McCarty, P.L., Semprini, L., Wilson, J.T., Kampbell, D.H., Reinhard, M., Bouwer, E.J., Borden, R.C., Vogel, T.M., Thomas, J.M., Ward, C.H., Eds.; Lewis Publishers: Boca Raton, Fla., **1994**; pp. 201-222

24. Miyamoto, K.; Urano, K. Reaction rates and intermediates of chlorinated organic compounds in water and soil. *Chemosphere* **1996**, 32(12), 2399-2408
25. Fells, I.; Moelwyn-Hughes, E. A. The kinetics of the hydrolysis of the chlorinated methanes. *J. Chem. Soc.* **1959**, 398-409
26. Valiev, M.; Garrett, B. C.; Tsai, M. -K.; Kowalski, K.; Kathmann, S. M.; Schenter, G. K.; Dupuis, M. Hybrid approach for free energy calculations with high-level methods: Application to the SN₂ reaction of CHCl₃ and OH⁻ in water. *J. Chem. Phys.* **2007**, 127, 051102-1-4
27. Amonette, J. E.; Jeffers, P. M.; Qafoku, O.; Russell, C. K.; Humphrys, D. R.; Wietsma, T. W.; Truex, M. J. *Abiotic degradation rates for carbon tetrachloride and chloroform: Progress in FY 2010*; PNNL-20044, Pacific Northwest National Laboratory: Richland, WA, **2010**; http://www.pnl.gov/main/publications/external/technical_reports/PNNL-20044.pdf
28. Golab, A. N.; Peterson, M. A.; Indraratna, B. Selection of potential reactive materials for a permeable reactive barrier for remediating acidic groundwater in acid sulphate soil terrains. *Q. J. Eng. Geol. Hydroge.* **2006**, 39, 209-223
29. Indraratna, B.; Regmi, G.; Nghiem, L. D.; Golab, A. Performance of a PRB for the remediation of acidic groundwater in acid sulfate soil terrain. *J. Geotech. Geoenviron.* **2010**, 136(7), 897-907
30. Regmi, G.; Indraratna, B.; Nghiem, L. D.; Guruprasad, A. N.; Guruprasad, B. Treatment of acid groundwater in acid sulphate soil terrain using recycled concrete: Column experiments. *J. Environ. Eng.* **2011**, 137(6), 433-443

31. Hwang, I.; Batchelor, B. Reductive dechlorination of tetrachloroethylene by Fe(II) in cement slurries. *Environ. Sci. Technol.* **2000**, 34(23), 5017-5022
32. Hwang, I.; Batchelor, B. Reductive dechlorination of chlorinated methanes in cement slurries containing Fe(II). *Chemosphere* **2002**, 48, 1019-1027
33. Hwang, I.; Park, H.-J.; Kang, W.-H.; Park, J.-Y. Reactivity of Fe(II)/cement systems in dechlorinating chlorinated ethylenes. *J. Hazard. Mater.* **2005**, B118, 103-111
34. Meckenstock, R. U.; Barbara Morasch, B.; Griebler, C.; Richnow, H. H. Stable isotope fractionation analysis as a tool to monitor biodegradation in contaminated aquifers. *J. Contam. Hydrol.* **2004**, 75, 215-255
35. Harrington, R. R.; Poulson, S. R.; Drever, J. I.; Colberg, P. J. S.; Kelly, E. F. Carbon isotope systematics of monoaromatic hydrocarbons: vaporization and adsorption experiments. *Org. Geochem.* **1999**, 30, 765-775
36. Poulson, S. R.; Drever, J. I. Stable isotope (C, Cl, and H) fractionation during vaporization of trichloroethylene. *Environ. Sci. Technol.* **1999**, 33(20), 3689-3694
37. Slater, G. F.; Ahad, J. M. E.; Sherwood Lollar, B.; Allen-King, R. M.; Sleep, B. E. Carbon isotope effects resulting from equilibrium sorption of dissolved VOCs. *Anal. Chem.* **2000**, 72(22), 5669-5672
38. Schüth, C.; Taubald, H.; Bolaño, N.; Maciejczyk, K. Carbon and hydrogen isotope effects during sorption of organic contaminants on carbonaceous materials. *J. Contam. Hydrol.* **2003**, 64, 269-281

39. Wang, Y.; Huang, Y. S. Hydrogen isotopic fractionation of petroleum hydrocarbons during vaporization: Implications for assessing artificial and natural remediation of petroleum contamination. *Appl. Geochem.* **2003**, 18(10), 1641-1651
40. Palau, J.; Marchesi, M.; Chambon, J.C.C.; Aravena, R.; Canals, À.; Binning, P.J.; Bjerg, P.L.; Otero, N.; Soler, A. Multi-isotope (Carbon and Chlorine) analysis for fingerprinting and site characterization at a fractured bedrock aquifer contaminated by chlorinated ethenes. *Sci. Total Environ.* (accepted)
41. Parkhurst, D.L. User's guide to PHREEQC-A computer program for speciation, reaction-path, advective-transport, and inverse geochemical calculations. U.S. Geological Survey Water-Resources Investigations Report **1995**, 95-4227, 143 pp.
42. Huskey, W.P. Enzyme mechanism from isotope effects. In *Enzyme mechanism from isotope effects*; Cook, P. F., Ed.; CRC Press: Boca Ratn, FL, **1991**; pp. 37-72
43. Chan, C. C. H.; Mundle, S. O. C.; Eckert, T.; Liang, X.; Tang, S.; Lacrampe-Couloume, G.; Edwards, E. A.; Sherwood-Lollar, B. Large carbon isotope fractionation during biodegradation of chloroform by Dehalobacter cultures. *Environ. Sci. Technol.* **2012**, 46, 10154-10160
44. Koenig, J. C.; Lee, M. J.; Manefield, M. Successful microcosm demonstration of a strategy for biodegradation of a mixture of carbon tetrachloride and perchloroethene harnessing sulfate reducing and dehalorespiring bacteria. *J. Hazard. Mater.* **2012**, 219-220, 169-175

45. Maymó-Gatell, X.; Nijenhuis, I.; Zinder, S. H. Reductive dechlorination of cis-1,2-dichloroethene and vinyl chloride by *Dehalococcoides ethenogenes*. *Environ. Sci. Technol.* **2001**, 35(3), 516-521

46. Engelsen, C.J.; van der Sloot, HA.; Wibetoe, G.; Petkovic, G.; Stoltenberg-Hansson, E.; Lund, W. Release of major elements from recycled concrete aggregates and geochemical modeling. *Cement Concrete Res.* **2009**, 39, 446-459

Supporting Information

The use of alkaline hydrolysis as a novel strategy for chloroform remediation: the feasibility of using construction wastes and evaluation of carbon isotopic fractionation

Clara Torrentó^(1,*), Carme Audí-Miró⁽¹⁾, Geneviève Bordeleau⁽²⁾, Massimo Marchesi^(1, 3), Mònica Rosell⁽¹⁾, Neus Otero⁽¹⁾ and Albert Soler⁽¹⁾.

(1) Grup de Mineralogia Aplicada i Medi Ambient, Departament de Cristal·lografia, Mineralogia i Dipòsits Minerals, Facultat de Geologia, Universitat de Barcelona (UB), Martí Franquès s/n, 08028. Barcelona, Spain

(2) National Scientific Research Institute (INRS-ETE), 490 de la Couronne, G1K 9A9 Quebec, QC, Canada

(3) Department of Earth & Environmental Sciences, University of Waterloo, 200 University Ave. W, N2L 3G1 Waterloo, Ontario, Canada

(*) Corresponding author: Clara Torrentó e-mail: clara.torrento@ub.edu Phone: +34 93 403 37 73 Fax: +34 93 402 13 40.

Total number of pages (including cover): 24

Figures: 12

Tables: 1

Experimental details

Materials and solutions

The different experimental treatments involved the use of either unweathered concrete particles, a filtered concrete solution, a filtered cement solution, or a chemical buffer. The concrete that was used consisted of aggregates, Portland-limestone cement of 41.2 MPa strength class (CEM II/A-L 42.5 R), water and supplementary cementitious materials. The concrete was crushed and sieved, and the 4-8 mm grain size fraction was used in the experiments. The filtered concrete solution was prepared by combining 333.3 g of these concrete particles with 500 mL of distilled water (the same proportion as in the vials of the unfiltered concrete experiments, see the main text) and stirring with a magnetic rod for two days until the pH reached a constant value. The concrete was able to buffer the pH of the solution at 12.37 ± 0.03 . Afterwards, the concrete was discarded and the solution was filtered through a 0.45- μm syringe nylon filter (Uptidisc 25 mm, Interchim, France). The filtered cement solution was prepared by combining 100 g of Portland cement CEM I 52.5 R with 600 mL of distilled water, stirring for two days and filtering with a 0.45- μm syringe nylon filter (Uptidisc 25 mm, Interchim, France). The cement was able to buffer the pH of the solution at 12.71 ± 0.02 . The chemical buffer solution (pH 12.02 ± 0.04) was prepared by dissolving 0.24 g of NaOH and 1.86 g of KCl in 500 mL of distilled water. A CF saturated solution was prepared by adding pure CF (99% Sigma Aldrich) to distilled water in a concentration exceeding its solubility at room temperature and stirring overnight in amber glass bottles without headspace. Contaminant stock solution containing 2080 mg L^{-1} of CF was prepared from the saturated solution and was preserved at $4 \text{ }^\circ\text{C}$ until use. Finally, to allow quenching of the reactions in the experimental vials, a pH 6 buffer solution was prepared by dissolving 14.89 g of sodium acetate trihydrate in 50 mL of 0.2 M acetic acid.

Measurement of physicochemical parameters at the field-scale experiments

Physicochemical parameters (pH, temperature, conductivity, Eh and dissolved oxygen) were measured in situ using a flow-through cell (Eijkelkamp, Netherlands) to avoid contact with the atmosphere. A Multi3410 multi-parameter meter (WTW, Weilheim, Germany) was used. Eh was measured with a WTW senTix ORP 900 electrode connected to a WTW senTix 980 pH electrode. All Eh measurements were corrected to the standard hydrogen electrode system (UH) by adding the reference electrode potential at the groundwater temperature to the measured potential. The concentration of dissolved oxygen was measured with a DO meter (WTW FDO 925). Conductivity was measured using a WTW TetraCon 325 conductivity sensor. Samples were collected after wells had been continuously pumped until Eh values were stabilized.

Concentration measurements

Concentrations of chlorinated volatile organic compounds (chloroform, CF; carbon tetrachloride, CT; perchloroethylene, PCE; and trichloroethylene, TCE) were determined by headspace (HS) analysis using a FOCUS Gas Chromatograph coupled with a DSQ II Mass Spectrometer (Thermo Fisher Scientific, Waltham, MA, USA). The GC-MS system was equipped with a split/splitless injector and a DB-624 capillary column (60 m × 0.32 mm i.d., 1.8 μm film thickness; Agilent, Palo Alto, CA, USA) operating with He as the carrier gas at 1.8 mL min⁻¹. The oven temperature program was kept at 60 °C for 2 min, heated to 220 °C at a rate of 8 °C min⁻¹ and finally held at 220 °C for 5 min. HS vials of 20 mL were filled with a sample volume of 15 mL, previously diluted with ultra-pure water (Milli-Q) at different dilution factors, depending on the expected concentration in each case. The vials were immediately closed with aluminum crimp caps containing a PTFE-lined silicone septum and placed on the automatic HS injector. A headspace volume of 0.75 mL was injected in split mode (split ratio of 22:1) at 220 °C and with 40 mL min⁻¹ of helium as the carrier gas. The HS procedure was conducted for 30 min at 80 °C. The error based on replicate measurements was 5%. The compounds were identified on the basis of the comparison of the retention times and mass spectra of selected ions with the calibration standards, and the concentrations were quantified using a set of multi-component external standards at different concentrations. A multi-component standard stock solution with a concentration of 1 mg L⁻¹ was prepared in methanol using the "Volatile Organics Calibration Mix" (Supelco, SS502/524, 2000 μg mL⁻¹ in methanol). Then, aqueous standards at various concentrations, depending on the approximate concentration of the target compounds in the samples, were prepared by diluting the analytes from the methanolic standard stock solution in Milli-Q water. These aqueous standards were analyzed together with the samples.

Isotopic analyses

Carbon isotope analyses of chlorinated compounds were performed using a Thermo Finnigan Trace GC Ultra instrument coupled via a GC-Isolink interface to a Delta V Advantage isotope ratio mass spectrometer (Thermo Scientific GmbH, Bremen, Germany). The GC-C-IRMS system was equipped with a Supelco SPB-624 column (60 m × 0.32 mm, 1.8 μm film thickness; Bellefonte, PA, USA). The oven temperature program was kept at 60 °C for 5 min, heated to 165 °C at a rate of 8 °C min⁻¹, heated to 220 °C at a rate of 25 °C min⁻¹ and finally held at 220 °C for 1 min. The injector was set to split mode with a split ratio of 1:5 at a temperature of 250 °C. Helium was used as a carrier gas with a gas flow rate of 2.2 mL min⁻¹. The chlorinated compounds were extracted from the aqueous samples by automated headspace solid-phase micro-extraction (HS-SPME) using a 75-μm Carboxen-PDMS fiber (Supelco, Bellefonte, PA, USA). The 20-mL vials filled with 10-mL aqueous samples (diluted in Milli-Q water depending on the analyte concentration) were placed in the TriPlus™ Autosampler equipped with a SPME holder (Thermo Fisher Scientific, Waltham, USA). The extraction of the analytes was done at 40 °C for 20 minutes at constant agitation (600 s).

Carbon isotope ratios are reported relative to an international standard (VPDB, Vienna Pee Dee Belemnite) using the delta notation

$$\delta = (R/R_{\text{std}} - 1) \times 1000 (\text{‰}) \quad (1)$$

where R and R_{std} are the isotope ratios of the sample and the standard, respectively. All the measurements were run in duplicate, and the standard deviations of the $\delta^{13}\text{C}$ values obtained were below $\pm 0.5\text{‰}$ (Sherwood Lollar et al., 2007). The analytical system was verified daily using control standards of chlorinated solvents with known carbon isotope ratios which were determined previously using a Flash EA1112 (Carlo-Erba, Milano, Italy) elemental analyzer (EA) coupled to a Delta C isotope ratio mass spectrometer (Thermo Fisher Scientific, Bremen, Germany) through a ConFlo III interface (Thermo Finnigan, Bremen, Germany) using four international reference materials (USGS 40, IAEA 600, IAEA CH6, IAEA CH7) with respect to the Vienna Pee Dee Belemnite (VPDB) standard, according to Coplen et al. (2006).

To correct slight carbon isotopic fractionation induced by the HS-SPME preconcentration technique, the delta values obtained for the samples were corrected by the daily values of the control standards.

Quantification of isotopic fractionation

Isotopic fractionation during chemical or biological transformation of a compound can be evaluated using the Rayleigh equation (Mariotti et al., 1981):

$$R_t = R_0 f^{(\alpha-1)} \quad (1)$$

where f is the fraction of reactant remaining, R_t is the isotope ratio of reactant at a remaining fraction f, R_0 is the initial isotope ratio of the reactant, and α is the fractionation factor.

The fractionation factor is defined by:

$$\alpha = R_t / R_0 \quad (2)$$

By using the delta notation for carbon isotope ratios and the relationship that links the fractionation factor (α) to the isotopic fractionation (ϵ), $\epsilon = 1000(\alpha - 1)$, Equation 1 can be transformed to:

$$\ln [(\delta_t + 1000)/(\delta_0 + 1000)] = (\epsilon/1000) \ln f \quad (3)$$

where δ_t is the isotope ratio of the reactant at a remaining fraction f and δ_0 is the initial isotope ratio of the reactant.

Hence, a plot of $\ln [(\delta_t + 1000) / (\delta_0 + 1000)]$ vs. $\ln f$ should give a straight line with a slope of $(\epsilon/1000)$.

The apparent kinetic carbon isotope effect (AKIE) can be estimated from the following simplified equation according to Elsner et al. (2005):

$$AKIE \approx 1/(1 + (n \varepsilon_{\text{bulk}}/1000)) \quad (4)$$

where “n” is the total number of carbon atoms considered to be in the reactive positions, and it is assumed that secondary isotope effects are negligible. The uncertainty of the KIE can be estimated by error propagation:

$$\text{error of AKIE} = \left| \frac{\partial AKIE}{\partial \varepsilon} \right| \times \text{error of } \varepsilon \quad (5)$$

Approach for the kinetics of alkaline hydrolysis

When using a pH buffer or a low enough contaminant concentration so that the nucleophile(s) is in great excess, the hydrolysis reaction can be considered pseudo-first order. The kinetics of the hydrolysis reactions under alkaline conditions in the batch experiments can therefore be described by the pseudo-first-order rate expression as follows:

$$dC/dt = -k'_{\text{obs}} C \quad (6)$$

where C is the target chlorinated compound concentration, t is time and k'_{obs} is the pseudo-first-order rate constant. By monitoring the concentration of the chlorinated compounds during the time course of the reaction at a given OH^- concentration, the pseudo-first-order rate constants k'_{obs} can be obtained using the integrated form of Equation 6:

$$\ln C = \ln C_0 - k'_{\text{obs}} t \quad (7)$$

where C_0 is the initial concentration of the chlorinated compound. The slopes of the semi-logarithmic plots of $\ln(C/C_0)$ vs. time yield the pseudo-first-order rate constants k'_{obs} . The half-life ($t_{1/2}$) can be calculated as follows:

$$t_{1/2} = \ln(2) / k'_{\text{obs}} \quad (8)$$

Because a compound may react by several competing reactions, k'_{obs} can be considered as the sum of the rate constants of the individual reactions:

$$k'_{\text{obs}} = k_{\text{SN}} + k_{\text{EN}} + (k_{\text{SB}} + k_{\text{EB}})C_{\text{OH}^-}^n + \sum_j k_{\text{N}_j} C_{\text{N}_j} \quad (9)$$

where k_{SN} is the (pseudo-)first-order rate constant for the neutral nucleophilic substitution reaction, k_{EN} is the (pseudo-)first-order rate constant for the neutral elimination reaction, k_{SB} is the second-order rate constant for the alkaline nucleophilic substitution reaction, k_{EB} is the second-order rate constant for the alkaline elimination reaction, C_{OH^-} is the OH^- concentration and k_{N_j} is the second-order rate constant for the SN_2 reaction with other nucleophile, j (Schwarzenbach et al., 2003).

For CF degradation in the batch experiments, Equation 9 can be simplified to:

$$k'_{\text{obs}} = k_{\text{N}} + k_{\text{B}} C_{\text{OH}^-}^n \quad (10)$$

where k_N is the first-order rate constant of neutral hydrolysis and k_B is the second-order rate constant of alkaline hydrolysis. Assuming negligible contribution from the neutral reaction at the pH tested in the experiments (pH 12.0-12.7) and using the OH^- concentration and k'_{obs} data, the second-order rate constant for alkaline hydrolysis can be obtained using the integrated form of Equation 10:

$$\ln k'_{\text{obs}} = \ln k_B + n \ln C_{[\text{OH}^-]} \quad (11)$$

In a logarithmic plot of $\ln k'_{\text{obs}}$ vs. $\ln C_{[\text{OH}^-]}$, the second-order rate constant can be calculated from the interception of the “y” axis by the regression line. The slope of the regression line yields the order of the reaction with respect to OH^- concentration (n).

Rate constants vary as a function of temperature according to the Arrhenius equation (Lasaga, 1983):

$$k_{\text{obs}} = A e^{(-E_A/RT)} \quad (12)$$

where A is a constant known as the pre-exponential factor (min^{-1}), E_A is the activation energy (J mol^{-1}), R is the universal gas constant ($8.314 \text{ J mol}^{-1} \text{ K}^{-1}$) and T is the absolute temperature in degrees Kelvin. The activation energies of the reactions in which halogens are removed from saturated carbons in organic molecules by a substitution or elimination mechanism are between 80 and 120 kJ mol^{-1} , which means that a 10 °C decrease in temperature results in a decrease of the reaction rate by a factor of 3-5 (Schwarzenbach et al., 2003). Therefore, these reactions are quite sensitive to temperature. Fells and Moelwyn-Hughes (1959) found that both neutral and alkaline hydrolysis reaction kinetics of CF do not conform to the Arrhenius equation. The authors proposed the following empirical expressions for the rate constant for CF hydrolysis under neutral/acidic and alkaline conditions, respectively:

$$\log k_{\text{obs}} = 149.6905 - 46.28 \log T - \frac{14108}{T} \quad (\text{neutral hydrolysis}) \quad (13)$$

$$\log k_{\text{obs}} = 212.80249 - 67.18 \log T - \frac{15132}{T} \quad (\text{alkaline hydrolysis}) \quad (14)$$

These temperature dependence relationships were used to extrapolate rate constants for the selected temperatures.

Figure S1

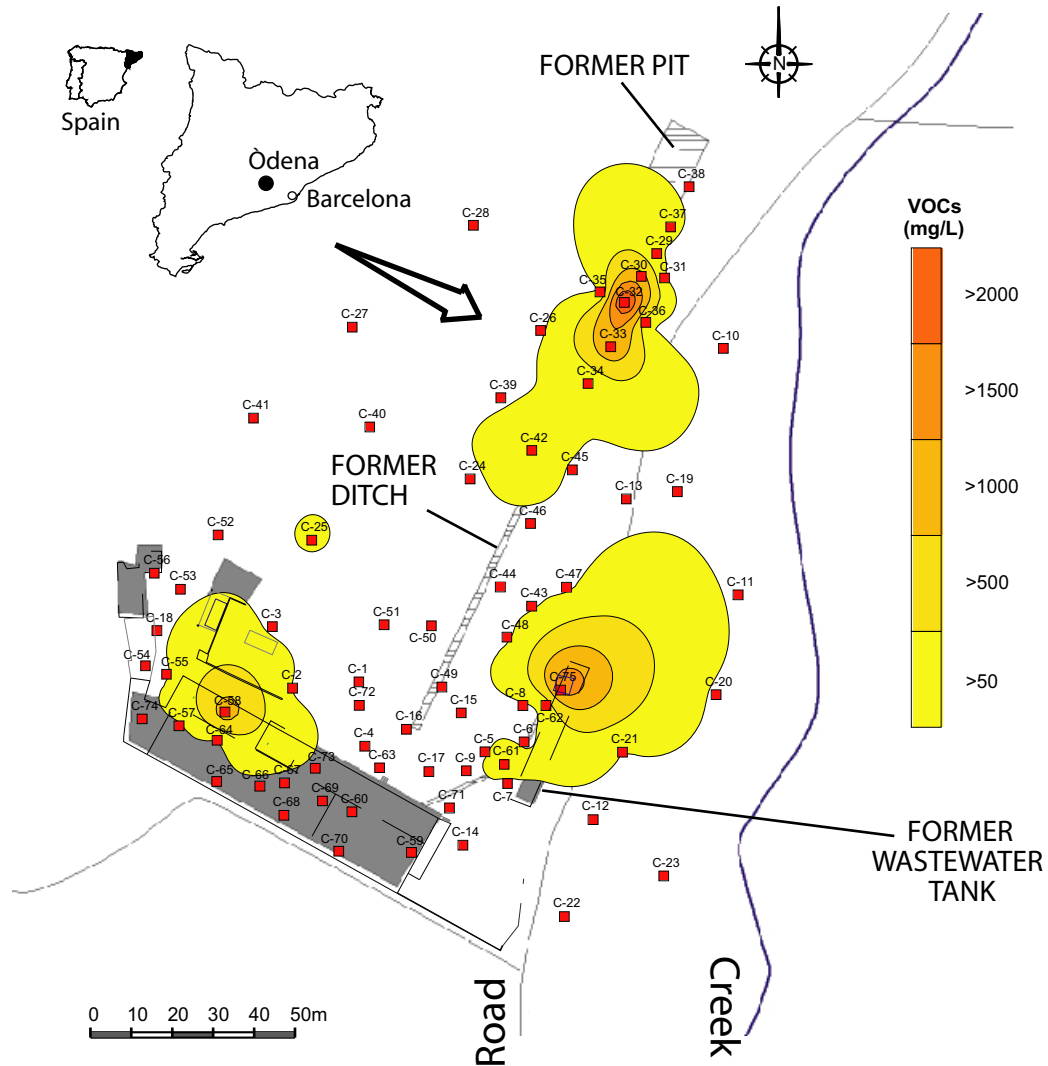


Figure S1. Field-scale pilot experiments. The location of the contaminated site, the location of the 75 trial pits excavated before the construction of the infiltration trenches and the isoconcentration lines for maximum total subsurface VOC concentrations are shown. The trial pits were excavated using a backactor excavator to depths up to 3 mBGL across the contaminated site. Contaminant concentration was screened using a photo-ionization detector (PID) every 0.5 m until the end of drilling. Around the wastewater tank and the former disposal pit, the highest VOC concentrations were detected.

Figure S2

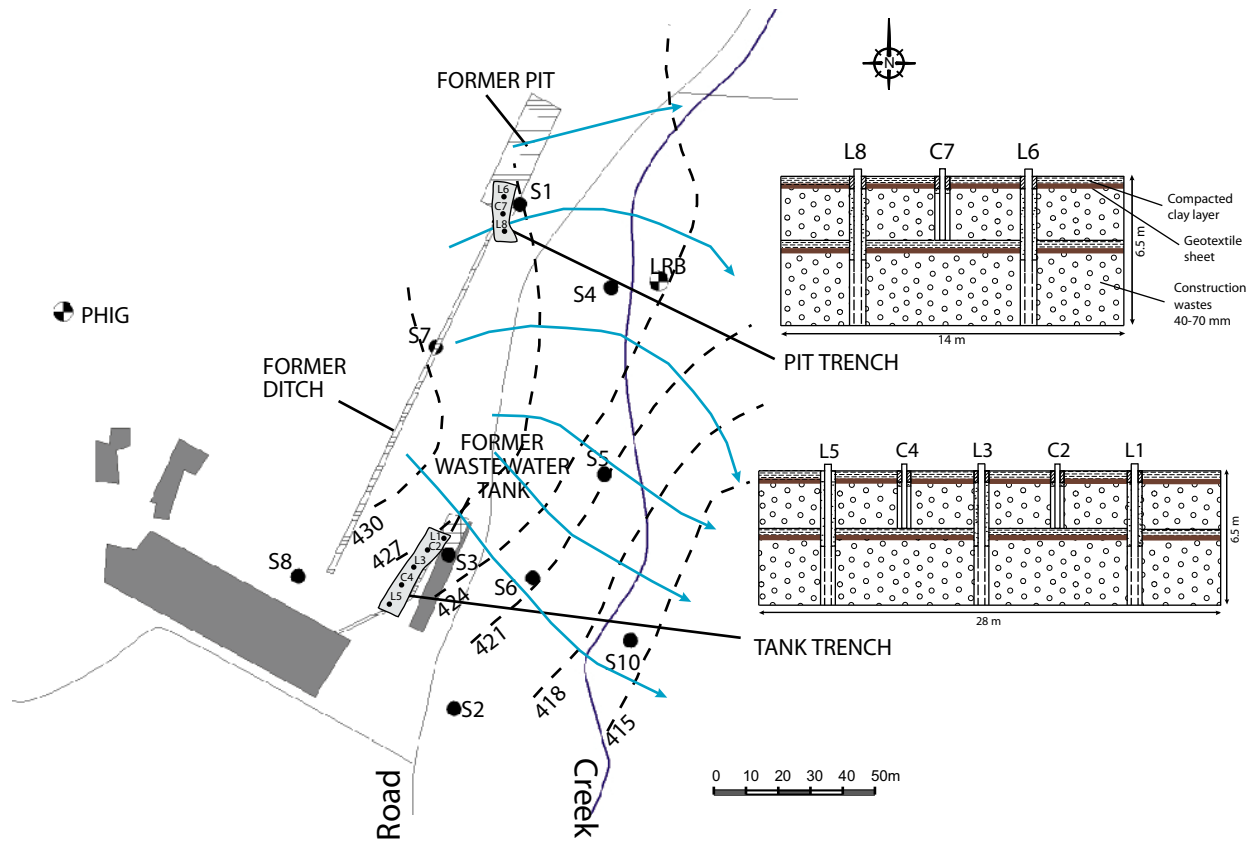


Figure S2. Location and schematic drawing (not to scale) of the trenches. The location of the multilevel monitoring aquifer wells, the piezometric surface (dashed lines in m above sea level) and groundwater flow lines (blue lines) are also shown. The represented groundwater flow system was calculated using the most predominant potentiometric data.

Figure S3

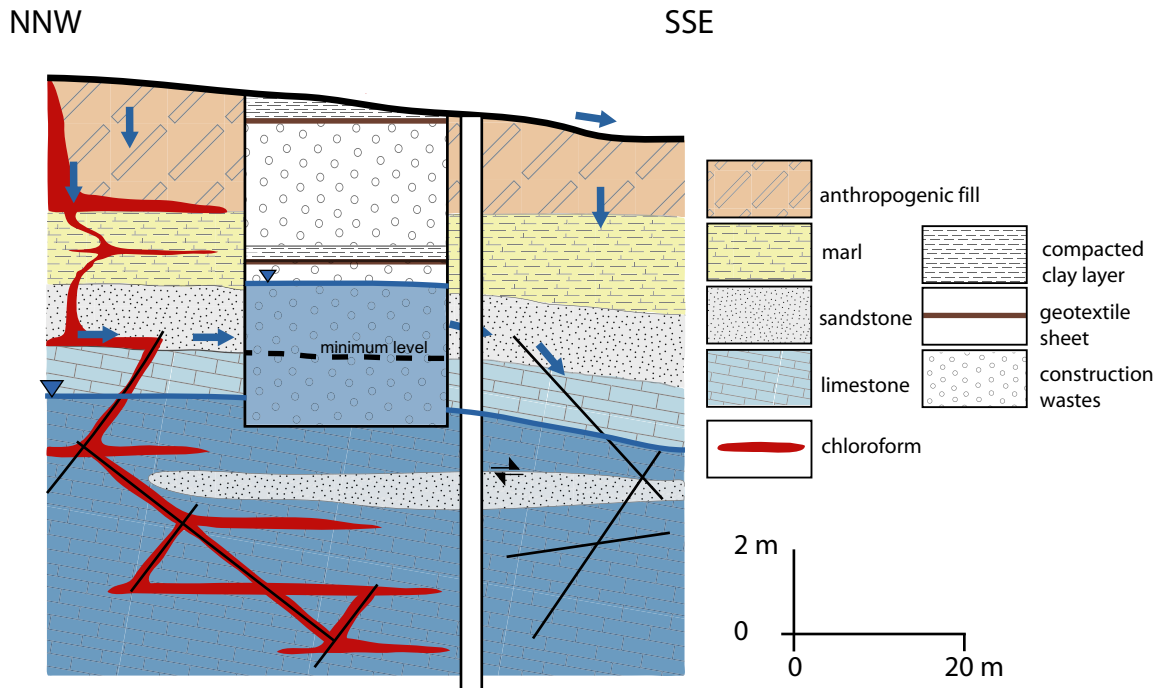


Figure S3. Schematic representation of the proposed hydrogeological performance of the interception trenches. Rainwater lixiviates contaminants retained in the unsaturated zone and infiltrates to the trenches. The “perched” trenches discharge to the unsaturated zone towards the SSE, following the main water flow direction until reaching a fracture connected to the underlying carbonated aquifer. The fractured bedrock unit consists of Eocene blue-gray limestone, which forms a low permeability matrix with conductive fractures and fissures. The bedrock is overlain, from base to top, by brown sandstone, altered yellow marl layers and soil (pit trench area) and/or anthropogenic fill (tank trench area). The anthropogenic fill is composed of a concrete slab and a mixture of fragments of bricks and sandy gravel material. The trenches discharge until a minimum level, which coincides with the contact between the brown sandstone and the fractured bedrock. Therefore, indirect hydraulic connectivity between the trenches and the saturated zone depends on the fracture network.

Figure S4

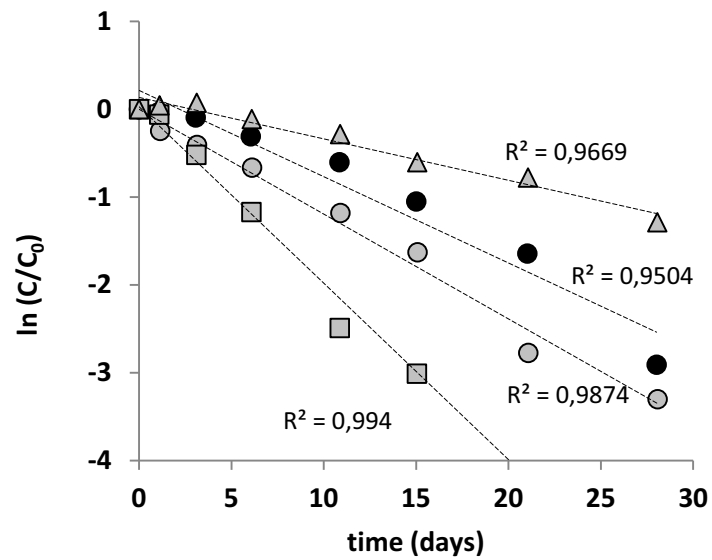


Figure S4. Evolution of $\ln(C/C_0)$ over time in the alkaline hydrolysis laboratory experiments: unfiltered concrete experiments (black circles), filtered concrete experiments (gray circles), filtered cement experiments (squares) and buffer experiments (triangles). Linear regression dashed lines and high correlation values (R^2) are evidence of pseudo-first-order kinetics.

Figure S5

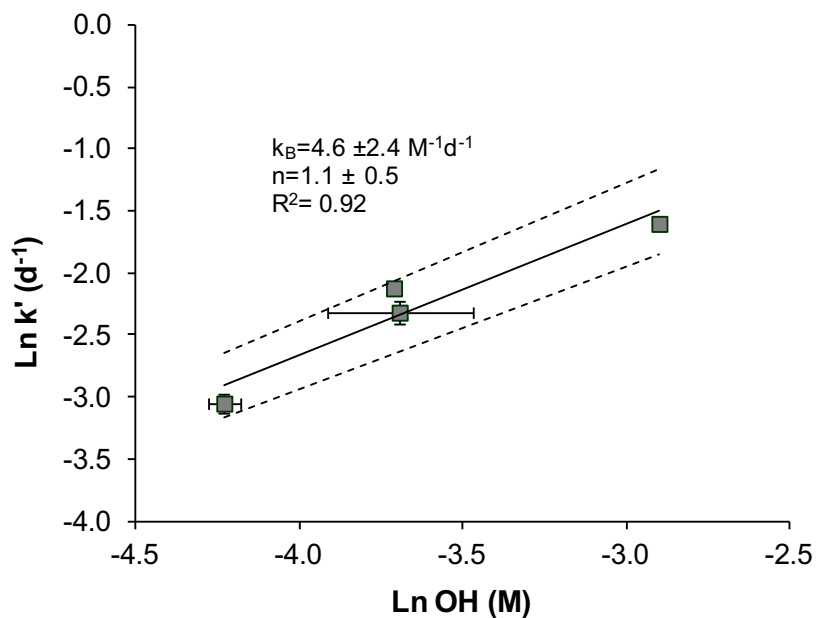


Figure S5. Correlation between the natural logarithm of the OH^- concentrations (estimated using the PHREEQC code) and the natural logarithm of the pseudo-first-order rate constants (k') for the alkaline hydrolysis lab-scale experiments. The uncertainty in the natural logarithm of k' was calculated by propagation of the first-order rate constant errors. Error bars are smaller than symbols when not visible. The dashed lines represent the corresponding 95% confidence interval. The second-order rate constant (k_B) and the reaction order with respect to $[\text{OH}^-]$ (n) have been obtained from the equation of the regression line according to Equation 11.

Figure S6

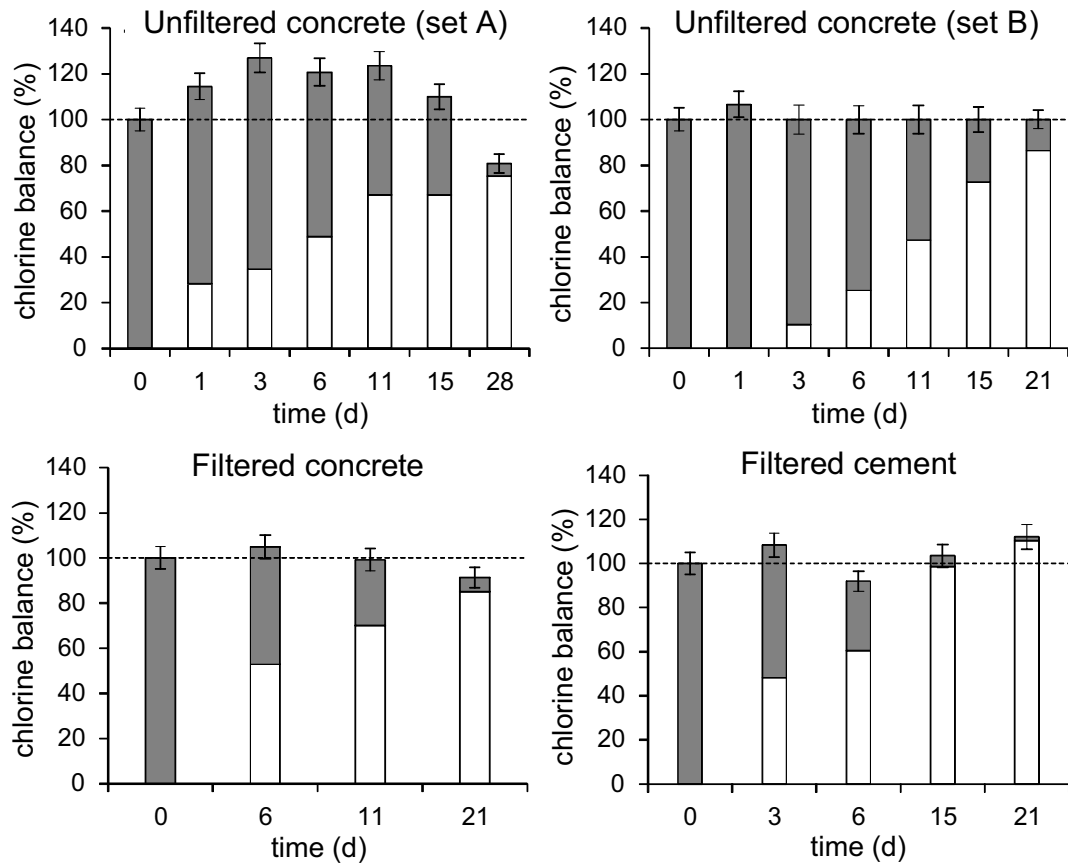


Figure S6. Chlorine mass balance (i.e., chloride released + chlorine in the remaining CF) throughout selected alkaline hydrolysis laboratory experiments. Error bars display the error calculated by propagation of the known total errors for CF (gray) and Cl⁻ (white) concentration measurements.

Figure S7

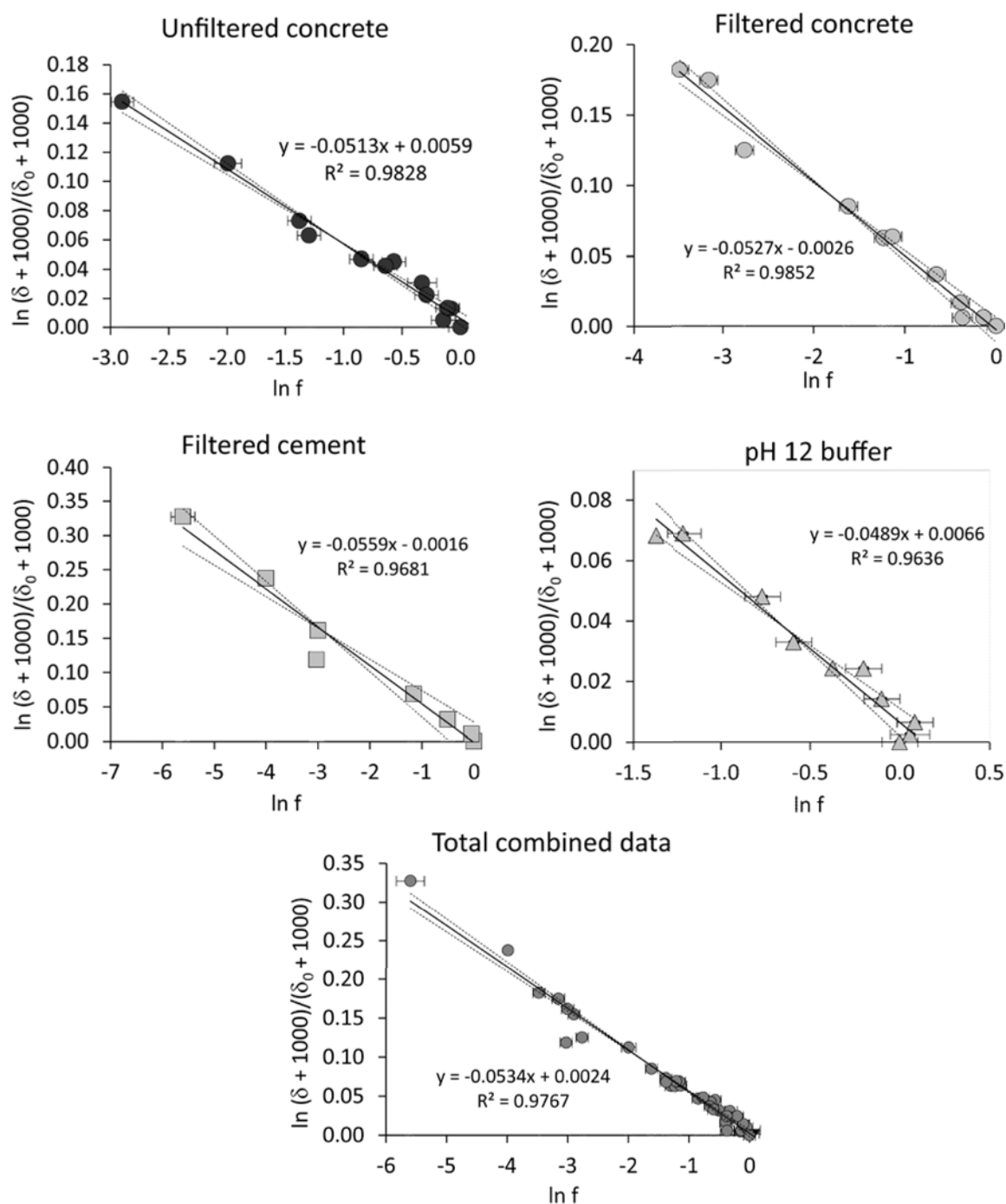
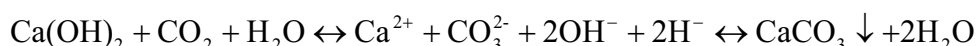


Figure S7. Carbon isotopic fractionation of the residual fraction of CF during degradation by alkaline hydrolysis for duplicated experiments and for total combined data. Following $\ln\left[\frac{(\delta_t + 1000)}{(\delta_0 + 1000)}\right] = (\epsilon/1000)\ln f$, the slope of the solid linear regression lines gives the ϵ_C values. The dashed lines represent the corresponding 95% confidence intervals. Error bars display the error calculated by propagation of the known total errors for concentration and $\delta^{13}\text{C}$ measurements. Obtained isotopic fractionations are listed in Table 2 in the main text.

Additional lab experiments of alkaline water and carbonate aquifer interaction

Additional lab experiments were performed to study the effect on the groundwater pH of the infiltration of the alkaline trench water to the aquifer. Soil CO₂ commonly diffuses upward to the atmosphere and downward to the water level. This last process produces a homogeneous profile of CO₂ within the unsaturated zone (Reardon et al., 1979; Walvoord et al., 2005). During the interaction of the alkaline trench water with the CO₂ of the unsaturated zone before reaching the saturated zone, precipitation of calcite could occur leading to the neutralization of pH. The overall reactions that could occur during these processes are as follow:



Batch and column experiments were performed using alkaline water and aquifer material. Alkaline water was sampled from the tank trench, and a sample of the limestone of the bedrock unit was obtained with a core barrel during the drilling of the S-5 core hole. The rock was a limestone with clasts of quartz, muscovite, biotite, calcite and dolomite and fossil fragments in a clay matrix with carbonate-based cement. Powder X-ray diffraction (XRD) of the core sample was performed using a Bruker D5005 diffractometer with Cu K α radiation over a 2 θ range from 0 to 60 degrees, with a scan speed of 0.025°/18 s. Rietveld analyses revealed that the sample was mainly composed of calcite (23 wt%), dolomite (20 wt%), quartz (21 wt%) and muscovite (28 wt%). Immediately before the start of the experiments, the core fragment was crushed to centimeter-sized fragments and these fragments were crushed and sieved to obtain a particle size that ranged from 5 to 15 mm.

The experiments were carried out at lab temperature (23±2 °C), and at 15.6 °C using an Excal controlled-temperature environmental test chamber (Climats, St Médard d'Eyrans, France). Solution pH and temperature were continuously measured (every 5 min) using a WTW 330i pH meter. For the batch experiments, 130 g of alkaline water was added to 100 g of the aquifer material. The alkaline water was sparged with air immediately before the start of the experiments to introduce air CO₂. In the column experiments, using a peristaltic pump, the alkaline water was circulated through a 15.5-cm long and 9.2-cm diameter column filled with 1800 g of the aquifer material and 740 g of the trench water with a flow rate of 51.9 mL d⁻¹, yielding a hydraulic retention time of 19.8 d. The aquifer material was not completely submerged in the water to simulate interaction of the alkaline water with the CO₂ of the unsaturated zone before reaching the saturated zone. After passing through the column, the water was circulated through a flow-cell to continuously measure pH and temperature.

In all batch and column experiments, neutralization of the pH until getting the range at which neutrophilic bacteria can live (between pH 5 and 8) was observed. After less than 10 days, a pH of 8 was achieved. A geochemical model using the PHREEQC code and the thermodynamic database MINTEQ.v4 (Parkhurst, 1995) proved that neutralization of pH values occurs by

calcite precipitation due to the interaction of the alkaline water with a CO_2 partial pressure of $10^{-2.5}$ atm.

The results obtained from these experiments show that neutralization of pH occurs naturally after only a few days. Therefore, water coming from the trenches should not represent any important effect on the natural attenuation processes existing in the aquifer.

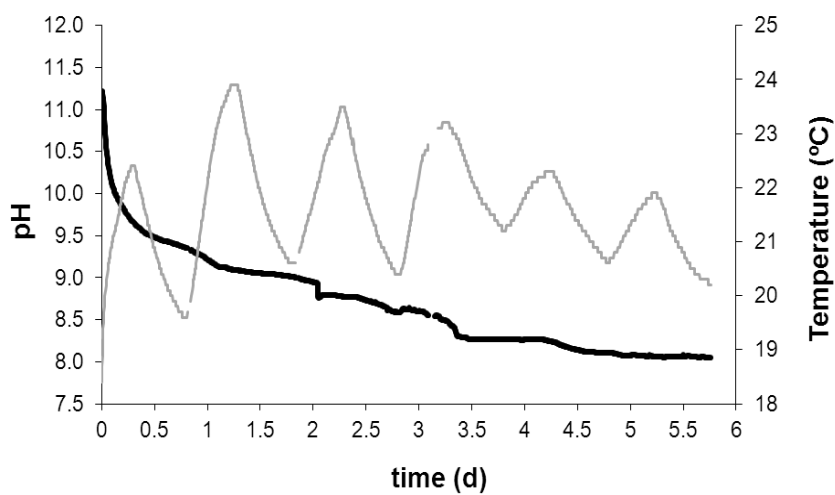


Figure S8. Evolution of the pH (black line) and temperature (gray line) in one of the batch experiments performed at lab temperature (23 ± 2 °C).

Figure S9

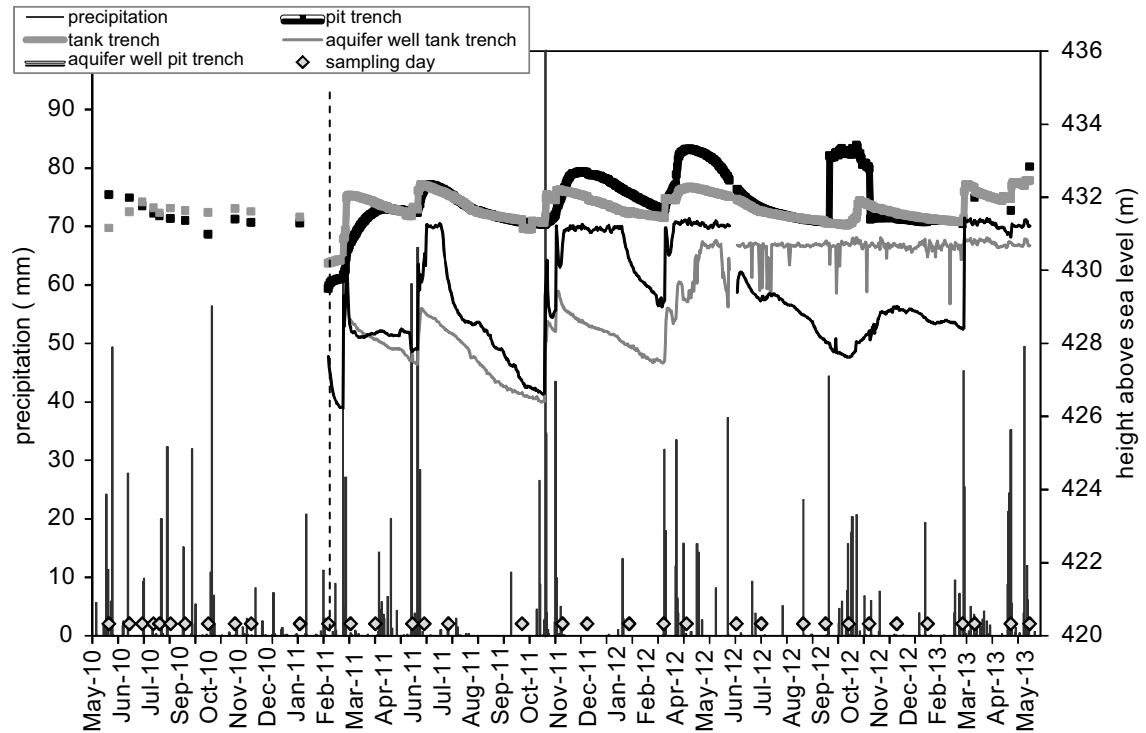


Figure S9. Variations in the water table elevation over time in the two interception trenches (pit and tank trenches) and in the two wells located downgradient from both trenches. Diamond symbols show the sampling days. Rainfall events during the study period are shown. The dashed line indicates the day when the trenches were completely emptied for the management of the contaminated water.

Discussion of cation release

The release of Ca, K, S, Sr, Ba, Li, Al and Zn in the unfiltered concrete experiments and in the field-scale experiments (Table S1) can be attributed to the dissolution of portlandite and hydrated phases, such as calcium silicate hydrate (CSH), and to the alteration of the minerals in the rock fraction of the concrete and construction wastes. Immobilization of heavy-metal (Cd, As, Zn, Cu, Ni, Pb, Ba and Cr) by concrete has been reported to occur via sorption and precipitation processes (Chen et al., 2009; Glasser, 1997). A drawback of using concrete in CF remediation approaches could therefore be the potential release of the concrete-sorbed heavy metals, which might require water post-treatment processing. Hence, care should be taken in the characterization of the concrete used as the reactant in remediation approaches. Nevertheless, in the present experiments, leaching of metals from the concrete and from the recycled concrete-based construction wastes was low, with metal concentrations at the end of the lab experiments and in trench water being below the maximum contaminants levels (MCLs) for drinking water set by the 98/83/EC European Drinking Water Directive. In accordance with these results, Coleman et al. (2005) reported that the 1-2 mm fine fraction of crushed concrete was highly resistant to the leaching of the sorbed heavy metals. The authors found that only a small fraction of the sorbed Cu, Zn and Pb was readily leachable from the crushed concrete, which it should therefore be proposed to be incorporated into permeable reactive barriers for in situ groundwater remediation.

Table S1. Concentration of cations in the alkaline hydrolysis laboratory experiments (unfiltered concrete, filtered concrete, filtered cement and buffer experiments) and in the field-scale experiments (pit and tank trenches).

samples	time (d)	Ba	Li	Mn	Zn	Al	Ca	K	Fe	S	Na	Mg	Sr	Si
		$\mu\text{g L}^{-1}$	mg L^{-1}	$\mu\text{g L}^{-1}$										
unfiltered concrete experiment (set A)	11	335	114	<0.1	<1	369	174	64	nd	4.3	<5	<0.1	1.2	1.2
	28	585	140	<0.1	48	127	240	80	nd	5.8	<5	<0.1	1.7	<0.2
unfiltered concrete experiment (set B)	11	285	123	<0.1	<1	502	162	64	nd	<0.5	43	<0.1	1.2	<0.2
	21	1087	121	0.81	25	92	241	71	nd	<0.5	<5	0.13	1.6	<0.2
filtered concrete experiment (set A)	11	242	520	<0.1	<1	101	292	468	nd	24	<5	<0.1	7.7	1.5
	28	272	513	<0.1	37	216	302	474	nd	25	<5	<0.1	7.8	5.8
filtered cement experiment (set A)	6	210	503	<0.1	<1	16	293	473	nd	25	<5	<0.1	7.8	0.6
	21	421	510	<0.1	<1	189	301	481	nd	25	52	<0.1	8.0	3.4
pH 12 buffer experiment (set A)	11	<0.1	<0.1	1.4	<1	434	<0.1	998	nd	<0.5	90	<0.1	<0.01	6.8
	28	<0.1	<0.1	2.9	123	851	<0.1	975	nd	<0.5	<5	<0.1	<0.01	6.7
tank trench		0.3	0.1	<10	0.10	636	95	107	0.07	nd	168	0.3	3.9	7.1
pit trench		0.1	0.2	<10	0.04	673	83	143	0.14	nd	289	0.1	4.8	7.2

nd: not
determined

Discussion of CT behavior

In both trenches, significant variations in the concentration of chlorinated volatile organic compounds were observed over time (Fig. S10). Regarding isotopic results, negligible changes in $\delta^{13}\text{C}$ values of TCE and PCE in the two trenches were found (Fig. S11). However, $\delta^{13}\text{C}$ -CT values showed significant enrichment during the two recharge periods in both trenches. In the tank trench, $\delta^{13}\text{C}$ -CT values increased from $-18.3\pm 0.2\text{‰}$ to $-13.2\pm 0.8\text{‰}$ in the first period and from $-19.0\pm 0.2\text{‰}$ to $-7.0\pm 0.1\text{‰}$ in the second period. In the pit trench, $\delta^{13}\text{C}$ -CT values increased from $-32.3\pm 1.3\text{‰}$ to $-20.4\pm 0.5\text{‰}$ and from $-29.2\pm 0.7\text{‰}$ to $-17.0\pm 0.5\text{‰}$, in the first and second periods respectively. CT transformation in the trenches is therefore occurring, especially in the tank trench. However, hydrolysis of CT, in contrast to CF degradation, is extremely slow (Jeffers et al., 1989). In this case, alkaline reactions are limited by two factors, namely, the high level of steric hindrance which prevents the occurrence of $\text{S}_{\text{N}}2$ reactions, and the absence of H atoms, which prevents the occurrence of β -elimination reactions (Moelwyn-Hughes, 1971). Furthermore, it is believed that the slow neutral hydrolysis rate of carbon tetrachloride is related to the absence of a C-H bond, which would provide the molecule with the vibration energy necessary to promote interaction with water. The rate-determining step of the neutral hydrolysis reaction is the breakdown of the CT molecule followed by reaction with either water or a hydroxide ion (Fells and Moelwyn-Hughes, 1959). Accordingly, several authors demonstrated that CT degradation by hydrolysis is pH independent (Fells and Moelwyn-Hughes, 1959; Jeffers et al., 1989). Jeffers et al. (1989) reported the first-order rate constant of the abiotic degradation of CT by neutral hydrolysis at 25 °C ($4.7\times 10^{-5} \text{ day}^{-1}$), which translates into a half-life of approximately 40 years.

Additional batch experiments were therefore performed to verify the low capability of concrete to hydrolyze carbon tetrachloride and to evaluate contaminant immobilization by adsorption. For the experiments with concrete particles, 39-mL glass vials were filled with 20 g of crushed concrete and approximately 30 mL of distilled water. For the experiments with the filtered concrete solution 26-mL glass vials were used. In all vials, the reaction was started by adding an appropriate volume of a 400 mg L^{-1} CT stock solution to provide an initial concentration of 30 mg L^{-1} . The experiments were started at different times to achieve reaction times varying from 0 to 50 d. After 50 d from the earliest prepared vials, all the vials were sacrificed at the same time ensuring that all samples experienced the same storage conditions before the analysis. Appropriate volumes of the pH 6 buffer solution were added to the vials to neutralize the solution to pH 6 and quench the alkaline hydrolysis reaction. In the experiments with concrete particles, the particles were discarded and the solution was filtered with a $0.45\text{-}\mu\text{m}$ syringe nylon filter (Uptidisc 25 mm, Interchim, France) before neutralization. Samples were held at 4 °C in darkness until analysis (within one week).

A decrease in CT concentration over time was observed in the experiments containing concrete particles (Fig. S12). After 28 d, a decrease of 64 % of CT was observed. However, no

reductions in concentrations were observed with the filtered concrete solution nor in the control experiments, which suggests that the decrease in concentration in the presence of concrete particles was most likely due to adsorption of CT onto the particles and not to hydrolysis, which is in accordance with the slow reaction rates anticipated for CT hydrolysis at environmental temperatures (Jeffers et al., 1989). Because approximately 75% of concrete consists of aggregates, the properties of the concrete may vary widely with the aggregates used. Therefore, heterogeneity in the specific surface area of concrete of recycled construction wastes must be accounted for to predict CT immobilization capability. Moreover, CT sorbed onto these particles could be slowly released back to the water, as shown in low organic carbon aquifer sediments after long contamination contact time (Riley et al., 2010). Long-term column desorption experiments using recycled concrete-based demolition wastes are therefore required for predicting CT immobilization or potential future rebound episodes.

In the unfiltered concrete series, the decrease in CT concentrations was not accompanied by a detectable change in the $\delta^{13}\text{C}$ values of the remaining CT (Fig. S11). Therefore, the significant isotopic fractionation observed in the field-scale experiments, especially in the tank trench, could indicate the occurrence of other degradation processes distinct from alkaline hydrolysis. Several studies reported carbon isotopic fractionation associated with abiotic reductive dechlorination of CT by Fe(II) sorbed onto iron minerals (Elsner et al., 2004; Zwank et al., 2005), by structural Fe(II) within magnetite or smectites (Neumann et al., 2009) or by Zn⁰ (Vanstone et al., 2008), with ϵC values ranging from -10.0 to -32‰. Moreover, the reactivity of iron minerals with CT is strongly pH dependent and is connected to the deprotonation of the mineral surface, which makes CT dechlorination faster at higher pH (Danielsen and Hayes, 2004; Lin and Liang, 2013). Although the mineral composition of the recycled concrete aggregates used in the field tests was not analyzed, a small content of iron phases, such as hematite, cannot be discarded (Engelsen et al., 2009). Geochemical speciation modeling using the code PHREEQC and the thermodynamic database MINTEQ.v4 (Parkhurst, 1995) showed that water samples collected from the trenches were supersaturated with respect to several iron oxy-hydroxides, such as goethite, hematite, magnetite and lepidocrocite. Therefore, CT degradation processes related to these iron minerals cannot be discarded although further research is needed. The potential formation of lighter CF by these CT degradation processes in the field trenches would have been another source of CF $\delta^{13}\text{C}$ variability.

Figure S10

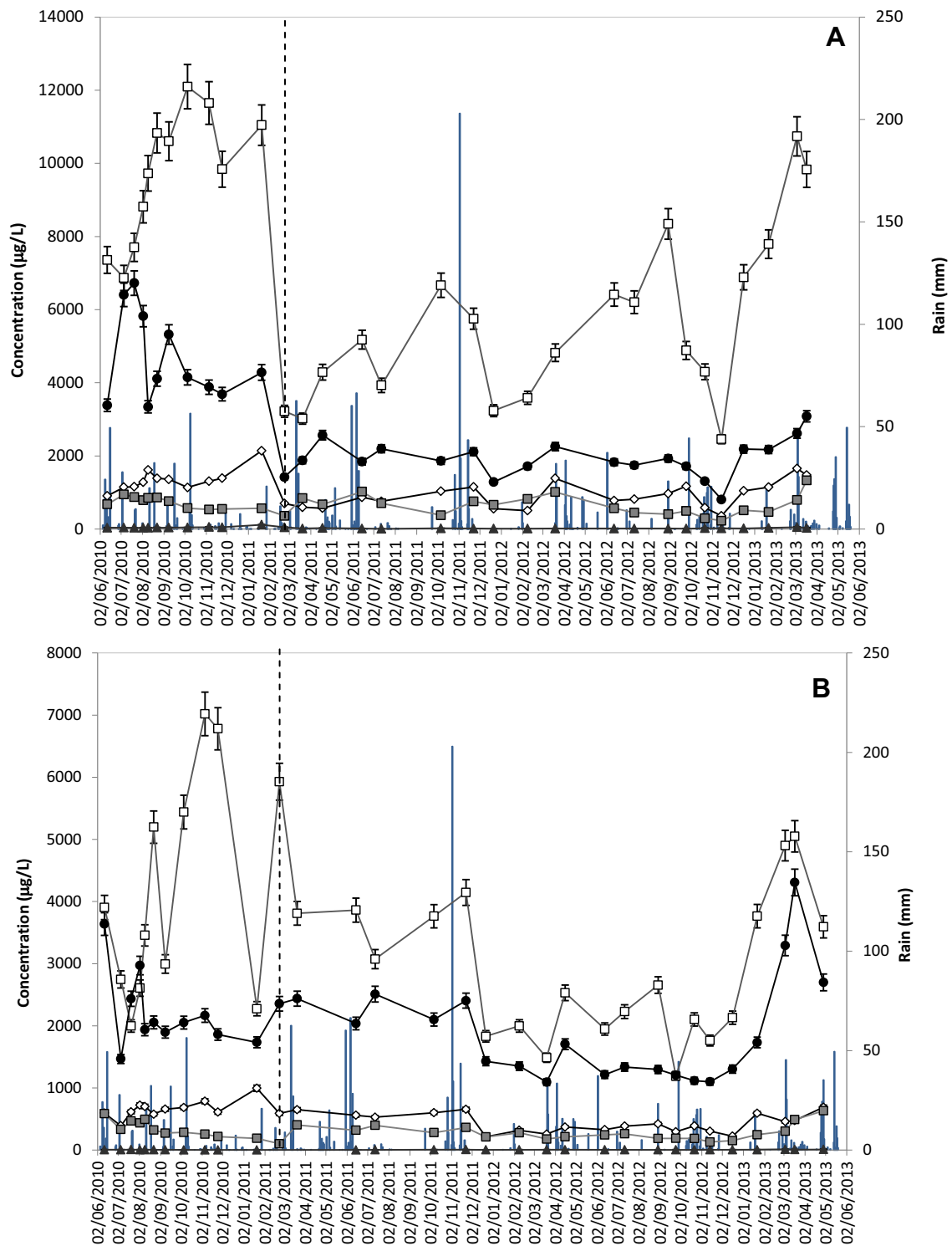


Figure S10. Evolution of the concentration of chlorinated volatile organic compounds over time in the (A) tank trench and (B) pit trench: CF (black circles), CT (gray squares), PCE (white diamonds) and TCE (white squares). Error bars display the accuracy based on replicate measurements of the concentration data. Rainfall events during the study period are also shown. Dashed lines indicate the days when the trenches were completely emptied for the management of the contaminated water.

Figure S11

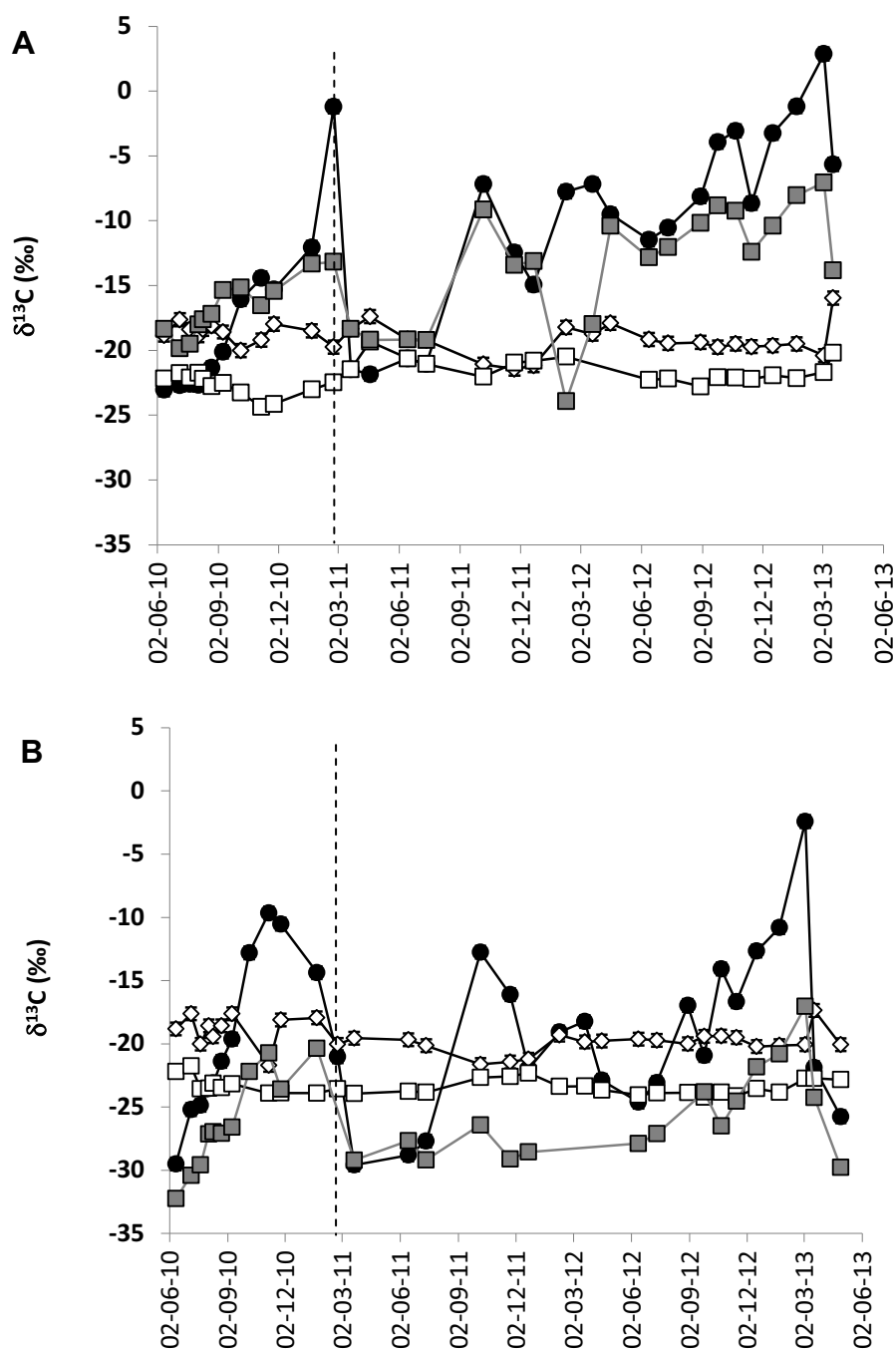


Figure S11. Variation over time of the carbon isotope ratios ($\delta^{13}\text{C}$) of the chlorinated compounds in the (A) tank trench and (B) pit trench during the studied period: CF (black circles), CT (gray squares), PCE (white diamonds) and TCE (white squares). The error bars show the standard deviation for replicate measurements of the isotopic data. Dashed lines indicate the days when the trenches were completely emptied for the management of the contaminated water.

Figure S12

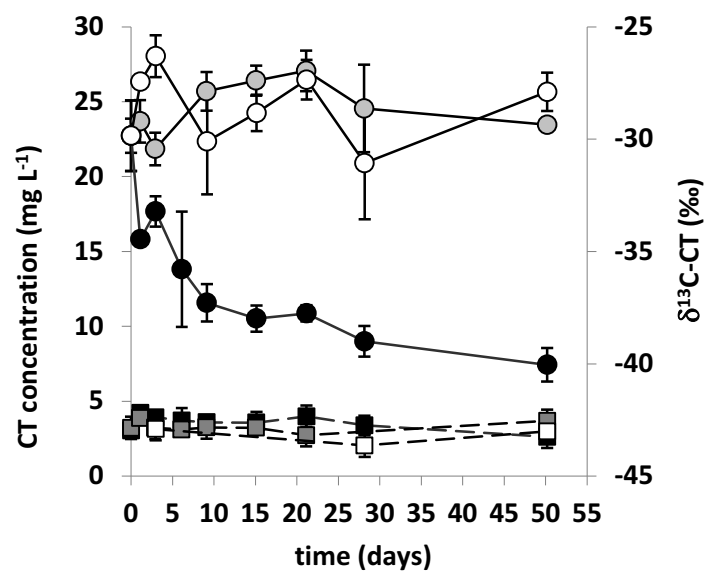


Figure S12. Variations in the concentration (circles) and $\delta^{13}\text{C}$ values (squares) of CT over time in the unfiltered concrete experiments (black symbols), filtered concrete experiments (gray symbols) and control experiments (white symbols). Error bars display the accuracy based on replicate measurements of the concentration and isotopic data.

References

- Chen, Q. Y.; Tyrer, M.; Hills, C. D.; Yang, X. M.; Carey, P. Immobilization of heavy metal in cement-based solidification/stabilization: A review. *Waste Manage.* **2009**, 29, 390-403.
- Coleman, N. J.; Lee, W. E.; Slipper, I. J. Interactions of aqueous Cu²⁺, Zn²⁺ and Pb²⁺ ions with crushed concrete fines. *J. Hazard. Mater.* **2005**, B121, 203-213.
- Coplen, T. B.; Brand, W.A.; Ghore, M.; Gröning, M.; Meijer, H. A. J.; Toman, B.; Verkouteren, R. M. New guidelines for $\delta^{13}\text{C}$ measurements. *Anal. Chem.* **2006**, 78, 2439-2441
- Danielsen, K. M.; Hayes, K. F. pH dependence of carbon tetrachloride reductive dechlorination by magnetite. *Environ. Sci. Technol.* **2004**, 38, 4745-4752
- Elsner, M.; Haderlein, S. B.; Kellerhals, T.; Luzi, S.; Zwank, L.; Angst, W.; Schwarzenbach, R. P. Mechanisms and products of surface-mediated reductive dehalogenation of carbon tetrachloride by Fe(II) on goethite. *Environ. Sci. Technol.* **2004**, 38(7), 2058-2066
- Elsner, M.; Zwank, L.; Hunkeler, D.; Schwarzenbach, R. P. A new concept linking observable stable isotope fractionation to transformation pathways of organic pollutants. *Environ. Sci. Technol.* **2005**, 39(18), 6896-6916.
- Engelsen, C.J.; van der Sloot, HA.; Wibetoe, G.; Petkovic, G.; Stoltenberg-Hansson, E.; Lund, W. Release of major elements from recycled concrete aggregates and geochemical modeling. *Cement Concrete Res.* **2009**, 39, 446-459
- Fells, I.; Moelwyn-Hughes, E. A. The kinetics of the hydrolysis of the chlorinated methanes. *J. Chem. Soc.* **1959**, 398-409
- Glasser, F. P. Fundamental aspects of cement solidification and stabilization. *J. Hazard. Mater.* **1997**, 52, 151-170.
- Lasaga, A.C. Rate laws of chemicals reactions. In: *Kinetics of geochemical processes*; Lasaga, A. C., Kirkpatrick, R. J., Eds.; Reviews in Mineralogy, 8. Mineralogical Society of America: Washington, DC **1983**; pp. 1-68
- Lin, Y-T.; Liang, C. Carbon tetrachloride degradation by alkaline ascorbic acid solution. *Environ. Sci. Technol.* **2013**, 47, 3299-3307
- Jeffers, P. M.; Ward, L. M.; Woytowltch, L. M.; Wolfe, N. L. Homogeneous hydrolysis rate constants for selected chlorinated methanes, ethanes, ethenes, and propanes. *Environ. Sci. Technol.* **1989**, 23(8), 965-969
- Mariotti, A. ; Germon, J. C. ; Hubert, P. ; Kaiser, P.; Létolle, R. ; Tardieux, A. ; Tardieux, P. Experimental determination of nitrogen kinetic isotope fractionation - Some principles - Illustration for the denitrification and nitrification processes. *Plant Soil* **1981**, 62, 413-430
- Moelwyn-Hughes, E.A. *The Chemical Statics and Kinetics of Solutions*. Academic Press Inc: London **1971**
- Neumann, A; Hofstetter, T.B.; Skarpeli-Liati, M.; Schwarzenbach, R.P. Reduction of polychlorinated ethanes and carbon tetrachloride by structural Fe(II) in smectites. *Environ. Sci. Technol.* **2009**, 43(11), 4082-4089

- Parkhurst, D.L. User's guide to PHREEQC--A computer program for speciation, reaction-path, advective-transport, and inverse geochemical calculations. U.S. Geological Survey Water-Resources Investigations Report **1995**, 95-4227, 143 pp.
- Reardon, E.J.; Allison, G.B.; Fritz, P. Seasonal chemical and isotopic variations of soil CO₂ at Trout Creek, Ontario. *J. Hydrol.* **1979**, 43,355-371
- Riley, R.G.; Szecsody, J.E.; Sklarew, D.S.; Mitroshkov, A.V.; Gent, P.M.; Brown, C.F.; Thompson, C.J. Desorption behavior of carbon tetrachloride and chloroform in contaminated low organic carbon aquifer sediments. *Chemosphere* **2010**, 79, 807-813
- Schwarzenbach, R.P.; Gschwend, P.M.; Imboden, D.M. *Environmental organic chemistry*. 2nd edition. John Wiley & Sons: Hoboken, NJ **2003**
- Sherwood Lollar, B.; Hirschorn, S.K.; Chartrand, M.M.G.; Lacrampe-Couloume, G. An approach for assessing total instrumental uncertainty in compound-specific carbon isotope analysis: implications for environmental remediation studies. *Anal. Chem.* **2007**, 79, 3469-3475
- Vanstone, N.; Elsner, M.; Lacrampe-Couloume, G.; Mabury, S.; Lollar, B. S. Potential for identifying abiotic chloroalkane degradation mechanisms using carbon isotopic fractionation. *Environ. Sci. Technol.* **2008**, 42(1), 126-132
- Walvoord, M.A.; Striegl, R.G.; Prudic, D.E.; Stonestrom, D.A. CO₂ dynamics in the Amargosa desert: Fluxes and isotopic speciation in a deep unsaturated zone. *Water Resour. Res.* **2005**, 41, W02006
- Zwank, L.; Elsner, M.; Aeberhard, A.; Schwarzenbach, R. P.; Haderlein, S. B. Carbon isotope fractionation in the reductive dehalogenation of carbon tetrachloride at iron (hydr)oxide and iron sulfide minerals. *Environ. Sci. Technol.* **2005**, 39(15), 5634-5641